uOttawa

L'Université canadienne
Canada's university

FACULTÉ DES ÉTUDES SUPÉRIEURES ET POSTOCTORALES

uOttawa

L'Université canadienne
Canada's university

FACULTY OF GRADUATE AND POSDOCTORAL STUDIES

Roza Tizvar

AUTEUR DE LA THÈSE / AUTHOR OF THESIS

M.A.Sc. (Chemical Engineering)

GRADE / DEGREE

Department of Chemical Engineering

FACULTÉ, ÉCOLE, DÉPARTEMENT / FACULTY, SCHOOL, DEPARTMENT

Investigation of Liquid-Liquid Extraction Process for Separation of Glycerol and Biodiesel

TITRE DE LA THÈSE / TITLE OF THESIS

Dr. David McLean

DIRECTEUR (DIRECTRICE) DE LA THÈSE / THESIS SUPERVISOR

CO-DIRECTEUR (CO-DIRECTRICE) DE LA THÈSE / THESIS CO-SUPERVISOR

EXAMINATEURS (EXAMINATRICES) DE LA THÈSE / THESIS EXAMINERS

Dr. X. Cao

Dr. A. Tremblay

Gary W. Slater

Le Doyen de la Faculté des études supérieures et postdoctorales / Dean of the Faculty of Graduate and Postdoctoral Studies

Investigation of Liquid-Liquid Extraction Process for Separation of Glycerol and Biodiesel

by

Roza Tizvar

Thesis submitted to the Faculty of Graduate and Postdoctoral Studies in partial fulfillment of the requirements for the degree

Master of Applied Science

in the Department of Chemical Engineering
Faculty of Engineering
University of Ottawa
June, 2007

Your file Votre référence
ISBN: 978-0-494-32483-7
Our file Notre référence
ISBN: 978-0-494-32483-7

To my mother

Abstract

Biodiesel is a sustainable and environmentally friendly source of energy which is now being used as an alternative for fossil fuels worldwide. Glycerol is the main by-product of biodiesel produced via transesterification and must be removed from biodiesel according to the ASTM Standard D-6751-02. This purification has usually been carried out with liquid-liquid extraction with water as a solvent for glycerol. In commonly-used alkali-catalyzed transesterification of waste cooking oil, the use of large quantities of water alone, as extraction solvent, results in formation of soaps, then emulsions and further difficulties in process downstream. This problem does not exist in acid-catalyzed transesterification of waste cooking oil.

The main objective of the current study was to evaluate the efficiency of other potential solvents, such as hexane and methanol, as well as water in a liquid-liquid extraction unit for separation of glycerol and biodiesel. In order to accomplish this task, first of all, the reliability of the UNIFAC activity coefficient model to predict the phase equilibria of such systems was evaluated. The technical feasibility of the use of hexane, methanol and water as solvents in a single-stage mixer-settler was then investigated. The biodiesel was produced via acid-catalyzed transesterification of waste cooking oil with methanol and the stream entering the mixer was assumed to be free of unconverted oil and acid catalyst, containing only biodiesel, glycerol and methanol. Furthermore, the biodiesel was assumed to have the properties of methyl oleate, which is the major component of biodiesel made from canola oil and methanol. The ASTM limit for glycerol content of biodiesel (<0.02 wt%), the residence time in the settler, the ratio of the liquid phase volumes in the settler and the biodiesel loss were the major performance measures considered. Four different solvent systems were found suitable: (1) water combined with residual methanol (with optimal mass ratio of biodiesel:methanol:water of 1:0.10:0.97), (2) a mixture of hexane and methanol (with optimal mass ratio of biodiesel:hexane:methanol of 1:1.15:1.62), (3) a mixture of hexane and water combined with residual methanol (with optimal mass ratio of biodiesel:hexane:methanol:water of

1:0.79:0.10:0.69) and (4) a mixture of hexane, methanol and water (with optimal mass ratio of biodiesel:hexane:methanol:water of 1:2.27:0.87:0.30).

In acid-catalyzed production of biodiesel from waste cooking oil and methanol, the units located following the mixer-settler were designed and used in the economic evaluation of the entire biodiesel plant. The technically feasible solvent systems were then optimized based on maximizing the after-tax return on investment as a measure of the annual profitability. Although all the processes showed poor economic potentials with negative annual after-tax return on investment, the relative values were important to compare these processes. The biodiesel plants using hexane and water solvents combined with residual methanol or additional methanol with optimal biodiesel:hexane:methanol:water mass ratio of 1:0.43:0.10:0.24 or 1:2.19:0.90:0.34, respectively, yielded the highest annual after-tax return on investment of -35%. The process using water combined with residual methanol, with optimal mass ratio of biodiesel:methanol:water of 1:0.10:0.86 showed to be the least economically beneficial system, mainly because of its relatively low annual revenue and low total capital investment. In contrast, the process using water combined with residual methanol and the process using a mixture of hexane and water combined with additional methanol yielded the lowest and the highest biodiesel break-even prices of 1.70 and 1.91 $/L, respectively.

Résumé

Le biodiesel est une source d'énergie soutenable écologique qui est maintenant employée comme alternative pour les combustibles fossiles dans le monde entier. Le glycérol est le sous-produit principal du biodiesel produit par l'intermédiaire de la transestérification et doit être enlevé du biodiesel selon la norme ASTM D-6751-02. Cette purification a été habituellement effectuée avec l'extraction liquide-liquide avec de l'eau comme solvant pour le glycérol. La méthode commence de transestérification alcali-catalysée utilise généralement l'huile usée de cuisine, et l'utilisation de grandes quantités seule de l'eau, comme solvant d'extraction, a comme conséquence la formation des savons, puis des émulsions et d'autres difficultés dans le processus en aval. Ce problème n'existe pas dans la transestérification acide-catalysée d'huile usée de cuisine de rebut.

L'objectif principal de cette l'étude était d'évaluer l'efficacité d'autres solvants potentiels, tels que l'hexane et le méthanol, aussi bien que l'eau dans une unité d'extraction liquide-liquide pour la séparation du glycérol et du biodiesel. Afin d'accomplir cette tache, tout d'abord, la fiabilité du modèle de coefficient d'activité d'UNIFAC pour prévoir que les équilibres de phase de tels systèmes a été évalué. La faisabilité technique de l'utilisation de l'hexane, du méthanol et de l'eau comme solvants dans un mélangeur-colonne en une seule étape a été alors étudiée. Le biodiesel a été produit par l'intermédiaire de la transestérification acide-catalysée d'huile usée de cuisine avec du méthanol et on a assumé que le jet entrant dans le mélangeur est exempt de catalyseur acidique et de pétrole nonconverti, contenant seulement le biodiesel, le glycérol et le méthanol. En outre, on a assumé que le biodiesel a les propriétés de l'oléate méthylique, qui est le composant principal du biodiesel fait à partir d'huile de canola et du méthanol. La limite d'ASTM pour la teneur en glycérol du biodiesel (<0.02 wt%), le temps de séjour dans la colonne, le rapport des volumes phasiques liquides dans le colonne et la perte de biodiesel étaient les mesures de performance principales considérées. Quatre systèmes solvants différents ont été trouvés appropriés : (1) l'eau combinée avec du méthanol résiduel (avec le rapport de masse optimal de biodiesel:méthanol:eau de 1:0.10:0.97), (2) un mélange d'hexane et de méthanol (avec le rapport de masse optimal de

biodiesel:hexane:méthanol de 1:1.15:1.62), (3) un mélange de l'hexane et de l'eau combinés avec du méthanol résiduel (avec le rapport de masse optimal de biodiesel:hexane:méthanol:eau de 1:0.79:0.10:0.69) et (4) un mélange d'hexane, de méthanol et d'eau (avec le rapport de masse optimal de biodiesel:hexane:méthanol:eau de 1:2.27:0.87:0.30).

Dans la production acide-catalysée du biodiesel de l'huile usée de cuisine et du méthanol, les unités placées après le mélangeur-colonne ont été conçues et employées dans l'évaluation économique de l'usine entière de biodiesel. Les systèmes solvants techniquement faisables ont été alors optimisés basés sur un maximum de retour après imposition sur l'investissement comme mesure de la rentabilité annuelle. Bien que tous les processus aient montré des potentiels économiques faibles avec le retour après imposition annuel négatif sur l'investissement, les valeurs relatives étaient importantes pour comparer ces processus. Les usines de biodiesel utilisant des solvants d'hexane et d'eau combinés avec le méthanol résiduel ou le méthanol additionnel avec le rapport de masse optimal de biodiesel:hexane:méthanol:eau de 1:0.43:0.10:0.24 ou 1:2.19:0.90:0.34, ont respectivement, rapporté le retour d'investissement après imposition annuel le plus élevé a -35%. Le processus combinant l'eau et le méthanol résiduel, avec le rapport de masse optimal de biodiesel:méthanol:eau de 1:0.10:0.86 a démontré qu'il était le système le moins économique, principalement en raison de son revenu annuel relativement bas et de son investissement réduit en capital total d'équipement. En revanche, le processus utilisant l'eau combinée avec le méthanol résiduel et le processus utilisant un mélange d'hexane et d'eau combinés avec du méthanol additionnel ont rapporté le plus bas et le plus haut biodiesel des prix équilibrés de 1.70 et 1.91 $/L, respectivement.

Acknowledgements

I take this opportunity to express my deep gratitude to everyone who helped me directly or indirectly throughout my master's studies.

Foremost, I would like to acknowledge my supervisors, Dr. Morris Kates and Dr. David D. McLean for giving me the opportunity to pursue this research project. Their encouraging trust, keen supervision and continual support were the great driving force for me to accomplish this work.

I am extremely grateful to Dr. Marc A. Dubé, for financially supporting me during my studies.

I would like to thank the examination committee, Dr. André Y. Tremblay, Dr. Xudong Cao and Dr. Jason Zhang for their great comments that helped me to improve the content of this thesis. Also, thanks to all the professors, fellow graduate students and staff at the Faculty of Chemical Engineering, University of Ottawa for their assistance and support.

I am beholden to my mother, Manijeh (Minoo) Alaghehbandha, for her admirable courage, unbelievable love and thoughtful guidance throughout my entire life. Without her, I would not be who I am.

My special thanks and best wishes to my dear friends at the University of Ottawa, Siamak Lashkari, Shahrzad Hashemi and Forouzan Sadeghi for being always there for me.

Table of Contents

List of Tables

List of Figures

Chapter 1

Introduction

This thesis deals with the development of a solvent extraction process for recovery of commercial grade biodiesel (i.e., fatty acid alkyl esters or FAAE), which specifically involves the separation of the glycerol by-product, resulting from the acid catalyzed transesterification of waste canola oil with methanol.

1.1 Why biofuels?

Nowadays, the impending scarcity of energy resources is one of the main concerns in the world. While just a few countries own huge and of course finite sources of fossil fuels, these fuels make up almost 80% of the total fuel consumed in the world (Lincoln, 2005). Even though Rudolph Diesel in 1885 employed vegetable oil in his newly invented ignition engine, and Henry Ford used biomass-made ethanol to run the 'model T' Ford in 1908, the availability of large sources of fossil fuels at low cost during most of the 20th century postponed serious consideration of renewable sources of energy until World War II, the energy crisis in the United States of America in the 1970's and later on the Gulf war in 1991 (yokAyo biofuels, 2006). Depletion of fossil fuel resources and the continually increasing demands for energy have led to an unstable market for such fuels (Lincoln, 2005). Furthermore, environmental degradation, caused by unrestricted consumption of fossil fuels, has raised serious questions about the use of these fuels (Koonin, 2006). Hence, finding renewable, sustainable and environmentally friendly sources of energy has become a vital task for governments, research institutes and industries. As a potential alternative to fossil fuels, renewable biofuels, particularly vegetable oil-based biodiesel and ethanol have been investigated widely during the last few decades (Fukuda et al., 2001; Ma and Hanna, 1999; Meher et al., 2006).

1.2 Why biodiesel?

In order to be considered a practical alternative for fossil fuels, biofuels, despite their renewability, should be evaluated to determine whether they are "technically feasible, economically competitive, environmentally reasonable and readily available" (Srivastava and Prasad, 2000).

Although there have been significant investments in hydrogen and ethanol as biofuels, technical difficulties associated with the production and storage of hydrogen and the lower energy generation per unit mass of ethanol compared to fossil fuels are the major drawbacks to their extensive production and use (Fernando and Jha, 2006). Almost all the requirements for an efficient substitute for petroleum-based diesel are satisfied by biodiesel (Encinar et al., 2005), which is a liquid biofuel made from vegetable oil or animal fat. Compared to petrodiesel, biodiesel has remarkable environmental benefits, such as lower emissions of CO and CO_2, zero sulfur content and therefore, less GHG environmental impact (Ali and Hanna, 1994; Fernando and Jha, 2006). The use of biodiesel will greatly reduce the dependency on foreign oil products and will support the agricultural sector by increasing the demand for "energy crops" (Koonin, 2006), such as canola, rapeseed and soybean. Moreover, the recent increase in the price of petroleum products may also result in a greater motivation for industrial-scale production, use and commercialization of biodiesel worldwide.

In spite of all the positive features of biodiesel, the major disadvantage that makes it less popular compared to petroleum-based diesel, is its higher cost (Environment Canada, 2006). For instance, biodiesel made in the U.S. sells at $1.28 per liter in Canada, while the price of petrodiesel is around $1.00 per liter (Blondeau et al., 2006). The higher cost of biodiesel is largely due to the cost of virgin vegetable oil feedstock. Employing waste cooking oil or non-edible oil as the raw material as well as process improvements and providing government tax credits are some of the practical solutions to lowering the cost of biodiesel (Al-Widyan and Al-Shyoukh, 2002; Bender, 1999; Canakci, 2007; Demirbas

and Karslioglu, 2007; Encinar et al., 2005; Felizardo et al., 2006; Haas et al., 2006; Korus et al., 1993; Zhang et al., 2003a,b; Zheng, 2003).

Biodiesel plants were first started in South Africa in 1981 and in Austria and New Zealand in 1982. Since then, biodiesel production and processing plants have been developed in different parts of the world, but mostly in Europe, North America and recently Asia. The amount of biodiesel sold in the U.S. has increased dramatically from 500,000 gallons in 1999 to 75 million gallons in 2005 (Canadian Renewable Fuels Association, 2006).

In Canada, 385 million liters of biodiesel was produced in the year 2005. This amount was only 2% of the total petroleum-based diesel consumed in Canada. BIOX, Milligan and Rothsay are three major biodiesel producers in Canada. Development in their production facilities by end of the year 2006 led to biodiesel that could supply the Canadian biodiesel market (Canadian Renewable Fuels Association, 2006).

1.3 Biodiesel production via transesterification

Biodiesel is commonly produced through transesterification (i.e., alcoholysis) of vegetable oils or animal fats (triglycerides) in the presence of an acid, alkali or enzyme catalyst. Briefly, transesterification is a catalyzed, reversible and equilibrium reaction of triglycerides with an alcohol (usually methanol or ethanol), in which one alcohol (e.g. methanol) replaces another one (e.g., glycerol) from an ester. The following reaction displays the transesterification of triglyceride and methanol.

$$\begin{array}{l} \begin{array}{lll} O & O & O \\ \| & \| & \| \\ R-C & C-R & C-R \\ | & | & | \\ O & O & O \\ | & | & | \end{array} \\ CH_2-CH-CH_2 + 3CH_3-OH \underset{\longleftarrow}{\xrightarrow{\text{catalyst}}} 3CH_3-O-\overset{\overset{O}{\|}}{C}-R + C_3H_5(OH)_3 \end{array} \qquad (1.1)$$

triglyceride + alcohol $\underset{\longleftarrow}{\xrightarrow{\text{catalyst}}}$ fatty acid methyl ester (FAME) + glycerol

Because of the reversible nature of this reaction, it can be forced to completion by using a large excess of alcohol (Encinar et al., 2005; Zhang et al., 2003a; Zheng et al, 2006).

The major by-product of transesterification is glycerol, which according to the ASTM Standard for biodiesel (ASTM D-6751-02, 2002), should be almost completely removed from biodiesel. Purification of biodiesel after the transesterification reaction so that it contains less than 0.02 %wt glycerol is required to meet this standard and is the main area of interest of the present work.

1.4 Biodiesel purification

While washing the reaction mixture with water has been the most common technique to separate impurities from biodiesel (Al-Widyan and Al-Shyoukh, 2002; Encinar et al., 2005; Karaosmanoglu et al., 1996), Nye et al. (1983), employed hexane as the solvent to separate biodiesel after transesterification of waste frying oil. Although hexane is not a cheap solvent and due to its flammability, there must be special safety considerations in the plant, it has been commonly used as a solvent for lipids in oilseed extraction processes since the 1930s (Mirghani and Che Man, 2003; Wan, 1997; Arnold and Juhl, 1954). Hexane dissolves biodiesel very well and, because of its relatively low normal boiling point (69°C), can be readily distilled off in biodiesel purification. It also reduces the density and viscosity of the biodiesel-rich stream, which enhances the phase separations. For alkali-catalyzed process of waste cooking oil, the presence of hexane was speculated to reduce the formation of emulsions (Zhang et al., 2003a).

Using HYSYS^{TM} simulation software, Zhang et al. (2003a,b) performed a thorough technical and economic assessment of four different biodiesel processing plants including biodiesel production by acid-catalyzed transesterification of waste frying oil and its purification by hexane/methanol/water extraction process. Moreover, in the studies of Dubé et al. (2004), McBride (1999) and Zheng et al. (2006), hexane and methanol/water solvents were used to purify biodiesel experimentally. This idea has been further investigated in the present study. The greatly different solubilities of biodiesel and

glycerol in hexane and methanol/water, respectively, suggest an effective method for separating glycerol and biodiesel. Because of the considerably lower miscibility of water in hexane, the presence of water results in improved separation of the hexane/FAME and methanol/glycerol/water phases (McBride, 1999; Zhang et al., 2003a). This liquid-liquid partitioning process was carried out at normal room temperature and atmospheric pressure.

1.5 Thesis objectives

The objectives of this thesis were:

1. To determine the phase equilibria for systems consisting of various mixtures of biodiesel or methyl oleate, glycerol, hexane, methanol and water at room temperature and atmospheric pressure. Due to the difficulties encountered during experimental analyses of this 5-component system, as the first step, the quaternary system of methyl oleate, glycerol, hexane and methanol was investigated. To accomplish this task, thermodynamic activity coefficient models (i.e., UNIFAC and Modified UNIFAC) were employed to investigate and predict the phase equilibria of such multicomponent system. To validate the model predictions, experimental measurements were taken to allow actual phase compositions to be determined.

2. To evaluate and optimize the technical performance of potential solvents individually or mixed together using a single-stage mixer-settler extraction system. This evaluation was based on various technical performance criteria to achieve optimal operation of the mixer-settler unit as well as to obtain biodiesel that met the relevant ASTM Standard for glycerol content. Quantity or compositions of the single or mixed solvents were then adjusted to obtain optimal values of the performance criteria.

3. To design and determine economically optimal solvent systems. This design has been carried out by adjusting the compositions of the technically feasible solvents to achieve maximum achievable economic profitability of the proposed biodiesel plants. To complete this task, annual after-tax return on investment was implemented as the measure of the economic profitability.

1.6 Thesis outline

This thesis continues with Chapter 2, which deals with the literature review and background of the biodiesel processing focusing on the available biodiesel purification techniques. Chapter 3 (Paper 1) deals with the study of the liquid-liquid equilibria of the quaternary system methyl oleate (biodiesel), glycerol, hexane and methanol at room temperature and atmospheric pressure. In Chapter 4 (Papers 2 & 3), the technical assessment and optimization of a single-stage mixer-settler system with hexane, methanol and/or water solvents are presented. The economic assessment and optimization of biodiesel processing plants with different solvents in a single-stage mixer-settler, used as the liquid-liquid extraction unit to separate glycerol and biodiesel is dealt with, in Chapter 5 (Paper 4). In the final chapter (Chapter 6), the conclusions and contributions of this study to the current knowledge of biodiesel purification and also the recommendations for the future work in this field are presented.

References

Arnold, L. K. and Juhl, W. G., "Solvent Extraction of Cottonseed Meats," J. Am. Oil Chem. Soc., 31(12), 613-618 (1954).

ASTM D-6751-02, Standard Specification for Biodiesel Fuel (B100) Blend Stock for Distillate Fuels, Designation D-6751-02, American Society for Testing and Materials, West Conshohocken, PA (2002).

Ali, Y. and Hanna, M. A., "Alternative Diesel Fuels from Vegetable Oils," Bioresource Technology, 50, 153-163 (1994).

Blondeau, J., Pon, G., Bresciani, S and Reaney M., Agriculture and Agri-Food Canada, "Analysis of Selected Diesel Fuel Markets in Canada: Markets for Canola Biodiesel-Executive Summary," http://res2.agr.ca, (May, 2006).

Bender, M., "Economic Feasibility Review for Community-Scale Farmer Cooperatives for Biodiesel," Bioresource Technology, 70, 81-87 (1999).

Canadian Renewable Fuels Association, "Biodiesel around the World," http://www.greenfuels.org (May, 2006).

Canakci, M., "The Potential of Restaurant Waste Lipids as Biodiesel Feedstocks," Bioresource Technology, 98, 183-190 (2007).

Dubé, M. A., Zheng, S., McLean, D. D. and Kates, M., "A Comparison of ATR-FTIR Spectroscopy and GPC for Monitoring Biodiesel Production," J. Am. Oil Chem. Soc., 81, 599-603 (2004).

Encinar, J. M., Gonzalez, J. F. and Rodriguez-Reinares, A., "Biodiesel from Used Frying Oil: Variables Affecting the Yields and Characteristics of the Biodiesel," Ind. Eng. Chem. Res, 44, 5491-5499 (2005).

Environment Canada, "A Critical Review of Biodiesel as a Transportation Fuel in Canada: Summary of Major Biodiesel Issues and Recommendations," http://www.ec.gc.ca (May, 2006).

Fernando, S., Hall, C. and Jha, S., "NO_x Reduction from Biodiesel Fuels," Energy & Fuels, 20, 376-382 (2006).

Felizardo, P., Correia, M. J. N., Raposo, I., Mendes, J. F., Berkemeier, R. and Bardado, J. M., "Production of biodiesel from waste frying oil," Waste Management, 26, 487-494 (2006).

Fukuda, H., Kondo, A. and Noda, H., "Biodiesel Fuel Production by Transesterification of Oils," Journal of Bioscience and Bioengineering, 92(5), 405-416 (2001).

Haas, M. J., McAloon, A. J., Yee, W. C. and Foglia T. A., "A Process Model to Estimate Biodiesel Production Costs," Bioresource Technology, 97, 671-678 (2006).

Koonin, S. E., "Getting Serious about Biofuels," Science Magazine, 311, 435 (2006).

Lincoln, S. F., "Fossil Fuels in the 21st Century," Ambio. 34(8), 621-627 (2005).

Ma, F. and Hanna, M. A., "Biodiesel Production: A Review," Bioresource Technology, 70, 1-15 (1999).

McBride, N., "Modeling the Production of Biodiesel from Waste Frying Oil," B. A. Sc. Thesis, 1999, Department of Chemical Engineering, University of Ottawa.

Meher L. C., Sagar, V. and Naik, S. N., "Technical Aspects of Biodiesel Production by Transesterification-A Review," Renewable & Sustainable Energy Reviews, 10, 248-268 (2006).

Mirghani, M. E. S. and Che Man Y. B., "Determination of Hexane Residues in Vegetable Oils with FTIR Spectroscopy," J. Am. Oil Chem. Soc., 80(7), 619-623 (2003).

Nye, M. J., Williamson, T. W., Deshpande, S., Schrader, J. H. and Snively, W. H., "Conversion of Used Frying Oil to Diesel Fuel by Transesterification: Preliminary Tests," J. Am. Oil Soc. Chem. 60(8), 1598-1601 (1983).

Srivastava, A. and Prasad, R., "Triglycerides-Based Diesel Fuels," Renewable Sustainable Energy Rev., 4, 111-133 (2000).

Wan, P.J., Hydrocarbon Solvents, in Technology and Solvents for Extracting Oilseeds and Nonpetroleum Oils, edited by P.J. Wan and P.J. Wakelyn, AOCS Press, Champaign, pp. 170–185 (1997).

yokAyo biofuels, "A History of Biodiesel," http://www.ybiofuels.org (May, 2006).

Zhang, Y., Dubé, M. A., McLean, D. D. and Kates, M., "Biodiesel Production from Waste Cooking Oil: 1. Process design and technological assessment," Bioresource Technology, 89, 1-16 (2003a).

Zhang, Y., Dubé, M. A., McLean, D. D. and Kates, M., "Biodiesel Production from Waste Cooking Oil: 2. Economic Assessment and Sensitivity Analysis," Bioresource Technology, 90, 229-240 (2003b).

Zheng, S., "Biodiesel Production from Waste Frying Oil: Conversion Monitoring and Modeling," M. A. Sc. Thesis, 2003, Department of Chemical Engineering, University of Ottawa.

Zheng, S., Kates, M., Dubé, M. A. and McLean, D. D., "Acid Catalyzed Production of Biodiesel from Waste Frying oil," Biomass and Bioenergy, 30, 267-272 (2006).

Chapter 2

Literature Review and Background

In this chapter, the notable advantages of biodiesel and its production techniques are reviewed briefly. Then a critical review of previous studies about biodiesel purification methods either as laboratory-scale experiments or process simulations is presented. Finally, the limitations of the available science and technology of biodiesel purification, which led to the objectives of the current research project, are addressed.

2.1 Biodiesel

Biodiesel is an environmentally friendly, nontoxic and biodegradable fuel. When using pure biodiesel (i.e., B100) or its mixture with petrodiesel (e.g., B20), there are considerably lower emissions of sulfur, carbon monoxide, carbon dioxide, solid particulates, unburned hydrocarbons and volatile organic compounds compared to the petroleum-based fuels (Ali and Hanna, 1994; Canakci, 2007a; Dorado et al., 2003; Fernando et al., 2006; Nabi et al., 2006; Ulusoy et al., 2004; Wang et al., 2000). Some researchers have also shown a significant reduction in the NO_x emissions by using pure biodiesel or its blend with petroleum-based fuels (Dorado et al., 2003; Kalam and Masjuki, 2002; Lin and Huang, 2003). In addition, using biodiesel instead of fossil fuels reduces the output of atmospheric green house gases and the chance of acid rain (Dorado, 2003; Fernando et al., 2006; Health Canada, 2006). Because the carbon molecules in biomass-made biofuels (e.g., fatty acid alkyl esters or ethanol) are biogenic and easily biodegradable, biodiesel and ethanol are considered to be biodegradable fuels (Holbein et al. 2004). It is also reported that other than a small portion of waste cooking oil that is reused as animal food, the rest is mostly discharged into the sewage system and enters the food chain (Buczek and Czepirski, 2004; Cvengros and Cvengrosova, 2004); while biodiesel industry is an excellent consumer of large quantities of waste cooking oil (Encinar, 2005; Kulkarni et al., 2006).

Since the global oil and gas market has been unstable during the last few decades, the ability to produce some of its energy needs would lead to a reduced dependency on foreign fuel products and thus to a more stable economy (McKillop, 2005). Moreover, since the raw material for biodiesel production is derived from domestically grown crops or animal fat, the agricultural sectors will be maintained and supported due to an increase in the demand for oil seed crops by the biodiesel industry (Bender, 1999; Koonin, 2006). Based on a study by the U.S. department of agriculture, developments in biodiesel industry result in an increase of $300 million in the average net income of crop farms annually by 2010 (National Biodiesel Board, 2006).

Another positive feature of biodiesel is its compatibility with compression-ignition engines without the need for any major modification in the engine (Agarwal and Das, 2001; Canakci, 2007a; Lang et al., 2001; Monyem and Van Gerpen, 2001; Ulusoy, 2004). Compared to petroleum diesel fuels, biodiesel has a higher flash point, which makes it safer and easier to transport and store. Biodiesel also improves the lubricity of the fuel when mixed with petroleum diesel and extends the engine life (Geller and Goodrum, 2004; Hertz, 2006; yokAyo biofuels, 2006). Compared to the ordinary petroleum-based diesel oil for mobile engine applications, biodiesel has no aromatic hydrocarbons and contains more than 10 wt% oxygen, which makes it easier to combust (Demirbas, 2005; Ulusoy, 2004). Moreover, in terms of energy savings, 0.85 kg of crude petroleum oil is saved per kilogram of biodiesel produced (Korbitz, 1999).

Despite all these benefits, poor cold flow properties and lubricity of the biodiesel made from the oils with high content of saturated fats (e.g. animal fat) is a major technical drawback (Kulkarni et al., 2006; Kulkarni and Dalai, 2006). This problem can be solved by employing vegetable oils (e.g. canola oil) as the biodiesel feedstock (Chiu et al, 2004; Coleman, 2006) or adding specific compounds to prevent gelation and viscosity increase at severely cold temperatures (Huang and Wilson, 2000).

2.2 Biodiesel production via transesterification

Due to the growing demand for large scale production of biodiesel during the last few decades, the number of studies on the production of biodiesel, particularly via transesterification reaction, has increased. There have been two major areas of interest for most of such studies: (a) to investigate the mechanism and kinetics of transesterification, especially the alkali- or acid-catalyzed reactions, through a series of bench-scale experiments; and (b) to analyze the effect of different factors, such as reaction temperature and the quantities of the reactants, on the reaction performance experimentally, followed by the optimization of these operating conditions to achieve the highest yield of fatty acid alkyl esters (i.e., biodiesel). Some studies have also recently dealt with the technological and economical evaluation of the biodiesel production and processing in large scale industrial plants.

As early as the 1940's, efforts to produce biodiesel via transesterification were summarized in a series of patents (e.g. Allen et al., 1945; Bradshaw and Meuly, 1944; Trent, 1945) (See Ma and Hanna, 1999 for more specific details).

Freedman et al. (1984, 1986), investigated the effect of different variables on the kinetics of transesterification reaction and explained its mechanism. In their first publication, the effect of the type of catalyst, initial molar ratio of alcohol to oil, reaction temperature and the quality of the oil feedstock on the yield of biodiesel were studied. The optimal operating conditions for both acid and base catalyzed transesterification reactions to achieve the highest yield of biodiesel were determined experimentally. When an alkaline catalyst was employed (e.g., sodium methoxide or sodium hydroxide), a 6:1 molar ratio of methanol, ethanol or butanol to the refined vegetable oil at 60°C resulted in a complete conversion of oil to fatty acid alkyl esters in 1 hour. With respect to the acid-catalyzed transesterification, temperature had a more significant effect than the type of alcohol on the reaction rate, in order to reach the highest conversion of virgin vegetable oil to esters. With 1% sulphuric acid and increased molar ratio of alcohol to oil of 30:1, high conversion of ~100% was observed at the temperature of 65°C after 69 hours

(Freedman et al., 1984). It was also reported that under identical reaction conditions, alkali-catalyzed transesterification proceeds much faster than acid-catalyzed reaction; however, formation of "gums and extraneous materials" during the alkali-catalyzed reaction was the major technical difficulty encountered.

The second study of Freedman et al. (1986) concentrated on the reaction kinetics and the mechanism of butanolysis and methanolysis of virgin soybean oil in the presence of an alkali (sodium butoxide) or an acid (sulphuric acid) at different temperatures. According to the experimental time-course data obtained, they confirmed the hypothesis of occurrence of a series of consecutive forward and reverse reactions during the transesterification. The mechanism of the transesterification was based on conversion of triglycerides to diglycerides, then diglycerides to monoglycerides and finally monoglycerides to glycerol, with the liberation, in each step, of a fatty acid alkyl ester. The authors also concluded that the forward reaction could be a pseudo-first order or sometimes second order, depending on the ratio of the alcohol to oil, type of catalyst and reaction temperature, but the reverse reaction was definitely a second order reaction.

While Freedman et al. (1986) pointed out the possibility of a "shunt" reaction, which was defined as the simultaneous reaction of three moles of alcohol and one mole of triglyceride to create fatty acid alkyl esters during transesterification under specific reaction conditions, Boocock et al. (1996, 1998) discussed the unlikelihood of such reactions. The latter authors also improved the methanolysis of virgin vegetable oil by adding a suitable co-solvent. They claimed that due to the low solubility of methanol in oil, the reactants form two phases and transesterification takes place mostly in the methanol-rich phase. The slow rate of reaction is thus the direct result of the relatively low concentration of oil in the methanol-rich phase. Using THF (i.e., tetrahydrofuran) as a suitable co-solvent in alkali-catalyzed transesterification, they achieved a fatty acid methyl ester yield of 95 wt% after 20 minutes at ambient temperature of 23°C, methanol to oil molar ratio of 6:1 and methanol to THF volume ratio of 1.25:1.

Using roughly the same operating conditions as Freedman et al., (1986), Noureddini and Zhu (1997), studied the effect of mixing and reaction temperature on the kinetics of alkali-catalyzed transesterification of soybean oil with methanol. Experimentally, they investigated the effect of mixing only on the slow initial mass transfer controlling stage of the reaction. The kinetically controlling fast period of the reaction and the final slow equilibrium controlling step were not influenced by mixing significantly. At the beginning, the reaction mixture formed two phases making the reaction highly diffusion resistant. However, after some time, due to the creation of fatty acid methyl esters, which also acted as solvent, there was only a single phase present. Hence, mixing reduced the mass transfer resistance period at the initial stages of the reaction. In terms of the impact of temperature on the reaction rate, the time interval associated with the mass transfer controlling step was reduced as the reaction temperature was increased. The "shunt reaction" theory of Freedman et al. (1986) was also rejected in their paper.

Ma and Hanna (1999) reviewed several methods of biodiesel production. The variables affecting the rate of transesterification reaction and its mechanism studied by the authors were the molar ratio of methanol to oil, reaction temperature, reaction time, type of catalyst and quality of the initial oil feedstock. Concerning the commercial production of biodiesel, the acid-catalyzed transesterification of waste cooking oil was recommended to be more economically beneficial, due to the lower price of waste cooking oil compared to that of virgin vegetable oil. They also suggested the use of a continuous, high capacity transesterification process with short reaction time. In addition, the recovery of high quality glycerol by-product resulted in the process becoming economically more attractive.

In a review paper by Fukuda et al. (2001), several unconventional, methods of biodiesel production such as lipase enzymatic-transesterification of vegetable oil, transesterification in presence of supercritical alcohol and acid-catalyzed transesterification were discussed. With respect to the latter, they mentioned the possibility of an "*in situ*" transesterification. In such system, the transesterification proceeds as a result of the contact of oil-bearing material with acidified alcohols. Because

the alcohol acts as an extraction solvent and esterification reagent at the same time, both transesterification of oil and separation of the biodiesel product from the reactants happen concurrently. They also stressed the significantly high yield of purified biodiesel obtained through this technique.

Recently, Demirbas and Karsioglu (2007) and Marchetti et al. (2007) have reviewed the available biodiesel production techniques, such as alkali, acid or enzyme-catalyzed reactions or the reaction in presence of supercritical methanol without any need to any type of catalyst. While the first paper reviews in details the kinetics of transesterification via each method with the corresponding rate expressions, the latter paper represents an overview of the parameters affecting transesterification, the biodiesel fuel properties and the current economy of biodiesel. The reaction in presence of supercritical methanol, which led to a conversion of 95% of triglycerides to methyl esters after 10 minutes (Demirbas and Karsioglu, 2007), was considered as a potential method to produce biodiesel.

Freedman et al. (1984) were not the first researchers who mentioned the sensitivity of the alkali-catalyzed transesterification to the quality of the initial oil. High content of free fatty acids and moisture of the oil feedstock notably reduces the yield of biodiesel and negatively impacts the ease of the separation of glycerol from biodiesel, as studied by Bradshaw and Meuly (1944), Feuge et al. (1949), Liu (1994), Ma et al. (1998), Meher et al. (2006) and Wright et al. (1944). Based on their findings about the alkali-catalyzed transesterification of waste cooking oil, the presence of a high quantity of free fatty acids and alkali leads to formation of soaps and water, which further results in formation of emulsions and increase in the viscosity of the reaction mixture. In the industrial scale production of biodiesel from non-edible oils by this method, an increase in the viscosity of the reaction mixture and emulsions results in serious difficulties in the process downstream (mainly glycerol separation step) and high losses of biodiesel (Canakci and Van Gerpen, 1999). Hence, usually a pre or post-treatment step must be designed to either convert the free fatty acids to alkyl esters before the main reaction or to separate the soaps after the reaction and prior to the separation units (Canakci and Van Gerpen,

1999; Canakci and Van Gerpen, 2001; Encinar et al., 2005; Freedman et al., 1984; Felizardo et al., 2006; Supple et al., 2002). Another solution to the problem of free fatty acids is to conduct the transesterification at considerably high pressure and temperature (Kreutzer, 1984), which is usually very costly and less practical.

The main advantage of alkali-catalyzed transesterification, which is the rapid rate of reaction, is weakened by its sensitivity to the presence of free fatty acids and moisture in the reactants. In the next section, the available technologies of the synthesis of biodiesel from waste cooking oil, which has relatively high content of free fatty acid and moisture, but considerably lower price compared to virgin vegetable oil, will be reviewed.

2.3 Biodiesel from waste cooking oil

The use of waste frying oil and non-edible seed oil as biodiesel feedstock has been suggested because of their significantly lower cost compared to virgin vegetable oil and the significant reduction in the total production cost of biodiesel (Al-Widyan and Al-Shyoukh, 2002; Canakci, 2007b; Demirbas and Karslioglu, 2007; Encinar et al., 2005; Felizardo et al., 2006; Haas et al., 2006; Korus et al., 1993; Zhang et al., 2003). However, the amount of free fatty acids and moisture in waste frying oil is relatively high and because of the issues mentioned previously (formation of soap and their conversion to emulsions), a pre or post-treatment step is needed in the alkali-catalyzed transesterification of such oils (Canakci, 2007b; Canakci and VanGerpen, 2001; Encinar et al., 2005; Felizardo et al., 2006).

To avoid the high expenses of high pressure operations or the treatment steps, it has been suggested to employ either an acid-catalyzed or an enzymatic process, both insensitive to the presence of free fatty acids in the reactants (Al-Widyan and Al-Shyoukh, 2002; Freedman et al., 1984; Fukuda et al., 2001; Keim, 1945; Zhang et al., 2003a,b; Zheng et al., 2006). The high price of the lipase catalyst and its much slower rate of reaction make it a less favourable choice and its commercial use in biodiesel production requires further research (Fukuda, 2001; Nelson et al., 1996; Watanabe et al.,

2001). The acid-catalyzed process is a potentially simple solution to the problems encountered during the alkali-catalyzed transesterification of waste cooking oil.

Using waste frying oil in presence of acid or base catalysts, Nye et al. (1983) studied the effect of temperature and type of alcohol on the yield of transesterification reaction. At 50°C and in presence of 0.4% potassium hydroxide, methanol and at 105°C and in presence of 0.1% concentrated sulphuric acid, butanol, 1-propanol and ethanol gave the highest yield of biodiesel after 24 and 40 hours, respectively. In addition, a yield of 78.1% was obtained by acid-catalyzed transesterification using butanol which was close to the yield of 79.3% obtained through base-catalyzed transesterification of waste cooking oil with methanol. Their study was one of the primary researches dealing with the use of acid catalyst in transesterification; although limited to some laboratory-scale experiments, this work was one of the motivating studies in this field.

Following the work of Nye et al. (1983), other research groups, for example Freedman et al. (1984 and 1986) considered the use of acid catalysts in transesterification of waste cooking oil as was reviewed above.

Regarding the acid-catalyzed transesterification of waste cooking oil, Ripmeester (1998) conducted a series of bench-scale experiments to study the kinetics of transesterification and finding the operating conditions that led to the highest yield of biodiesel. When the molar ratio of methanol:H_2SO_4:oil of 245:4:1 was used, a complete conversion of oil to fatty acid methyl esters was reached in 3 hours at temperature and pressure of 70°C and ~12 psig, respectively.

Following the work of Ripmeester (1998), McBride (1999) investigated the kinetics of transesterification of waste canola oil with an acid catalyst and found a strong dependency of the reaction rate on the initial molar ratio of methanol to oil. A nearly 100% conversion was achieved after 3½ hours for a minimum molar ratio of methanol:oil of 50:1, at 70°C and 170-180 kPa. Linear models were developed to predict the time to reach half conversion of oil to fatty acid methyl ester as well as the overall reaction rate.

However, it was mentioned that a more detailed experimental study would improve the reliability of the suggested models.

Canakci and Van Gerpen (1999) studied the biodiesel production via transesterification of waste frying oil with methanol using sulphuric acid, as catalyst. They observed that increasing the molar ratio of alcohol to vegetable oil, temperature, quantity of catalyst and reaction time would increase the yield of biodiesel. In contrast, an increase in water content or amount of free fatty acids in the oil above 0.5% and 5%, respectively, decreased the biodiesel yield below 90%.

Al-Widyan and Al-Shyoukh (2002), compared the reaction performance of alkali and acid catalysts in transesterification of waste palm oil with ethanol. Utilizing HCL or H_2SO_4 as catalysts, they could experimentally eliminate the formation of soaps during transesterification. In this reaction, the conversion of oil to esters in ethanolysis of waste palm oil with sulfuric acid was similar to the equivalent alkali-catalyzed reaction. Without mentioning the effect of temperature on the reaction rate of acid-catalyzed transesterification, the authors concluded that the reaction time required to achieve a certain conversion could be reduced by either increasing the catalyst concentration or the molar ratio of alcohol to oil.

In another study on this topic, Zullaikah et al. (2005) examined a two-stage acid-catalyzed transesterification with methanol in order to get high conversion of rice bran oil to fatty acid alkyl esters. Rice bran oil is an inexpensive raw material that contains high amounts of free fatty acids and is produced as a co-product of rice milling. In the first stage, at 60°C and atmospheric pressure, 55 to 90% FAME was obtained in 2 hours. The second stage is basically the reaction of the organic phase remaining from the first step with methanol at 100°C and atmospheric pressure to achieve a yield of 98^{+}% of FAME in less than 8 hours.

Zheng et al. (2006) studied the effect of feed composition (the ratio of oil:methanol:catalyst), reaction temperature and rate of mixing on the reaction kinetics

and biodiesel yield of the acid-catalyzed methanolysis of waste canola oil. They achieved a yield of 99^{+}% of biodiesel in a one-step reaction at 80°C and methanol:oil:acid molar ratio of 245:1:3.8 after 4 hours. They concluded that to achieve high yield of biodiesel, any decrease in the temperature and pressure of the reaction should be compensated by increasing the amount of input alcohol or concentration of the acid catalyst.

Lotero et al. (2005), reported on the effectiveness of two types of acid catalysts, liquid (i.e., homogeneous catalyst) and solid (i.e., heterogeneous catalyst), re-stating the success of acid-catalyzed process in both transesterification of fatty acids and esterification of free fatty acids. With liquid catalysts, such as sulphuric acid and hydrofluoric acid, which have been more commonly used than solid catalysts, the reaction rate is more dependent on temperature and also the rate of reaction is 4000 times slower than the reaction rate with a homogeneous alkali catalyst. They mentioned the hesitant belief regarding the use of solid catalysts due to the presupposed even lower reaction rates than the liquid catalysts and undesirable side reactions. Although not experimentally verified, the authors speculate that solid acid catalysts contain large interconnected pores and strong acid sites, which are favourable in both transesterification and esterification reaction. In addition, the solid catalysts do not cause any contamination and environmental problems and are easier to be removed from the biodiesel product.

Recently, Kulkarni and Dalai (2006) provided a complete review of several biodiesel production techniques from waste cooking oil. The techniques re-analyzed in their paper were acid-, alkali-, enzyme-catalyzed and catalyst-free transesterification in presence of supercritical fluids. The authors concluded that due to the positive and negative features of each method, there is a need for a careful economical and technological study before starting a new biodiesel plant.

2.4 Overall technical and economic assessment of biodiesel plants

Regarding the biodiesel production via acid or alkali-catalyzed transesterification of virgin vegetable oil or waste cooking oil, other than the patents, there have only been a few articles focusing on the technical and economic assessment of biodiesel processing plants.

Nelson et al. (1994) assessed the economics of a biodiesel plant with alkali-catalyzed transesterification of low or high quality feedstocks. They found a biodiesel break-even price range of 0.96$/gallon for cheap raw material to 3.39 $/gallon for more expensive raw material. The cost of feedstock was determined to be the most significant factor in the final price of biodiesel, while plant size and glycerine by-product value were of secondary concern.

Bender (1999) stated that biodiesel production with animal fat as feedstock is not economically feasible and more research and technological development is required to advance it. A biodiesel plant with capacity of 10,560 tonne per year with biodiesel break-even price of 420 $/tonne and $3.12 million was under investigation. In order to make biodiesel a more competent fuel, the author recommended providing the farmers with government subsidies, which would allow them to produce biodiesel crops without paying extra money to buy the protein meal.

On the same subject, Noordam and Withers (1996) studied the economic feasibility of a 7600 tonne per year biodiesel production plant carried out by alkali-catalyzed transesterification of canola oil. They found that the final price of biodiesel is much more affected by the cost of raw material (virgin vegetable oil) than the glycerine value and reported a break-even price of 763 $/tonne for biodiesel. Although their study was one of the first approaches in economic assessment of such a biodiesel process, in calculation of the total production cost, they did not take into account some of the expenses, nor did they exactly address the basis of their economic evaluations.

Van Gerpen (2005) recently reviewed some of the previous technical studies about the commercial biodiesel processes in the U.S. He reiterated that alkali-catalyzed transesterification has been favoured due to its high rate of reaction; although pre-processing is essential to deal with the free fatty acids and moisture in the feedstock. The suggested block flow diagram of the entire plant, which is based on the alkali-catalyzed reaction of virgin vegetable oil, is shown in Figure 2.1. This process consists of three major steps utilized in most biodiesel plants: (1) production of biodiesel, (2) separation of impurities from biodiesel and (3) purification of the glycerol by-product. He mentioned the possibility of a continuous process employing two CSTR reactors in series to increase the performance of the reaction significantly. 80% of the raw material reacted in the first step and the remainder was converted to FAME in the second step.

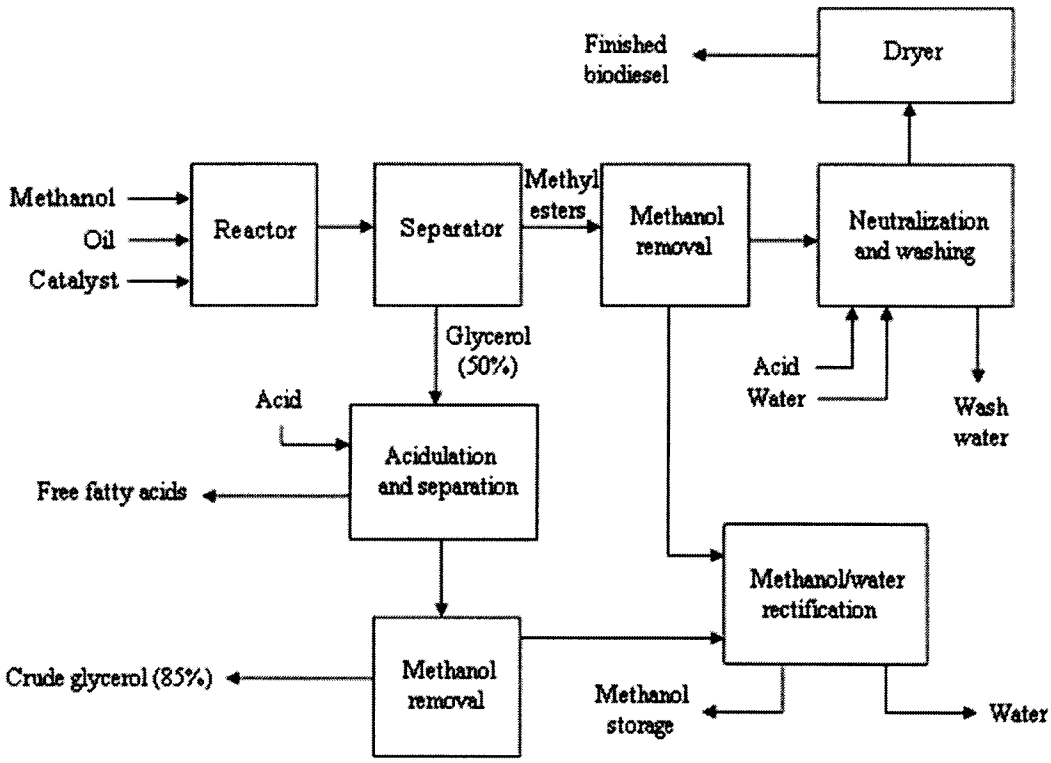

Figure 2.1 An archetypal block flow diagram for biodiesel processing, Van Gerpen (2005)

Meher et al. (2006) reviewed the technical aspects of a biodiesel processing plant. In their work, various operating variables involved in the transesterification, different

analytical methods to detect reactants and products (fatty acid alkyl esters, glycerol, di- and tri- and mono-glycerides, alcohol, catalyst) and the properties of the final biodiesel product were studied. Even though the biodiesel production step is discussed in detail, the paper does not deal with the processes after the reaction, such as purification of biodiesel and the by-products.

Using ASPEN PLUS^{TM} (2001) Process Simulation Software, Haas at al. (2006) developed a process model to estimate the biodiesel production costs. The authors emphasized the flexibility of their cost model with respect to the feedstock, price of glycerol as the by-product, process technology and equipment. Yet, later in the paper the authors declared the failure of their model to predict the production costs of biodiesel when waste cooking oil was the feedstock. Figure 2.2 shows the process flow diagram, they used in the cost estimation of the biodiesel production process. The entire proposed process can be divided into three major parts: (1) transesterification of vegetable oil, (2) biodiesel purification and (3) glycerol recovery. For a plant capacity of 10^7 gallons of biodiesel per year by alkali-catalyzed transesterification of virgin soybean oil and methanol at 60°C in two reactors (ESTER 1 and 2, Figure 2.2) with overall conversion of 90% of oil to fatty acid methyl esters, the total calculated capital and gross operating cost were $11,350,000 and $20,041,000, respectively. The purification stage of biodiesel in this plant consists of a water-washing step, centrifugation to separate the aqueous phase and then drying under vacuum (Figure 2.2). Linear relationships between the biodiesel production cost and feedstock cost and also a linear relationship between the biodiesel production cost and the value of purified glycerol by-product was reported.

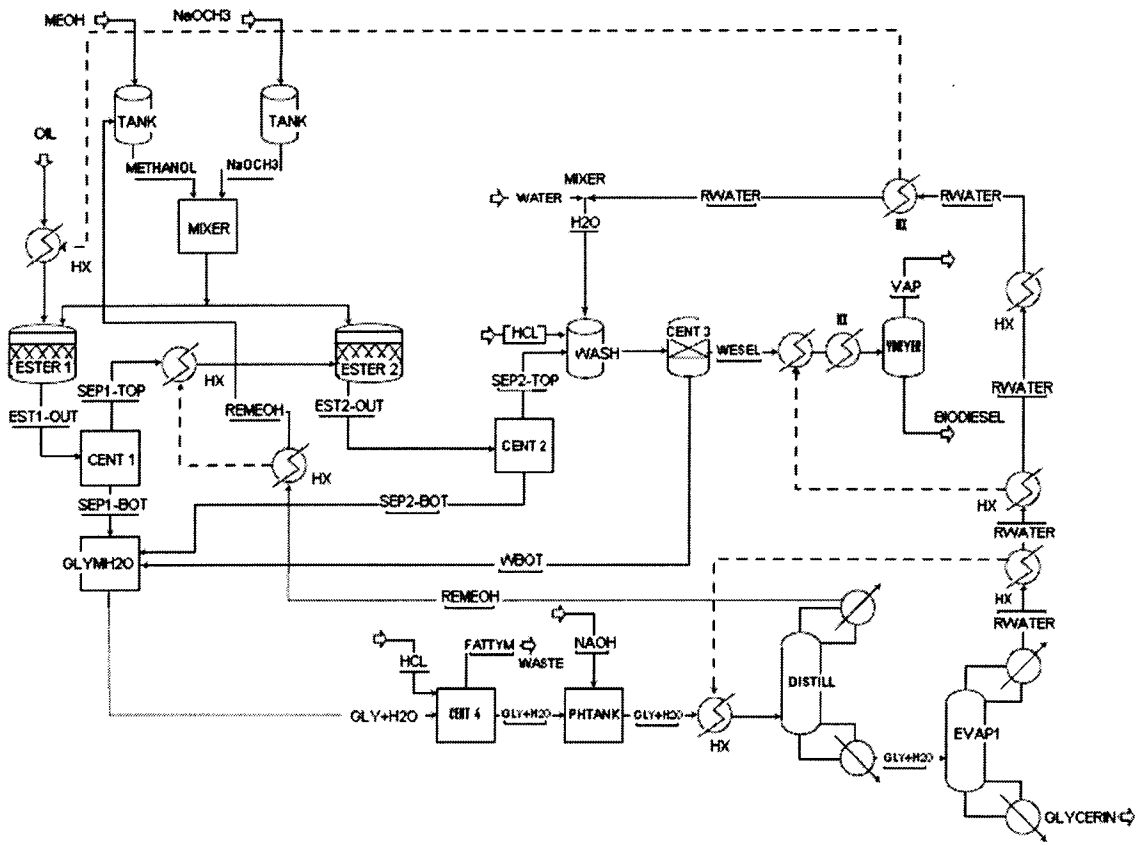

Figure 2.2 Process flow diagram of the biodiesel production process from soybean oil (Hass et al., 2006)

"Flowsheet for the modeled production of biodiesel from soybean oil; CENT: centrifuge; ES1-, 2-OUT: post-transesterification ester mixture exiting reactors 1 and 2, respectively; FATTYM: free fatty acid waste stream; GLYH2O: glycerol–water stream, GLYMH2O: crude glycerol accumulation tank; HX: heat exchanger; dashed lines indicate heat transfer; MEOH: methanol; NAOCH3: sodium methoxide; PHTANK: pH adjustment tank, REMEOH: recovered methanol; RWATER: recovered water; SEP1-, 2-BOT: heavy (glycerol-rich) layer exiting centrifugal separators 1 and 2, respectively; SEP1-, 2-TOP: light layer (containing ester product) exiting centrifugal separators 1 and 2, respectively; VAP: water vapour; VDRYER: vacuum dryer; WBOT: aqueous stream recovered after a water-wash of crude biodiesel, WDESEL: biodiesel–water mixture. Solid lines indicate the flow of liquid streams, dashed lines the flow of heat."

In contrast to the statement of Haas et al. (2006) that no thorough economic analysis of biodiesel production processes had been reported in previous biodiesel-related studies, Zhang et al. (2003a,b) provided a detailed study of four potential processes of biodiesel production in terms of their technical and economical feasibility using the HYSYS^{TM} Process Simulation Software. The processes included those using virgin vegetable oil or waste cooking oil with an alkali catalyst (Process *I* and *II*). In the other two processes (Processes *III* and *IV*) waste cooking oil was transesterified in presence of an acid catalyst. These processes were somehow different in their method of biodiesel

purification. The results revealed that all the proposed processes were technically viable. Among those processes, biodiesel production via alkali-catalyzed transesterification of virgin vegetable oil, Process *I*, had the lowest capital cost, due to the simplicity of the reaction and no need to any pre-treatment unit. On the other hand, acid-catalyzed transesterification of waste frying oil had the lowest operating cost due to the use of waste cooking oil instead of virgin vegetable oil, with no major technical issue associated with the formation of emulsions. The authors claimed acid-catalyzed transesterification of waste frying oil should be considered as an alternative for the widespread alkali-catalyzed reaction in biodiesel industry.

2.5 Biodiesel purification

After transesterification, removing the impurities from biodiesel to meet the relevant ASTM Standard D-6751-02 is a critical task to be accomplished. Up to this point, there have been only a few studies dealing specifically with the purification of biodiesel. However, the basic fundamentals of different methods to separate the impurities from biodiesel can be found through the experimental procedures of the reaction and kinetics studies, discussed previously. It should also be mentioned that most of the studies of biodiesel purification are limited to bench-scale experiments. The industrial-scale technical or economic feasibility of the methods proposed for such purification has not been addressed in most studies reported in the literature.

Nye et al. (1983) carried out consecutive stages of washing the biodiesel product with different solvents. The solvents were subsequently removed to obtain the ultimate biodiesel product. First, in a hexane extraction stage, due to the high solubility of biodiesel in hexane, two liquid phases of mostly biodiesel/hexane and glycerol/methanol/catalyst were formed. Then the top phase, which contained biodiesel, hexane and catalyst, was separated and washed with dilute hydrochloric acid or saturated sodium bicarbonate followed by water. Finally, anhydrous sodium sulphate was used to dry the mixture. The remaining hexane was evaporated by holding the mixture for 48 hours at room temperature. The solid residuals, which were not exactly addressed in their

paper, were removed using gravity filtration. The filtration step was repeated after keeping the sample for a week at 5°C. The authors did not mention the formation of soaps or emulsions through the alkali-catalyzed transesterification of waste frying oil and the way to separate them from the product. Moreover, they did not report the effectiveness of their biodiesel purification process or the purity of the final biodiesel product.

McBride (1999) and Ripmeester (1998) employed hexane or low boiling petroleum ether and 10% aqueous methanol to separate glycerol and biodiesel by a solvent partitioning process. TLC analysis was conducted in order to detect the remaining glycerol in the purified biodiesel. No glycerol was detected in the purified biodiesel; however, the TLC analysis was not precise enough to show very small traces of glycerol in the biodiesel. The efficiency of the biodiesel purification step and the purity of the final biodiesel product were not determined in that study.

In another bench-scale study, after acid-catalyzed transesterification of waste cooking oil with ethanol and formation of separate biodiesel- and glycerol-rich phases, Al-Widyan and Al-Shyoukh (2002) water-washed the biodiesel-rich phase to remove the ethanol and catalyst. This step was done using 40 mL of water at each step and was repeated until the remaining water was completely neutral. The samples were then dried in an oil bath under vacuum (25 mmHg) at 110°C for 1 hour. Not mentioning the yield of biodiesel via such purification method, the authors state that to obtain a high quality biodiesel, the suggested procedure should be repeated for 1 to 4 times.

Encinar et al. (2005) employed sedimentation, following the transesterification reaction, to separate the liquid phase rich in fatty acid methyl esters and glycerol-rich phase, which also contained soap, excess methanol and catalyst. They continued the purification by distilling off the excess methanol from the methyl ester-rich phase at 80°C. The base catalyst was then removed by several steps of water-washing. The final biodiesel product was obtained by drying the wet biodiesel with calcium chloride

followed by filtration. Again, the efficiency of their proposed purification process and the purity of the final biodiesel product are questionable.

Felizardo et al. (2006) also removed the alkali catalyst by first washing the biodiesel with water, followed by a dilute HCl solution (0.5%) and finally with water again. They dried the wet samples with magnesium sulphate as moisture absorbent and then filtered the samples under vacuum to completely recover the purified alkyl esters. Although the authors mentioned the possibility of the formation of soaps and emulsions in alkali-catalyzed transesterification of waste cooking oil and utilized a pre-treatment step to reduce the content of free fatty acid and moisture of the oil and make it more suitable for such reaction (water content of 0.07-0.13 wt% and acid value of 0.42-2.07 mg of KOH per each gram of refined oil), the formation or non-formation of soaps in their experiments and the way to remove them were not mentioned clearly. Moreover, it was not reported how well the impurities were separated from the biodiesel product and the yield of biodiesel via the purification step was not determined.

Bryan (2005) noted the disadvantages of water-washing as a common way to purify biodiesel. Inefficiency in removing the solid residuals, the relatively high loss of esters in the water effluent and the cost and time consumption of the drying steps were some of the points emphasized on. To overcome these difficulties, it is suggested to employ the synthetic magnesium silicate adsorbent as a commercially feasible and technically efficient way to separate the methyl esters from moisture, methanol and other impurities such as color, chlorophyll and metals. However, no experimental data or theoretical explanation was presented to confirm the usefulness of such method.

In a detailed and unique study, Karaosmanoglu et al. (1996) concentrated on the refining step of biodiesel produced by alkali-catalyzed transesterification of rapeseed oil. Three different refining processes were proposed and experimentally evaluated: (1) washing the reaction mixture with hot distilled water, (2) dissolving the mixture in petroleum ether then washing with distilled water and (3) neutralizing the mixture with an acid and then removing the resulted salt. Although the latter appears to be useful only

in removing the alkali catalyst and not the glycerol, the purification yield was determined as the ratio of the amount of purified fatty acid alkyl esters to the initial vegetable oil used in transesterification. In the first method, the reaction mixture was washed with hot distilled water and kept in a separatory funnel to reach room temperature and separate into two liquid phases. The alkali catalyst was removed in the solid state and the upper liquid phase was washed with hot distilled water five times in total, twice without stirring and three times with stirring. In order to free the biodiesel of moisture and other impurities such as methanol, the washed fatty acid alkyl esters were dried over sodium sulphate for 12 hours then filtered. The refining yield of this system was reported to be 84.2%, 80.0% and 79.5% for three different water temperatures of 50, 65 and 80°C, respectively. In the second technique, the catalyst was first separated in the solid form in a separatory funnel. The biodiesel and glycerol phases were then separated. After removing the remaining methanol in the alkyl ester-rich phase using a rotary vacuum evaporator, the ester phase was returned to the separatory funnel. Distilled water and petroleum ether were added to the ester phase (equal to the volume of the ester phase) and acetic acid was added to the mixture to neutralize the solution. The water-washing step was repeated three times. Drying the ester phase over heated sodium sulphate and then filtration, followed by removing the petroleum ether in a rotary vacuum evaporator yielded a high purity biodiesel. The refining yield was found to be 82.6% for this method. In the third system, the catalyst could be in the form of either solid or as a solution in methanol. For both systems, sulphuric acid was added to the system to neutralize the alkali catalyst, and the resulting salt was separated by centrifugation. The remaining methanol in the methyl ester-rich phase was removed by a rotary evaporator and the glycerol was separated by water-washing the mixture three times. The refining yield of 81.2% and 80.9% was obtained as the refining yield of the solid and dissolved form of the catalyst. The most successful refining process was reported to be the first process. Even though, the authors mention considering the biodiesel purity and refining cost in this study, there was no clear discussion on the effect of those parameters on the selection of the first method as the best. Moreover, rather than the block flow diagrams of the biodiesel processing focusing on the refining steps, the applicability of their suggested methods to the large-scale biodiesel plants was not discussed. However, it should be

mentioned that their work is one of the rare studies in the field of biodiesel purification and refining.

Using the HYSYS^{TM} process simulation software, Zhang et al. (2003a,b) studied the technical and economical feasibility of a hexane/methanol/water extraction process in an acid-catalyzed transesterification of waste frying oil with methanol (Process *IV*). The solvent extraction system operated on the basis of phase partitioning between hexane and methanol. Due to the high solubility of biodiesel in hexane and that of glycerol in methanol/water, two liquid phases of biodiesel/hexane and glycerol/methanol/acid catalyst were formed. Addition of water to the system was suggested to decrease the solubility of hexane in anhydrous methanol. The hexane and remaining methanol solvent were further distilled off and biodiesel was obtained with a purity of 99.6%. Glycerol was obtained as a valuable by-product, which could be further treated to a high purity of 85^{+}%. Although this process was not found economically reasonable with a return on investment and biodiesel break-even price of -21.5% and 702 $/tonne, respectively, the technical practicability of such hexane extraction system as an alternative for the common water-washing technique was verified. In the same study, water-washing was utilized to separate impurities, mainly glycerol, from biodiesel in the Processes *I*, *II* and *III*. In Processes *I* and *II*, a water-washing column with 4 theoretical stages were employed to separate fatty acid methyl esters from glycerol, methanol and catalyst. The remaining water in the biodiesel-rich phase was further distilled off to yield biodiesel with a purity of 99.6%. Glycerol by-product with a purity of 92% was obtained after neutralizing the base catalyst and removing the water and methanol by distillation. Since the main objective of the work of Zhang et al. (2003a,b) was the technical and economical assessment of the proposed biodiesel processes (Processes *I* to *IV*), the hexane extraction unit was not studied and designed in detail. Moreover, although not giving similar results, the NRTL and UNIQUAC thermodynamic models available in HYSYS^{TM} were employed to predict the phase separations in the extraction and distillation units. The interaction parameters of such models in HYSYS^{TM} were derived from the available experimental vapor-liquid-liquid equilibrium data. Due to the limited equilibrium data for methyl oleate or triolein (vegetable oil), more accurate values of the

interaction parameters can be obtained by doing a series of equilibrium experiments for the systems containing methyl oleate, glycerol, hexane, methanol, water, oil and acid or base catalyst and adjusting the existing parameters for the systems under study.

Recently, feasibility of the separation of biodiesel from its impurities using hexane partitioning system was confirmed experimentally once more by Dubé et al. (2004) and Zheng et al. (2006) in our laboratory. In their experiments, hexane or low boiling petroleum ether and methanol/water (10:1 on a volume basis) were added to the reaction mixture with the volume ratio of solvent to the reaction mixture of 90:10 or 10:1, respectively. Clearly separated liquid phases of biodiesel/hexane (or biodiesel/petroleum ether) and methanol/water/glycerol/sulphuric acid were formed. Purified biodiesel was obtained after washing the biodiesel phase with methanol/water and evaporating the hexane or petroleum ether by a rotary evaporator. Almost no glycerol was detected during the analysis of different samples of the purified biodiesel with GPC. Since the main objective of their study was to study the reaction kinetics of acid catalyzed transesterification, the efficiency of the hexane (or petroleum ether) extraction step was not specified.

2.6 Limitations of the existing research

Based on the literature survey about biodiesel purification methods, some of the most crucial limitations of the existing research are:

- The increasing demand for biodiesel as a reasonable alternative for petroleum diesel necessitates a thorough study of each unit in the biodiesel processing plant, including the separation steps. The ASTM Standard for biodiesel (D-6751-02) specifies the allowable quantity of the impurities in the purified, consumable biodiesel. In contrast to the biodiesel production-related studies (e.g., mechanism and kinetics of transesterification), purification of biodiesel has not been studied comprehensively. Thus, there should be more effort to study and evaluate different biodiesel purification processes technically and economically.

- In the alkali-catalyzed transesterification, which has been the most common technique to produce biodiesel, water-washing has been the usual method for removing the impurities from biodiesel. In spite of the inexpensive and easy availability of water as the solvent, the problem of saponification and formation of unwanted emulsions has always been present in alkali-catalyzed reactions. This issue becomes more critical when waste cooking oil is employed as the raw material. It should also be mentioned that even for water-washing systems, there are few literature sources dealing with technical and economical feasibility, design and optimization of such a process as a part of the entire biodiesel plant. Hence, to advance biodiesel technology, other alternatives for separation of impurities from biodiesel should be studied and carefully assessed.

- Hexane/aqueous methanol extraction has been experimentally and theoretically shown to be a potential technique for separating impurities (mainly glycerol) from biodiesel made by both acid-catalyzed transesterification of waste cooking oil and alkali-catalyzed transesterification of virgin vegetable oil. However, there has not been any detailed study about the applicability of such a process to the industrial scale production of biodiesel, or its technical and economical design and optimization. Therefore, the present research project deals with the technical and economical study, design and optimization of the biodiesel purification by hexane/aqueous methanol partitioning technique.

References

Agarwal, A. K. and Das, L. M., "Biodiesel Development and Characterization for Use as a Fuel in Compression Ignition Engines," Journal of Engineering for Gas Turbines and Power, 123, 440-447 (2001).

Ali, Y. and Hanna, M. A., "Alternative Diesel Fuels from Vegetable Oils," Bioresource Technology, 50, 153-163 (1994).

Allen, H. D., Rock, G. and Kline, W. A., "Process or Treating Fats and Fatty Oils," US Patent 2, 383-579 (1945).

Al-Widyan, M. I. and Al-Shyoukh, A. O., "Experimental Evaluation of the Transesterification of Waste Palm Oil into Biodiesel," Bioresource Technology, 85, 253-256 (2002).

Bender, M., "Economic Feasibility Review for Community-Scale Farmer Cooperatives for Biodiesel," Bioresource Technology, 70, 81-87 (1999).

Boocock, D. G. B., Konar, S, Mao, V. and Sidi, H, "Fast One-Phase Oil-Rich Processes for the Preparation of Vegetable Oil Methyl Esters," Biomass and Bioenergy, 11(1), 43-50 (1996).

Boocock, D. G. B., Konar, S. K., Mao, V., Lee, C. and Buligan, S., ""Fast Formation of High-Purity Methyl Esters from Vegetable Oils," J. Am. Oil Soc. Chem., 75(9), 1167-1172 (1998).

Bradshaw, G. B. and Meuly, W. C., "Preparation of Detergents," US Patent 2, 360-844 (1944).

Bryan, T., "Adsorbing it All," Biodiesel Magazine, 40-43 (March, 2005).

Buczek, B. and Czepirski, L., "Applicability of Used rapeseed Oil for Production of Biodiesel," Inform, 15(3), 186-188 (2004).

Canakci, M. and Van Gerpen, J., "Biodiesel Production via Acid Catalysis," Trans. ASAE, 42(5), 1203-1210 (1999).

Canakci, M. and Van Gerpen, J., "Biodiesel Production from Oils and Fats with High Free Fatty Acids," Trans. ASAE, 44(6), 1429-1436 (2001).

Canakci, M., "Combustion Characteristics of a Turbocharged DI Compression Ignition Engine with Petroleum Diesel Fuels and Biodiesel," Bioresource Technology, 98, 1167-1175 (2007a).

Canakci, M., "The Potential of Restaurant Waste Lipids as Biodiesel Feedstocks," Bioresource Technology, 98, 183-190 (2007b).

Coleman, B., "Canola: An Excellent Feedstock for Biodiesel," Biodiesel Magazine, 50 (January 2006).

Chiu, C. W., Schumacher, L. G. and Suppes, G. L., "Impact of Cold Flow Improvers on Soybean Biodiesel Blend," Biomass and Bioenergy, 27, 485-491 (2004).

Cvengros, J. and Cvengrosova, Z., "Used Frying Oils and Fats and Their Utilization in the Production of Methyl Esters of Higher Fatty Acids," Biomass Bioenergy, 27, 173-181 (2004).

Demirbas, A., "Biodiesel Impacts on Compression Ignition Engines (CIE): Analysis of Air Pollution Issues Relating top Exhaust Emissions," Energy Sources, 27, 549-558 (2005).

Demirbas, A. and Karslioglu, S., "Biodiesel Production Facilities from Vegetable Oils and Animal Fats," Energy Sources, Part A, 29, 133-141 (2007).

Dorado, M. P., Ballesteros, E., Arnal J. M., Gomez, J. and Lopez F. J., "Exhaust Emissions from a Diesel Engine Fueled with Transesterified Waste Olive Oil," Fuel, 82, 1311-1315 (2003).

Dubé, M. A., Zheng, S. McLean, D. D. and Kates, M., "A Comparison of ATR-FTIR Spectroscopy and GPC for Monitoring Biodiesel Production," J. Am. Oil Chem. Soc. 81, 599-603 (2004).

Eckey, E. W., "Esterification and Interesterification," J. Am. Oil Chem. Soc., 33, 575-579 (1956).

Encinar, J. M., Gonzalez, J. F. and Rodriguez Reinares, A., "Biodiesel from Used Oil. Variables Affecting the Yields and Characteristics of the Biodiesel," Ind. Eng. Chem. Res., 44, 5491-5499 (2005).

Felizardo, P., Joana Neiva Correia, M., Raposo, I., Mendes, J. F., Berkemier, R. and Bordado, J. M., "Production of Biodiesel from Waste Frying Oil," Waste Management, 26, 487-494 (2006).

Fernando, S., Hall, C. and Jha, S., "NO_x Reduction from Biodiesel Fuels," Energy & Fuels, 20, 376-382 (2006).

Feuge, R. O., Grose, T., "Modification of Vegetable Oil. VII. Alkali-catalyzed Interesterification of Peanut Oil with Ethanol," J. Am. Oil Soc. Chem., 26, 97-102 (1949).

Freedman, B., Pryde, E. H. and Mounts, T. L., "Variables Affecting the Yields of Fatty Esters from Transesterified Vegetable Oils," J. Am. Oil Soc. Chem., 61(10), 1638-1643 (1984).

Freedman, B., Butterfield, R. O. and Pryde, E. H., "Transesterification Kinetics of Soybean Oil," J. Am. Oil Soc. Chem., 63(10), 1375-1380 (1986).

Fukuda, H., Kondo, A. and Noda, H., "Biodiesel Fuel Production by Transesterification of Oils," Journal of Bioscience and Bioengineering, 92(5), 405-416 (2001).

Geller, D. P. and Goodrum J. W., "Effects of Specific Fatty Acid Methyl Esters on Diesel Fuel Lubricity," Fuel, 83, 2351-2356 (2004).

Haas, M. J., McAloon, A. J., Yee, W. C. and Foglia T. A., "A Process Model to Estimate Biodiesel Production Costs," Bioresource Technology, 97, 671-678 (2006).

Health Canada, "Health Benefits of Reducing Greenhouse Gas Emissions," www.hc-sc.gc.ca (2006).

Hertz, P. B., "Extending Engine Life and Fuel Economy with Canola Based Fuel Additives," Department of Mechanical Engineering, University of Saskatchewan, Saskatoon, Canada, www.milliganbiotech.com (2006).

Holbein, B. E., Stephen, J. D. and Layzell D. B., "Canadian Biodiesel Initiative," Final Report, BIOCAP Canada, Kingston, Ontario, Canada (2004).

Huang, C. and Wilson, D., "Improving the Cold Flow Properties of Biodiesel," 91st AOSC Annual Meeting, San Diego, CA, www.nationalbiodieselboard.com (2000).

Kalam, M. A. and Masjuki M. M., "Biodiesel from Palm Oil-An Analysis of its Properties and Potential," Biomass Bioenergy, 23, 471-479 (2002).

Karaosmanoglu, F., Cigizoglu, K. B., Tuter, M. and Ertekin S. "Investigation of the Refining Step of Biodiesel Production," Energy and Fuels, 10, 890-895 (1996).

Keim, G. I., "Process for Treatment of Fatty Glycerides," US Patent 2,383,601 (August, 1945).

Koonin, S. E., "Getting Serious about Biofuels," Science Magazine, 311, 435 (2006).

Korbitz, W., "Biodiesel Production in Europe and North America, an Encouraging Prospect," Renewable Energy, 16, 1078-1083 (1999).

Korus, R.A., Hoffman, D.S., Bam, N., Peterson, C.L., Drown, C., "Transesterification Process to Manufacture Ethyl Ester of Rape Oil," In: The Proceedings of the First Biomass Conference of the Americas: Energy, Environment, Agriculture, and Industry, National Renewable Energy Laboratory, Golden Co., 2, 815–826 (1993).

Kreutzer, U. R., "Manufacture of Fatty Alcohols Based on Natural Fats and Oils," J. Am. Oil Soc. Chem., 61(2), 343-348 (1984).

Kulkarni, G., M. and Dalai, A. K., "Waste Cooking Oil-An Economical Source for Biodiesel: A Review," Ind. Eng. Chem. Res., 45, 2901-2913 (2006).

Kulkarni, G. M., Dalai, A. K. and Bakhshi, N. N., "Utilization of Green Seed Canola Oil for Biodiesel Production," Journal of Chemical Technology and Biotechnology, 81, 1886-1893 (2006).

Lang, X., Dalai, A. K., Bakhshi, N. N., Reaney, M. J. and Hertz, P. B., "Preparation and Characterization of Bio-Diesels from Various Bio-Oils," Bioresource Technology, 80(1), 53-62 (2001).

Lin, C. Y. and Huang, J. C., "An Oxygenating Additive for Improving the Performance and Emission Characteristics of Marine Diesel Engines," Ocean Engineering, 30, 1699-1715 (2003).

Liu, K. S., "Preparation of Fatty Acid Methyl Esters for Gas Chromatographic Analysis of Lipids in Biological Materials," J. Am. Oil Soc. Chem., 71(11), 1179-1187 (1994).

Lotero, E., Liu, Y., Lopez, D. E., Suwannakarn, K., Bruce, D. A. and Goodwin, J. G., "Synthesis of Biodiesel via Acid Catalysis," Ind. Eng. Chem. Res., 44, 5353-5363 (2005).

Ma, F. and Hanna, M. A., "Biodiesel Production: A Review," Bioresource Technology, 70, 1-16 (1999).

Ma, F., Clements, L. D. and Hanna, M. A., "The Effects of Catalyst, Free Fatty Acids and Water on Transesterification of Beef Tallow," Trans. ASAE, 41, 1261-1264 (1998).

Marchetti, J. M., Miguel, V. U. and Errazu, A. F., "Possible Methods for Biodiesel Production," Renewable and Sustainable Energy Reviews, 11, 1300-1311 (2007).

McBride, N., "Modeling the Production of Biodiesel from Waste Frying Oil," B.A. Sc. Thesis, Department of Chemical Engineering, University of Ottawa (1999).

McKillop, A., "Oil: No Supply Side Answer to the Coming Energy Crisis," Refocus, 6(1), 50-53 (2005).

Meher, L. C., Vidya Sagar, D. and Naik, S. N., "Technical Aspects of Biodiesel Production by Transesterification-A Review," Renewable & Sustainable Energy Reviews, 10, 248-268 (2006).

Monyem, A. and Van Gerpen, J. H., "The Effect of Biodiesel Oxidation on Engine Performance and Emissions," Biomass and Bioenergy, 20, 317-325 (2001).

Nabi, Md. N., Akhter, Md. S. and Zaglul Shahadat, Md. M., "Improvement of Engine Emissions with Conventional Diesel Fuel and Diesel-Biodiesel Blend," Bioresource Technology, 97, 372-378 (2006).

Nelson, L. A., Foglia, T. A. and Marmer, W. N., "Lipase-Catalyzed Production of Biodiesel," J. Am. Oil Soc. Chem., 73(8), 1191-1195 (1996).

Nelson, R. G., Howell, S. A. and Weber, J. A., "Potential Feedstock Supply and Costs for Biodiesel Production," Bioenergy'94, Proceedings of the Sixth National Bioenergy Conference, Reno/Sparks, Nevada (1994).

Noordam. M. and Withers, R., "Producing Biodiesel from Canola in the Island Northwest: An Economic Feasibility Study," Idaho Agricultural Experiment Station Bulletin No. 785, University of Idaho, College of Agriculture, Moscow, Idaho, p.12 (1996).

Noureddini, H. and Zhu, D., "Kinetics of Transesterification of Soybean Oil," J. Am. Oil Soc. Chem., 74(11), 1457-1463 (1997).

Nye, M. J., Williamson, T. W., Deshpande, S., Schrader, J. H., Snively, W. H., Yurkewich, T. P. and French, C. L., "Conversion of Used Frying Oil to Diesel Fuel by Transesterification: Preliminary Tests," J. Am. Oil Soc. Chem., 60(8), 1598-1601 (1983).

Ripmeester, W. E., "Modeling the Production of Biodiesel from Waste Cooking Oil," B.A. Sc. Thesis, Department of Chemical Engineering, University of Ottawa (1998).

Supple, B., Holward-Hildige, R., Gonzalez-Gomez, E. and Leahy, J. J., "The Effect of Steam Treating Waste Cooking Oil on the Yield of Methyl Ester," J. Am. Oil Chem. Soc., 79(2), 175-178 (2002).

Trent, W. R., "Process of Treating Fatty Glycerides," US Patent 2, 383-632 (1945).

Ulusoy, Y., Tekin, Y., Cetikaya, M. and Karaosmanoglu, F., "The Engine Tests of Biodiesel from Used Frying Oil," Energy Sources, 26, 927-932 (2004).

Van Gerpen, J., "Biodiesel Processing and Production," Fuel Processing Technology, 86, 1097-1107 (2005).

Wang, W. G., Lyons, D. W., Clark, N. N. and Gautam, M., "Emissions from Nine Heavy Trucks Fueled by Diesel and Biodiesel Blend without Engine Modification," Environ. Sci. Technol, 34, 933-939 (2000).

Watanabe, Y., Shimada, Y., Sugihara, A. and Tominaga, Y., "Enzymatic Conversion of Waste Edible Oil to Biodiesel Fuel in a Fixed-Bed Bioreactor," J. Am. Oil Soc. Chem., 78(2), 703-707 (2001).

Wright, H. J., Segur, J. B., Clark, H. V., Coburn, S. K., Langdon, E. E. and DuPuis, R. N., "A Report on Ester Interchange," Oil and Soap, 21, 145-148 (1944).

yokAyo biofuels, "Benefits: Agriculture and Performance," http://www.ybiofuels.org (May, 2006).

Zhang, Y., Dubé, M. A., McLean, D. D. and Kates, M., "Biodiesel Production from Waste Cooking Oil: 1. Process design and technological assessment," Bioresource Technology, 89, 1-16 (2003a).

Zhang, Y., Dubé, M. A., McLean, D. D. and Kates, "Biodiesel Production from Waste Cooking Oil: Economic Assessment and Sensitivity Analysis," Bioresource Technology, 90, 229-240 (2003b).

Zheng, S., Kates, M., Dubé, M. A. and McLean, D. D., "Acid-catalyzed Production of Biodiesel from Waste Frying oil," Biomass and Bioenergy, 30, 267-272 (2006).

Zullaikah, S., Lai, C. C., Vali, S. R. and J, Y. H., "A Two-Step Acid-Catalyzed Process for The Production of Biodiesel from Rice Bran Oil," Bioresource Technology, 96, 1889-1896 (2005).

Chapter 3 (Paper 1)

Liquid-Liquid Equilibria of the System: Methyl Oleate, Glycerol, Hexane and Methanol at Room Temperature and Atmospheric Pressure

Roza Tizvar[1], David D. McLean[1*], Morris Kates[2], Marc A. Dubé[1]
[1] Department of Chemical Engineering, University of Ottawa
[2] Department of Biochemistry, Microbiology and Immunology, University of Ottawa
Ottawa, Ontario, K1N 6N5

Abstract

Liquid-liquid equilibria of the quaternary system methyl oleate, glycerol, hexane and methanol were experimentally quantified at room temperature and atmospheric pressure. UNIFAC and Modified UNIFAC activity coefficient models were used to predict the properties of the co-existing phases at equilibrium. These models employed the previously reported binary group interaction parameters of Magnussen et al. (1981) and Gmehling et al. (1993), respectively, without any regression. Overall, the predicted tielines showed no significant lack of fit when compared to the experimental tielines for both models; however, the precision of the experimental data was insufficient to verify achievement of the ASTM Standard for glycerol content of the methyl oleate-rich phase. Nevertheless, the hexane/methanol solvent system showed potential to achieve the required separation.

Keywords: biodiesel purification, methyl oleate, quaternary system, liquid-liquid equilibria, UNIFAC, Modified UNIFAC

* Corresponding author, Tel: +1-613-562-5800 x6110; Fax: +1-613-562-5172.
Email: mclean@genie.uottawa.ca

3.1 Introduction and background

Biodiesel (i.e., fatty acid alkyl esters) is one of the best substitutes for petroleum-based fuels mainly due to its renewability and biodegradability (Fernando et al., 2006; Hertz, 2006; Nabi et al., 2006). Biodiesel is usually produced by catalytic transesterification of triglycerides with an alcohol. The main by-product is glycerol, which impacts negatively on the properties of the biodiesel fuel (Prankl et al., 2004). Based on the ASTM Standard for biofuels (ASTM D-6751-02), the maximum allowable quantity of free glycerol in biodiesel is 0.02 wt% (ASTM D-6751-02, 2002). Hence, before its use, biodiesel must be almost completely separated from the glycerol by-product, which has an economic value in the pharmaceutical and other industries. Consecutive stages of water washing have been commonly used to purify biodiesel, sometimes together with another extraction solvent such as hexane or petroleum ether (Al-Widyan and Al-Shyoukh, 2002; Encinar et al., 2005; Felizaro et al., 2006; Karaosmanoglu et al., 1996). The main disadvantage of water washing is the formation of emulsions, which results in a significant reduction in the efficiency of the purification process. This phenomenon is especially severe when biodiesel is made via alkali-catalyzed transesterification of waste cooking oil, due to the formation of soaps from the free fatty acids in the waste oils (Kulkarni and Dalai, 2006), but is greatly reduced when biodiesel is made by the acid-catalyzed reaction (Kulkarni and Dalai, 2006; Zhang et al., 2003; Zheng et al., 2006).

In a bench-scale study, Nye et al. (1983) added hexane to the alkali-catalyzed reaction mixture, which contained biodiesel, glycerol, residual methanol and catalyst, to form a biodiesel/hexane phase and a glycerol/methanol/catalyst phase. This method was one of the first approaches for hexane extraction of biodiesel.

At ambient temperature and atmospheric pressure, solvent extraction with hexane, water and methanol (with the volume ratio of water to methanol of 1:9) was experimentally found to be a suitable technique to separate glycerol and biodiesel (Dubé et al., 2004; McBride, 1999; Zheng et al., 2006). When hexane and aqueous methanol are

added to the reaction mixture, which mainly contains biodiesel, glycerol and some methanol, two liquid phases will form. Due to the relatively high solubility of biodiesel in hexane and that of glycerol in methanol-water, the hexane phase contains almost all of the biodiesel and the methanol-water phase contains almost all of the glycerol. In this way the biodiesel and glycerol are well separated and can be readily isolated by distillation or flash evaporation of the respective extraction solvents.

To our knowledge, quantitative examination of the phase equilibria of the five component liquid system, biodiesel/glycerol/hexane/methanol/water, involved in the purification of biodiesel has not been reported. Such information is required for detailed design of biodiesel isolation and purification processes. The liquid-liquid phase equilibria of ternary systems of methyl oleate (biodiesel fuel)/glycerol/methanol (Negi et al., 2006; Gutschke et al., 1988; Komers et al., 1995), biodiesel fuel/methanol/water (Stloukal et al., 1997) and hexane/water/methanol (Liu et al., 2002) have been studied previously. Negi et al. (2006) reported five experimental liquid-liquid equilibrium data points for the methyl oleate/glycerol/methanol system. They compared these experimental results with the predictions of the UNIFAC and UNIFAC-Dortmund (i.e., Modified UNIFAC) activity coefficient models and concluded that both models were capable of predicting the phase equilibria at 60°C. Working on roughly the same system, Gutschke et al. (1988) and Komers et al. (1995) studied the liquid-liquid equilibria of the ternary system biodiesel fuel/methanol/glycerol. The ternary phase diagram of biodiesel fuel/methanol/water in the temperature range of 25-65°C was investigated by Stloukal et al. (1997). In another study, Liu et al. (2002) experimentally investigated the liquid-liquid equilibria for the ternary system of methanol/water/hexane at temperatures of 25, 35 and 45°C. Although the authors did not make any predictions of phase equilibria of that system with the available models, they covered a rather wide range of experimental compositions.

In our work, difficulties were encountered in the experimental study of the five-component system due to the lack of precise analytical procedures for simultaneous analysis of the five components, particularly for water. Thus, as a first step, the present study deals with the experimental study and prediction of liquid-liquid equilibria of the

quaternary system consisting of biodiesel, glycerol, hexane and methanol at room temperature and atmospheric pressure. UNIFAC and Modified UNIFAC activity coefficient models were used for the liquid-liquid equilibria predictions. The results obtained using the models were compared with the experimental data. The 3-dimensional plot of the phase diagram of such multicomponent systems was simulated using the UNIFAC activity coefficient model. Since biodiesel consists of a range of fatty acid alkyl esters, methyl oleate, which is the main product of the transesterification of canola oil with methanol, was employed as a substitute for biodiesel.

3.2 Experimental details

3.2.1 Materials

Methyl oleate, hexane, methanol and glycerol were supplied by Sigma-Aldrich with purities of 99%, 99^{+}%, 99.93% and 99.5^{+}%, respectively. All chemicals were employed as received, without any further purification or pretreatment. HPLC-grade tetrahydrofuran (THF) was supplied by Fisher Scientific.

3.2.2 Methods

Varying quantities of the components, methyl oleate, glycerol, hexane and methanol (Table 3.1), were weighed into 15 mL graduated screw cap tubes using a Mettler Toledo (model AG204) balance and mixed for 4½ hours in an automatic rotator at laboratory temperature of ~20°C and atmospheric pressure. After 16 hours at rest at the same temperature and pressure, two separate transparent liquid phases were obtained. The volume of each liquid phase was recorded. One to four samples were taken from both upper and lower phases, diluted with THF (0.04 g of sample diluted to 2 g with THF) and filtered. The diluted samples were then analyzed quantitatively by Gel Permeation Chromatography (GPC). The GPC was equipped with two 300x7.5 mm Phenogel columns with pore sizes of 3 μm and 100 Å, installed in series. The pump and

autosampler were models Waters 600-MS and Waters 717, respectively. The detector was a Waters 410 differential refractometer. The mobile phase was HPLC-grade tetrahydrofuran, which was pumped into the column at a flow rate, temperature and pressure of 0.5 mL/min, 25°C and 732 psi, respectively. In order to ensure that the phase equilibria had been reached at that point, randomly selected samples were re-analyzed after a significantly longer time (72 hours). Since the composition of each phase after 3 days was the same as that after 16 hours, it was concluded that the selected duration of 16 hours was sufficient to reach thermodynamic equilibrium. The GPC chromatograms showed discrete peaks for each component in the mixtures. The mass and mole fractions of methyl oleate, glycerol, hexane and methanol in the samples of the upper and lower phases were determined from the GPC calibration equations for each component. Details of the calibration of the GPC and sample chromatograms of the upper and lower phases are given in Appendix A of this thesis.

3.3 Model calculations

The multicomponent multiphase equilibria of the system methyl oleate, glycerol, hexane and methanol were calculated with the method suggested by Bunz et al. (1991) and Nelson (1987). This method is capable of predicting up to three co-existing phases at equilibrium; one vapour and two liquid phases. The UNIFAC (Magnussen et al., 1981) or Modified UNIFAC (Gmehling et al., 1993) activity coefficient models were employed to estimate the properties of the liquid phases and the SRK equation of state (Holderbaum and Gmehling, 1991) was used to predict the properties of the vapour phase. Necessary computer codes in MATLAB® (version 7.1.0.246, R14 developed by MathWorks Inc.) were developed to determine the composition, density, the amount of each phase and other physical characteristics of the phases at equilibrium. Although the phase equilibria calculations were carried out for vapour-liquid-liquid equilibria, the quantity of the components in the vapour phase was found to be negligible ($<10^{-11}$ wt%) for the quaternary system under investigation.

3.4 Results and discussion

3.4.1 Experimental results

The experimental overall compositions of the system methyl oleate/glycerol/hexane/methanol, as well as the equilibrium compositions of the upper and lower separated phases are given in Table 3.1 as mole and mass fractions. The phase compositions are expressed as means of 1 to 4 replicate analyses in approximate 95% confidence interval in the following form,

$$\overline{x} \pm 2\frac{s}{\sqrt{N}} \tag{3.1}$$

where $\overline{x}$ is the sample mean mole or mass fraction, s is the sample standard deviation associated with each set of replicated data and N is the number of replicates for each overall composition.

Among the experimental tielines, Tielines 6 and 8 gave the best separation of glycerol and methyl oleate (Table 3.1); however, the analytical instrument (GPC) lacked sufficient precision to test the achievement of the ASTM-based glycerol content of methyl oleate-rich phase.

Table 3.1 Overall compositions and average liquid-liquid equilibria compositions for the quaternary system: methyl oleate, glycerol, hexane and methanol at 20°C and 1 bar

Tieline	Experimental overall composition				Methyl oleate-rich phase (upper phase)				Glycerol-rich phase (lower phase)			
	methyl oleate	glycerol	hexane	methanol	methyl oleate	glycerol	hexane	methanol	methyl oleate	glycerol	hexane	methanol
Mole Fractions												
1	0.033	0.412	0.386	0.169	$0.076^{\pm 0.009*}$	$0.012^{\pm 0.001}$	$0.888^{\pm 0.008}$	$0.024^{\pm 0.002}$	$0.007^{\pm 0.014}$	$0.774^{\pm 0.005}$	$0.008^{\pm 0.006}$	$0.211^{\pm 0.013}$
2	0.042	0.457	0.416	0.085	0.093	0.006	0.901	n.d.	0.003	0.860	0.002	0.135
3	0.067	0.394	0.329	0.210	$0.172^{\pm 0.026}$	n.d.	$0.806^{\pm 0.025}$	$0.013^{\pm 0.005}$	$0.006^{\pm 0.007}$	$0.666^{\pm 0.014}$	$0.010^{\pm 0.009}$	$0.318^{\pm 0.019}$
4	0.083	0.416	0.331	0.170	$0.208^{\pm 0.031}$	$0.012^{\pm 0.010}$	$0.768^{\pm 0.036}$	$0.012^{\pm 0.010}$	$0.002^{\pm 0.003}$	$0.755^{\pm 0.004}$	$0.002^{\pm 0.000}$	$0.241^{\pm 0.007}$
5	0.085	0.352	0.272	0.291	$0.247^{\pm 0.013}$	$0.007^{\pm 0.001}$	$0.689^{\pm 0.058}$	$0.057^{\pm 0.045}$	$0.003^{\pm 0.004}$	$0.635^{\pm 0.013}$	n.d.	$0.362^{\pm 0.007}$
6	0.089	0.459	0.369	0.083	$0.204^{\pm 0.003}$	n.d.	$0.796^{\pm 0.003}$	$0.000^{\pm 0.000}$	$0.002^{\pm 0.000}$	$0.858^{\pm 0.001}$	$0.002^{\pm 0.002}$	$0.138^{\pm 0.002}$
7	0.100	0.376	0.275	0.249	$0.273^{\pm 0.024}$	n.d.	$0.689^{\pm 0.034}$	$0.028^{\pm 0.007}$	$0.005^{\pm 0.004}$	$0.636^{\pm 0.010}$	$0.004^{\pm 0.003}$	$0.355^{\pm 0.007}$
8	0.113	0.422	0.299	0.166	$0.291^{\pm 0.002}$	n.d.	$0.687^{\pm 0.005}$	$0.022^{\pm 0.006}$	$0.002^{\pm 0.000}$	$0.749^{\pm 0.002}$	$0.002^{\pm 0.001}$	$0.247^{\pm 0.002}$
9	0.125	0.375	0.250	0.250	0.343	0.019	0.601	0.037	0.002	0.607	0.001	0.390
10	0.135	0.460	0.322	0.083	$0.307^{\pm 0.021}$	n.d.	$0.680^{\pm 0.009}$	$0.008^{\pm 0.001}$	$0.008^{\pm 0.000}$	$0.854^{\pm 0.002}$	n.d.	$0.135^{\pm 0.002}$
11	0.146	0.415	0.274	0.165	$0.363^{\pm 0.008}$	n.d.	$0.617^{\pm 0.012}$	$0.018^{\pm 0.009}$	$0.005^{\pm 0.003}$	$0.744^{\pm 0.004}$	$0.002^{\pm 0.002}$	$0.250^{\pm 0.006}$
12	0.183	0.456	0.277	0.084	0.388	0.014	0.528	0.070	0.022	0.850	0.005	0.123
Mass Fractions												
1	0.113	0.439	0.385	0.063	$0.223^{\pm 0.022}$	$0.011^{\pm 0.000}$	$0.758^{\pm 0.022}$	$0.008^{\pm 0.001}$	$0.026^{\pm 0.049}$	$0.882^{\pm 0.033}$	$0.009^{\pm 0.007}$	$0.084^{\pm 0.009}$
2	0.134	0.452	0.385	0.029	0.261	0.005	0.734	n.d.	0.011	0.936	0.002	0.051
3	0.218	0.398	0.311	0.074	$0.422^{\pm 0.046}$	n.d.	$0.575^{\pm 0.042}$	$0.003^{\pm 0.001}$	$0.024^{\pm 0.028}$	$0.827^{\pm 0.029}$	$0.012^{\pm 0.011}$	$0.137^{\pm 0.010}$
4	0.254	0.395	0.294	0.056	$0.477^{\pm 0.045}$	$0.009^{\pm 0.007}$	$0.512^{\pm 0.049}$	$0.003^{\pm 0.003}$	$0.008^{\pm 0.013}$	$0.891^{\pm 0.008}$	$0.002^{\pm 0.000}$	$0.099^{\pm 0.004}$
5	0.279	0.359	0.259	0.103	$0.542^{\pm 0.027}$	$0.005^{\pm 0.001}$	$0.440^{\pm 0.038}$	$0.014^{\pm 0.011}$	$0.013^{\pm 0.018}$	$0.824^{\pm 0.022}$	n.d.	$0.163^{\pm 0.002}$
6	0.256	0.410	0.308	0.026	$0.469^{\pm 0.004}$	n.d.	$0.531^{\pm 0.004}$	$0.000^{\pm 0.000}$	$0.007^{\pm 0.002}$	$0.938^{\pm 0.001}$	$0.002^{\pm 0.002}$	$0.053^{\pm 0.001}$
7	0.309	0.361	0.247	0.083	$0.573^{\pm 0.031}$	n.d.	$0.420^{\pm 0.032}$	$0.006^{\pm 0.002}$	$0.021^{\pm 0.016}$	$0.816^{\pm 0.020}$	$0.005^{\pm 0.004}$	$0.158^{\pm 0.004}$
8	0.324	0.376	0.249	0.051	$0.590^{\pm 0.002}$	n.d.	$0.405^{\pm 0.002}$	$0.005^{\pm 0.001}$	$0.008^{\pm 0.001}$	$0.888^{\pm 0.003}$	$0.002^{\pm 0.001}$	$0.102^{\pm 0.001}$
9	0.366	0.341	0.213	0.079	0.650	0.011	0.331	0.008	0.009	0.809	0.001	0.181
10	0.355	0.376	0.246	0.024	$0.607^{\pm 0.024}$	n.d.	$0.391^{\pm 0.016}$	$0.002^{\pm 0.000}$	$0.028^{\pm 0.001}$	$0.919^{\pm 0.003}$	n.d.	$0.051^{\pm 0.001}$
11	0.392	0.346	0.214	0.048	$0.667^{\pm 0.010}$	n.d.	$0.329^{\pm 0.009}$	$0.004^{\pm 0.002}$	$0.019^{\pm 0.012}$	$0.876^{\pm 0.007}$	$0.002^{\pm 0.002}$	$0.102^{\pm 0.004}$
12	0.442	0.342	0.194	0.022	0.701	0.008	0.277	0.014	0.073	0.878	0.005	0.044

n.d. : not detectable (a peak area corresponding to an injected mass of less than ~0.003 mg of glycerol or ~0.001 mg of hexane or ~0.0005 mg of methanol could not be detected).

* : $\pm 2s/\sqrt{N}$ (Equation 3.1); no value indicates a single observation.

Some authors (Liu et al., 2002; Awwad et al., 2005; Ince and Kirbaslar, 2003; Resa et al., 2006) created the Othmer-Tobias plot (Othmer and Tobias, 1942), as a proof of the reliability of their experimental data. In our work also, reliability of the experimental tielines was evaluated by checking the linearity of the Othmer-Tobias plot, as shown in Figure 3.1. All the individual tielines were plotted in this figure. The coefficient of determination, R^2, for the top, middle and bottom lines were 0.94, 0.95 and 0.89, respectively, indicating strong linearity.

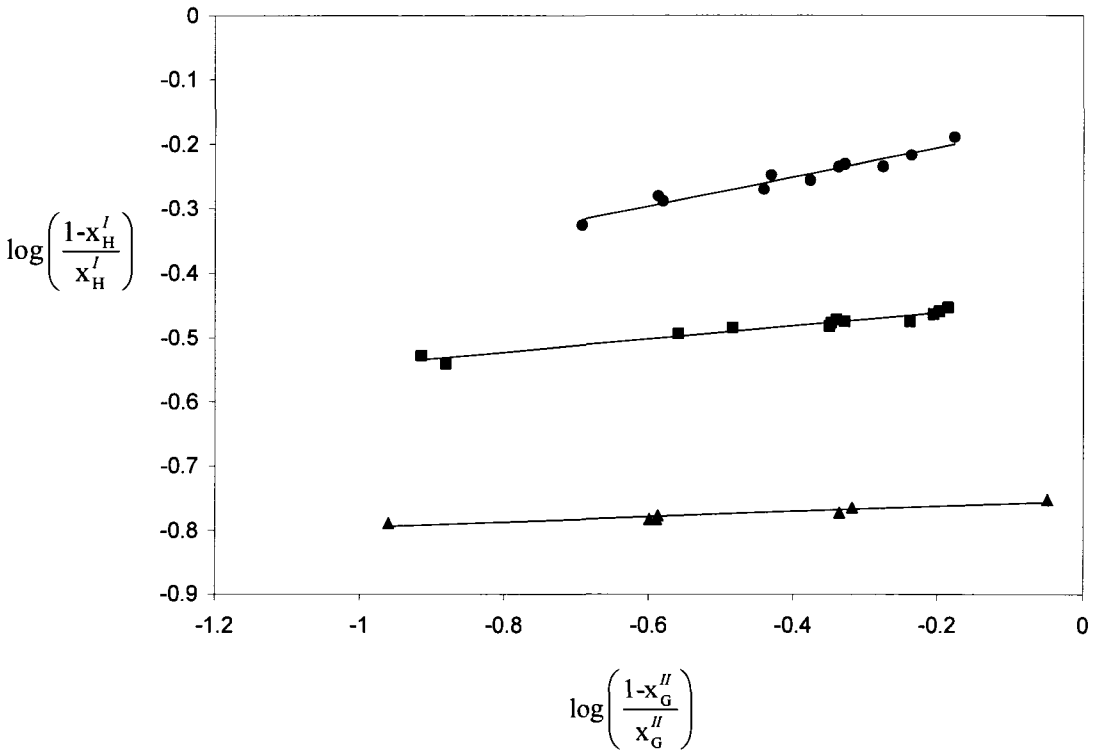

Figure 3.1 Othmer-Tobias plots of methyl oleate, glycerol, hexane and methanol at 20°C and 1 bar:
(•)$(\text{glycerol/methanol})_{\text{overall-mole}} = \sim 1$, (■)$(\text{glycerol/methanol})_{\text{overall-mole}} = \sim 2$,
(▲)$(\text{glycerol/methanol})_{\text{overall-mole}} = \sim 5$; x_H^I and x_G^{II} are mole fraction of hexane in Phase *I* (methyl oleate-rich phase) and that of glycerol in Phase *II* (glycerol-rich phase), respectively.

3.4.2 Phase equilibria predictions

3.4.2.1 UNIFAC model

The equilibrium phase compositions were calculated using the UNIFAC activity coefficient model (Magnussen et al., 1981). A complete set of UNIFAC equations can be found in Appendix *3.I.* The binary interaction parameters of UNIFAC functional groups (CH_3, CH_2, CH, CH=CH, OH, CH_3COO) as well as the group volume and surface area parameters for this system were also taken from the paper by Magnussen et al. (1981). Table 3.2 contains the predicted molar phase compositions corresponding to the overall compositions given in Table 3.1.

Table 3.2 Predicted mole fractions at equilibrium of the quaternary system: methyl oleate, glycerol, hexane and methanol using UNIFAC activity coefficient model at 20°C and 1 bar

Tieline	Methyl oleate-rich phase (upper phase)				Glycerol-rich phase (lower phase)			
	methyl oleate	glycerol	hexane	methanol	methyl oleate	glycerol	hexane	methanol
1	0.078	0.000	0.892	0.030	0.000	0.713	0.017	0.271
2	0.091	0.000	0.894	0.015	0.000	0.841	0.015	0.144
3	0.165	0.000	0.791	0.043	0.000	0.661	0.016	0.323
4	0.197	0.000	0.767	0.036	0.000	0.718	0.015	0.267
5	0.229	0.000	0.703	0.068	0.000	0.560	0.016	0.424
6	0.194	0.000	0.789	0.017	0.000	0.847	0.014	0.140
7	0.258	0.000	0.683	0.059	0.000	0.615	0.015	0.371
8	0.269	0.000	0.692	0.038	0.000	0.728	0.013	0.259
9	0.319	0.001	0.618	0.063	0.000	0.617	0.013	0.370
10	0.294	0.000	0.687	0.019	0.000	0.850	0.012	0.138
11	0.339	0.001	0.619	0.041	0.000	0.730	0.011	0.259
12	0.394	0.001	0.584	0.021	0.000	0.852	0.010	0.138

3.4.2.2 Modified UNIFAC model

The Modified UNIFAC model was also used to predict the molar composition of the liquid phases at equilibrium. The equations of this model are summarized in Appendix *3.II.* The surface, volume and interaction parameters of the functional groups involved in

this system (CH_3, CH_2, CH, CH=CH, OH, CH_3OH, CH_3COO) are reported by Gmehling et al. (1993). Table 3.3 contains the predicted mole fractions of the components in both phases for the global compositions presented in Table 3.1.

Table 3.3 Predicted mole fractions at equilibrium of the quaternary system: methyl oleate, glycerol, hexane and methanol using Modified UNIFAC activity coefficient model at 20°C and 1 bar

Tieline	Methyl oleate-rich phase (upper phase)				Glycerol-rich phase (lower phase)			
	methyl oleate	glycerol	hexane	methanol	methyl oleate	glycerol	hexane	methanol
1	0.078	0.000	0.915	0.007	0.000	0.712	0.001	0.287
2	0.091	0.000	0.906	0.003	0.000	0.845	0.001	0.154
3	0.166	0.000	0.819	0.015	0.000	0.658	0.001	0.341
4	0.198	0.000	0.789	0.013	0.000	0.716	0.001	0.283
5	0.232	0.000	0.738	0.030	0.000	0.556	0.001	0.443
6	0.193	0.000	0.801	0.006	0.000	0.850	0.001	0.149
7	0.261	0.000	0.713	0.026	0.000	0.611	0.001	0.388
8	0.271	0.000	0.713	0.016	0.000	0.726	0.001	0.273
9	0.324	0.000	0.645	0.031	0.000	0.611	0.001	0.388
10	0.294	0.000	0.699	0.008	0.000	0.851	0.001	0.148
11	0.342	0.000	0.639	0.019	0.000	0.725	0.001	0.274
12	0.395	0.000	0.595	0.010	0.000	0.851	0.001	0.148

3.4.3 Comparison of the model predictions and experimental results

The discrepancies between the experimental and predicted molar compositions were determined using Equations 3.2 and 3.3, which define the mean squared deviation (*MSD*) and mean absolute deviation (*MAD*) of the experimental compositions from the calculated, respectively,

$$MSD = \frac{\sum_{i=1}^{I}\sum_{l=1}^{L}\sum_{k=1}^{K}\sum_{u=1}^{n_k}\left(x_{ilku}^{\exp} - x_{ilku}^{cal}\right)^2}{IL\sum_{k=1}^{K} n_k} \tag{3.2}$$

$$MAD = \frac{\sum_{i=1}^{I}\sum_{l=1}^{L}\sum_{k=1}^{K}\sum_{u=1}^{n_k}\left|x_{ilku}^{\exp} - x_{ilku}^{cal}\right|}{IL\sum_{k=1}^{K} n_k} \tag{3.3}$$

where $x_{ilku}^{\exp}$ and x_{ilku}^{cal} denote the experimental and calculated compositions of component i in phase l that belongs to tieline k and replicate data point of u, respectively. I, L, K and n_k represent the number of components, number of phases, number of experimental tielines and total number of replicated data points for the k^{th} tieline respectively. In the current study, I, L and K are 4, 2 and 12, respectively. n_k varies for each tieline from 1 to 4 replicates and the total number of individual measurements, $\sum_{k=1}^{K} n_k$, is 30. The mean squared deviation and mean absolute deviation of the calculated tielines from the experimental ones show that both models are well capable of predicting the phase behaviour of this system (Table 3.4). The 95% confidence intervals for the expected true values of mean squared deviation and mean absolute deviation, E[*MSD*] and E[*MAD*] respectively, were also calculated over 240 single data points and are reported in Table 3.4. No significant difference was observed between the E[*MAD*] using the UNIFAC and Modified UNIFAC activity coefficient models. Similarly, no significant difference was found between the E[*MSD*] using the UNIFAC model and Modified UNIFAC model.

Table 3.4 Deviation of the experimental and calculated mole fractions using UNIFAC and Modified UNIFAC activity coefficient models, as defined in Equations 3.2 and 3.3

	UNIFAC	Modified UNIFAC
MSD	0.00046±0.00013[a]	0.00061±0.00019[a]
MAD	0.0151±0.0020[b]	0.0157±0.0025[b]

[a, b] calculations of 95% confidence intervals are given in Appendix *3.III.*

To graphically illustrate the closeness of the model predictions to the experimental tielines, the experimental compositions were plotted versus the corresponding predicted compositions (Figure 3.2). The predicted compositions for both phases show good agreement with the observed data.

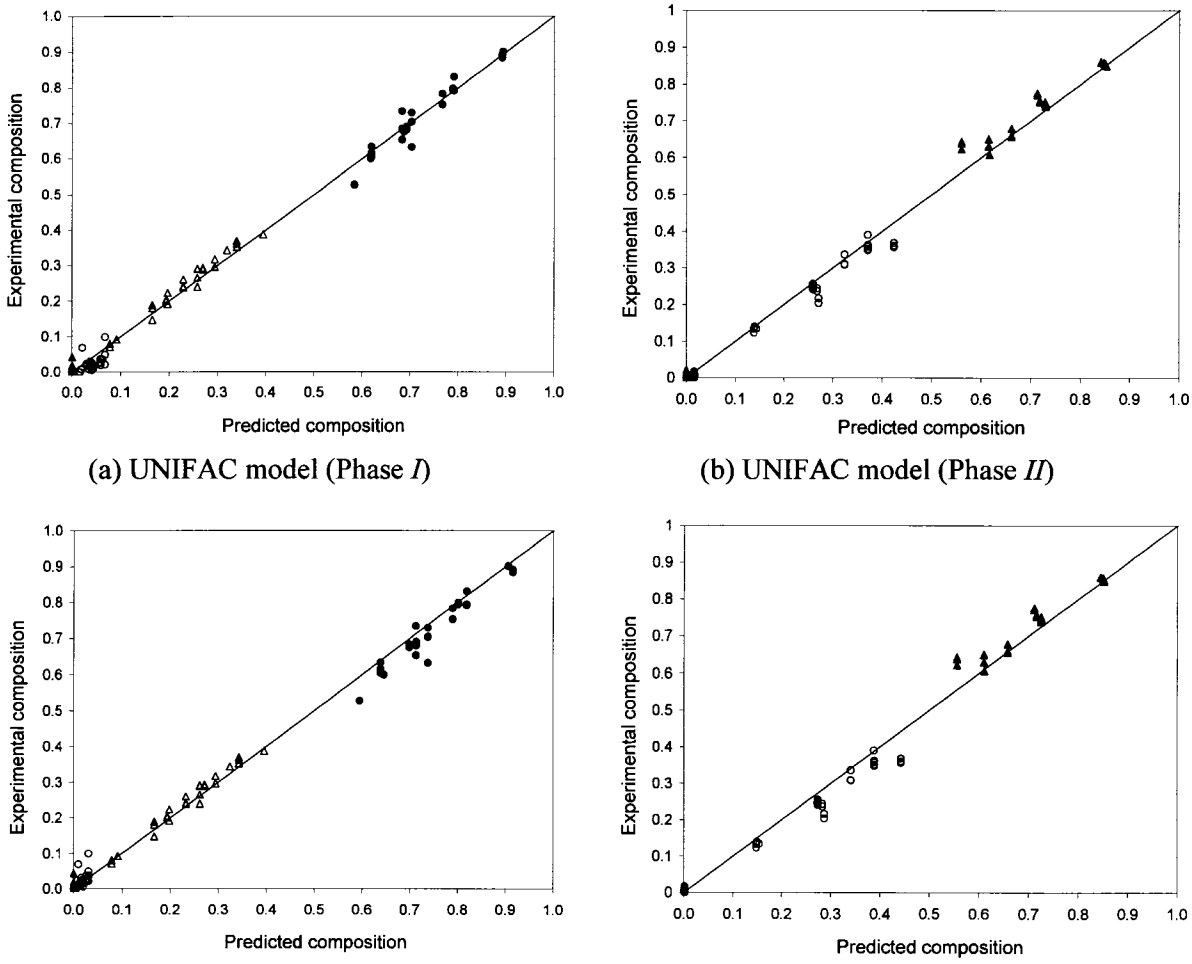

(a) UNIFAC model (Phase *I*)

(b) UNIFAC model (Phase *II*)

(c) Modified UNIFAC model (Phase *I*)

(d) Modified UNIFAC model (Phase *II*)

Figure 3.2 Predicted mole fractions vs. experimental mole fractions for methyl oleate (△), glycerol (▲), hexane (•) and methanol (○) in: (a) and (b) phases *I* and *II* with UNIFAC model, respectively; (c) and (d) phases *I* and *II* with Modified UNIFAC model, respectively.

3.4.4 Simulation of the quaternary phase diagram

The liquid-liquid phase diagram of quaternary systems can be displayed graphically by plotting the data in a pyramid, each of the corners of which represent one of the four components. Figure 3.3 represents the estimated 3-dimensional surface of the two-phase region shown by the shaded area, for the system methyl oleate, glycerol, hexane and methanol at room temperature and atmospheric pressure obtained using the UNIFAC activity coefficient model. Every point inside the two-phase region, which is surrounded by the surface shown, represents a mixture of the four components and will be separated into two liquid phases at physical equilibria. One end of both sample experimental tielines shown in Figure 3.3 is roughly on the methanol/glycerol edge of the pyramid, having approximately no hexane or methyl oleate in that phase. The other ends of the tielines are close to the hexane/methanol/methyl oleate face, closer to the edge of hexane/methyl oleate, carrying almost no glycerol in that phase. This simulation is consistent with the results obtained in the liquid-liquid equilibria experiments of the current work (Table 3.1), which showed the separation of the mixture of methyl oleate, glycerol, hexane and methanol into two liquid phases, one rich in methyl oleate and hexane and the other rich in glycerol and methanol.

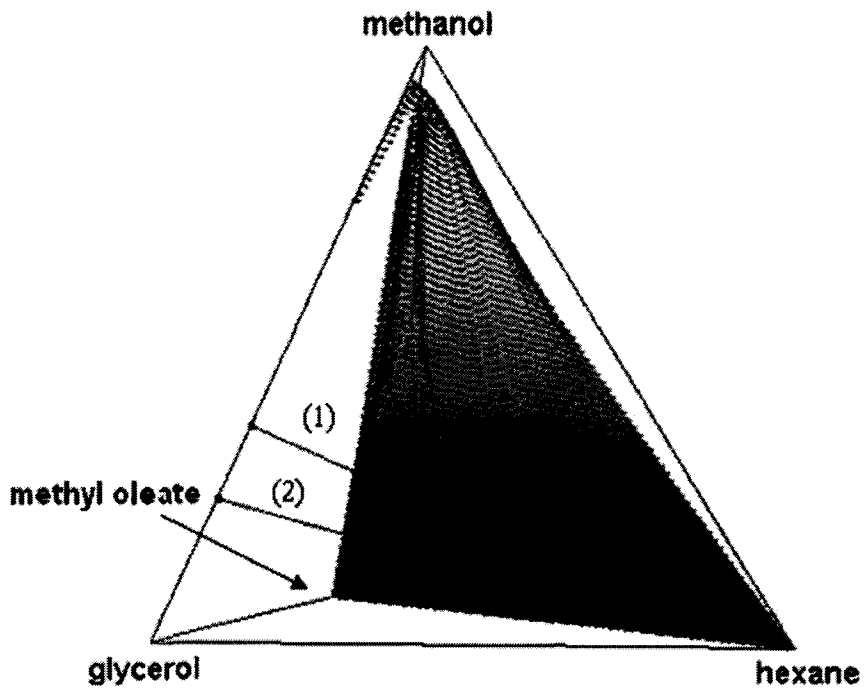

(a)

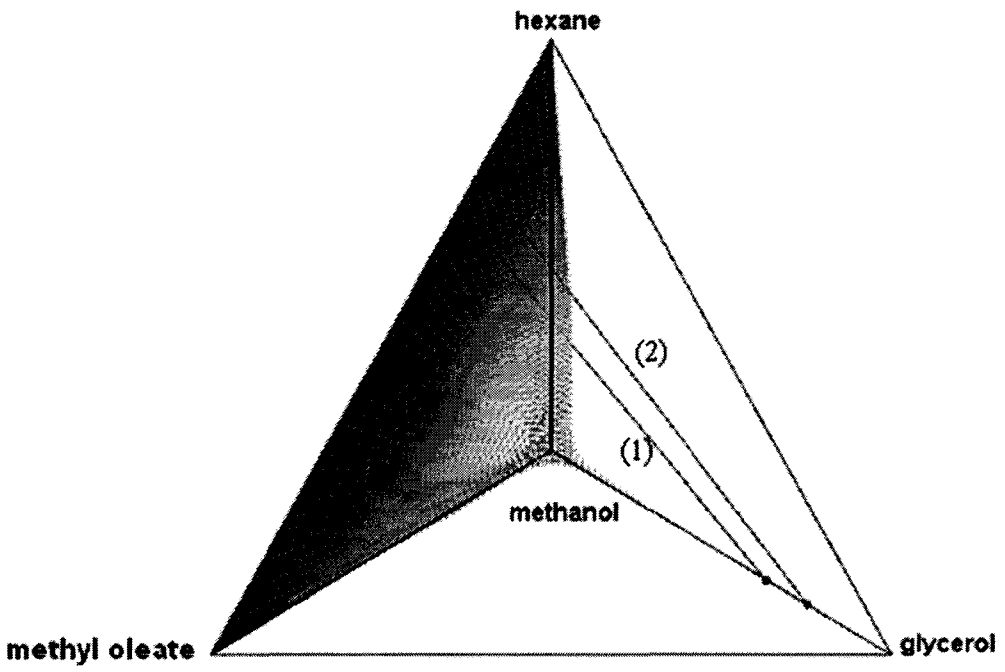

(b)

Figure 3.3 Schematic image of the quaternary phase diagram using UNIFAC model for the system: methyl oleate, glycerol, hexane and methanol at 20°C, •—•: sample experimental tielines
(a: side view b: top view)
(1) Tieline 4 in Table 3.1 (2) Tieline 5 in Table 3.1

3.5 Conclusions

From the study of the phase equilibria of the quaternary system methyl oleate, glycerol, hexane and methanol at room temperature of ~20°C and atmospheric pressure, it was found that the multicomponent phase equilibria predictions using UNIFAC or Modified UNIFAC activity coefficient models are both in good agreement with the experimental data. However, because of the insufficient precision of the experimental equilibrium compositions, achievement of the ASTM Standard for the glycerol content of the methyl oleate-rich phase could not be verified. The interaction parameters of these models were the ones previously reported elsewhere, without any need for regression using the experimental data. This gave confidence that either UNIFAC or Modified UNIFAC models can be used for design of separation processes for this quaternary system. The results of the present study showed that the hexane/methanol solvent system has potential for the separation of glycerol from methyl oleate that could satisfy the ASTM requirement. Further investigation on the use of such solvent systems for separation of glycerol and methyl oleate (i.e., biodiesel) is dealt with in the next chapter of this thesis.

Acknowledgements

The financial support of Natural Sciences and Research Council of Canada (NSERC) is greatly acknowledged. The authors also wish to thank Dr. Benjamin C. Y. Lu for his assistance with some thermodynamic concepts.

Appendices

3.I UNIFAC activity coefficient model

The equations in UNIFAC activity coefficient model can be represented as follows (Magnussen et al., 1981),

$$\ln \gamma_i = \ln \gamma_i^C + \ln \gamma_i^R$$

$$\ln \gamma_i^C = \ln \frac{\phi_i}{x_i} + 1 - \frac{\phi_i}{x_i} - \frac{1}{2} z q_i \left(\ln \frac{\phi_i}{\theta_i} + 1 - \frac{\phi_i}{\theta_i} \right)$$

$$\phi_i = \frac{x_i r_i}{\sum_{j=1}^{n} x_j r_j} \quad \text{and} \quad \theta_i = \frac{x_i q_i}{\sum_{j=1}^{n} x_j q_j}$$

$$r_i = \sum_t \nu_{ti} R_t \quad \text{and} \quad q_i = \sum_t \nu_{ti} Q_t$$

$$\ln \gamma_i^R = \sum_t \nu_{ti} \left(\ln \Gamma_t - \ln \Gamma_t^{(i)} \right)$$

$$\ln \Gamma_t = Q_t \left[1 - \ln \left(\sum_b \theta_b \psi_{bt} \right) - \sum_b \left(\frac{\theta_b \psi_{tb}}{\sum_d \theta_d \psi_{db}} \right) \right]$$

$$\psi_{db} = \exp\left(\frac{-a_{db}}{T} \right)$$

$$\theta_b = \frac{Q_b X_b}{\sum_d Q_d X_d}$$

$$X_b = \frac{\sum_{j=1}^{n} \nu_{bj} x_j}{\sum_{j=1}^{n} \sum_d \nu_{dj} x_j}$$

where $\sum_t$, $\sum_d$ and $\sum_j$ are summations over the groups.

3.II Modified UNIFAC activity coefficient model

The following equations represent the Modified UNIFAC activity coefficient model (Gmehling et al., 1993).

$$\ln \gamma_i = \ln \gamma_i^C + \ln \gamma_i^R$$

$$\ln \gamma_i^C = \ln V_i^{'} + 1 - V_i^{'} - 5q_i\left(\ln \frac{V_i}{F_i} + 1 - \frac{V_i}{F_i}\right)$$

$$V_i^{'} = \frac{r_i^{3/4}}{\sum_{j=1}^{n} x_j r_j^{3/4}} \text{ and } V_i = \frac{r_i}{\sum_{j=1}^{n} x_j r_j}, \text{ where } r_i = \sum_t \nu_{ti} R_t$$

$$F_i = \frac{q_i}{\sum_{j=1}^{n} x_j q_j} \text{ where } q_i = \sum_t \nu_{ti} Q_t$$

$$\ln \gamma_i^R = \sum_t \nu_{ti}\left(\ln \Gamma_t - \ln \Gamma_t^{(i)}\right)$$

$$\ln \Gamma_t = Q_t\left[1 - \ln\left(\sum_b \theta_b \psi_{bt}\right) - \sum_b\left(\frac{\theta_b \psi_{tb}}{\sum_d \theta_d \psi_{db}}\right)\right]$$

$$\theta_b = \frac{Q_b X_b}{\sum_d Q_d X_d} \text{ and } X_b = \frac{\sum_{j=1}^{n} \nu_{bj} x_j}{\sum_{j=1}^{n}\sum_d \nu_{dj} x_j}$$

$$\psi_{db} = \exp\left(-\frac{a_{db} + e_{db}T + h_{db}T^2}{T}\right)$$

where $\sum_t$, $\sum_b$, $\sum_j$ and $\sum_d$ are summations over the groups.

3.III Calculation of the confidence intervals for *MSD* and *MAD*

a:

Squared Deviation $SD = \left(x_{ilku}^{\exp} - x_{ilku}^{cal}\right)^2$

$$Var(SD) = \frac{1}{IL\sum_{k=1}^{K} n_k - 1} \sum_{i=1}^{I}\sum_{l=1}^{L}\sum_{k=1}^{K}\sum_{u=1}^{n_k}\left(SD - MSD\right)^2$$

where *MSD* (i.e., Mean Squared Deviation) is calculated from Equation 3.2 in the manuscript. The 95% confidence interval for E[*MSD*] is,

$$MSD - 1.96\sqrt{\frac{Var(SD)}{IL\sum_{k=1}^{K} n_k}} \le E[MSD] \le MSD + 1.96\sqrt{\frac{Var(SD)}{IL\sum_{k=1}^{K} n_k}}$$

b:

Absolute Deviation $AD = \left|x_{ilku}^{\exp} - x_{ilku}^{cal}\right|$

$$Var(AD) = \frac{1}{IL\sum_{k=1}^{K} n_k - 1} \sum_{i=1}^{I}\sum_{l=1}^{L}\sum_{k=1}^{K}\sum_{u=1}^{n_k}\left(AD - MAD\right)^2$$

where *MAD* (i.e., Mean Absolute Deviation) is calculated from Equation 3.3 in the manuscript. The 95% confidence interval for E[*MAD*] is,

$$MAD - 1.96\sqrt{\frac{Var(AD)}{IL\sum_{k=1}^{K} n_k}} \le E[MAD] \le MAD + 1.96\sqrt{\frac{Var(AD)}{IL\sum_{k=1}^{K} n_k}}$$

Nomenclature

$\bar{x}$	Mean value of the mole/mass compositions for the replicated data of each tieline
s	Standard deviation for the replicated data of each tieline
N	Total number of replicates in each set of experimental tieline
MAD	Mean absolute deviation of experimental compositions from predicted
MSD	Mean squared deviation of experimental compositions from predicted
E[*MSD*]	Expected true value of *MSD*
E[*MAD*]	Expected true value of *MAD*
L	Total number of phases
K	Number of experimental tielines
I	Total number of components
U	Total number of replicated data points
n_k	Number of replicates in the k^{th} tieline
a	Binary group interaction parameter (K)
e	Binary group interaction parameter in Modified UNIFAC model
F	Surface-related parameter in Modified UNIFAC model
h	Binary group interaction parameter in Modified UNIFAC model (K^{-1})
q, Q	Surface area parameter
r, R	Volume parameter
T	Temperature (K)
V	Auxiliary property in Modified UNIFAC model (volume fraction/mole fraction)
V'	Empirically modified V-value
x	Molar composition
z	Coordination number = 10

Greek Letters:

γ_i	Activity coefficient of component i
Γ	Parameter defined for mixtures
$\Gamma^{(i)}$	Parameter defined for pure component i
ν	Number of groups in a molecule
θ	Surface fraction in the liquid phase
ϕ	Volume parameter in UNIFAC model
X	Group mole fraction in the liquid phase
ψ	UNIFAC binary group interaction parameter

Superscripts and subscripts:

C	Combinatorial part of the activity coefficient

R	Residual part of the activity coefficient
j, s, f, b, d, t	Groups
i	Components
l	Phases
k	Tielines
u	Replicates

References

Al-Widyan, M. I. and Al-Shyoukh, A. O., "Experimental Evaluation of the Transesterification of Waste Palm Oil into Biodiesel," Bioresource Technology, 85, 253-256 (2002).

ASTM D-6751-02, Standard Specification for Biodiesel Fuel (B100) Blend Stock for Distillate Fuels, Designation D-6751-02, American Society for Testing and Materials, West Conshohocken, PA (2002).

Awwad, A. M.; Al-Dujaili, A. H.; Al-Heideri, A.; Essa, H. M. Liquid-Liquid Equilibria for Sulfolane + 2-Methoxyethanol + Octane + Toluene at 293.15 K. J. Chem. Eng. Data, 50, 788-791 (2005).

Bunz, A. P., Dohrnt, R. and Prausnitz, J. M., "Three Phase Flash Calculations for Multicomponent Systems," Computers Chem. Eng., 15, 47-51(1991).

Dubé, M. A., Zheng, S., McLean, D. D. and Kates, M., "A Comparison of ATR-FTIR Spectroscopy and GPC for Monitoring Biodiesel Production," J. Am. Oil Chem. Soc., 81, 599-603 (2004).

Encinar, J. M., Gonzalez, J. F. and Rodriguez Reinares, A., "Biodiesel from Used Oil. Variables Affecting the Yields and Characteristics of the Biodiesel," Ind. Eng. Chem. Res., 44, 5491-5499 (2005).

Felizardo, P., Joana Neiva Correia, M., Raposo, I., Mendes, J. F., Berkemier, R. and Bordado, J. M., "Production of Biodiesel from Waste Frying Oil," Waste Management, 26, 487-494 (2006).

Fernando, S., Hall, C. and Jha, S., "NO_x Reduction from Biodiesel Fuels," Energy & Fuels, 20, 376-382 (2006).

Hertz, P. B., "Extending Engine Life and Fuel Economy with Canola Based Fuel Additives," Department of Mechanical Engineering, University of Saskatchewan, Saskatoon, Canada, www.milliganbiotech.com, 2006.

Holderbaum, T. and Gmehling, J., "A Group Contribution Equation of State Based on UNIFAC," Fluid Phase Equilibria, 70, 251-265 (1991).

Gmehling, J., Li, J. and Schiller, M., "A Modified UNIFAC Model 2. Present Parameter Matrix and Results for Different Thermodynamic Properties," Ind. Eng. Chem. Res., 32, 178-193 (1993).

Gutschke, B., Peukert, E. and Jeromin, L., "Glycerolysis Design of Chemical Reaction of Immiscible Liquids," Fat. Sci. Technol., 90, 507 (1988).

Ince, E. and Kirbaslar, I., "(Liquid + Liquid) Equilibria of (Water + Ethanol + Dimethyl Glutarate) at Several Temperatures," J. Chem. Thermodynamics, 35, 1671-1679 (2003).

Karaosmanoglu, F., Cigizoglu, K. B., Tuter, M. and Ertekin S., "Investigation of the Refining Step of Biodiesel Production," Energy and Fuels, 10, 890-895 (1996).

Komers, K., Tichy, J. and Skopal, F., "Ternares Phasen Diagramm Biodiesel-Methanol-Glyzerin," J. Prakt. Chem., 337, 328-331 (1995).

Kulkarni, M. G. and Dalai, A. K., "Waste Cooking Oil: An Economic Source for Biodiesel," Ind. Eng. Chem. Res., 45, 2901-2913 (2006).

Liu, J., Qin, Z. and Wang, J., "Liquid-Liquid Equilibria for Methanol + Water + Hexane Ternary Mixtures," J. Chem. Eng. Data, 47, 1243-1245 (2002).

McBride, N., "Modeling the Production of Biodiesel from Waste Frying Oil," B.A.Sc. Thesis, Department of Chemical Engineering, University of Ottawa (1999).

Magnussen, T., Rasmussen, P. and Fedenslund, A., "UNIFAC Parameter Table for Prediction of Liquid-liquid Equilibria," Ind. Eng. Chem. Process Des. Dev., 20 331-339 (1981).

Nabi, Md. N., Akhter, Md. S. and Zaglul Shahadat, Md. M., "Improvement of Engine Emissions with Conventional Diesel Fuel and Diesel-Biodiesel Blend," Bioresource Technology, 97, 372-378 (2006).

Negi, D. S., Sobotka, F., Kimmel, T., Wozny, G. and Schomäcker, R., "Liquid-Liquid Phase Equilibrium in Glycerol-Methanol-Methyl Oleate and Glycerol-Monoolein-Methyl Oleate Ternary Systems," Ind. Eng. Chem. Res., 45, 3693-3696 (2006).

Nelson, P. A., "Rapid Phase Determination in Multi-Phase Flash Calculations," Computers Chem. Eng., 11(6), 581-591(1987).

Nye, M. J., Williamson, T. W., Deshpande, S., Schrader, J. H., Snively, W. H., Yurkewich, T. P. and French, C. L., "Conversion of Used Frying Oil to Diesel Fuel

by Transesterification: Preliminary Tests," J. Am. Oil Soc. Chem., 60(8), 1598-1601 (1983).

Othmer, D. F. and Tobias, P. E., "Tieline Correlation," Ind. Eng. Chem., 34(6), 693-696 (1942).

Prankl, H., Korbitz, W., Mittelbach, M. and Worgetter, M., "Review on Biodiesel Standardization World-wide," BLT Wieselburg, www.blt.bmlfuw.gv.at, 2006.

Resa, J. M., Goenaga, J. M., Iglesias, M., Gonzalez-Olmoz, M. and Pozuelo, M., "Liquid-Liquid Equilibrium Diagrams of Ethanol + Water + (Ethyl Acetate or 1-Pentanol) at Several Temperatures," J. Chem Eng. Data, 51, 1300-1305 (2006).

Stloukal, R., Komers, K. and Machek, J., "Ternary Phase Diagram Biodiesel Fuel-Methanol-Water," J. Prakt. Chem., 339, 485-487 (1997).

Zhang, Y., McLean, D. D., Kates, M. and Dubé, M. A., "Biodiesel Production from Waste Cooking Oil: 1. Process design and technological assessment," Bioresource Technology, 89, 1-16 (2003).

Zheng, S., Kates, M., Dubé, M. A. and McLean, D. D., "Acid Catalyzed Production of Biodiesel from Waste Frying oil," Biomass and Bioenergy, 30, 267-272 (2006).

Chapter 4 (Papers 2 & 3)

Optimal Separation of Glycerol and Biodiesel via Liquid-Liquid Extraction

Roza Tizvar[1], David D. McLean[1*], Morris Kates[2], Marc A. Dubé[1]
[1] Department of Chemical Engineering, University of Ottawa
[2] Department of Biochemistry, Microbiology and Immunology, University of Ottawa
Ottawa, Ontario, K1N 6N5

Abstract

To meet ASTM D-6751-02 for biodiesel, impurities, particularly glycerol, must be reduced to acceptable levels. The major criteria for investigating the technical feasibility of a process to separate glycerol and biodiesel are acceptability of the separation of glycerol and biodiesel, how close the volume ratio of the liquid phases is to 1:1, how high the recovery of biodiesel is and how short the residence time of the liquid phases in the settler is. In the present study, liquid-liquid extraction processes using hexane, methanol or water, alone or mixed together as a multi-solvent, in a single-stage mixer-settler were investigated. Three multi-solvent systems, hexane/methanol, hexane/water and hexane/methanol/water were found to be technically feasible. The optimal compositions of each system were determined based on use of the UNIFAC activity coefficient model.

Keywords: biodiesel purification, transesterification, liquid-liquid extraction, phase equilibria, mixer-settler, liquid residence time

* Corresponding author, Tel: +1-613-562-5800 x6110; Fax: +1-613-562-5172.
Email: mclean@genie.uottawa.ca

4.1 Introduction and background

Biodiesel, a renewable, biodegradable and clean-burning source of energy, is considered to be an appropriate alternative for fossil fuels. Biodiesel is compatible with most diesel engines without any need for engine modifications (Agarwal and Das, 2001; Ali and Hanna, 1994; Fernando and Jha, 2006; McKillop, 2005; Monyem and Van Gerpen, 2001; Nabi et al., 2006; Ulusoy et al., 2004; Wang et al., 2000). Biodiesel is produced by transesterification of vegetable oils or animal fat, with an alcohol. Because of the significantly lower price of waste cooking oil compared to virgin vegetable oil, the use of the former as a biodiesel feedstock has been widely studied (Encinar et al., 2005; Mangesh and Dalai, 2006). Glycerol is the main by-product of transesterification but its presence in biodiesel reduces the quality of the fuel (Prankl et al., 2004). According to the ASTM Standard for biodiesel, glycerol must comprise less than 0.02 wt% of the purified biodiesel (ASTM D-6751-02, 2002).

There have been few studies focusing on the purification of biodiesel; however, bench-scale experiments for purification of biodiesel can be found in the studies that dealt primarily with the kinetics or mechanism of transesterification. Although these studies provided little rigor in the analysis of separations, they offer a source of potential methodologies.

In many studies, removal of glycerol, excess alcohol and catalyst, was achieved by several consecutive stages of water washing (Al-Widyan and Al-Shyoukh, 2002; Encinar et al., 2005; Felizaro et al., 2006; Karaosmanoglu et al., 1996). In alkali-catalyzed transesterification of waste cooking oil, which has a relatively high content of free fatty acids, the major difficulty is the formation of emulsions due to soaps. This problem becomes more serious when water is added to the system in large amounts, since emulsions may lead to large losses of biodiesel in the washing step.

Karaosmanglu et al. (1996) removed the alkali catalyst from the reaction mixture in the solid from. The biodiesel-rich phase was separated from the glycerol-rich phase by

keeping them for 5 hours to rest in a separatory funnel. The authors compared three different methods for further separation of impurities from the biodiesel made by alkali-catalyzed reaction of virgin rapeseed oil. In the first method, the biodiesel-rich phase was washed with hot distilled water and then left over heated Na_2SO_4 and finally filtered. In the second method, the biodiesel-rich phase was dissolved in petroleum ether and then washed with distilled water. The PH of the solution was adjusted to 7 by adding acetic acid. Again, the mixture was left over Na_2SO_4 and then filtered. The third purification technique, which is neutralization of the alkali catalyst with sulfuric acid, was applied to two types of catalyst; solid form and dissolved in methanol. In the first experiment, the salt resulted from the reaction of acid and solid alkali was separated from the ester phase by centrifugation. The ester phase was further treated the same as previous methods. In the second experiment, in which the alkali was dissolved in methanol and fed initially to the reactor, the reaction mixture was neutralized with sulfuric acid and the resulting salt was separated by centrifugation. The remaining mixture was transferred to a separatory funnel. After formation of ester phase and glycerol-rich phases, the ester phase was washed three times with water, left over Na_2SO_4 and then filtered. In their experimental study, the refining yield was calculated by dividing the mass of the purified biodiesel to the mass of initial vegetable oil consumed in the transesterification. The refining yield of 82-84% was reported for the separation of glycerine, excess alcohol, catalyst and fatty acids from the alkyl esters produced. The first method with 84.2% refining yield was found to be the most attractive process from the separation point of view.

Nye et al. (1983) added hexane to the alkali-catalyzed reaction mixture to form a biodiesel/hexane phase and a glycerol/methanol phase. The biodiesel-rich phase was purified by washing with dilute hydrochloric acid and then with water. This method was one of the first approaches for biodiesel purification but the efficiency of the purification process was not reported.

Later, Dubé et al. (2004), McBride (1999), Ripmeester (1998) and Zheng et al. (2006) employed hexane or low boiling petroleum ether and 10% aqueous methanol to purify biodiesel by solvent partitioning. No glycerol was detected in the purified biodiesel by

TLC (McBride 1999; Ripmeester, 1998). However, the TLC used was not capable of precisely determining the glycerol content in the purified biodiesel and the efficiency of the biodiesel purification step was not reported.

Zhang et al. (2003a,b) used HYSYS^{TM} process simulation software to design and evaluate four possible biodiesel processing plants: an alkali-catalyzed process using virgin vegetable oil or waste cooking oil (Processes *I* and *II*, respectively), acid-catalyzed process using waste cooking oil with a water washing process (Process *III*), and acid-catalyzed process using waste cooking oil with a hexane/methanol/water extraction process (Process *IV*). Based on their findings for the latter process, partitioning of the biodiesel and glycerol components between hexane and methanol was improved by adding water to the methanol solvent. The focus of the study by Zhang et al., (2003a,b) was on technical and economical evaluation of the overall biodiesel plants. Detailed technical assessment of the biodiesel purification sections were not carried out.

This task was the main objective of the current study. Some parts of the results of the plants designed by Zhang et al. (2003a), such as the reaction, methanol distillation and catalyst removal units, were employed in this study. All these units are located prior to the purification unit. In the present study, a single-stage mixer-settler employing the solvents hexane, methanol and water, alone or mixed together was used for separation of glycerol and biodiesel. Optimal quantities of each solvent was determined so as to achieve the ASTM Standard for biodiesel purity, with respect to its glycerol content, as well as minimal liquid residence time in the settler, desirable phase volume ratio in the settler and minimal loss of biodiesel. The assessment of the performance of each potential solvent and also determination of the optimal composition of the solvent systems were carried out by means of the multi-component multi-phase equilibria calculations.

4.2 Process description

4.2.1 Overall process scheme

Using hexane, methanol and water as extraction solvents results in the formation of two liquid phases. One phase contains mostly hexane and biodiesel and the other phase contains mostly glycerol, methanol and water. The driving force for this separation is the high solubility of biodiesel in hexane and that of glycerol in methanol or aqueous methanol. On shaking the mixture, the continuous phase was experimentally found to be the biodiesel/hexane phase and the dispersed phase was the glycerol/methanol/water phase. The time required for the separation of the two liquid phases in the settler is defined as the residence time. Following the experimental studies by Dubé et al. (2004), McBride (1999), Ripmeester (1998) and Zheng et al. (2006) and the HYSYS^{TM} process simulation results of Zhang et al. (2003a,b), the properties of the extraction system were calculated at a temperature of 20°C and atmospheric pressure.

4.2.2 Feed properties

In the biodiesel plant (Process *IV*), the stream exiting the methanol recovery distillation column after the acid-catalyzed transesterification reactor contains biodiesel, glycerol, small amounts of unreacted oil (~2% triglycerides), the acid catalyst and the remaining methanol (Figure 5, stream 203 by Zhang et al., 2003a). This stream was used as the feed to the mixer-settler unit except that it was assumed to be free of acid catalyst and unreacted oil. This assumption was based on the results of previous experiments by Zheng et al. (2006), showing that high conversion of oil to biodiesel (~99.7 wt%) could be achieved by acid-catalyzed reaction without the formation of free fatty acids.

Although biodiesel consists of a variety of esters with different chain lengths and physical properties, methyl oleate was substituted for biodiesel in the calculations. This choice was made because methyl oleate is the major component of biodiesel made from canola oil.

With these assumptions, the mole/mass fractions of methyl oleate, glycerol and methanol in the feed entering the mixer were found to be 0.434/0.826, 0.146/0.087 and 0.420/0.087, respectively.

The ternary phase diagram of the system methyl oleate/glycerol/methanol, which also represents the feed stream entering the extractor, is shown in Figure 4.1. The tieline corresponding to the feed composition indicates the separation of the feed mixture into two liquid phases, consisting of a bottom phase of mostly glycerol and methanol and a top phase of mostly methyl oleate and some methanol. Although there is a spontaneous partitioning between the two liquid phases, the quantity of $M_G^I/(M_G^I+M_{MO}^I)$, which is the definition of the ASTM Standard for the glycerol content in biodiesel, is ~0.0003 (0.0008 on a mole basis). Comparing this value to the corresponding ASTM value of 0.0002 (equivalent to ~0.00064 on a molar basis), one finds that the ASTM Standard is not met and further purification using a suitable solvent must be carried out.

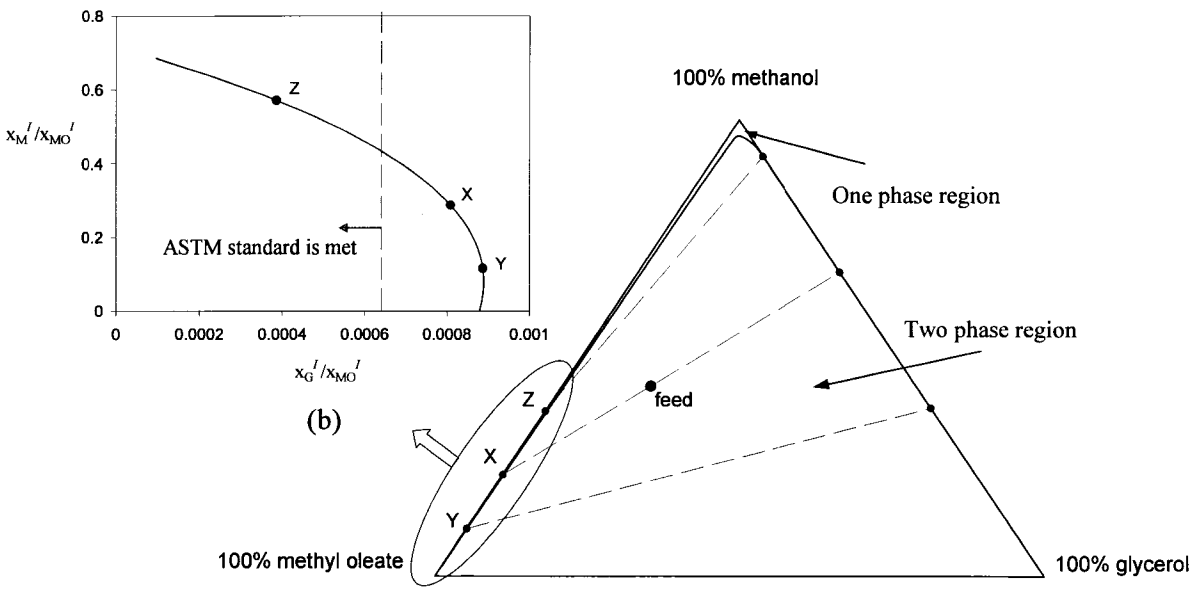

Figure 4.1 (a) Ternary phase diagram of methyl oleate, glycerol and methanol and the sample tielines (X, Y, Z) at 293.15 K and 1 bar (based on mole%) (b) x_M^I/x_{MO}^I vs. x_G^I/x_{MO}^I in methyl oleate-rich phase —; ASTM D-6751-02 ——; x_G^I, x_M^I and x_{MO}^I are mole fractions of glycerol, methanol and methyl oleate in methyl oleate-rich phase, respectively.

4.3 Methods

4.3.1 Phase equilibria calculations

The fugacity-matching method developed by Bunz et. al. (1991) and Nelson (1987) was employed to determine the multi-component, multi-phase equilibria compositions at 20°C and atmospheric pressure. As part of this method, a stability test was carried out to indicate the number and nature of the phases at equilibrium (Bunz et al., 1991; Nelson, 1987). The fugacity-matching method can handle up to three co-existing phases at equilibrium, one vapor and two liquid phases. The material balance, the $\gamma - \phi$ equations (Smith et al., 1996) along with the SRK equation of state for predicting the vapor phase properties (Holderbaum and Gmehling, 1991; Walas, 1985) were employed for the phase equilibria calculations. To predict the properties of the liquid phases, the UNIFAC group contribution method of Magnussen et al. (1981) was used. This choice was made because of the reasonable phase equilibria predictions of the UNIFAC activity coefficient model for the quaternary system of methyl oleate, glycerol, hexane and methanol, as studied in Chapter 3 (Paper 1) of this thesis. By developing the necessary computer codes in MATLAB® (version 7.1.0.246, R14 developed by MathWorks Inc.) and employing an appropriate nonlinear optimization solver, the composition and physical properties of the co-existing phases at equilibrium were determined for every given overall composition. The quantity of the components in the vapor phase was found to be negligible over the entire composition range used for the extraction systems under investigation. Therefore, the system was assumed to contain only two liquid phases at equilibrium. A detailed description of the multicomponent vapor-liquid-liquid equilibria calculations used in this work and some of the codes in MATLAB® are presented in Appendices C and E of this thesis, respectively.

4.3.2 Design criteria

The technical feasibility of various extraction processes was determined relative to the following criteria:

1. The ratio of the mass of glycerol to the mass of methyl oleate plus that of glycerol in the methyl oleate-rich phase must meet the corresponding ASTM Standard (ASTM D-6751-02, 2002) such that:

$$\frac{M_G^I}{M_{MO}^I + M_G^I} \leq 0.0002 \tag{4.1}$$

where M_G^I and M_{MO}^I are the masses of glycerol and methyl oleate in the methyl oleate-rich phase, respectively.

2. For effective operation of a mixer-settler system, the volume ratio of the two liquid phases should be close to 1:1. The more equivalent the phase volumes are, the better the contact of the molecules in the mixture, and accordingly, the more effective the mass transfer. In continuous discharge of both top and bottom liquid phases, equivalent phase volumes results in lessened sensitivity of the mixer-settler operation to changes in flow or composition of the inlets. The mathematical expression of this criterion is:

$$\frac{V^I}{V^{II}} \approx 1 \tag{4.2}$$

where V^I and V^{II} are the volumes of phase *I* (methyl oleate-rich phase) and phase *II* (glycerol-rich phase), respectively. This criterion was implemented as a soft inequality constraint as following:

$$\max\left\{\frac{V^I}{V^{II}}, \frac{V^{II}}{V^I}\right\} - n \leq 0 \tag{4.3}$$

where n represents an upper limit for the phase ratio. For instance, when n is equal to five, the phase volume ratio will be less than 5:1.

3. A highly effective extraction process is a system with a low loss of methyl oleate in the glycerol-rich phase, which can be expressed as $M_{MO}^{II}/\left(M_{MO}^{II} + M_{MO}^{I}\right)$, where

M_{MO}^{I} and M_{MO}^{II} denote the mass of methyl oleate in phases *I* and *II*, respectively. This quantity was used as one of the performance measures.

4. The size of the settler unit depends largely on the residence time of the phases in the settler. The shorter the liquid residence time, the smaller the settler. The residence time is expressed as:

$$T = 0.1\left[\frac{\mu}{\rho_b - \rho_t}\right] \tag{4.4}$$

where T is the residence time in hours, μ is the viscosity of the continuous phase (methyl oleate-rich phase) in cp and ρ_b and ρ_t are the specific gravities of the bottom phase and top phases, respectively (Branan, 2002). Any decrease in the viscosity of the methyl oleate-rich phase or increase in the difference between the densities of the two liquid phases results in reduction of the residence time. Minimization of T was also an element of the performance measure.

5. Since water may be used as a solvent, some residual water may appear in the methyl oleate-rich phase. Consequently, it must be minimized to simplify the removal of water after the extraction unit to achieve the relevant ASTM Standard of the water content of biodiesel (<0.050 volume% or 0.12 wt% of water in biodiesel at normal temperature and pressure). This criterion is expressed as following:

$$\min\left\{\frac{M_W^I}{M_{MO}^I}\right\} \tag{4.5}$$

where M_W^I and M_{MO}^I are the masses of water and methyl oleate in the methyl oleate-rich phase, respectively.

4.3.3 Optimization method

In order to determine the optimal relative ratios of the extraction solvents (hexane, methanol and/or water), the performance measures and constraints, presented in Section 4.3.2, were coded in MATLAB® and solved by means of a nonlinear multi-objective solver (i.e., fgoalattain). This multi-objective optimization routine simultaneously minimizes a set of performance measures by sequential quadratic programming (SQP). The formulation for this problem was the goal attainment problem of Gembicki (Gembicki, 1974). This entailed the specification of goals for each performance measure (MATLAB® Help, 2005). The performance measures to be minimized were the criteria 3, 4 and 5 of the Design criteria (Section 4.3.2) and introduced to the code as follow:

$$\underline{F}(\underline{x}) - \underline{weight}.\gamma \leq \underline{goal} \tag{4.6}$$

In this implementation, the slack variable, γ, was used as a dummy argument to minimize the vector of performance measures, *F(x)*, simultaneously, and was introduced to the optimization problem by the solver itself. *goal* was a set of target values that the optimizer attempts to attain. Generally, prior to the optimization, it was not known whether the performance measures would reach the goals (under-attainment) or exceed the goals (over-attainment). A weighting vector, *weight*, controlled the relative under-attainment or over-attainment of the objectives (MATLAB® Help, 2005). In this study, equal weights were introduced to the performance measures.

Besides the minimization of a set of objective functions, this optimizer was capable of handling constraints, such as criteria 1 and 2 of the Design criteria (Section 4.3.2). The formulation for such nonlinear constraints is,

$$\underline{C}(\underline{x}) \leq 0 \text{ and } \underline{lb} \leq \underline{x} \leq \underline{ub} \tag{4.7}$$

The vector of the constraints, the glycerol content of the methyl oleate-rich phase and the liquid phase volume ratio, were defined as *C(x)* and *lb* and *ub* were the lower bound

and upper bounds of the variables x, respectively. The vector of variables, $\underline{x}$, contained three elements, which were the mole ratios of each hexane, methanol and water, to the methyl oleate fed initially into the extractor.

4.4 Results and discussion

4.4.1 Methanol alone as the solvent

When methanol alone is employed as the extraction solvent, the ASTM Standard for glycerol content in biodiesel is met at a methanol to methyl oleate mass ratio of 0.243 (Figure 4.2). Because of the high solubility of glycerol in methanol, which can be seen from the ternary phase diagram of methyl oleate/glycerol/methanol (Figure 4.1), the more methanol added, the better the separation of glycerol and methyl oleate would be. This ternary system forms two liquid phases for a large range of overall compositions; mostly methyl oleate and some methanol in one phase and glycerol and methanol in the other phase (Figure 4.1). As shown in Figure 4.2, on adding methanol to this ternary mixture, the quantity of glycerol in the in methyl oleate-rich phase reduces to significantly lower values than the relevant ASTM Standard value of 0.0002 (Figure 4.2). However, when the concentration of methanol in the ternary mixture of methyl oleate, glycerol and methanol becomes very large, there is a chance of formation of a single liquid phase (Figure 4.1).

The phase volume ratio becomes closer to unity by adding more methanol to the reaction mixture, since most of the methanol remains in the glycerol-rich phase. The recovery of methyl oleate[1] was found to be in the range of 96-99% and decreases to 96% on adding methanol solvent.

[1] The recovery of methyl oleate (i.e. biodiesel) is defined as the ratio of the mass of methyl oleate in the methyl oleate-rich phase to the initial mass of methyl oleate fed to the mixer. Due to the small changes in the recovery of methyl oleate using the solvents under study, it is not shown in the figures.

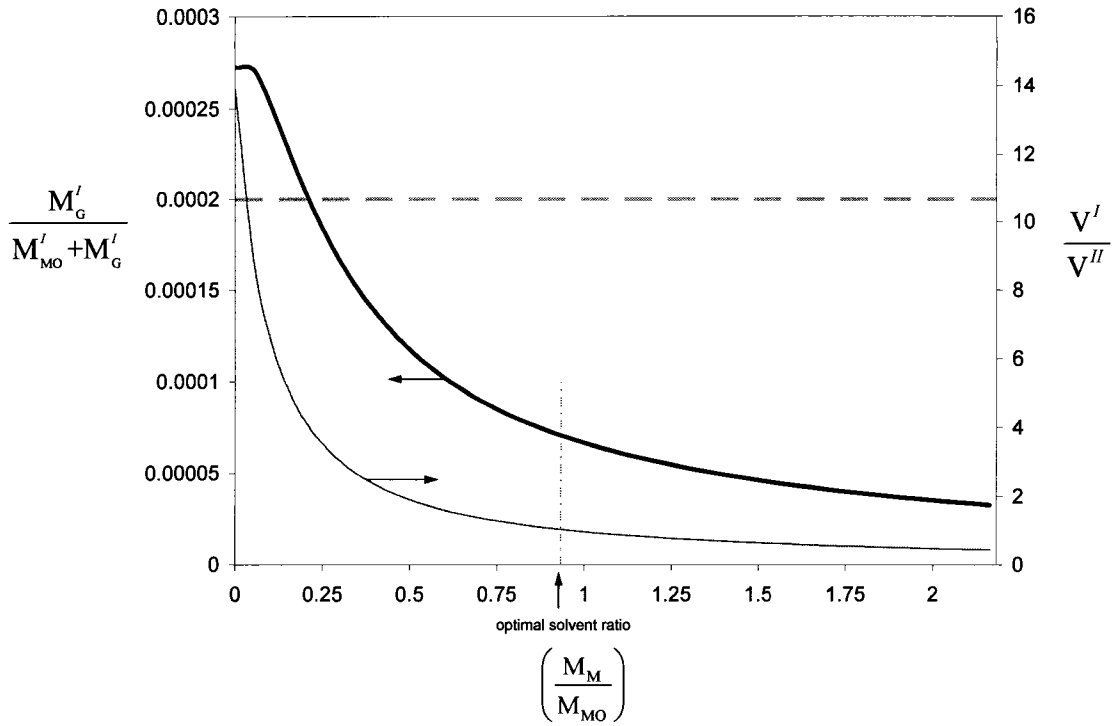

(a)

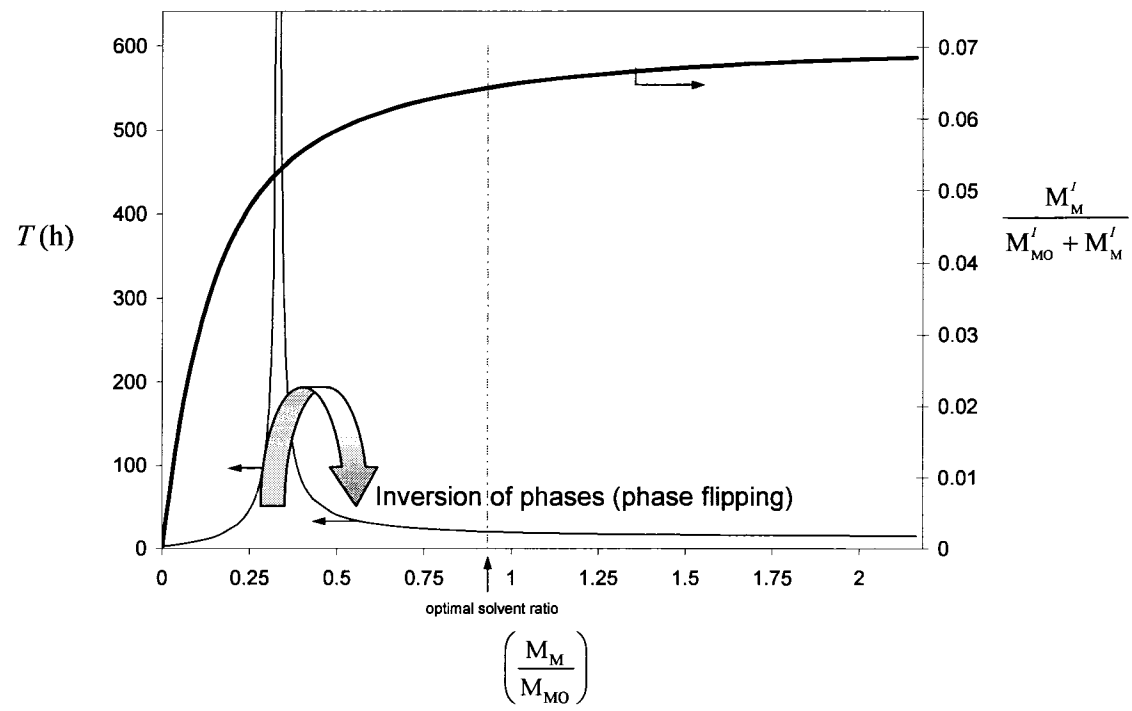

(b)

Figure 4.2 Effects of addition of methanol for (M_G/M_{MO})=0.104 :

(a) $M_G^I/(M_{MO}^I+M_G^I)$ —; ASTM D-6751-02 – –; V^I/V^{II} —

(b) $M_M^I/(M_{MO}^I+M_M^I)$ —; Residence time in the settler (T) —

While methanol as a solvent for glycerol seems to be a good choice, at a methanol-to-methyl oleate mass ratio of ~0.3, the difference between the densities of the top and bottom phases approaches zero, the liquid residence time in the settler increases to an infinite value and the phase separation becomes practically impossible without any specific apparatus, such as a centrifuge (Figure 4.2). After that point, phase inversion (i.e., phase flipping) occurs on adding more methanol and the residence time decreases to a minimum of ~15 h. The inversion of phases occurs because of the presence of the methanol solvent in the mixture that results in a decreased density of the glycerol-rich phase, which originally has a greater density than methyl oleate-rich phase (Table 4.1). From the practical point of view, in order to have the extractor in a steady state operation, it is desired to be far from the phase flipping region (methanol to methyl oleate mass ratio of 0.2 to 0.5 as shown in Figure 4.2).

Table 4.1 Density and viscosity of the components involved in the extractor

Components	Density*$_{@20°C}$ (gr/cm^3)	Viscosity$_{@20°C}$ (cP)
Feed:		
methyl oleate	0.874	8.307
glycerol	1.262	92.10
methanol	0.791	0.577
Solvents:		
hexane	0.659	0.310
water	1.008	1.025

* given by Sigma-Aldrich

Table 4.2 contains the phase separation properties for the optimal quantity of methanol, which is the mass ratio of methyl oleate:methanol of 1:0.93 (equivalent to the mole ratio of 1:8.63). For this tieline, the calculated residence time is ~20 h, which is relatively lengthy. The recovery of methyl oleate for the optimal solvent ratio was found to be ~99%.

Table 4.2 Phase separation properties for the optimal quantity of methanol as the extraction solvent, $(M_M/M_{MO})=0.933$, when $(M_G/M_{MO})=0.104$

Components	Overall mole fraction	Overall mass fraction	Mole fraction phase *I*	Mole fraction phase *II*	Mass fraction phase *I*	Mass fraction phase *II*	$\frac{V^I}{V^{II}}$	Density phase *I* $\left(\frac{gr}{cm^3}\right)$	Density phase *II* $\left(\frac{gr}{cm^3}\right)$
methyl oleate	0.1003	0.4909	0.6108	0.0012	0.9355	0.0102			
glycerol	0.0336	0.0511	0.0001	0.0401	0.0001	0.1063	1.04	0.811	0.842
methanol	0.8661	0.4580	0.3891	0.9587	0.0644	0.8835			

To conclude, although methanol is capable of separating glycerol from methyl oleate, it is not a suitable solvent due to the lengthy residence time it needs for separation of the liquid phases in the settler. Furthermore, because of the phenomenon of phase flipping and the chance of formation of a single liquid phase at high methanol concentrations, one should be cautious in choosing methanol as the only extraction solvent for the separation of glycerol from biodiesel.

4.4.2 Water-methanol as the solvent

Figure 4.3 shows the changes in the content of glycerol in the methyl oleate-rich phase, $M_G^I/(M_G^I+M_{MO}^I)$, and the phase volume ratio, V^I/V^{II}, on adding water solvent to the feed mixture, which contains methyl oleate, glycerol and methanol. The glycerol content in the methyl oleate-rich phase is decreased as the quantity of water is increased. Because glycerol has a much higher solubility in water than in methyl oleate, even small amounts of water, methyl oleate:methanol:water mass ratio of 1:0.104:0.007 (equivalent to mole ratio of 1:0.96:0.12), leads to achieving the ASTM-based separation of glycerol and methyl oleate (Figure 4.3). Concerning the phase volumes, since water dissolves in the glycerol-rich phase, which initially has a smaller volume compared to the methyl oleate-rich phase, addition of water will equalize the volumes of the liquid phases. The recovery of methyl oleate by water washing remains roughly constant at ~99-100%, making this purification processes a low loss system.

The quantity of water in the methyl oleate-rich phase, upon adding water, increases slightly to a constant value of $M_W^I/\left(M_{MO}^I + M_W^I\right)$=0.001 (Figure 4.3). The methanol content in the methyl oleate-rich phase $\left(M_M^I/M_{MO}^I + M_M^I\right)$ decreases on adding water to the system, to a minimum of ~0.003. The small quantities of water and methanol remaining in the methyl oleate-rich phase can easily be removed by flash evaporation at reduced pressure.

Since water dissolves in the glycerol/methanol phase (usually the bottom phase, when methanol to methyl oleate mass ratio is constant at 0.104), its addition results in an increase in the density of the bottom phase and a greater difference between the densities of the top and bottom phases (Table 4.3). Consequently, the residence time is reduced to a minimum of ~5½ hours (Figure 4.3).

From the discussion above, it can be seen that water, mixed with some methanol (which already exists in the reaction mixture), is a very good solvent for glycerol. However, the relatively lengthy residence time in the settler indicates this mixed solvent is not the ultimate choice. Moreover, the formation of emulsions in alkali-catalyzed transesterification of waste cooking oil becomes more problematic in presence of water. The properties of the two phases separated for the optimal methyl oleate:methanol:water mass ratio of 1:0.104:0.973 (equivalent to the mole ratio of 1:0.96:16.02), which satisfies the design criteria, is shown in Table 4.3. For the optimal tieline, the liquid residence time in the settler and the recovery of methyl oleate are 5.4 h and ~100%, respectively. Although this solvent shows to satisfy all the design objectives, due to the chance of formation of a single phase at high water concentrations and also formation of emulsions due to soaps in alkali-catalyzed transesterification of waste cooking oil, its use in alkali-catalyzed transesterification of waste cooking oil should be conducted with specific considerations.

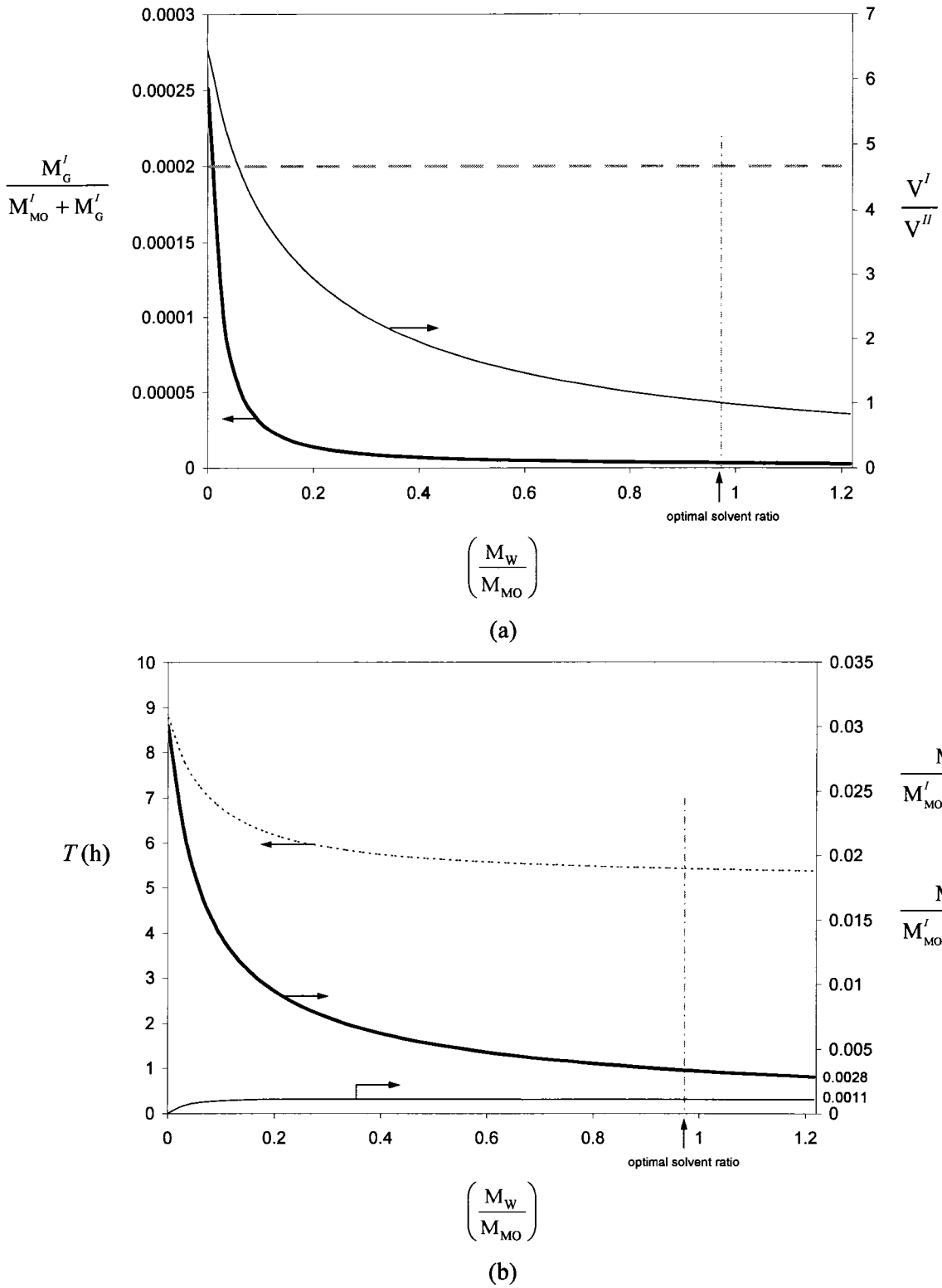

Figure 4.3 Effects of addition of water for (M_M/M_{MO})=0.104 and (M_G/M_{MO})=0.104 :
(a) $M_G^I/(M_{MO}^I + M_G^I)$ —; ASTM D-6751-02 — —; V^I/V^{II} —
(b) $M_M^I/(M_{MO}^I + M_M^I)$ —; $M_W^I/(M_{MO}^I + M_W^I)$ —; Residence time in the settler (T) ....

Table 4.3 Phase separation properties for the optimal quantity of water solvent, $(M_W/M_{MO}) = 0.973$, when $(M_M/M_{MO}) = 0.104$ and $(M_G/M_{MO}) = 0.104$

Components	Overall mole fraction	Overall mass fraction	Mole fraction phase *I*	Mole fraction phase *II*	Mass fraction phase *I*	Mass fraction phase *II*	$\frac{V^I}{V^{II}}$	Density phase *I* $\left(\frac{gr}{cm^3}\right)$	Density phase *II* $\left(\frac{gr}{cm^3}\right)$
methyl oleate	0.0546	0.4584	0.9529	0.0000	0.9955	0.0000	~1	0.874	1.024
glycerol	0.0183	0.0477	0.0000	0.0194	0.0000	0.0884			
methanol	0.0525	0.0476	0.0298	0.0539	0.0034	0.0854			
water	0.8746	0.4463	0.0173	0.9267	0.0011	0.8262			

Complete removal of methanol from the mixture leaving the reactor before the extraction unit was also considered. When water is used as the only solvent, with no methanol in the stream entering the mixer, the ASTM Standard for glycerol content in biodiesel is met at the methyl oleate:water mass ratio of 1:0.009. This ratio is slightly higher than the ratio found when some methanol remains in the feed (Figure 4.3), because of the fact that methanol was also found to be a good solvent for glycerol. In the absence of methanol, adding water to the mixture of glycerol and methyl oleate leads to the reduction in the density of the glycerol-rich phase and therefore an increase in the residence time (Table 4.1). In this case, the phase volume ratio, V^I/V^{II}, decreases to ~0.9, the water content of the methyl oleate-rich phase, $M_W^I/\left(M_W^I + M_{MO}^I\right)$, increases to 0.0010 and the recovery of methyl oleate remains almost constant at 99% on increasing the quantity of water solvent to the mass ratio of $(M_W/M_{MO}) = 1.2$.

4.4.3 Hexane-methanol as the solvent

The ASTM Standard for biodiesel is never met by adding hexane as the extraction solvent, and the quantity of glycerol in the methyl oleate-rich phase increases on adding hexane solvent to the feed mixture (Figure 4.4). Mainly due to partial miscibility of methanol in hexane and complete miscibility of glycerol in methanol, the more hexane added, the more methanol and accordingly, more glycerol enters the hexane-rich phase. This miscibility continues to the point where at very high concentration of hexane, for

example at overall mass fraction of methyl oleate:glycerol:hexane:methanol of 0.0170:0.0053:0.9758:0.0018 a single liquid phase is formed.

The ratio of the phase volumes is increased significantly by adding hexane to the reaction mixture. This is due to the fact that methyl oleate ($1.06\ m^3/kmol$) and hexane ($0.368\ m^3/kmol$) molecules, which form one phase, are larger in size compared to glycerol ($0.255\ m^3/kmol$) and methanol ($0.127\ m^3/kmol$). The recovery of methyl oleate remains roughly constant at ~99% and the quantity of methanol in the methyl oleate-rich phase, $M_M^I/\left(M_{MO}^I + M_M^I\right)$, increases to the value of ~0.08 on adding hexane solvent (Figure 4.4).

The major advantage of hexane as the extraction solvent in this system is the significant reduction in the residence time it causes (Figure 4.4). The residence time decreases to 0.10 h on adding hexane up to 5.8 times more than methyl oleate on a mass basis (Figure 4.4). Hexane decreases the density of the methyl oleate-rich phase, which is the upper phase. It also decreases the viscosity of the methyl oleate-rich phase, as the continuous phase and results in an easier and faster separation of the two liquid phases in the settler (Equation 4.4 and Table 4.1).

It can be concluded that even in presence of some methanol in the feed stream entering the mixer, which acts as a solvent for glycerol, neither the ASTM Standard for glycerol content of biodiesel is met, nor the similar phase volume ratio is achieved; however, the liquid residence time in the settler decreases significantly on adding hexane solvent to the feed mixture.

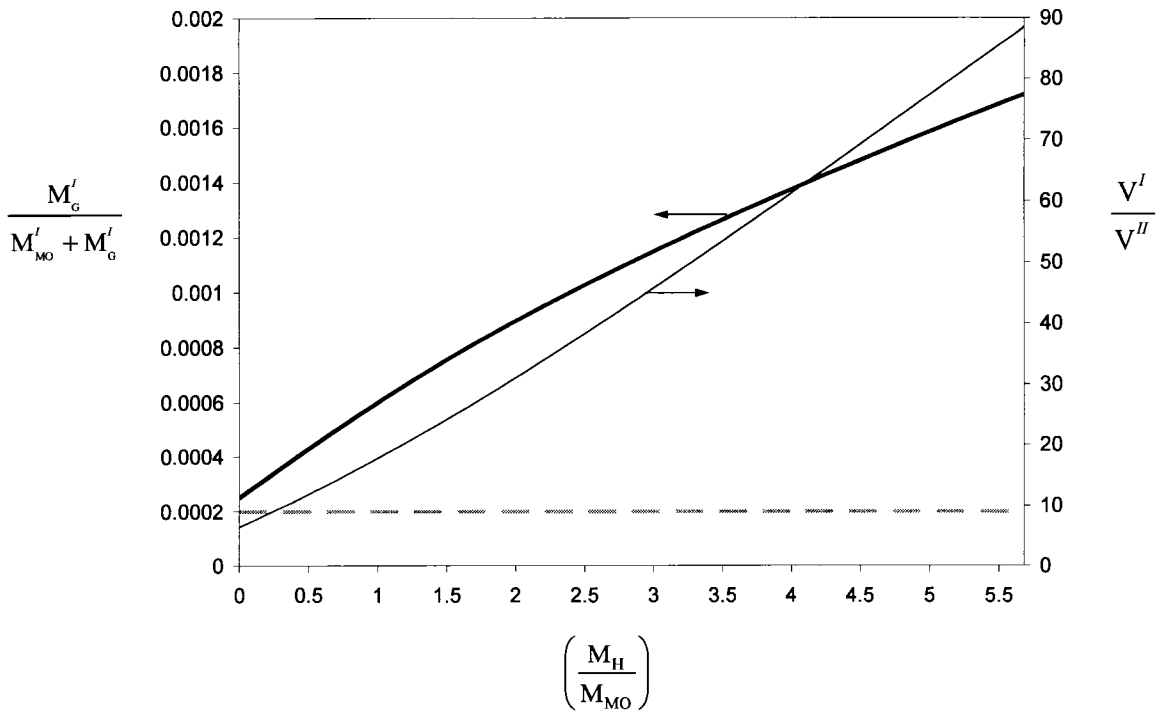

(a)

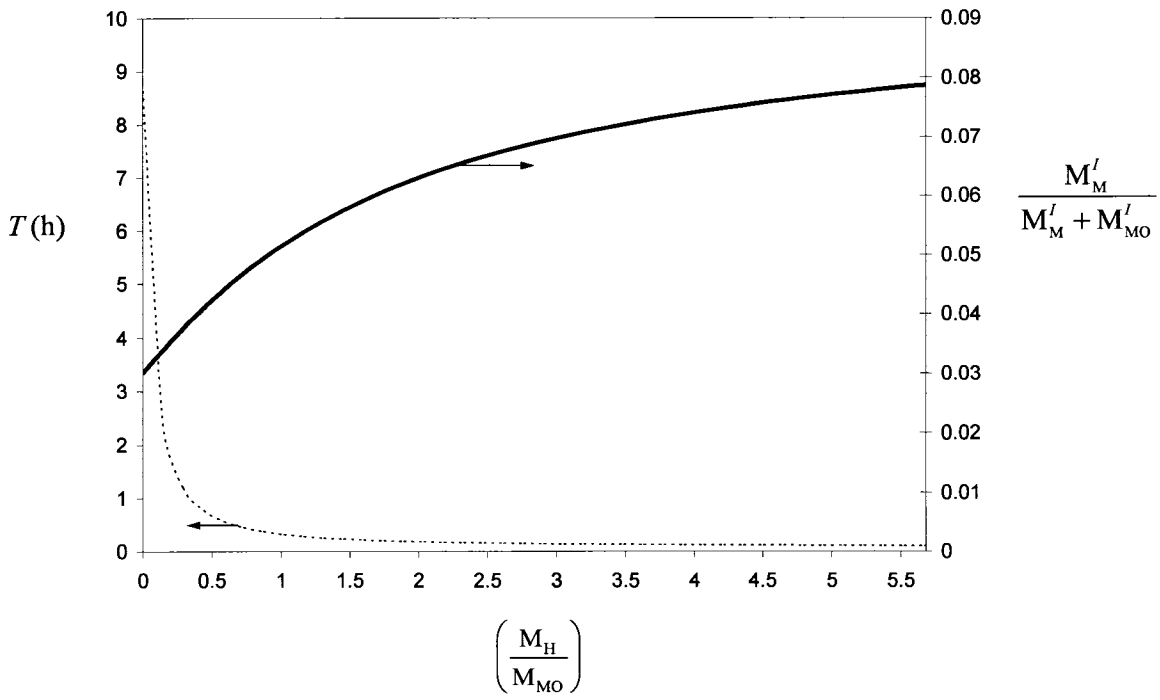

(b)

Figure 4.4 Effects of addition of hexane for (M_G/M_{MO})=0.104 and (M_M/M_{MO})=0.104 :

(a) $M_G^I/\left(M_{MO}^I + M_G^I\right)$ —; ASTM D-6751-02 — —; V^I/V^{II} —

(b) $M_M^I/\left(M_{MO}^I + M_M^I\right)$ —; Residence time in the settler (T) ....

Figure 4.5 shows the effects of addition of hexane on the quantity of glycerol remaining in the methyl oleate-rich phase and on the liquid residence time if the excess methanol were completely distilled off prior to the extraction. Again, the ASTM Standard for glycerol content of biodiesel is not met and the phase volumes are very different. However, because of the absence of methanol, the liquid residence time in the settler decreases to a slightly lower value of 0.07 h (Figure 4.5), compared to the liquid residence time of 0.10 h in Figure 4.4.

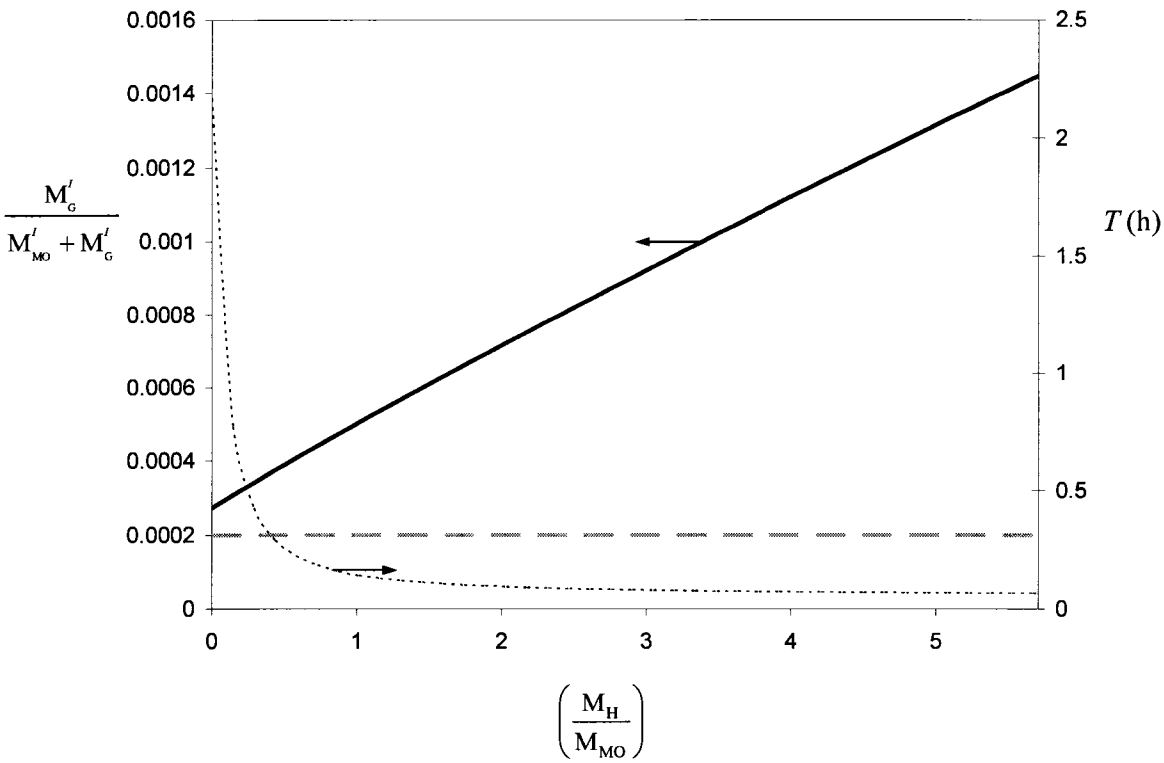

Figure 4.5 Effect of addition of hexane for (M_G/M_{MO})=0.104 and (M_M/M_{MO})=0: $M_G^I/(M_{MO}^I + M_G^I)$ —; ASTM D-6751-02 — —; Residence time in the settler (T) ....

From the previous discussions in Section 4.4 about the use of methanol, water or hexane as solvent, it can be concluded that the ASTM Standard for biodiesel, which is the key performance measure for this separation, is never met when hexane, alone or with residual methanol in the stream entering the extractor, is used as the solvent. When water

or methanol alone is the solvent, the ASTM Standard is satisfied. However, a major drawback of the use of water or methanol solvents is the relatively high residence times in the settler (>15 h and >5½ h for methanol and water, respectively), which necessitates a large settler. On the other hand, hexane was shown to require a much shorter time for separation of the two liquid phases, compared to methanol or water (~10 min). Hence, in order to simultaneously reduce the residence time and meet the ASTM Standard, a mixture of methanol and hexane or water and hexane or all the three can be employed as solvent.

Due to the relatively lengthy residence time of the liquid phases in the settler, when methanol alone or water alone is used as extraction solvent, a mixture of them as a dual solvent without any hexane is not considered a practical alternative.

4.4.4 Methanol and hexane as a dual solvent

Due to the merits of hexane in dissolving methyl oleate and reducing the liquid residence time in the settler, and that of methanol in effectively dissolving glycerol, the potential of a mixture of hexane and methanol, for separation of glycerol and methyl oleate was studied. The glycerol content in the methyl oleate-rich hexane phase and the ratio of the liquid phase volumes, are shown in Figure 4.6. As the level of methanol increases, the amount of glycerol in the methyl oleate-rich phase increases and then declines, the extent of these changes increases at higher hexane levels. The ASTM Standard for glycerol is achieved only at relatively low levels of hexane and high levels of methanol. Since hexane and methanol remain in the methyl oleate-rich and glycerol-rich phases, respectively, the more methanol and less hexane added, the more equal the volumes of the two liquid phases become (Figure 4.6).

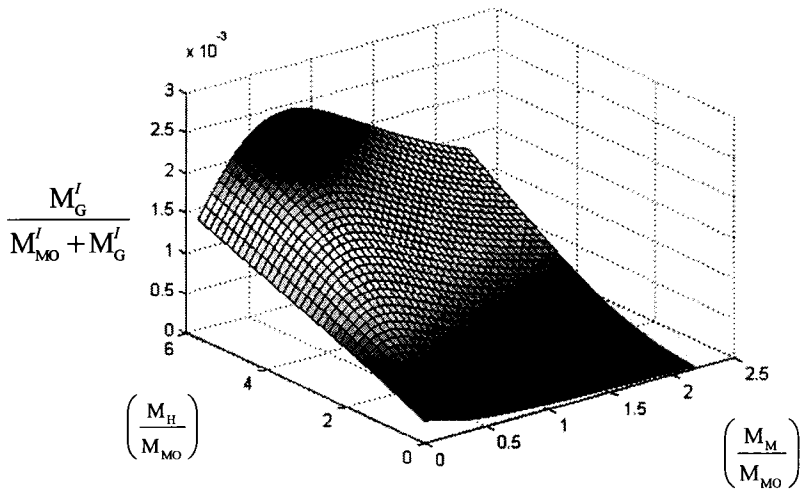

(a)

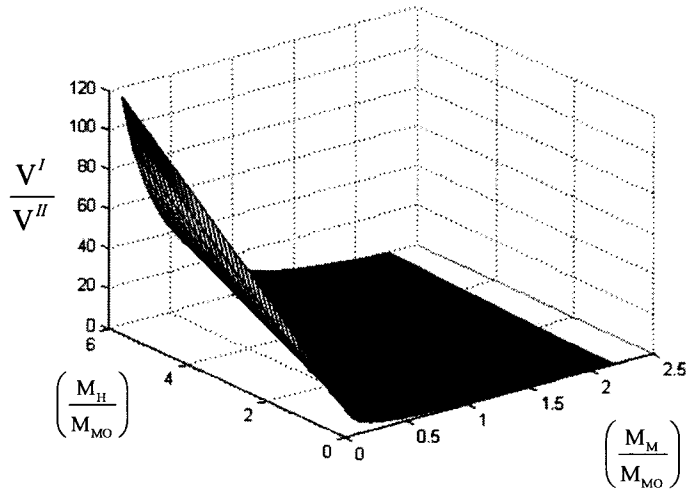

(b)

Figure 4.6 Effect of methanol and hexane solvents for (M_G/M_{MO})=0.104 on:
(a) $M_G^I/(M_{MO}^I + M_G^I)$; (b) V^I/V^{II}

Given that the most important separation criterion is achieving the ASTM Standard for glycerol content of biodiesel, the term $M_G^I/(M_{MO}^I + M_G^I)$ was set at the maximum allowable standard value of 0.02 wt%, and the minimum required mass ratios of methanol to methyl oleate for the given mass ratios of hexane to methyl oleate were calculated and plotted in Figure 4.7, while the mass of glycerol to methyl oleate in the feed was fixed at 0.104. The corresponding liquid volume ratios and the residence time of the liquid phases in the settler, for different quantities of hexane are shown in Figure 4.7.

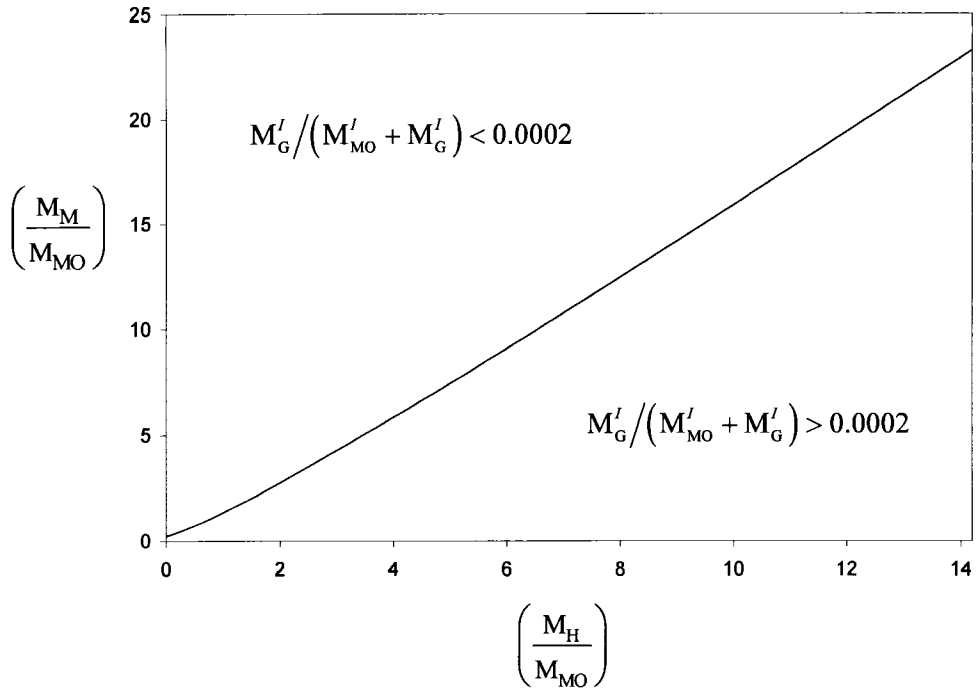

(a)

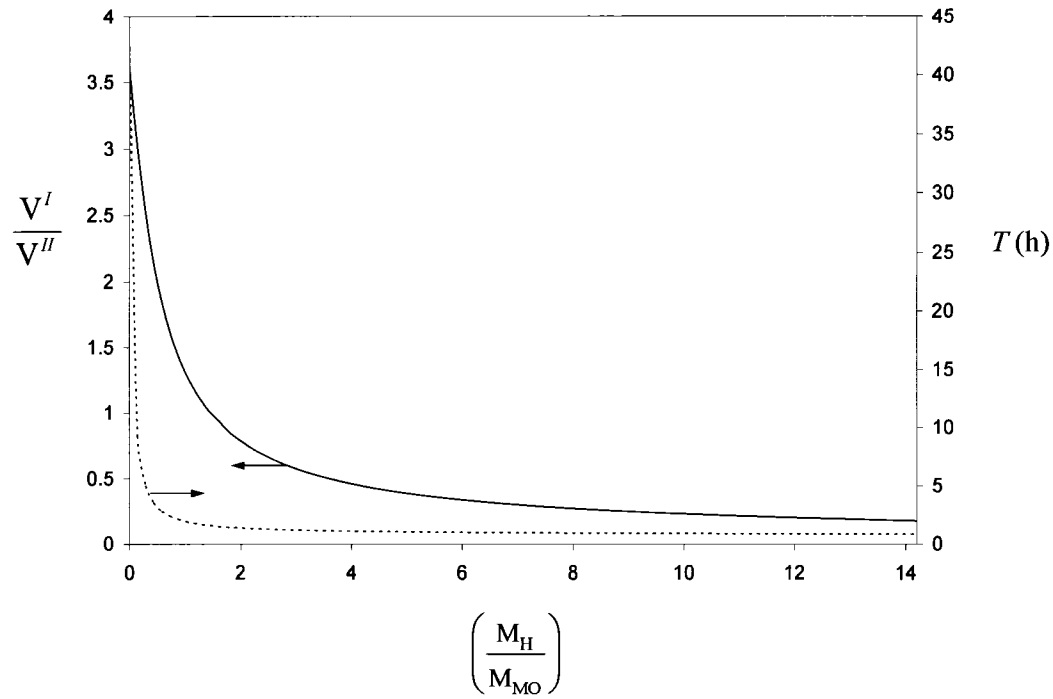

(b)

Figure 4.7 For (M_G/M_{MO})=0.104, (a) The required quantity of methanol for given quantities of hexane to meet the ASTM D-6751-02$(M_G^I/M_G^I + M_{MO}^I = 0.0002)$, (b) The ratio of the liquid phase volumes and residence time for varying quantities of hexane

The quantities of hexane and methanol as a dual solvent were also optimized to satisfy the separation objectives. The optimal quantities of methyl oleate:hexane:methanol on a mass basis was found at 1:1.15:1.62 (equivalent to the mole ratio of 1:3.97:15.01) for $(M_G/M_{MO}) = 0.104$. The composition and some physical properties of the separated phases, for the optimum point are shown in Table 4.4. The corresponding residence time of the liquid phases in the settler and methyl oleate recovery are 1.82 h and 98%, respectively. The slightly lower recovery of methyl oleate compared to other solvents is because of slightly higher quantity of methanol or the absence of water, which results in considerably low miscibility of methyl oleate in the glycerol-rich phase.

Table 4.4 Phase separation properties for the optimal quantity of methanol and hexane as a dual solvent, when $(M_G/M_{MO}) = 0.104$

Components	Overall mole fraction	Overall mass fraction	Mole fraction Phase *I*	Mole fraction Phase *II*	Mass fraction Phase *I*	Mass fraction Phase *II*	$\frac{V^I}{V^{II}}$	Density phase *I* $\left(\frac{gr}{cm^3}\right)$	Density phase *II* $\left(\frac{gr}{cm^3}\right)$
methyl oleate	0.0492	0.2576	0.1813	0.0011	0.4926	0.0095	1.13	0.736	0.793
glycerol	0.0165	0.0268	0.0001	0.0225	0.0001	0.0552			
hexane	0.1954	0.2974	0.5382	0.0709	0.4250	0.1627			
methanol	0.7389	0.4182	0.2804	0.9055	0.0823	0.7726			

4.4.5 Hexane and water as a dual solvent

When hexane and water are employed as a dual solvent, with no methanol in the mixture, the quantity of glycerol in the methyl oleate-rich phase, $M_G^I/(M_{MO}^I + M_G^I)$, the ratio of the phase volumes, V^I/V^{II}, and the liquid residence time in the settler, *T*, are shown in Figure 4.8. Due to the high miscibility of glycerol in water, the separation of glycerol and methyl oleate is enhanced on adding water to the mixture. In terms of the phase volume ratio, the more water and less hexane, the more equal the phase volumes become.

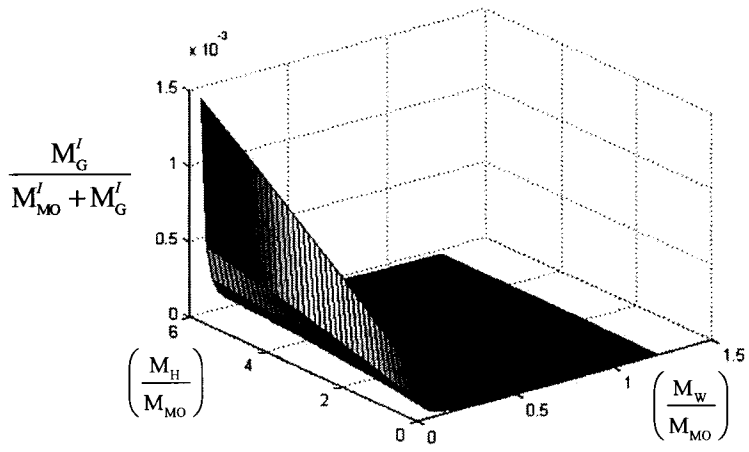

(a)

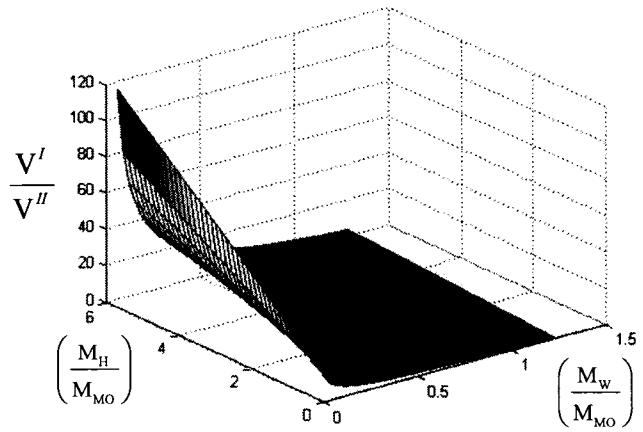

(b)

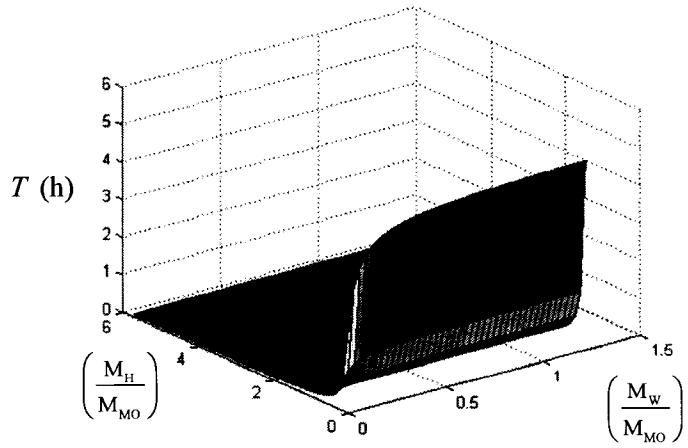

(c)

Figure 4.8 The effect of water and hexane solvents for (M_G/M_{MO})=0.104 and (M_M/M_{MO})=0 on: (a) $M_G^I/\left(M_{MO}^I + M_G^I\right)$; (b) V^I/V^{II} ; (c) Residence time in the settler (T)

Although, in the presence of some methanol in the feed to the extractor, water reduces the liquid residence time (Figure 4.3), in the absence of methanol, adding water results in a relatively lower density of the glycerol-rich phase and therefore, a slight increase in the liquid residence time in the settler (Table 4.1 and Figure 4.8). The residence time is decreased on adding hexane, due to the reduction in the density and viscosity of the methyl oleate-rich phase (Table 4.1, Figures 4.5 and 4.8).

For the fixed glycerol quantity of $(M_G/M_{MO}) = 0.104$ in the feed stream entering the mixer and different mass ratios of hexane to methyl oleate, the minimum quantity of water required to meet the ASTM Standard of the glycerol content of biodiesel and the corresponding ratios of the liquid phase volumes as well as the liquid residence time in the settler were determined and shown in Figure 4.9.

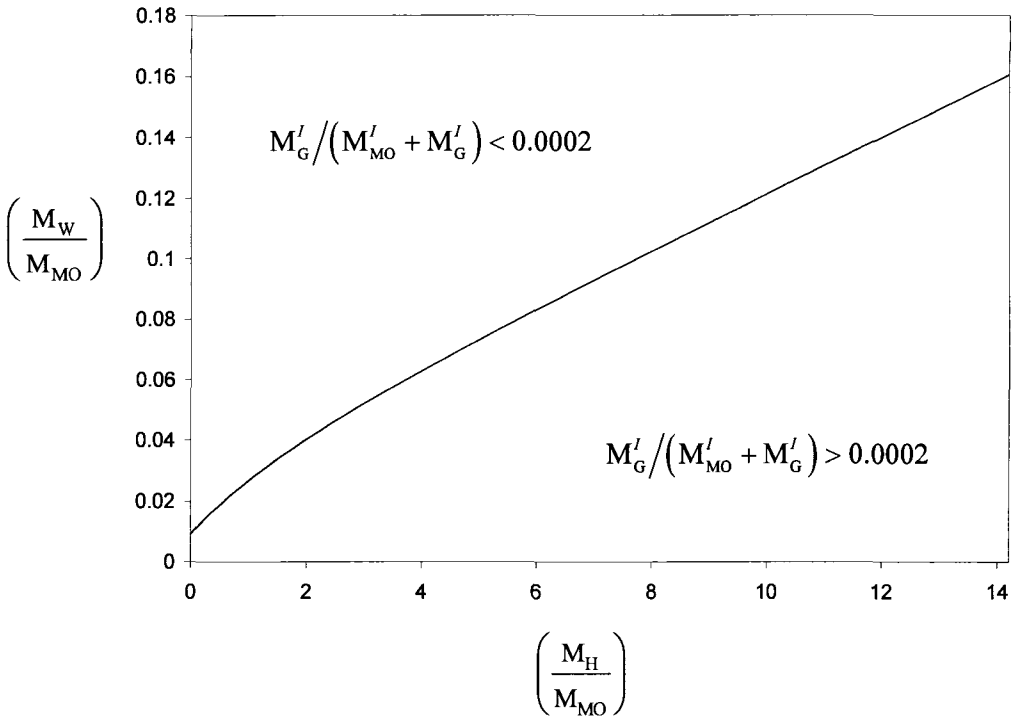

(a)

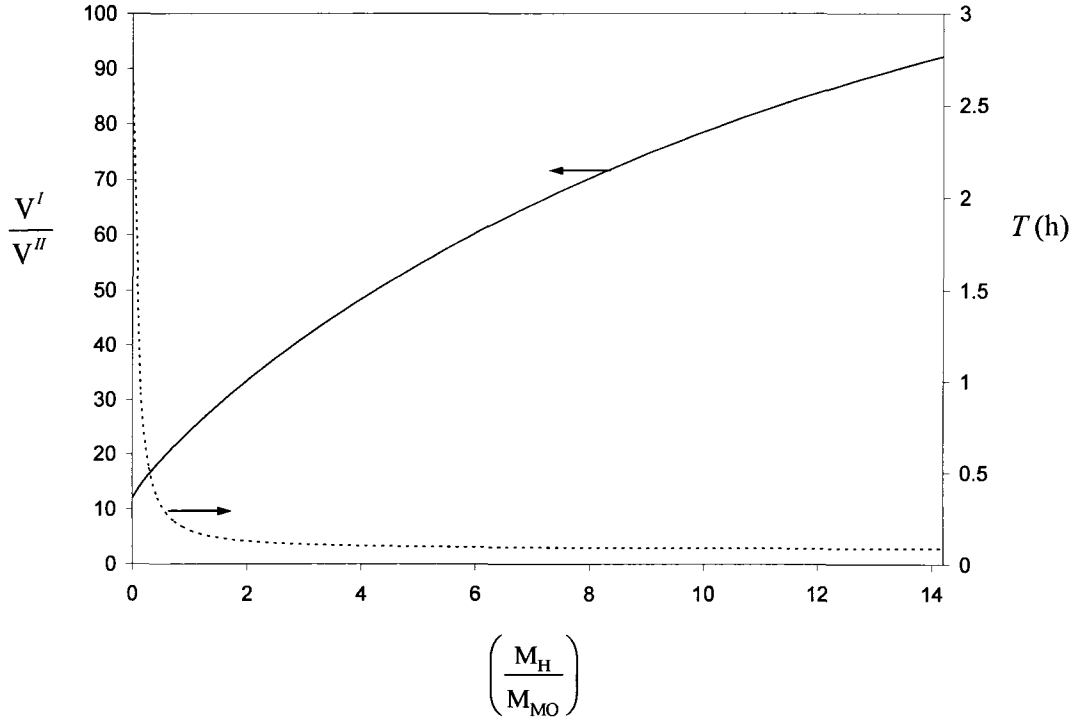

(b)

Figure 4.9 For (M_G/M_{MO})=0.104 and (M_M/M_{MO})=0, (a) The required quantity of water for given quantities of hexane to meet the ASTM D-6751-02$(M_G^I/M_G^I + M_{MO}^I = 0.0002)$
(b) The ratio of the liquid phase volumes and residence time for varying quantities of hexane

For the case where no methanol is present, the quantities of hexane and water were optimized to satisfy the extraction objectives simultaneously. The optimized mass ratio of methyl oleate:hexane:water of 1:3.76:1.36 (equivalent to the mole ratio of 1:12.93:22.38) yields a residence time of 0.12 h or ~7.2 min and almost complete recovery of methyl oleate. Table 4.5 contains the properties of the partitioned phases for the optimized quantity of hexane and water solvents.

Table 4.5 Phase separation properties for the optimal quantities of water and hexane as a dual solvent, (M_M/M_{MO})=0 and (M_G/M_{MO})=0.104

Components	Overall mole fraction	Overall mass fraction	Mole fraction phase *I*	Mole fraction phase *II*	Mass fraction phase *I*	Mass fraction phase *II*	$\frac{V^I}{V^{II}}$	Density phase *I* $\left(\frac{gr}{cm^3}\right)$	Density phase *II* $\left(\frac{gr}{cm^3}\right)$
methyl oleate	0.0273	0.1608	0.0717	0.0000	0.2103	0.0000			
glycerol	0.0092	0.0166	0.0000	0.0147	0.0000	0.0709	4.98	0.677	1.035
hexane	0.3528	0.6039	0.9264	0.0001	0.7894	0.0003			
water	0.6107	0.2187	0.0019	0.9852	0.0003	0.9288			

4.4.6 Methanol, water and hexane as a mixed solvent

4.4.6.1 Fixed quantity of methanol

In this case, water and hexane were fed to the extraction unit, while the quantity of methanol entering the extractor remains constant such that (M_M/M_{MO})=0.104. Figure 4.10 shows the quantity of glycerol in the hexane phase, the ratio of the phase volumes and the liquid residence time in the settler. The minimum required quantities of water for varying quantities of hexane that satisfy the ASTM Standard of the glycerol content of biodiesel along with the corresponding residence times and phase volume ratios are shown in Figure 4.11. Due to the limited capability of hexane to achieve the separation of glycerol and methyl oleate, the more hexane added, the more water is required to meet the relevant ASTM Standard.

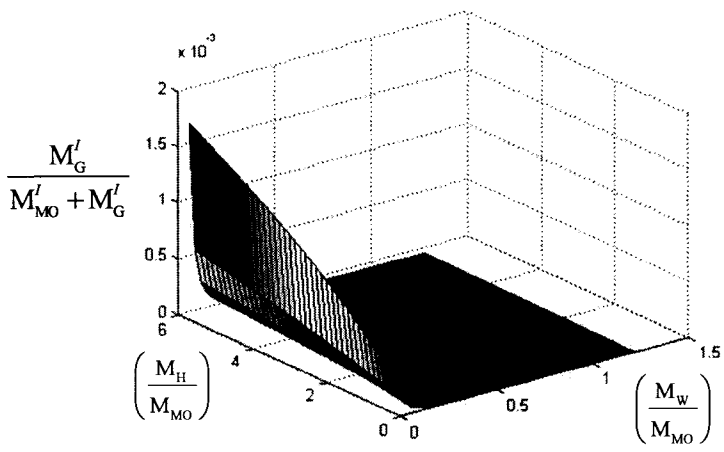

(a)

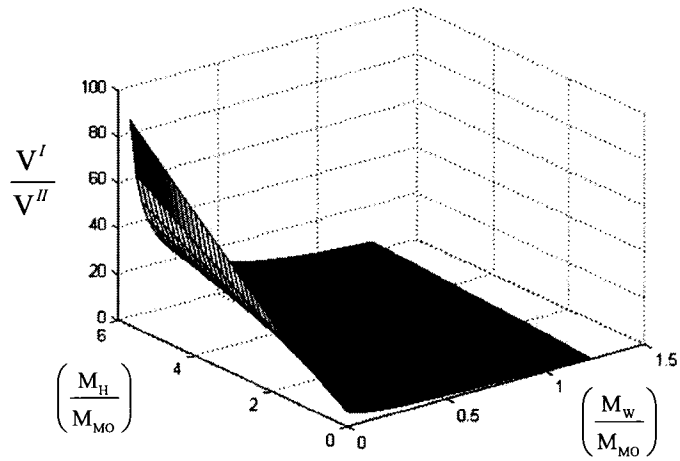

(b)

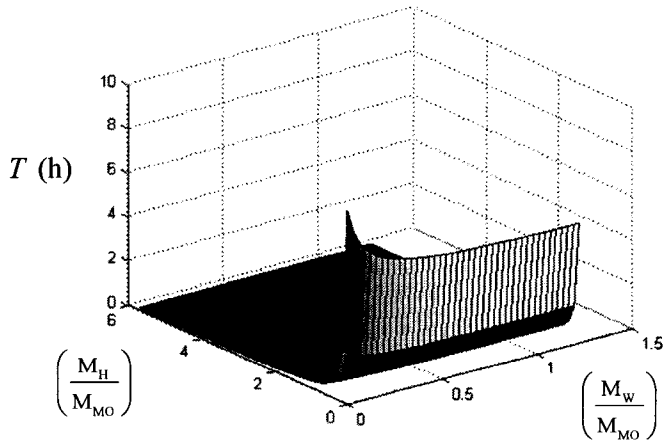

(c)

Figure 4.10 The effect of water and hexane solvents for (M_G/M_{MO})=0.104 and (M_M/M_{MO})=0.104 on: (a) $M_G^I/(M_{MO}^I + M_G^I)$; (b) V^I/V^{II} ; (c) Residence time in the settler (T)

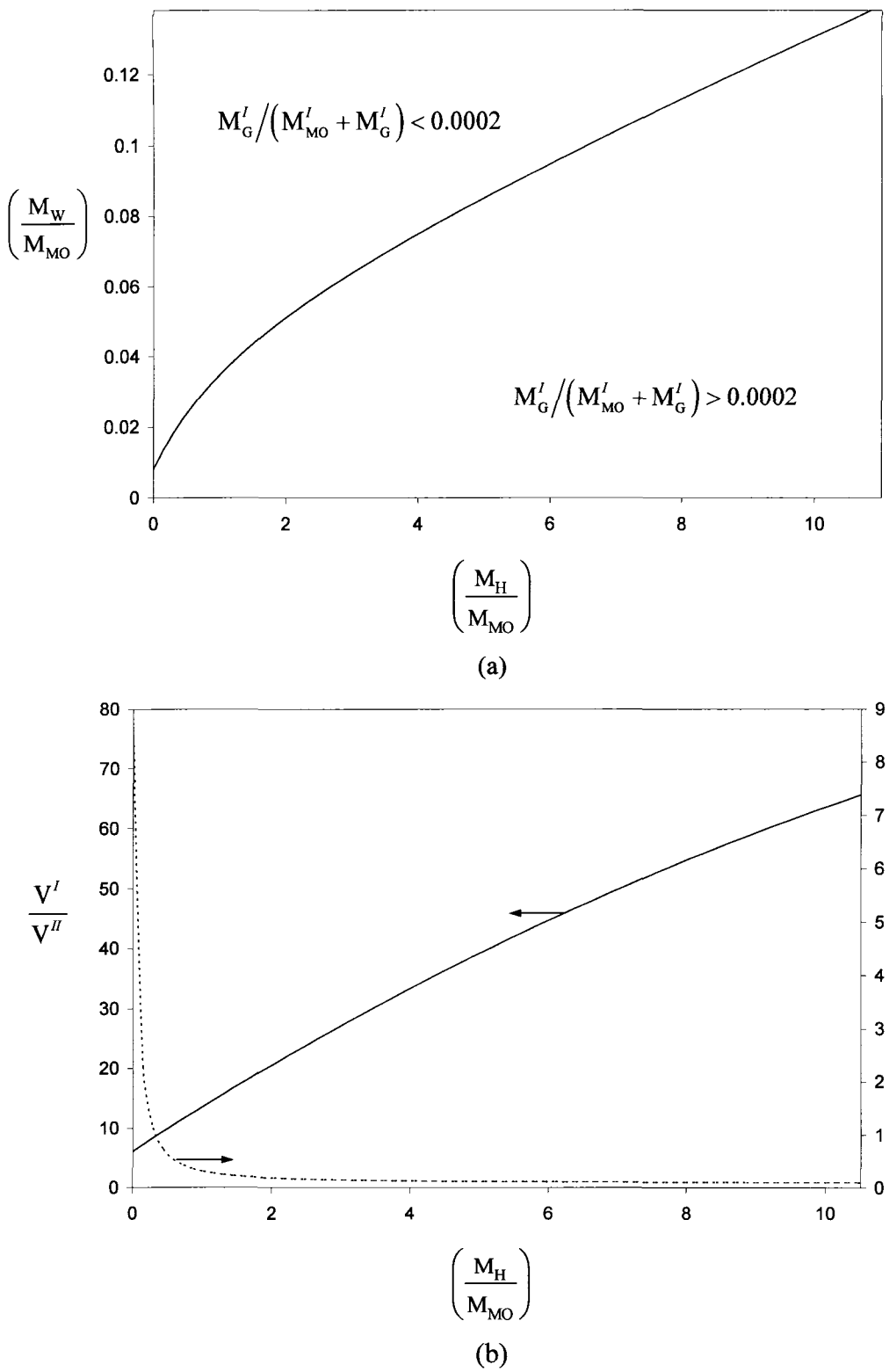

Figure 4.11 For (M_G/M_{MO})=0.104 and (M_M/M_{MO})=0.104, (a) The required quantity of water for given quantities of hexane to meet the ASTM D-6751-02$\left(M_G^I/M_G^I + M_{MO}^I = 0.0002\right)$ (b) The ratio of the liquid phase volumes and residence time for varying quantities of hexane

For the fixed amount of methanol in the mixture fed to the mixer, the mass ratio of methyl oleate:hexane:water of 1:0.79:0.69 (equivalent to the molar ratio of 1:2.74:11.35) was found to be the ratio providing the optimal separation. The compositions and some physical properties of the two liquid phases are given in Table 4.6 with the corresponding liquid residence time of 0.31 h (~19 min) and the ratio of the phase volumes, V^{I}/V^{II}, of 2.87. The recovery of methyl oleate in this case is ~100%.

Table 4.6 Properties of separation for the optimal quantities of water and hexane, when (M_M/M_{MO})=0.104 and (M_G/M_{MO})=0.104

Components	Overall mole fraction	Overall mass fraction	Mole fraction Phase *I*	Mole fraction Phase *II*	Mass fraction Phase *I*	Mass fraction Phase *II*	$\frac{V^{I}}{V^{II}}$	Density phase *I* $\left(\frac{gr}{cm^3}\right)$	Density phase *II* $\left(\frac{gr}{cm^3}\right)$
methyl oleate	0.0610	0.3711	0.2608	0.0000	0.5540	0.0000			
glycerol	0.0205	0.0387	0.0000	0.0268	0.0000	0.1175			
hexane	0.1672	0.2956	0.7140	0.0002	0.4408	0.0009	2.87	0.721	1.021
methanol	0.0586	0.0385	0.0195	0.0705	0.0045	0.1075			
water	0.6927	0.2561	0.0057	0.9025	0.0007	0.7741			

4.4.6.2 Methanol added to the system

When additional methanol is fed to the extractor along with hexane and water as solvents, the mass ratio of methyl oleate:hexane:methanol:water of 1:2.27:0.87:0.30 (equivalent to the mole ratio of 1:7.81:8.05:4.94) provided the optimal separation. The properties of the separated phases for the optimized values of each solvent are presented in Table 4.7. For this optimal tieline, the liquid residence time in the settler was 0.29 h and the ratio of the phase volumes was 3.54. Methyl oleate is almost completely recovered with the optimal composition of the extraction solvent. Comparing this system with the case where the quantity of methanol was fixed, one can observe an increase in the phase volume ratio from 2.87 (Table 4.6) to 3.54 (Table 4.7). This is due to the higher content of hexane required to compensate the reduction in the residence time in the settler, caused by the presence of larger quantity of methanol solvent in the mixture.

Table 4.7 Properties of separation for optimized amounts of methanol, water and hexane as a mixed solvent, when (M_G/M_{MO})=0.104

Components	Overall mole fraction	Overall mass fraction	Mole fraction Phase *I*	Mole fraction Phase *II*	Mass fraction Phase *I*	Mass fraction Phase *II*	$\frac{V^I}{V^{II}}$	Density phase *I* $\left(\frac{gr}{cm^3}\right)$	Density phase *II* $\left(\frac{gr}{cm^3}\right)$
methyl oleate	0.0452	0.2202	0.1027	0.0000	0.2997	0.0001			
glycerol	0.0151	0.0228	0.0000	0.0270	0.0000	0.0861			
hexane	0.3528	0.4995	0.7844	0.0138	0.6654	0.0412	3.54	0.699	0.897
methanol	0.3637	0.1914	0.1077	0.5648	0.0340	0.6265			
water	0.2232	0.0661	0.0052	0.3944	0.0009	0.2461			

To ease the comparison of the optimal solvents found and the values of each performance measure, the optimal compositions of the potential solvents found in the present chapter are summarized in Table 4.8 and the values of the performance measures and constraints for these solvents are presented in Table 4.9.

Table 4.8 Summary of the optimal quantities of the solvents, for (M_G/M_{MO})=0.104

	Methyl oleate	Hexane	Methanol	Water
Solvent 1	1	--	0.93	--
Solvent 2	1	--	0.10	0.97
Solvent 3	1	1.15	1.62	--
Solvent 4	1	3.76	--	1.36
Solvent 5	1	0.79	0.10	0.69
Solvent 6	1	2.27	0.87	0.30

Note: Values are given in mass

Table 4.9 Quantity of each performance measure (Section 4.3.2) for the optimal ratios of the solvents given in Table 4.8

	Solvent 1	Solvent 2	Solvent 3	Solvent 4	Solvent 5	Solvent 6
$\frac{M_G^I}{M_G^I + M_{MO}^I}$	0.0001	0.0000	0.0002	0.0000	0.0000	0.0000
$\frac{V^I}{V^{II}}$	1.04	1.00	1.13	4.98	2.87	3.54
$\frac{M_{MO}^I}{M_{MO}^I + M_{MO}^{II}}$	0.99	~1	0.98	~1	~1	~1
T (hr)	20.22	5.42	1.82	0.12	0.31	0.29
$\frac{M_W^I}{M_W^I + M_{MO}^I}$	--	0.0011	--	0.0014	0.0013	0.0030

With respect to the separation of glycerol from methyl oleate, since the allowable ASTM value for the glycerol content of the methyl oleate-rich phase (0.02 wt%) was implemented as a hard constraint, this condition is met for all the optimized quantities of the solvent systems. However, the glycerol content was reduced significantly when water was added to the mixer as one of the solvents.

In terms of the phase volume ratio, Solvent 2 with both water and methanol solvents, led to the most equal phase volume ratio. On the other hand, Solvent 4, with relatively higher quantity of hexane resulted in a ratio of the methyl oleate-rich phase to the glycerol-rich phase of roughly 5, which is the set maximum value of the phase volume ratio (Tables 4.8 and 4.9).

The recovery of methyl oleate is not changing significantly for different solvent systems; however, in presence of water (Solvents 2, 4, 5 and 6), a high recovery of ~100% for methyl oleate was obtained. Between Solvent 1 and 3, due to the lower content of methanol in Solvent 1, the recovery of methyl oleate is slightly higher (Tables 4.8 and 4.9).

The liquid residence time in the settler, varies significantly for different solvents (~7 min in Solvent 4 to ~20 h in Solvent 1). Due to the presence of large amount of hexane and absence of methanol, Solvent 4 yielded the shortest residence time among the other solvents. On the other hand, Solvent 1, with only methanol solvent, resulted in a significantly lengthy residence time in the settler of ~20 h (Tables 4.8 and 4.9).

The quantity of water that enters the methyl oleate-rich phase, $M_W^l/\left(M_W^l+M_{MO}^l\right)$, is minimum for Solvent 2 and maximum for Solvent 6. Due to the complete miscibility of water and methanol and also partial miscibility of hexane and methanol, the presence of methanol resulted in having moisture in the methyl oleate-rich phase. The effect of the quantity of methanol on the water content of the methyl oleate-rich phase can be demonstrated by comparing Solvents 5 and 6. Although the quantity of water in Solvent 6 is half of that in Solvent 5, due to the relatively greater quantity of methanol in the former solvent system, the term $M_W^l/\left(M_W^l+M_{MO}^l\right)$ of Solvent 6 is greater than that of Solvent 5.

Due to the chance of phase flipping and lengthy residence time in Solvent 1 and also the possibility of formation of a single liquid phase at high methanol concentrations, this solvent system is not an appropriate choice for the separation of glycerol and methyl oleate (i.e., biodiesel) via a single-stage mixer-settler. Hence, from the technical point of view, without considering the effect of the type of catalyst in the production of biodiesel, among the proposed solvent systems, Solvents 2, 3, 4, 5 and 6 (Table 4.8), were found to be the most practical solvents.

4.5 Conclusions

Based on the findings in the present study, it can be concluded that washing the reaction mixture, with hexane alone, cannot satisfy the ASTM D-6751-02. However, the advantage of using hexane is the significant reduction in the residence time in the settler, due to the high solubility of methyl oleate in hexane and the reduction in density and viscosity of the phase rich in methyl oleate. In contrast, methanol alone or water alone

was successful in separating glycerol from methyl oleate to meet the ASTM Standard. However, with methanol alone, residence time in the settler is very large and with water alone, formation of emulsions particularly in alkali catalyzed transesterification of waste cooking oil could become problematic. There is also the possibility of formation of a single liquid phase in the settler at high methanol or water concentrations.

The above-mentioned advantages of hexane and methanol led to examination of a mixture of hexane and methanol without water. A solvent having a mass ratio of methyl oleate:hexane:methanol of 1:1.15:1.62 provided overall optimal performance with residence time of 1.82 h. Although this solvent system yielded a large residence time relative to the systems using water and hexane together, it would be suitable when formation of emulsions is of concern. However, besides its relatively lengthy residence time, in the absence of water, there is a possibility of formation of a single liquid phase at high methanol or hexane concentrations.

When formation of emulsions is of no concern, for example when waste cooking oil is used for biodiesel production in an acid-catalyzed transesterification, a mixture of hexane and water with some methanol in the feed entering to the mixer $\left(M_M/M_{MO}=0.104\right)$ with the mass ratio of methyl oleate:hexane:water of 1:0.79:0.69 (Solvent 5) or a mixture of hexane, methanol and water solvents with the mass ratio of methyl oleate:hexane:methanol:water of 1:2.27:0.87:0.30 (Solvent 6) are good solvents, leading to a residence times of ~19 and ~17 minutes, respectively. These were found to be the most effective solvents, for the presence of water and hexane together ensures the formation of a two-phase liquid system in the settler. Another feasible solvent is a mixture of water and methanol, which already exists in the feed stream to the extractor, with the optimal mass ratio of methyl oleate:methanol:water of 1:0.10:0.97 (Solvent 2). Although this solvent satisfies all the mixer-settler design criteria, it yielded a relatively longer residence time of 5.4 h and there is the possibility of formation of a single liquid phase at high water concentration. In order to reduce the residence time in the settler, the quantity of methanol entering the extractor must be minimized and a mixture of only hexane and water must be employed as the extraction solvent. This is possible by

distilling off the entire methanol present in the reaction mixture prior to the extraction unit. In this case, an optimum mass ratio of methyl oleate:hexane:water of 1: 3.76:1.36 (Solvent 4) with the residence time of ~7 min provided overall optimal performance.

Acknowledgements

The financial support of Natural Sciences and Research Council of Canada (NSERC) is greatly acknowledged.

Nomenclature

x_M^I	Mole fraction of methanol in the methyl oleate-rich phase
x_{MO}^I	Mole fraction of methyl oleate in the methyl oleate-rich phase
x_G^I	Mole fraction of glycerol in the methyl oleate-rich phase
M_G^I	Mass of glycerol in the methyl oleate-rich phase
M_{MO}^I	Mass of methyl oleate in the methyl oleate-rich phase
M_{MO}^{II}	Mass of methyl oleate in the glycerol-rich phase
M_W^I	Mass of water in the methyl oleate-rich phase
M_M^I	Mass of methanol in the methyl oleate-rich phase
V^I	Volume of the methyl oleate-rich phase
V^{II}	Volume of the glycerol-rich phase
T	Liquid residence time in the settler
M_M	Overall mass of methanol in the mixer
M_{MO}	Overall mass of methyl oleate in the mixer
M_W	Overall mass of water in the mixer
M_H	Overall mass of hexane in the mixer

Greek letters:

μ	Viscosity of the methyl oleate-rich phase
ρ_b	Specific gravity of the bottom phase
ρ_t	Specific gravity of top phase

Abbreviations:

min	Minimum of the performance measure

References

Agarwal, A. K. and Das, L. M., "Biodiesel Development and Characterization for Use as a Fuel in Compression Ignition Engines," Journal of Engineering for Gas Turbines and Power, 123, 440-447 (2001).

Ali, Y. and Hanna, M. A., "Alternative Diesel Fuels from Vegetable Oils," Bioresource Technology, 50, 153-163 (1994).

Al-Widyan, M. I. and Al-Shyoukh, A. O., "Experimental Evaluation of the Transesterification of Waste Palm Oil into Biodiesel," Bioresource Technology, 85, 253-256 (2002).

ASTM D-6751-02, Standard Specification for Biodiesel Fuel (B100) Blend Stock for Distillate Fuels, Designation D-6751-02, American Society for Testing and Materials, West Conshohocken, PA (2002).

Branan, C., "Rules of Thumb for Chemical Engineers," 3rd edition, Gulf Professional Publishing, Houston (2002), pp. 131-135.

Bunz, A. P., Dohrnt, R. and Prausnitz, J. M., "Three Phase Flash Calculations for Multicomponent Systems," Computers Chem. Eng. 15, 47-51(1991).

Dubé, M. A., Zheng, S. McLean, D. D. and Kates, M., "A Comparison of ATR-FTIR Spectroscopy and GPC for Monitoring Biodiesel Production," J. Am. Oil Chem. Soc. 81, 599-603 (2004).

Encinar, J. M., Gonzalez, J. F. and Rodriguez Reinares, A., "Biodiesel from Used Oil. Variables Affecting the Yields and Characteristics of the Biodiesel," Ind. Eng. Chem. Res., 44, 5491-5499 (2005).

Felizardo, P., Joana Neiva Correia, M., Raposo, I., Mendes, J. F., Berkemier, R. and Bordado, J. M., "Production of Biodiesel from Waste Frying Oil," Waste Management, 26, 487-494 (2006).

Fernando, S., Hall, C. and Jha, S., "NO_x Reduction from Biodiesel Fuels," Energy & Fuels, 20, 376-382 (2006).

Gembicki, F.W., "Vector Optimization for Control with Performance and Parameter Sensitivity Indices," Ph.D. Dissertation, Case Western Reserve University, Cleveland, OH (1974).

Holderbaum, T. and Gmehling, J., "A Group Contribution Equation of State Based on UNIFAC," 70, 251-265 (1991).

Karaosmanoglu, F., Cigizoglu, K. B., Tuter, M. and Ertekin S. "Investigation of the Refining Step of Biodiesel Production," Energy and Fuels, 10, 890-895 (1996).

Magnussen, T., Rasmussen, P. and Fedenslund, A., "UNIFAC Parameter Table for Prediction of Liquid-liquid Equilibria," Ind. Eng. Chem. Process Des. Dev. 20, 331-339 (1981).

Mangesh, G. K., Dalai, A. K., "Waste Cooking Oil-An Economical Source for Biodiesel: Review," Ind. Eng. Chem. Res. 45, 2901-2913 (2006).

MATLAB® Help, MATLAB® version 7.1.0.246, R14 developed by MathWorks Inc. (2005).

McBride, N., "Modeling the Production of Biodiesel from Waste Frying Oil," B.A.Sc. Thesis, Department of Chemical Engineering, University of Ottawa (1999).

McKillop, A., "Oil: No Supply Side Answer to the Coming Energy Crisis," Refocus, 6(1), 50-53 (2005).

Monyem, A. and Van Gerpen, J. H., "The Effect of Biodiesel Oxidation on Engine Performance and Emissions," Biomass and Bioenergy, 20, 317-325 (2001).

Nabi, Md. N., Akhter, Md. S. and Zaglul Shahadat, Md. M., "Improvement of Engine Emissions with Conventional Diesel Fuel and Diesel-Biodiesel Blend," Bioresource Technology, 97, 372-378 (2006).

Nelson, P. A., "Rapid Phase Determination in Multi-Phase Flash Calculations," Computers Chem. Eng. 11(6), 581-591(1987).

Nye, M. J., Williamson, T. W., Deshpande, S., Schrader, J. H., Snively, W. H., Yurkewich, T. P. and French, C. L., "Conversion of Used Frying Oil to Diesel Fuel by Transesterification: Preliminary Tests," J. Am. Oil Soc. Chem., 60(8), 1598-1601 (1983).

Prankle, H., Korbitz, W., Mittelbach, M. and Worgetter, M., "Review on Biodiesel Standardization World-wide," BLT Wieselburg, www.blt.bmlfuw.gv.at, 2006.

Ripmeester, W. E., "Modeling the Production of Biodiesel from Waste Cooking Oil," B.A. Sc. Thesis, Department of Chemical Engineering, University of Ottawa (1998).

Smith, J. M., Van Ness, H. C. and Abbott, M. M., "Introduction to Chemical Engineering Thermodynamics," 5th edition, McGraw Hill Companies, Inc., New York (1996), p. 434.

Ulusoy, Y., Tekin, Y., Cetikaya, M. and Karaosmanoglu, F., "The Engine Tests of Biodiesel from Used Frying Oil," Energy Sources, 26, 927-932 (2004).

Walas, S. M., "Phase Equilibria in Chemical Engineering," Butterworth Publishers, Boston, MA (1985), 202-203.

Wang, W. G., Lyons, D. W., Clark, N. N. and Gautam, M., "Emissions from Nine Heavy Trucks Fueled by Diesel and Biodiesel Blend without Engine Modification," Environ. Sci. Technol, 34, 933-939 (2000).

Zhang, Y., Dubé, M. A., McLean, D. D. and Kates, M., "Biodiesel Production from Waste Cooking Oil: 1. Process design and technological assessment," Bioresource Technology, 89, 1-16 (2003a).

Zhang, Y., Dubé, M. A., McLean, D. D. and Kates, M., "Biodiesel Production from Waste Cooking Oil: Economic Assessment and Sensitivity Analysis," Bioresource Technology, 90, 229-240 (2003b).

Zheng, S., Kates, M., Dubé, M. A. and McLean, D. D., "Acid Catalyzed Production of Biodiesel from Waste Frying oil," Biomass and Bioenergy, 30, 267-272 (2006).

Chapter 5 (Paper 4)

Economic Assessment of Biodiesel Production with a Variety of Liquid-Liquid Extraction Systems

Roza Tizvar[1], David D. McLean[1*], Morris Kates[2], Marc A. Dubé[1]
[1] Department of Chemical Engineering, University of Ottawa
[2] Department of Biochemistry, Microbiology and Immunology, University of Ottawa
Ottawa, Ontario, K1N 6N5

Abstract

The economic feasibility of continuous biodiesel processing plants, using a liquid-liquid extraction unit for the ASTM-based separation of glycerol and biodiesel with four potential solvents, was evaluated. In the systems under investigation, biodiesel was produced by acid-catalyzed transesterification of waste cooking oil with methanol. The optimal quantities of the potential solvents were determined on the basis of the maximum attainable return on investment along with meeting the technical criteria associated with the operation of a single-stage mixer-settler. There was not a significant difference between different biodiesel plants in terms of their annual revenue, total production cost and return on investment. None of the processes were appeared to be economically attractive. A maximum return on investment of ~-35% was achieved with optimal solvent mass ratios of biodiesel:hexane:methanol:water of 1:0.43:0.10:0.24 and 1:2.19:0.90:0.34. Although the water-washing process required the lowest total production cost and total capital investment, its net annual loss resulted in its low return on investment.

Keywords: biodiesel purification, liquid-liquid extraction, mixer-settler, return on investment, biodiesel break-even price

* Corresponding author, Tel: +1-613-562-5800 x6110; Fax: +1-613-562-5172.
Email: mclean@genie.uottawa.ca

5.1 Introduction and background

The rising demand for energy resources has led to an increased interest in renewable, sustainable and environmentally friendly non-fossil fuels, such as biodiesel. Biodiesel is usually made by catalytic transesterification of triglycerides (e.g., virgin vegetable oil or animal fat) with an alcohol (e.g., methanol). Alkali catalysts have usually been used because of the high reaction rate achieved. The main by-product of transesterification is glycerol, which cannot be more than 0.02 wt% of the biodiesel product (ASTM D-6751-02, 2002). Despite the renewability and environmental advantages of biodiesel, its higher cost compared to petroleum-based fuels has been a barrier to its commercialization (Bender, 1999; Kulkarni and Dalai, 2006; Zhang et al., 2003a,b). This higher cost is largely due to the high price of virgin vegetable oil feedstock. Hence, efforts to reduce the cost of biodiesel have focused on ways to reduce the cost of the raw material. One possible solution is the use of waste cooking oil instead of virgin vegetable oil (Korus et al., 1993; Kulkarni and Dalai, 2006; Nelson et al., 1994; Zhang et al., 2003a,b).

In alkali-catalyzed transesterification there is the problem of soap formation and emulsions due to the high content of free fatty acids in waste cooking oil. These emulsions can lead to high biodiesel losses in the process downstream (Zhang et al., 2003a). To prevent this, the use of acid catalysis, in which the free fatty acids are converted to methyl esters, has been suggested (Supple et al., 1999; Zhang et al., 2003a; Zheng et al., 2006). Although the reaction rate of acid-catalyzed transesterification is significantly lower than that of alkali-catalyzed reaction (Canakci and Van Gerpen, 1999; Lotero et al., 2005; Zullaikah et al., 2005), the yield of methyl esters can reach 99^{+} mol%, using a large excess of methanol to force the reaction to completion (Zheng et al., 2006).

Bender (1999), Nelson et al. (1994) and Noordam and Withers (1996), studied the economics of biodiesel production plants using alkali-catalyzed transesterification, and considered various criteria, such as the break even price of biodiesel, as the basis for their economic evaluations. According to Nelson et al. (1994), the cost of biodiesel is greatly affected by the cost of raw material, plant size and value of the glycerine by-product.

Noordam and Withers (1996) also noted the large impact of raw material expenses in the total production cost of biodiesel. While Noordam and Withers (1996) reported a break-even price of 763 $/tonne for the biodiesel made from virgin canola oil, Bender (1999) and Nelson et al. (1994) found relatively close biodiesel break even prices of 340 and 420 $/tonne, respectively. However, none of these studies dealt with the use of low quality feedstock in an acid-catalyzed reaction (Zhang et al., 2003b).

Employing ASPEN PLUS™ (2001), Haas et al. (2006) developed a process model to estimate the biodiesel capital and production costs. The production of biodiesel in that study was carried out through transesterification of purified soybean oil with methanol in the presence of sodium methoxide. Although the authors expressed the flexibility of their model for different feedstocks, glycerol price and process technology, they concluded that their model was not capable of predicting the costs of the processes in which the oil feedstock contains a high content of free fatty acids.

Using HYSYS™, Zhang et al. (2003b) assessed the economics of a 8000 tonne/yr biodiesel production plant using four different biodiesel production processes: alkali-catalyzed process using virgin vegetable oil or waste cooking oil (Processes *I* and *II*, respectively), acid-catalyzed process using waste cooking oil with a water washing process or with a hexane extraction unit to purify biodiesel (Processes *III* or *IV*, respectively). All were reported to be technically feasible (Zhang et al., 2003a). Due to the simplicity of Process *I* and the least amount of equipment, the alkali-catalyzed process using virgin vegetable oil had the lowest total capital investment required (Zhang et al., 2003b). In Process *II*, waste cooking oil, which has a relatively high content of free fatty acids, was transesterified in an alkali-catalyzed process. Despite the significantly lower price of waste cooking oil compared to virgin vegetable oil, a pre-treatment unit (i.e., acid-catalyzed esterification) was required before the main alkali-catalyzed reactor. This resulted in a higher total capital investment and a lower economic feasibility for Process *II* compared to Process *I*. In the acid-catalyzed processes using waste cooking oil (Processes *III* and *IV*), because of its insensitivity to the free fatty acid content of the feedstock, a lower total production cost than the alkali-catalyzed reaction of waste

cooking oil (Process *II*) was obtained. The authors concluded that the acid-catalyzed processes of waste cooking oil (Processes *III* and *IV*) were economically competitive to the alkali-catalyzed process of waste cooking oil (Zhang et al., 2003b). The break even prices of biodiesel were found to be 857, 884, 644 and 702 $/tonne for the Processes *I*, *II*, *III* and *IV*, respectively. In addition, an after-tax return on investment of -85, -51, -16 and -21% were calculated for these processes, respectively. Even though none of these processes were found to be economically attractive, the study by Zhang et al. (2003b) gave an overall overview to the variety of biodiesel processing plants. A sensitivity analysis of these processes showed that the price of raw material, the final price of biodiesel and plant capacity were the major factors affecting the return on investment of a biodiesel plant.

In Process *IV*, a hexane/methanol/water extraction unit was successfully utilized for separating the glycerol by-product from biodiesel. The available thermodynamic activity coefficient models, NRTL and UNIQUAC, were employed for design of the proposed biodiesel plants; however, their capability to predict the systems under investigation was not evaluated experimentally. Furthermore, in the same process, instead of a real extraction unit, a component splitter, which does not carry out the phase equilibria-based calculations in order to converge, was utilized. Therefore, although the results obtained gave an overall idea about the technical and economic feasibility of the proposed biodiesel plants, they could be improved by using a more suitable thermodynamic model and a liquid-liquid equilibria-based extraction unit.

A thorough evaluation of the technical feasibility of a single-stage mixer-settler for such separation was carried out in Chapter 4 (Papers 2 & 3) of this thesis. Hexane, methanol and water solvents, alone or mixed together were assessed and their quantities optimized for (1) their ability to satisfy the ASTM standard of glycerol content in biodiesel (<0.02 wt%), and (2) the efficient operation of a mixer-settler system, such as ~1:1 ratio of the liquid phase volumes, high recovery of biodiesel and short liquid residence time in the settler. When formation of emulsions is of concern (e.g., in alkali-catalyzed transesterification of waste cooking oil), a mixture of hexane and methanol was

found to be a suitable solvent for the biodiesel purification. When formation of emulsions is of no concern (e.g., in acid-catalyzed transesterification of waste cooking oil), water alone, a mixture of hexane and water or a mixture of hexane, methanol and water were found to be efficient solvents.

The current study focuses on the economic evaluation and design of biodiesel processing plants with a mixer-settler extraction system and a variety of extraction solvents for separating glycerol and biodiesel. Return on investment (ROI), which is the net annual profit as a percentage of the total capital investment, was chosen as the basis for such economic evaluation. The compositions of the potential extraction solvents were adjusted to satisfy the biodiesel ASTM Standard of the glycerol content (ASTM D-6751-02), to maintain the selected liquid volume ratio and finally to achieve the maximum economic profitability of the biodiesel plant. As another measure of the economic feasibility of this plant, the break even price of biodiesel product, where the total production cost of the plant is equal to the total annual sales revenue, was also calculated for the optimal composition of each solvent system.

5.2 Process description

A schematic diagram of the proposed biodiesel processing plant is shown in Figure 5.1. Table 5.1 gives the major components in each stream for the proposed biodiesel plant in Figure 5.1. Since the streams R1 to R4 and W1 to W4 are a part of the streams T1 to T4, their compositions were similar and not shown in Table 5.1. For the simulation of such a plant, the entire process was divided into two parts:

- Pre-extraction units, which are the same as process *III* in the study by Zhang et al. (2003a,b).
- Extraction and post-extraction units, which are the main focus of the present study.

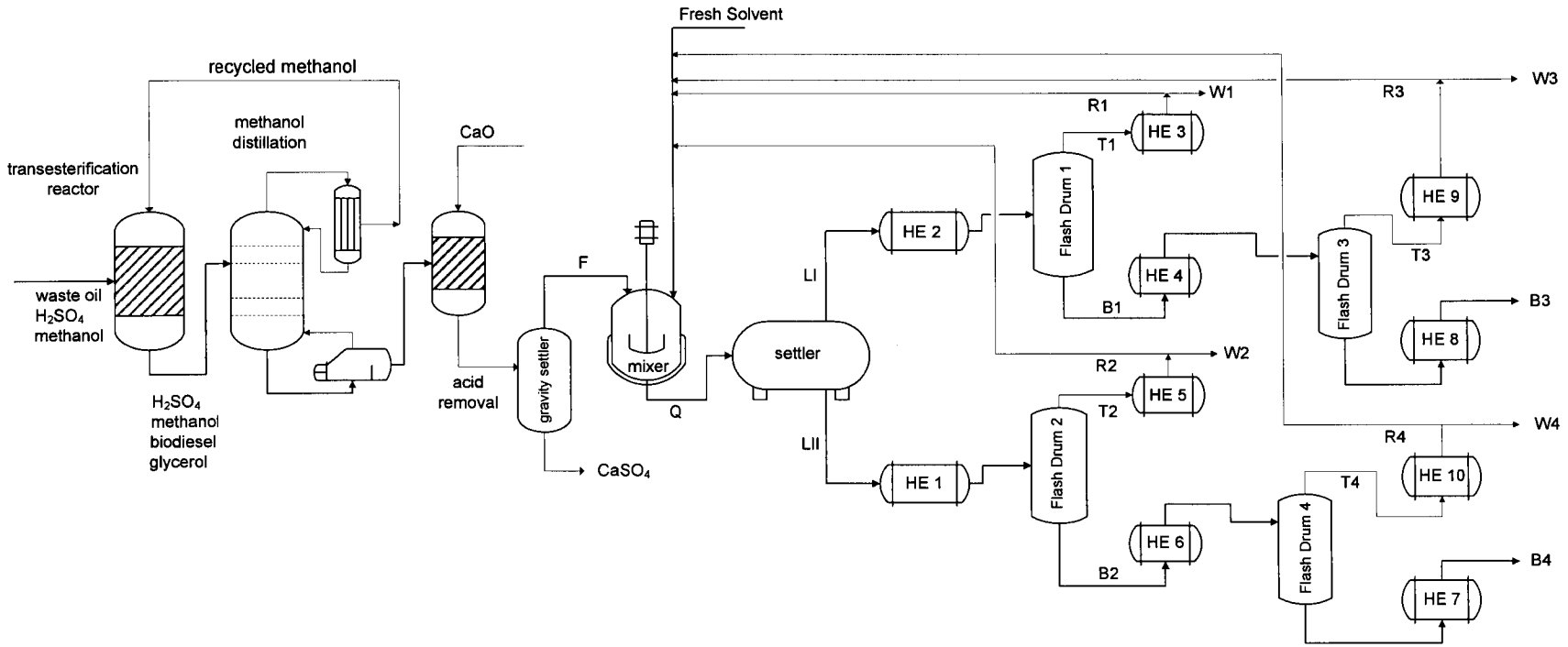

Table 5.1 The major components in the streams in Figure 5.1
(Streams R and W are the same as stream T)

	F	Q	LI	LII	B1	B2	B3	B4	T1	T2	T3	T4
Biodiesel	✓	✓	✓		✓		✓					
Glycerol	✓	✓		✓		✓		✓				
Hexane		✓	✓		✓				✓		✓	
Methanol	✓	✓		✓		✓				✓		✓
Water		✓		✓		✓				✓		✓

B: Streams leaving the bottom of the flash drums
F: Feed to the mixer
HE: Heat exchanger
LI: Biodiesel-rich phase (usually the top phase)
LII: Glycerol-rich phase (usually the bottom phase)
Q: Stream entering the settler (feed plus solvents)
R: Recycle
T: Streams leaving the top of the flash drums
W: Vent (waste)

Figure 5.1 Schematic diagram of the biodiesel plant (production of biodiesel from acid-catalyzed transesterification of waste cooking oil)

5.2.1 Pre-extraction

In the process under study, biodiesel was made by transesterification of waste cooking oil with methanol in presence of sulfuric acid. The pre-extraction section consisted of the transesterification reactor, methanol distillation column and acid removal unit (Zhang et al., 2003a).

Waste cooking oil, methanol and acid were fed to the reactor, which operated at 80°C and 4 bar. The resulting reaction mixture contained biodiesel, glycerol, acid catalyst, methanol and unconverted oil. To achieve a high conversion of oil to fatty acid methyl esters (i.e., biodiesel), methanol was initially fed into the reactor in excess amounts (100:1 on a molar basis) (Zhang et al., 2003a; Zheng et al., 2006). Since complete conversion of oil to biodiesel was achieved after four hours, no unconverted oil was assumed to be present in the feed stream to the extractor. A distillation column was provided following the reactor to recover and recycle excess methanol and accordingly reducing the size of the following units (Zhang et al., 2003a). The acid catalyst was completely removed from the reaction mixture with CaO after the methanol distillation unit. Hence, the mixture leaving the acid removal unit and entering the extractor contained biodiesel, glycerol and methanol and was free of unconverted oil and acid catalyst.

5.2.2 Extraction and post-extraction

In this investigation four solvent systems for biodiesel purification via liquid-liquid extraction were evaluated: Process *A*, water alone as solvent with methanol in the feed to the mixer, Process *B*, a mixture of hexane and methanol; Process *C*, a mixture of hexane and water with methanol in the feed to the mixer; and Process *D*, a mixture of hexane, methanol and water. These multi-solvent systems were previously found to be technically suitable for the separation of glycerol and biodiesel in a single-stage mixer-settler (Chapter 4, Papers 2 & 3).

In Process *A*, after separation of the biodiesel- and glycerol-rich phases, no further separation was required due to the very small amounts of methanol and water in the biodiesel-rich phase (Stream LI, Figure 5.1). However, the methanol and water remained in the glycerol-rich phase (Stream LII, Figure 5.1) and were removed via a flash separator operating at 147°C and atmospheric pressure (Flash Drum 2, Figure 5.1). This system yielded a high-purity biodiesel (99^{+} wt%) and glycerol (92^{+} wt%).

In Processes *B*, *C* and *D*, after separation of the two liquid phases in the settler, the upper hexane-biodiesel phase (Stream LI) was fed to Flash Drum 1, which operated at 100°C and 0.5 bar. Due to the significantly lower boiling points of hexane, water and methanol compared to biodiesel, the vapor phase contained mostly hexane and traces of methanol and/or water and the liquid phase contained mostly biodiesel and only traces of solvents (hexane, methanol and/or water). In order to achieve a high quality biodiesel, another flash drum (Flash Drum 3 at an average temperature of 140°C and 0.5 bar) was required to remove the remaining solvent from the biodiesel-rich phase. The final biodiesel product with 97 wt% biodiesel and 3% hexane was the liquid phase exiting Flash Drum 3 after being cooled down to the ambient temperature of 25°C (Stream B3).

In the mixer-settler, the bottom phase (Stream LII) contained mostly methanol and glycerol and/or water and traces of hexane. This stream was fed to Flash Drum 2, which operated at atmospheric pressure and temperatures varying for different solvent systems from 70 to 147°C. The vapor phase contained the solvents and the liquid phase contains mostly glycerol. The liquid phase was fed to Flash Drum 4 operating at 140°C and 0.5 bar to obtain a high quality glycerol by-product (92^{+} wt%). The purified glycerol was the liquid phase exiting this flash drum after being cooled down to the ambient temperature of 25°C (Stream B4). The streams to be recycled depended on the composition of the solvent mixtures required in the extractor. In Process *B*, the recycle streams were the vapor streams of all the flash drums (Streams R1, R2, R3 and R4) after being cooled down to the temperature of the extractor. In Process *C*, the recycle streams were the vapor phase in Flash Drums 1 and 3 (Streams R1 and R3). In Process *D*, which uses a mixture of hexane, methanol and water, recycles were the vapor phase in Flash Drums 1

to 4 (Streams R1, R2, R3 and R4). When a mixture of hexane and methanol was used as the extraction solvent without any water, Streams W2 and W4 contained mostly methanol and were recycled back to the transesterification reactor. For the case where water is one of the solvents and no methanol is added as solvent (i.e., Processes *A* and *C*), due to the negligible impact of the price of water solvent in the economic evaluations, the streams containing water (vapor phases of Flash Drums 2 and 4) were not recycled.

5.3 Methods

5.3.1 Profitability calculations

After-tax return on investment (ROI), which is profit as a percentage of investment (Seider et al, 2004), given by,

$$\text{ROI}=\frac{(1-t)(\text{S-TPC})}{\text{TCI}}\times 100\% \tag{5.1}$$

was the main criterion selected for the profitability calculations herein. In Equation 5.1, t refers to the provincial corporate tax rate. S is the annual sales revenue and is the total yearly income from selling the biodiesel and glycerol products. TCI and TPC denote the total capital investment and annual total production cost, respectively.

In the economic calculations and design of the biodiesel plant in the current study, the following assumptions and considerations were applied:

- The provincial corporate tax rate of 0.5 was applied in the calculations (Equation 5.1).
- The quantities of the solvents in processes *A*, *B*, *C* and *D* were optimized for the flow rate of the feed to the extractor of 7.71 kmol/h (1203 kg/h) with a mass ratio of biodiesel: glycerol: methanol of 1:0.10:0.10.
- No makeup solvent was assumed for the processes.

- Since the acid catalyst was removed from the reaction mixture prior to the extraction unit, carbon steel was selected as the construction material for all the subsequent units.
- Based on 334 working days in a year, the yearly working hours of 8016 h was used in the calculations.
- Superheated steam at 185°C and cooling water at 15°C were used as the heating and cooling media in the heat exchangers, respectively.
- All prices are reported in US$.
- The approximate cost of the feed to the extractor (Stream F, Figure 5.1) (60 $/kmol) was based on the costs of waste cooking oil, methanol, sulfuric acid and the equipment cost of all the units located before the mixer-settler, as reported by Zhang et al. (2003b). The prices were updated using the Marshall and Swift cost index of the 2nd quarter of the year 2006, (I_{2006}=1306.3), (Chemical Engineering Magazine, October 2006).
- The purity of the final biodiesel product was 97 wt% and that of glycerol was 92 wt%. Further separation of the solvent (i.e., hexane, methanol or water) from the biodiesel- or glycerol-rich streams can be achieved via distillation. Although the 3 wt% hexane remaining in the biodiesel product is considered as impurity, the allowable quantity of hexane solvent in the ultimate biodiesel product is not specified in the corresponding ASTM standard. However, the effect of hexane will appear in the flash point of the fuel. Flash point of pure biodiesel is 150°C and that of pure hexane is -23°C. A rough calculation showed that the presence of 3 wt% hexane in biodiesel results in a flash point of ~130°C, which acceptably meets the corresponding ASTM Standard (the minimum flash point according to ASTM-D-6751-02 for biodiesel is 130°C). In the same way, the effect of residual hexane on density, viscosity, pour point and other properties of biodiesel can be studied in details. However, in the present study, due to the fact that hexane is a fuel by itself, it is assumed that its presence in biodiesel does not negatively impact on the properties of biodiesel, significantly.
- Fixed capital cost consists of the equipment cost, and the cost of land, piping, installation and services, electrical, material, building and yard improvements,

engineering and supervision, contractor's fee, legal expenses and contingency. The equipment cost was directly calculated from the design of the plant as shown in Figure 5.1; other costs were defined as a percentage of the equipment cost. For instance, land, building, piping, installation, services, electrical and yard improvements were considered to make up 6%, 16%, 80%, 25%, 45%, 20% and 15% of the equipment cost, respectively. The summation of engineering and supervision, contingency, legal expenses and contractor's fee were assumed to be 75% of the total purchased equipment cost. These percentages are the average values suggested by Peters et al. (2003).

- Fixed capital cost and working capital costs, which are the elements of total capital investment, are assumed to make up 85% and 15% of the total capital investment, respectively. These percentages are suggested as average quantities for a typical chemical processing plant (Peters et al., 2003).
- The temperature and pressure of the flash separators (Flash Drums 1 to 4 in Figure 5.1) were selected to attain the most effective separation of the volatile and non-volatile components. Since raising the temperature of the biodiesel-rich product streams may cause decomposition or polymerization of biodiesel, temperatures were kept as low as possible (<150°C) and reduce the pressure whenever the flash separation of the solvents and biodiesel or glycerol was not easily accomplished at moderate conditions.
- No pumps were shown in Figure 5.1; however, a total pump cost of $50 000, determined by Zhang et al. (2003b), was employed in the calculations after being updated to the 2nd quarter of the year 2006.
- The total equipment cost of the reactor, methanol distillation column, catalyst removal unit and heat exchangers located prior to the extractor were taken from the study by Zhang et al. (2003b) and updated for the 2nd quarter of the year 2006.
- Depreciation was assumed to be 10% of the fixed capital investment (Peters et al., 2003).
- Except the raw material expense, which was directly obtained from the plant design, all the other contributors to the total production cost were given as percentages of either total production cost or fixed capital investment. These

percentages for the contributors to the total production cost as suggested by Peters et al. (2003) and also their averages employed in the current study are summarized in Table 5.2.

Table 5.2 Contributors to the total production cost in a typical chemical processing plant

	%Total production cost suggested by Peters et al. (2003)	%Total production cost used in the current study
	Manufacturing Cost	
Variable production cost:		
Raw material	10-60	determined directly from design
Operating labour	10-20	15
Utilities	10-20	15
Maintenance and repairs	2-10*	6*
Operating supplies	0.3-1.5*	1*
Laboratory supplies	1-4	2
Royalties	0-6	3
Fixed Charges:		
Depreciation	10*	10*
Property tax	2-4*	2*
Insurance	1*	1*
Financing	negligible	negligible
Rent	negligible	negligible
Overhead costs	5-15	10
	General Expenses	
Administrative	2-5	3
Distribution and marketing	2-20	10
Research and development	5	5

* given as a percentage of fixed capital investment

- Since hexane and methanol were the most expensive solvents (Table 5.3), the streams containing large quantities of hexane (i.e., R1 and R3) or methanol (i.e., R2 and R4) were recycled and reused in the extraction unit. The streams containing large quantities of water and small quantities of methanol were not recycled.

- Some of the equations applied in the current study to determine the size and cost of each piece of equipment (e.g., flash drums and heat exchangers) in the proposed plants are given in Appendix D of this thesis.

The unit prices of the solvents, products and the raw materials for the reaction are summarized in Table 5.3.

Table 5.3 Unit price of the materials in the biodiesel plant and their web sources

	Price ($/tonne)	References
Products:		
Biodiesel (B100)	944	www.b100fuel.com
Glycerol (92^{+} wt%)	1303	www.findarticles.com
Raw materials:		
Waste cooking oil	200	www.studio255.com
Sulfuric acid	60	www.the-innovation-group.com
Methanol	593	www.methanex.com
Solvents:		
Hexane	737	www.icispricing.com
Water	0.22	www.kpmg.com.cn

Note: All prices are reported for the 2nd half of the year 2006

5.3.2 Optimization

In Chapter 4 (Papers 2 & 3), the quantities of the solvents were determined by employing a nonlinear multi-objective optimization solver (i.e., fgoalattain) in MATLAB® (version 7.1.0.246, R14 developed by MathWorks Inc.), which was capable of handling constraints. The ASTM-based glycerol content of biodiesel (≤0.02 wt%) and equal liquid phase volumes were introduced to the MATLAB® code in the form of a hard and soft constraint, respectively. Low biodiesel loss through the purification step and short residence time of the liquid phases in the settler, were treated as performance measures to be minimized. In the present work, the return on investment, as a measure of the economic profitability of the entire biodiesel plant, was applied as the performance measure. The glycerol content of biodiesel, which must meet the corresponding ASTM

standard, was introduced as a hard constraint and the phase volume ratio was implemented as a soft constraint. It was assumed that the phase volume ratio, which was between 0.2 and 5, as was applied as a soft constraint, does not have any impact on the structural design of the settler and therefore its capital cost. The other two technical criteria, which were the amount of biodiesel loss and liquid residence time in the settler, were neglected, since they directly impact on the after-tax return on investment, the basis for the economic performance measure for this chapter. The constrained nonlinear solver, fgoalattain, was also employed in the current study.

5.4 Results and discussion

In Chapter 4 (Papers 2 & 3), five solvent systems (solvent systems 2, 3, 4, 5 and 6) were found to be technically feasible. Due to the lack of information about the capital costs of the equipment located before the extraction unit, the case where methanol is completely distilled off prior to the extraction (Solvent 4) was not considered. Thus, for the economic analysis of the biodiesel plant only Solvents 2, 3, 5 and 6 were investigated in the present work. For these technically optimal solvent systems, the return on investment (ROI), total production cost (TPC), purchased equipment cost (PEC), the total annual biodiesel and glycerol sales revenue (S) and the break-even price of biodiesel (BEP) were determined and summarized in Table 5.4.

Table 5.4 ROI, TPC, PEC, S and BEP for the previously optimized quantities of the potential solvents given in Chapter 4 (Papers 2 & 3)

Solvent System	Mass ratios of solvents relative to biodiesel				ROI	TPC	PEC	S	BEP
	Biodiesel	Hexane	Methanol	Water	(%)	($/yr×10^{-6})	($×10^{-6})	($/yr×10^{-6})	($/L)
2	1	0	0.10	0.97	-42.8	15.17	1.55	9.22	1.71
3	1	1.15	1.62	0	-38.8	16.94	2.14	9.49	1.84
5	1	0.79	0.10	0.69	-35.9	16.87	2.17	9.86	1.78
6	1	2.27	0.87	0.30	-35.6	17.54	2.43	9.80	1.92

Solvent systems 2, 3, 5 and 6 represent the biodiesel processing plants with the optimized quantities of the solvents considering only the technical feasibility of the mixer-settler system given in Chapter 4 (Papers 2 & 3) of this thesis.

Although there was not a significant difference between the economic terms calculated for the proposed solvent systems, the plant using solvent 6, which consisted of hexane, methanol and water as a multi-solvent, was found the most economically beneficial process in terms of the after-tax return on investment (-35.6%). However, this plant had the largest purchased equipment cost and also total production cost compared to the other potential solvent systems. Solvent 5 with the same components, but fixed quantity of methanol in the feed stream entering the extractor, led to a close after-tax return on investment of -35.9%. This process yielded the largest annual revenue from selling the biodiesel and glycerol products. Solvent 3, which consisted of a mixture of hexane and methanol with no water added, also showed a roughly similar ROI value of -38.8% (Table 5.4).

Since the unit price of water is negligible compared to that of hexane or methanol, Solvent 2 showed to require the lowest total production cost among the processes studied. In addition, due to the fewest number of processing equipment and the small size of the required heat exchangers, this process had the lowest purchased equipment cost as well. In contrast, due to its low annual revenue, Solvent 2 was the least economically attractive process in terms of the after-tax return on investment (Table 5.4).

In terms of the break-even price of biodiesel, the biodiesel processing plant with water and some methanol in the feed stream to the mixer, as the extraction solvent (Solvent 2) showed the lowest biodiesel break-even price of 1.71 $/L. The highest biodiesel break-even price of 1.92 $/L was found for Solvent 6, which contained a mixture of hexane, methanol and water (Table 5.4).

In the current work, the technically optimal solvent systems were adjusted to achieve the maximum annual after-tax return on investment, while maintaining the ASTM Standard of biodiesel along with the selected phase volume ratio in the settler. Solvent systems *A*, *B*, *C* and *D* represent the re-adjusted compositions of the solvent systems 2, 3, 5 and 6, respectively.

Table 5.5 contains the optimal mass and mole ratios of the solvents relative to 1 kilogram or 1 mole of biodiesel entering the settler for Processes *A*, *B*, *C* and *D*. The flow rate, component mass fractions, temperature and pressure of the streams shown in Figure 5.1 are summarized in Table 5.6. The flow rates of the fresh solvents required for each process are summarized in Table 5.7. Table 5.8 contains a summary of the operating conditions, equipment sizing and cost of the mixer-settler and the units following them. A summary of the economic terms, profitability calculations and the properties of the final products for the processes under investigation are presented in Table 5.9.

Table 5.5 Optimal compositions of the solvent systems (Stream Q, Figure 5.1). Ratios are given relative to 1 mole or 1 kg of biodiesel fed to the mixer

Solvent system	Mole ratios				Mass ratios			
	biodiesel	hexane	methanol	water	biodiesel	hexane	methanol	water
A	1	0	0.96	14.23	1	0	0.10	0.86
B	1	2.10	8.21	0	1	0.61	0.89	0
C	1	1.47	0.96	3.87	1	0.43	0.10	0.24
D	1	7.54	8.32	5.58	1	2.19	0.90	0.34

Table 5.6a Properties of the streams in Process *A* for the optimal quantity of water (Table 5.5)

Stream:	F	Q	LI	LII	B1	B2	B3	B4	T1	T2	T3	T4	R1	R2	R3	R4	W1	W2	W3	W4
Volume flow (m^3/h)	1.25	2.10	1.13	1.10	--	0.09	--	--	--	0.98	--	--	--	--	--	--	--	0.98	--	--
Mass flow (kg/h)	1203	2064	1000	1064	--	97	--	--	--	967	--	--	--	--	--	--	--	967	--	--
Molar flow (kmol/h)	7.71	55.49	3.53	51.96	--	1.39	--	--	--	50.57	--	--	--	--	--	--	--	50.57	--	--
Temperature (°C)	20	20	20	20	--	147	--	--	--	147	--	--	--	--	--	--	--	147	--	--
Pressure (bar)	1	1	1	1	--	1	--	--	--	1	--	--	--	--	--	--	--	1	--	--
Mass fractions:																				
biodiesel	0.828	0.482	0.995	0.000	--	0.000	--	--	--	0.000	--	--	--	--	--	--	--	0.000	--	--
glycerol	0.086	0.050	0.000	0.098	--	0.920	--	--	--	0.015	--	--	--	--	--	--	--	0.015	--	--
methanol	0.000	0.050	0.004	0.094	--	0.003	--	--	--	0.103	--	--	--	--	--	--	--	0.103	--	--
water	0.086	0.418	0.001	0.808	--	0.077	--	--	--	0.882	--	--	--	--	--	--	--	0.882	--	--

Table 5.6b Properties of the streams in Process *B* for the optimal quantity of each hexane and methanol (Table 5.5)

Stream:	F	Q	LI	LII	B1	B2	B3	B4	T1	T2	T3	T4	R1	R2	R3	R4	W1	W2	W3	W4
Volume flow (m^3/h)	1.25	3.10	1.95	1.23	1.27	0.30	1.25	0.10	0.72	1.19	0.12	0.18	0.72	1.19	0.12	0.01	--	--	--	0.17
Mass flow (kg/h)	1203	2592	1607	985	1096	259	1017	112	511	726	79	147	511	726	79	44	--	--	--	103
Molar flow (kmol/h)	7.71	39.2	12.8	26.4	4.74	5.74	3.69	1.37	8.06	20.66	1.05	4.37	8.06	20.66	1.05	1.32	--	--	--	3.05
Temperature (°C)	20	20	20	20	100	70	25	25	100	70	138	125	25	25	25	25	--	--	--	25
Pressure (bar)	1	1	1	1	1	1	1	1	1	1	0.55	1	1	1	1	1	--	--	--	1
Mass fractions:																				
biodiesel	0.828	0.384	0.614	0.007	0.900	0.027	0.970	0.010	0.000	0.000	0.003	0.041	0.000	0.000	0.003	0.041	--	--	--	0.041
glycerol	0.086	0.040	0.000	0.105	0.000	0.401	0.000	0.920	0.000	0.000	0.000	0.003	0.000	0.000	0.000	0.003	--	--	--	0.003
hexane	0.000	0.235	0.314	0.106	0.093	0.005	0.029	0.000	0.788	0.142	0.912	0.009	0.788	0.142	0.912	0.009	--	--	--	0.009
methanol	0.086	0.341	0.072	0.782	0.007	0.567	0.001	0.070	0.212	0.858	0.085	0.947	0.212	0.858	0.085	0.947	--	--	--	0.947

Table 5.6c Properties of the streams in Process *C* for the optimal quantity of each hexane and water (Table 5.5)

Stream:	F	Q	LI	LII	B1	B2	B3	B4	T1	T2	T3	T4	R1	R2	R3	R4	W1	W2	W3	W4
Volume flow (m^3/h)	1.25	2.14	1.77	0.47	1.32	0.13	1.18	0.11	0.47	0.33	0.15	0.01	0.47	--	0.15	--	--	0.33	--	0.01
Mass flow (kg/h)	1203	1878	1444	434	1127	126	1026	112	317	308	101	14	317	--	101	--	--	308	--	14
Molar flow (kmol/h)	7.71	26.05	8.86	17.19	4.90	2.35	3.71	1.61	3.96	14.84	1.19	0.74	3.96	--	1.19	--	--	14.84	--	0.74
Temperature (°C)	20	20	20	20	110	120	25	25	110	120	139	130	25	--	25	--	--	25	--	25
Pressure (bar)	1	1	1	1	1	1	1	1	1	1	0.47	0.6	1	--	1	--	--	1	--	1
Mass fractions:																				
biodiesel	0.828	0.531	0.690	0.000	0.884	0.000	0.970	0.000	0.000	0.000	0.003	0.000	0.000	--	0.003	--	--	0.000	--	0.000
glycerol	0.086	0.055	0.000	0.239	0.000	0.816	0.000	0.920	0.000	0.002	0.000	0.009	0.000	--	0.000	--	--	0.002	--	0.009
hexane	0.000	0.227	0.300	0.003	0.115	0.000	0.030	0.000	0.960	0.004	0.985	0.000	0.960	--	0.985	--	--	0.004	--	0.000
methanol	0.086	0.062	0.009	0.209	0.001	0.018	0.000	0.003	0.036	0.288	0.012	0.131	0.036	--	0.012	--	--	0.288	--	0.131
water	0.000	0.125	0.001	0.549	0.000	0.166	0.000	0.077	0.004	0.706	0.000	0.860	0.004	--	0.000	--	--	0.706	--	0.860

Table 5.6d Properties of the streams in Process *D* for the optimal quantity of each hexane, methanol and water (Table 5.5)

Stream:	F	Q	LI	LII	B1	B2	B3	B4	T1	T2	T3	T4	R1	R2	R3	R4	W1	W2	W3	W4
Volume flow (m^3/h)	1.25	5.73	4.39	1.51	1.34	0.12	1.18	0.10	3.08	1.37	0.18	0.01	3.08	1.20	0.18	--	--	0.17	--	0.01
Mass flow (kg/h)	1203	4513	3236	1277	1144	115	1026	109	2092	1162	118	6.05	2092	1018	118	--	--	144	--	6.05
Molar flow (kmol/h)	7.71	76.53	31.58	44.95	5.11	1.78	3.71	1.53	26.47	43.17	1.40	0.25	26.47	37.80	1.40	--	--	5.37	--	0.25
Temperature (°C)	20	20	20	20	105	120	25	25	105	120	141	126	25	25	25	--	--	25	--	25
Pressure (bar)	1	1	1	1	1	1	1	1	1	1	0.5	0.7	1	1	1	--	--	1	--	1
Mass fractions:																				
biodiesel	0.828	0.221	0.307	0.000	0.870	0.000	0.970	0.000	0.000	0.000	0.004	0.000	0.000	0.000	0.004	--	--	0.000	--	0.000
glycerol	0.086	0.023	0.000	0.081	0.000	0.873	0.000	0.920	0.000	0.002	0.000	0.006	0.000	0.002	0.000	--	--	0.002	--	0.006
hexane	0.000	0.483	0.659	0.038	0.128	0.000	0.030	0.000	0.949	0.042	0.981	0.001	0.949	0.042	0.981	--	--	0.042	--	0.001
methanol	0.086	0.198	0.033	0.619	0.002	0.050	0.000	0.022	0.049	0.676	0.015	0.570	0.049	0.676	0.015	--	--	0.676	--	0.570
water	0.000	0.075	0.001	0.262	0.000	0.077	0.000	0.058	0.002	0.280	0.000	0.423	0.002	0.280	0.000	--	--	0.280	--	0.423

Table 5.7 Quantities of the components in Fresh Solvent stream in Figure 5.1

Solvent system	Molar flow (kmol/h)			Mass flow (kg/h)		
	hexane	methanol	water	hexane	methanol	water
A	0	0	47.78	0	0	860.92
B	0.35	0.05	0	30.18	1.59	0
C	0.26	0	12.93	22.40	0	233.00
D	0.41	0	2.74	35.68	0	49.41

Table 5.8 Equipment cost, sizing and operating condition of the extraction and post-extraction units

	Number of units	Total cost ($\$\times10^{-6}$)	Size D×H (m×m)	T (°C)	P (bar)
Process *A*					
Mixer	1	0.050	0.6x0.6	20	1
Settler	1	0.042	1.7x5.0	20	1
Drum2	1	0.038	0.3x1.0	147	1
Heat exchangers	2	0.044	113*	--	--
Process *B*					
Mixer	1	0.050	0.7x0.7	20	1
Settler	1	0.039	1.6x4.7	20	1
Drum1	1	0.105	0.3x2.7	100	1
Drum2	1	0.080	0.3x1.7	70	1
Drum3	1	0.101	0.3x2.6	138	0.55
Drum4	1	0.058	0.2x1.9	125	1
Heat exchangers	10	0.336	277*	--	--
Process *C*					
Mixer	1	0.050	0.6x0.6	20	1
Settler	1	0.021	0.8x2.4	20	1
Drum1	1	0.106	0.3x2.8	110	1
Drum2	1	0.067	0.3x1.3	120	1
Drum3	1	0.102	0.3x2.6	139	0.47
Drum4	1	0.058	0.2x1.9	130	0.6
Heat exchangers	10	0.432	227*	--	--
Process *D*					
Mixer	1	0.050	0.9x0.9	20	1
Settler	1	0.022	0.9x2.6	20	1
Drum1	1	0.105	0.5x1.8	105	1
Drum2	1	0. 103	0.8x1.0	120	1
Drum3	1	0.102	0.3x2.6	141	0.5
Drum4	1	0.057	0.2x1.9	126	0.7
Heat exchangers	10	0.602	401*	--	--

* represents the total area required by all the heat exchangers (m^2)

Table 5.9 Summary of the economic calculations and the properties of the biodiesel and glycerol products in the proposed biodiesel plants

		Process *A*	Process *B*	Process *C*	Process *D*
Equipment cost	($\times 10^{-6}$)	1.53	2.12	2.19	2.39
Fixed capital investment	($\times 10^{-6}$)	5.85	8.08	8.38	9.16
Total capital investment	($\times 10^{-6}$)	6.88	9.51	9.85	10.77
Raw material cost	($/yr$\times 10^{-6}$)	4.43	4.61	4.56	4.63
Total production cost	($/yr$\times 10^{-6}$)	15.13	16.83	16.84	17.47
Annual sales revenue	($/yr$\times 10^{-6}$)	9.26	9.62	9.87	9.81
Annual net profit	($\times 10^{-6}$)	-5.87	-7.21	-6.97	-7.67
Annual net profit after-tax	($\times 10^{-6}$)	-2.93	-3.61	-3.48	-3.83
Depreciation	($\times 10^{-6}$)	0.59	0.81	0.84	0.92
After-tax rate of return	(%)	-42.7	-37.9	-35.4	-35.6
Break-even price of biodiesel	($/L)	1.70	1.80	1.77	1.91
Recovery of biodiesel	(%)	99.9	99.0	99.9	99.9
Recovery of glycerol	(%)	86.0	99.6	99.6	97.3
Purity of the biodiesel product	(wt%)	99.5	97	97	97
Purity of the glycerol product	(wt%)	92	92	92	92
Rate of production of biodiesel	(kg/h)	1000	1017	1026	1026
Rate of production of glycerol	(kg/h)	97	112	112	109

5.4.1 Total capital investment

Among the four processes studied, Process *D* requires the largest initial capital investment for building the biodiesel plant. The total capital investment was calculated from the fixed capital investment, and the fixed capital investment was directly determined from the equipment cost plus the cost of land, piping, installation, services, overhead, material, etc. Due to the relatively high flow rate of the solvents added to the mixer in Process *D* (Tables 5.5 and 5.6d), the size and therefore, the average cost of the mixer-settler, flash drums and heat exchangers are greater than those in Processes *A*, *B* or *C*. Although Process *C* has the lowest flow rate of the solvent added to the mixer (1875 kg/h), because of it having the fewest pieces of equipment, Process *A* showed the lowest equipment cost and lowest total capital investment required for building the biodiesel plant. Although the flow rate of the solvent stream in Process *B* was found to be greater than that in Process *C*, the higher price of heat exchangers in Process *B*, which was

because of their operation at reduced pressure, led to a slightly higher purchased equipment cost and total capital investment of Process *C* compared to Process *B* (Table 5.9).

5.4.2 Total production cost

The total production cost was calculated as the summation of the raw material expense and other costs presented in Table 5.2. Some of these costs were reported as a percentage of the fixed capital investment. Thus, the greater the cost of raw material and fixed capital investment, the greater the total production cost. Because of the higher flow rate of the extraction solvents required, especially hexane and methanol, which are more expensive compared to water, the raw material cost and total production cost of Process *D* were determined to be larger than the other processes. Although none of the streams containing large quantities of water were recycled and reused as extraction solvent, due to the considerably low price of distilled water, Process *A* has the lowest raw material cost. Consequently, this process had the lowest total production cost among the processes studied (Tables 5.3 and 5.9). On average, for all the processes, the cost of raw materials was found to cover 27% of the total production cost.

5.4.3 Annual sales revenue

Biodiesel and glycerol were the products of this plant. Process *C* has the highest annual revenue from selling the biodiesel and glycerol product streams. This process with the lowest loss of biodiesel and glycerol compared to Processes *B* and *D* had 99.9% recovery[1] of biodiesel and 99.6% recovery of glycerol. Since the purity of the final biodiesel and glycerol products were 97 wt% and 92 wt%, respectively, for all the processes, the higher the recovery of the products, the greater the flow rate of the product streams. Hence, the sum of the flow rates of the biodiesel and glycerol product streams in Process *C* were found to be greater than those in Processes *B* or *D* (Table 5.9). Despite

[1] Recovery of biodiesel or glycerol is defined as the quantity of the final product (biodiesel or glycerol) as a percentage of the initial amount of biodiesel or glycerol fed into the mixer in stream F, Figure 5.1.

the lower per kilogram cost of biodiesel compared to glycerol (biodiesel: 0.94 $/kg; glycerol: 1.30 $/kg), due to considerably greater production rate of biodiesel-rich product stream in all the proposed processes (>1000 kg/h) than that of glycerol (>97 kg/h), the share of the flow rate of the biodiesel-rich product stream in the total annual sales revenue is roughly seven times more than that of glycerol-rich product stream. Therefore, between Processes *B* and *D*, Process *D* with a slightly higher recovery of biodiesel (99.9 wt%) and higher rate of biodiesel production (1026 kg/h) has the next highest annual sales revenue, although the recovery of glycerol in Process *D* is slightly lower compared to that in Process *B* (Table 5.9).

The annual sales revenue in Process A was found the lowest among the four systems, mainly due to the undesirably high purity of the final biodiesel product (99^{+} wt%) and therefore, low flow rate of the biodiesel-rich product stream. In addition, the recovery of glycerol and as a result, the rate of production of glycerol-rich product stream is relatively low (Table 5.9).

5.4.4 Return on investment (ROI)

Each process yielded a negative net annual profit (the difference between the annual revenue and total production cost, which is defined as the numerator in Equation 5.1) and accordingly negative annual after-tax return on investment. Due to the variations in the raw material prices or the assumptions made, there are uncertainties associated with the numbers calculated. However, to compare these systems, the relative values of the numbers are important.

Although Process *B* has the lowest equipment cost and total capital investment, among the Processes *B*, *C* and *D*, the lower raw material cost for Process *C* compensates more than for its higher equipment cost leading to Process *C* having the lowest total production cost, the highest annual net profit from selling glycerol and biodiesel products and -35% annual return on investment, the most economically beneficial process. Even though Process *D* has the highest raw material cost among the three Processes *B*, *C* and

D, due to its slightly higher recovery of biodiesel and annual revenue compared to Process *B*, Process *D* has essentially the same ROI, -36% (Table 5.9). The high recovery of biodiesel in Processes *C* and *D* is due to the presence of water and hexane solvents together. When a mixture of hexane and methanol, without water, is used as the extraction solvent, as in Process *B*, a lower recovery of biodiesel was resulted (Table 5.9).

Because of the considerably higher purity of biodiesel (99^{+} wt%) obtained through washing the reaction mixture with water, Process *A* with the lowest annual sales revenue is an exception and can not be compared to the other three processes. However, in this case, 26 kg/h of a "suitable" component can be added to the biodiesel product stream as an impurity, to reduce the undesired high purity of biodiesel to 97 wt% and increase the flow rate of the biodiesel product stream. For example on adding this quantity of hexane to the biodiesel product, the annual revenue and total production cost will increase to 9.46×10^{6} and 15.25×10^{6} \$/y, respectively. Annual after-tax return on investment will be -42%, which is not significantly changed. Moreover, a maximum value for ROI can be found by adding 26 kg/h of a "suitable" component, which costs nothing. In this case, TPC remains constant at 15.13×10^{6} \$/y (Table 5.9), while the annual sales revenue will increase to 9.46×10^{6} \$/y and ROI will reach to a slightly higher value of -41%, which is still lower than the other processes. Thus, Process *A* with the lowest TPC, but the lowest TCI and lowest annual sales revenue, which is largely due to the low recovery of 92 wt% glycerol (86%), was found to have the least after-tax return on investment (Table 5.9).

5.4.5 Biodiesel break-even price

In the proposed biodiesel Processes *A*, *B*, *C* and *D*, the break-even price of biodiesel was found to be 1.70, 1.80, 1.77 and 1.91 \$/L, respectively. Process *D*, resulted in the highest break-even price of biodiesel product, while Process *A*, resulted in the lowest break-even price of biodiesel product. These break-even prices are comparable to that of gasoline (0.52 \$/L) (Delucchi et al., 2000), the average price of gasoline (0.60 \$/L) or the average price of petroleum diesel (0.67 \$/L) for the month October, 2006 (eia, Energy Information Administration, 2006).

5.5 Conclusions

Based on the results obtained from the economic analysis of four biodiesel plants utilizing different extraction solvent systems in a single-stage mixer-settler for separation of glycerol from biodiesel (Processes *A*, *B*, *C* and *D*), none of them were found to be economically beneficial. Despite their negative net annual profit and negative after-tax return on investment, in order to compare these processes, the relative values of the numbers reported are of importance.

Process *C* with a mixture of hexane, water and residual methanol in the stream entering the extractor, was found to be the most economically attractive process. In this process, the optimal mass ratio of biodiesel:hexane:methanol:water of 1:0.43:0.10:0.24 (36% water in methanol) resulted in a -35% after-tax return on investment. This process has a high recovery of both biodiesel and glycerol (99.9% and 99.6%, respectively) and accordingly, the greatest production rate of the biodiesel- and glycerol-rich product streams and highest annual sales revenue.

Due to its considerably higher purity of biodiesel product (99.5 wt%), Process *A* was an exception. Although this process had the lowest total production cost, its after-tax return on investment was found to be -43%, mainly due to its net annual loss and also low total capital investment required. In order to be able to fairly compare this process with the other systems, the purity of biodiesel in the final biodiesel product stream must be reduced to 97 wt%. This can be carried out by adding 26 kg/h of a "suitable" component, which does not affect the biodiesel fuel properties, is not toxic and is cheap enough. However, ROI did not change significantly and reached the value of -41%.

Process *D* with the same recovery of biodiesel as Process *C*, but somewhat lower recovery of glycerol by-product, higher raw material expense and higher total production cost, led to an after-tax return on investment of -36%. Process *B* with higher raw material expense and lower total capital investment compared to Processes *C* and *D* and lower annual revenue led to a slightly lower after-tax return on investment of -38%.

In terms of the initial capital investment for building such biodiesel plants, Process *A* with the least number of equipment and low flow rate of the solvents, was the cheapest plant to build. On the contrary, Process *D* (with the optimal mass ratio of biodiesel:hexane:methanol:water of 1:2.19:0.90:0.34) with a relatively higher flow rate of the solvents, and therefore, larger size of equipment, needed the greatest initial investment to build the plant.

Regarding the biodiesel break-even price, Processes *A* and *D* with 1.70 and 1.91 $/L had the lowest and the highest break-even price of biodiesel, respectively.

The present study gives a rough idea about the costs involved in a biodiesel processing plant using a single-stage mixer-settler unit, with hexane/methanol/water as extraction solvents, to yield biodiesel that satisfies the ASTM Standard of its glycerol content. As discussed earlier, each of the economic terms obtained in the present study (e.g., the return on investments and the biodiesel break-even prices), may vary significantly due to the variations in the assumptions made, the flow rates or the unit prices of the raw materials. In addition, the government subsidise for the alternative and renewable energy sector or an increase in the price of the petroleum diesel may have a great impact on the results obtained.

Acknowledgements

The financial support of Natural Sciences and Research Council of Canada (NSERC) is greatly acknowledged.

References

ASTM D-6751-02, Standard Specification for Biodiesel Fuel (B100) Blend Stock for Distillate Fuels, Designation D6751-02, American Society for Testing and Materials, West Conshohocken, PA (2002).

Bender, M., "Economic Feasibility Review for Community-Scale Farmer Cooperative for Biodiesel," Bioresource Technology, 70, 81-87 (1999).

Canakci, M. and Van Gerpen, J., "Biodiesel Production via Acid Catalysis", Trans. ASAE, 42(5), 1203-1210 (1999).

Chemical Engineering Magazine, "Economic Indicators," p. 72, www.che.com/pindex, 2006.

Delucchi, M., Burke, A., Lipman, T. and Miller, M. "Electric and Gasoline Vehicle Lifecycle Cost and Energy-Use Model," Institute of Transportation Studies, University of California, Davis, paper UCD-ITS-RR-99-4, www.repositories.cdlib.org, 2000.

eia, Energy Information Administration, Official Energy Statistics from the U.S. Government, www.eia.doe.gov, 2006.

Haas, M. J., McAloon, A. J., Yee, W. C. and Foglia T. A., "A Process Model to Estimate Biodiesel Production Costs", Bioresource Technology, 97, 671-678 (2006).

Haas, M. J., "Improving the Economics of Biodiesel Production Through the Use of Low Value Lipids as Feedstocks: Vegetable Oil Soapstock," Fuel Processing Technology, 86, 1087-1096 (2005).

Kulkarni, M. G. and Dalai, A. K., "Waste Cooking Oil: An Economic Source for Biodiesel," Ind. Eng. Chem. Res., 45, 2901-2913 (2006).

Korus, R.A., Hoffman, D.S., Bam, N., Peterson, C.L., Drown, C., "Transesterification Process to Manufacture Ethyl Ester of Rape Oil," In: The Proceedings of the First Biomass Conference of the Americas: Energy, Environment, Agriculture, and Industry, National Renewable Energy Laboratory, Golden Co., 2, 815–826 (1993).

Lotero, E., Liu, Y., Lopez, D. E., Suwannakarn, K., Bruce, D. A. and Goodwin, J. G., "Synthesis of Biodiesel via Acid Catalysis", Ind. Eng. Chem. Res., 44, 5353-5363 (2005).

Nelson, R. G., Howell, S. A. and Weber, J. A., "Potential Feedstock Supply and Costs for Biodiesel Production," Bioenergy'94, Proceedings of the Sixth National Bioenergy Conference, Reno/Sparks, Nevada (1994).

Noordam. M. and Withers, R., "Producing Biodiesel from Canola in the Island Northwest: An Economic Feasibility Study," Idaho Agricultural Experiment Station Bulletin No. 785, University of Idaho, College of Agriculture, Moscow, Idaho, p.12 (1996).

Peters, M. S., Timmerhaus, K. D. and West, R. E., "Plant Design and Economics for Chemical Engineers," 5th edition, McGraw Hill Inc., New York (2003).

Seider, W. D., Seader, J. D. and Lewin D. R., "Product and Process Design Principles: Synthesis, Analysis and Evaluation," 2nd edition, John Wiley and Sons, Inc.New York (2004), p.582.

Supple, B., Howard-Hildige, R., Gonzalez-Gomez, E., Leahy, J. J., "The Effect of Steam Treating of Waste Cooking Oil on the Yield of Methyl Ester," J. Am. Oil Soc. Chem., 79(2), 175-178 (1999).

Zhang, Y., Dubé, M. A., McLean, D. D. and Kates, M., "Biodiesel Production from Waste Cooking Oil: 1. Process design and technological assessment", Bioresource Technology, 89, 1-15 (2003a).

Zhang, Y., Dubé, M. A., McLean, D. D. and Kates, M., "Biodiesel Production from Waste Cooking Oil: Economic Assessment and Sensitivity Analysis", Bioresource Technology, 90, 229-240 (2003b).

Zheng, S., Kates, M., Dubé, M. A. and McLean, D. D., "Acid Catalyzed Production of Biodiesel from Waste Frying oil", Biomass and Bioenergy, 30, 267-272 (2006).

Zullaikah, S., Lai, C. C., Vali, S. R. and J, Y. H., "A Two-Step Acid-Catalyzed Process for The Production of Biodiesel from Rice Bran Oil", Bioresource Technology, 96, 1889-1896 (2005).

Chapter 6

Conclusions, Contributions and Recommendations

In this chapter, a summary of the conclusions derived from this thesis will be presented. The contribution of this work to the existing science and technology of biodiesel purification and also the recommendations for further research in this area will be stated.

6.1 Conclusions

The focus of the current study was the technical and economic assessment of the biodiesel purification process via solvent partitioning in a single-stage mixer-settler, with the aim of separating glycerol and biodiesel to achieve the relevant ASTM standard (D-6751-02). The reaction mixture containing biodiesel, glycerol and methanol was fed into the mixer, while hexane, methanol and water were the extraction solvents to be evaluated. Because of the difficulties encountered during the experimental study of this 5-component system, the liquid-liquid equilibria experiments of the quaternary system of methyl oleate (i.e., biodiesel), glycerol, hexane and methanol, were carried out using GPC analysis. The experimental results showed the separation of two liquid phases with mostly hexane and methyl oleate in the upper phase and methanol and glycerol in the lower phase. The UNIFAC and Modified UNIFAC activity coefficient models were found to provide good predictions of the phase equilibria of this system. However, the precision of the experimental data was not sufficient enough to verify achievement of the ASTM Standard of the glycerol content of the methyl oleate-rich phase.

The potential solvents, hexane, methanol and water, were studied individually or mixed together for their capability (1) to yield biodiesel that fulfills the ASTM standard for its glycerol content (<0.02 wt%) and (2) to satisfy the technical criteria required for the efficient operation of the mixer-settler unit. The compositions of the solvents that satisfied these criteria were determined via application of a constrained multi-objective

optimization routine. The following conclusions were made based on the technical assessment of the potential solvents, either alone or mixed together.

1. Using hexane alone as solvent, a short liquid residence time was obtained in the settler, due to the significant decrease in the density and viscosity of the biodiesel-rich phase relative to the glycerol-rich phase. However, neither the ASTM standard, nor the ideal 1:1 ratio of the liquid phase volumes was obtainable.

2. The use of methanol alone as the extraction solvent resulted in biodiesel meeting the ASTM standard for glycerol content in biodiesel; however, the lengthy residence time, the likelihood of phase inversion and possibility of formation of a single liquid phase at high methanol concentrations were the major barriers to its use.

3. The addition of water to the feed stream to the extractor, which contains some methanol, was a very good solvent for glycerol and the ASTM standard was satisfied. As well, the phase volumes were close to being equal. A minimum achievable residence time in the settler of ~5½ h was also found. However, in alkali-catalyzed transesterification of waste cooking oil, free fatty acids are converted to soaps, which in the presence of large quantities of water form emulsions. The emulsion problem does not exist in acid-catalyzed transesterification of waste cooking oil. Thus, despite the merits of water, its use for separating glycerol and biodiesel is not free of difficulty for alkali-catalyzed systems.

4. From the technical point of view, the most appropriate solvents were found to be (1) water combined with residual methanol in the stream entering the extractor (with the optimal biodiesel:methanol:water mass ratio of 1:0.10:0.97) (2) a mixture of hexane and methanol (with optimal mass ratio of biodiesel:hexane:methanol of 1:1.15:1.62), (3) a mixture of hexane and water combined with residual methanol in the feed to the mixer-settler (with optimal

mass ratio of biodiesel:hexane:methanol:water of 1:0.79:0.10:0.69) and (4) a mixture of hexane, methanol and water (with optimal mass ratio of biodiesel:hexane:methanol:water of 1:2.27:0.87:0.30). For all the optimal compositions, the residual methanol in the feed to the mixer was included.

The economic assessment was also carried out for the plants, which produced biodiesel via acid-catalyzed transesterification of waste cooking oil with methanol and purified it via a single-stage mixer-settler with the four technically feasible solvent systems. The ultimate biodiesel-rich and glycerol-rich product streams contained 97 wt% and 92 wt% pure biodiesel and glycerol, respectively. No significant difference was observed between the annual revenue, total production cost and annual after-tax returns on investment of these four plants. However, in terms of the total capital investment, the water-washing system (Process *A*) required a considerably less initial investment to build the plant. Regardless of the negative annual after-tax returns on investment found for these biodiesel processes, in order to compare the economics of these processes, the relative values of total production costs, total capital investments, annual revenue, return on investments and biodiesel break-even prices are of importance. The following conclusions were made based on the economic study of the proposed biodiesel plants:

1. When water was combined with the residual methanol to form a biodiesel:methanol:water mass ratio of 1:0.10:0.86 (Process *A*), an after-tax return on investment of -43% and a biodiesel break-even price of 1.70 $/L were found. Despite the very high recovery of biodiesel in this system (99.9%), its relatively low annual after-tax return on investment was because of its relatively low annual revenue and low total capital investment. Its low total annual revenue was due to the higher purity of biodiesel in the final biodiesel-rich product stream (99.5 wt%), compared to the other systems (97 wt%), which resulted in a smaller rate of production of the biodiesel-rich product stream. It was also found that even on adding a component, which cost nothing, to the biodiesel-rich product stream to increase its flow rate and reduce the purity of biodiesel to 97 wt%, the ROI would increase to the value of -41%.

2. When a mixture of hexane and water was combined with residual methanol to form a mass ratio of biodiesel:hexane:methanol:water of 1:0.43:0.10:0.24 (Process *C*), the highest return on investment of -35% was achieved with a break-even price of biodiesel of 1.77 $/L.

3. When hexane and additional methanol were combined with the residual methanol to form a biodiesel:hexane:methanol mass ratio of 1:0.61:0.89 (Process *B*), a return on investment and biodiesel break-even price of -38% and 1.80 $/L, respectively were found. Compared to Processes *C* and *D*, the recovery of biodiesel and accordingly, the total annual revenue were lower due to the absence of water.

4. When hexane, water and additional methanol were combined to form a biodiesel:hexane:methanol:water mas ratio of 1:2.19:0.90:0.34 (Process *D*), has the highest raw material expense, its recovery of biodiesel and glycerol and accordingly the total annual sales revenue is higher than that of Processes *A* and *B*. Therefore this process with -36% after-tax return on investment was economically more acceptable than Processes *A* and *B*, but less economically beneficial than Process *C*. This process showed the highest break-even price of biodiesel of 1.91 $/L among the processes studied.

5. In terms of the annual after-tax return on investment, the best processes were found to be Processes *C* and *D*, both having a mixture of hexane, methanol and water as extraction solvent, while in terms of break-even price of biodiesel or total capital investment, Process *A* showed to be the best process.

6.2 Contributions

The main contributions of this study in the science and technology of biodiesel purification, especially the separation of the glycerol by-product from biodiesel are summarized as follows:

1. The UNIFAC activity coefficient model was shown to acceptably predict the phase equilibrium behavior of the system methyl oleate, glycerol, hexane and methanol at room temperature of ~20°C and atmospheric pressure without any parameter adjustment. The liquid-liquid equilibrium of such a system has not been experimentally and theoretically studied previously.

2. While water-washing has been the most widespread technique to remove glycerol and other impurities from biodiesel, the current study investigates alternative approaches involving the use of hexane and methanol solvents along with water for such separations. Although the use of hexane to purify biodiesel was previously mentioned by a few researchers, their work was restricted to the bench-scale extraction of biodiesel with hexane and did not provide detailed technical and economic assessment of such systems. In the present work, the technical feasibility of single or mixed solvent systems, containing hexane, methanol and/or water, was evaluated and their compositions optimized. This evaluation was based on the operation of a single-stage mixer-settler unit. The economics of the biodiesel plants with such solvent extraction systems was assessed considering annual after-tax return on investment, break-even price of biodiesel, total capital investment, total production cost and annual sales revenue.

3. In most studies, the separation of methanol, water and other extraction solvents from the biodiesel or glycerol has been carried out by distillation or vacuum drying, which is costly and sometimes these methods did not yield a high quality glycerol. In the present work, four inexpensive flash separators located after the mixer-settler unit were designed to separate the hexane, methanol and water from the biodiesel-rich and glycerol-rich phases exiting the top and bottom of the settler, respectively. Even though two of these flash drums operate at atmospheric pressure and relatively low temperatures, glycerol and biodiesel with purities of 97 wt% and 92 wt%, respectively, were obtained. Easier operation of the flash drums compared to distillation columns or vacuum dryers and their lower equipment costs make them more favorable choices.

6.3 Recommendations

The following recommendations are proposed for further research and studies in this field:

1. An appropriate analytical method should be developed to study the phase equilibria of the system methyl oleate, glycerol, hexane, methanol and water experimentally. Gas chromatography (i.e., GC) equipped with an FID (Flame Ionization Detector) and a factor four capillary column (type VF-5HT from Varian Inc.) with length×ID of 15m×0.32 mm is suggested for such analysis. Since water cannot be detected with an FID detector, a GC equipped with a Thermal Conductivity Detector (TCD) or the Karl-Fischer titration technique is recommended for detecting the water content of the samples. These experimental data could then be employed for estimation of the binary interaction parameters of the selected activity coefficient models (e.g., NRTL or UNIQUAC). Such models may provide better prediction of liquid-liquid phase equilibria for this system and thereby more reliable process design.

2. In order to simplify the calculations in this study, methyl oleate ($C_{19}H_{36}O_2$) was employed as a substitute for biodiesel. Although biodiesel consists of fatty acids with different chain lengths, this assumption is practical because oleic acid is the major constituent of the waste canola oil feedstock. To improve the reliability of the current results, one may consider using mixtures involving other fatty acids, such as palmitic, linoleic and stearic acid as methyl esters.

3. In the current study, the stream entering the mixer was assumed to contain biodiesel, glycerol and methanol and was free of unconverted oil and free fatty acids. The presence of unconverted oil and free fatty acids in the mixer-settler system should have a slight effect on the results, since both unconverted oil and free fatty acids remain in the biodiesel/hexane phase. Appropriate experiments

and phase equilibria calculations should be conducted in order to obtain more reliable results.

4. The operating conditions of the flash separators located after the extraction unit (flash drums 1 to 4 in Figure 1, Chapter 5) were set to achieve biodiesel and glycerol product streams with 97 wt% and 92 wt% purity, respectively. It was also attempted to operate at relatively low temperatures due to the chance of polymerization or decomposition of biodiesel at high temperatures. In order to obtain more reliable results of the plant design, these flash drums should be re-investigated and their temperatures and pressures optimized for the maximum profitability of the biodiesel plant as well as the desired vapor-liquid phase separation (i.e., solvent separation).

5. Although the flash separators were found to be suitable for the separation of hexane, methanol and water solvents from the biodiesel-rich and glycerol-rich phases in this study, feasibility of other solvent separation techniques such as distillation, rotary evaporation, membrane separation or adsorption, could also be evaluated technically and economically. Especially, as was previously studied, the use of distillation columns result in better separation of the solvents from the upper and lower phases exiting the extractor (biodiesel-rich and glycerol-rich phases, respectively) and consequently, achieving purer and more valuable biodiesel or glycerol product streams (Zhang et al., 2003a,b).

6. Due to its toxicity and flammability, the presence of hexane solvent in the biodiesel extraction unit necessitates special safety considerations. For instance, changes in operating temperatures and pressures or type of heat exchangers, can be applied to overcome or reduce the hexane emissions (Tunisian Cleaner Production Centre, 2007). In addition, treatment of used water and removal of residual hexane to prevent the hexane emissions into the environment is another important task to be considered. For further investigation of such biodiesel

production and processing, these considerations should be included in the technical design and economic assessment of the plant.

7. The evaluation of the economic feasibility of the biodiesel plant was carried out based on the overall design and equipment cost of the reactor, methanol distillation column and acid removal unit, reported earlier by Zhang et al. (2003b). A thorough plant design along with simultaneous economic assessment and optimization of the entire biodiesel plant should be carried out to achieve more accurate results.

8. Although the extraction system under investigation was designed for the acid-catalyzed transesterification of waste cooking oil, it may also be applied to the alkali-catalyzed reaction of virgin vegetable oil or waste cooking oil, provided the fatty acid soaps have been converted to methyl esters by acid-catalyzed methanolysis in a pre-treatment step. In this case, a complete knowledge of soap formation, its role in emulsion formation and its effect on the downstream processes might help to ensure a more industrially reliable design and optimization of the purification system.

References

Tunisian Cleaner Production Centre (CP3), INEM Casebook, http://www.p2pays.org, 2007.

Zhang, Y., Dubé, M. A., McLean, D. D. and Kates, M., "Biodiesel Production from Waste Cooking Oil: 1. Process design and technological assessment," Bioresource Technology, 89, 1-16 (2003a).

Zhang, Y., Dubé, M. A., McLean, D. D. and Kates, M., "Biodiesel Production from Waste Cooking Oil: Economic Assessment and Sensitivity Analysis," Bioresource Technology, 90, 229-240 (2003b).

Appendix A

Calibration of Gel Permeation Chromatograph

In order to convert the peak areas obtained from the GPC chromatograms to the injected mass or moles and then to mass or mole fractions, the GPC (i.e., Gel Permeation Chromatography) was calibrated for the components involved in the liquid-liquid equilibrium experiment of this thesis (methyl oleate or FAME, glycerol, hexane, methanol). This section deals with the analysis of the calibration data and developing appropriate equations to reliably interpret the experimental results.

A.1 Materials and operating conditions

Standard solutions of FAME, glycerol, hexane, methanol and methyl oleate were prepared and employed for calibrating the GPC for each component. FAME was produced in one of our laboratories through the alkali catalyzed transesterification of canola oil with methanol and then washed with water. In order to remove any moisture in the FAME, it was dried over sodium sulphate. High purity of FAME was verified analytically by GPC before using to prepare the standard solutions. The components, methyl oleate, glycerol, hexane and methanol were supplied by Sigma-Aldrich with the purity of 99%, 99^{+}%, 99.93% and 99.5^{+}%, respectively. These components were employed without any purification or further treatment. Calibration of GPC for each component was done separately, since their chromatographic peaks were found to be clearly resolute. The GPC operating temperature was set at 25°C, with tetrahydrofuran (THF) as the carrier fluid pumped into the column at the pressure and flow rate of ~732 psi 0.5 mL/min, respectively. 20 μL of each sample was injected twice into the GPC with an autosampler. The above operating conditions for the GPC calibration were the same as those applied for the GPC analyses of the liquid-liquid equilibria experiments, as described in Chapter 3 (Paper 1) of this thesis.

A.2 Resolution of the peaks

When analyzing a sample of more than one component with an analytical instrument such as GC (i.e., gas chromatography) or GPC, the resolution of the peaks should be studied carefully. This indicates if the selected analytical method is suitable to yield clearly separated peaks. If peak overlap or abnormal broadening of the peaks occurs, the resulting mass or mole fractions will be erroneous.

To study the resolution of the peaks in the system under investigation, each of the components (FAME, glycerol, hexane and methanol) was diluted with a 3:1 molar ratio of FAME to glycerol. This sample was then mixed in an automatic rotator and kept without mixing for 12 hours to allow to separation into two liquid phases. Figure A.1 shows the chromatograms of the upper and lower phases of that sample. Clearly, the four peaks associated with the four components are well separated and acceptably resolute in both phases. However, the proximity of the peaks of hexane and methanol could be a potential problem if peak broadening with increased amounts of these solvents leads to overlapping of their peaks. This issue has been solved by developing a MATLAB® code (version 7.1.0.246, R14 developed by MathWorks Inc.), which calculates the area under the peak of hexane or methanol by taking the overlapped region into account. Since the retention times of FAME and methyl oleate were found to be very close, the same conclusion can be made for the resolution of the peaks in the mixture of methyl oleate, glycerol, hexane and methanol.

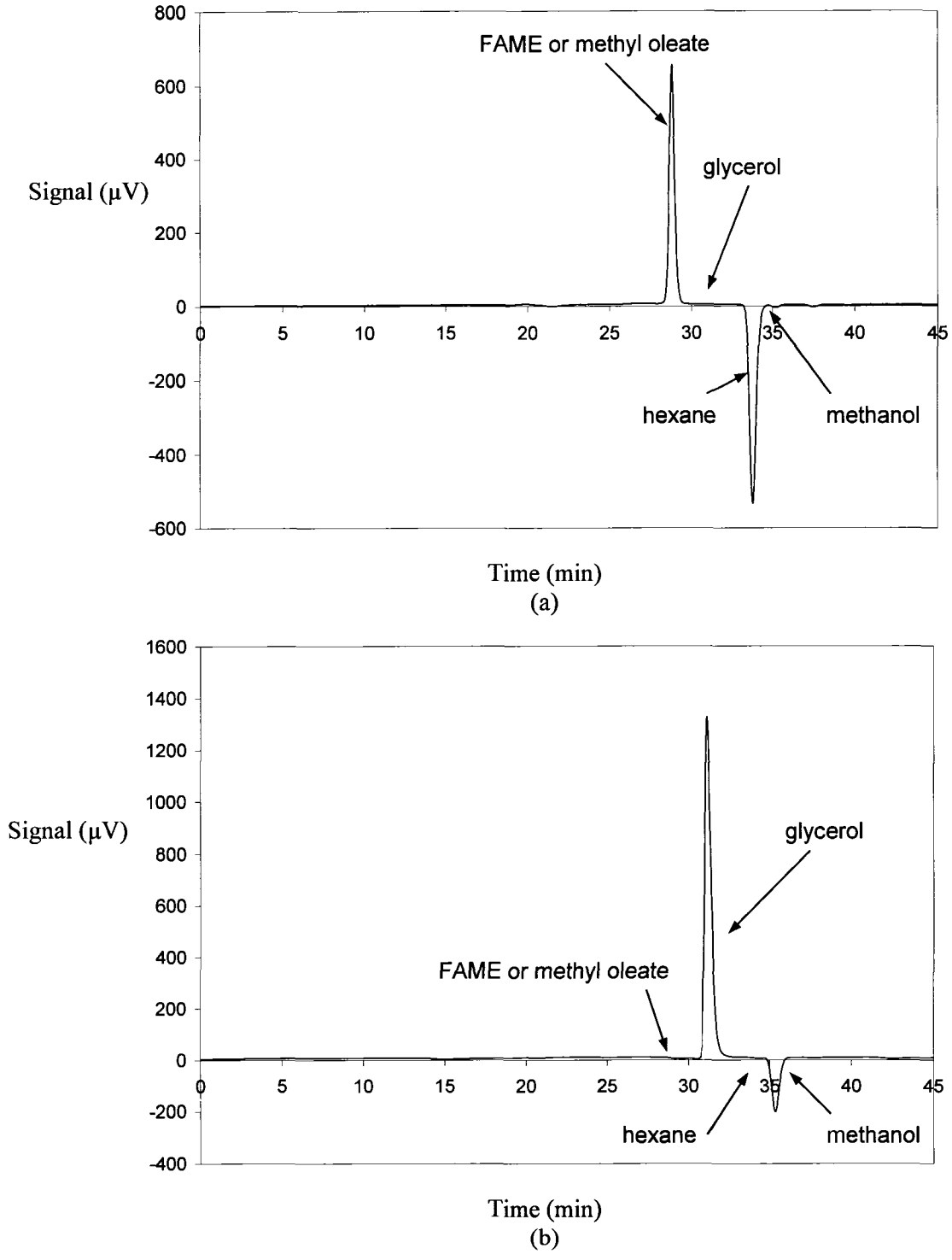

Figure A.1 Sample experimental chromatograms with mole/mass fractions of the components in the upper and lower liquid phases:
(a) Methyl oleate-rich phase: methyl oleate: 0.2046/0.4710, glycerol: 0.0076/0.0054, hexane: 0.7797/0.5216, methanol: 0.0081/0.0020
(b) Glycerol-rich phase: methyl oleate: 0.0013/0.0050, glycerol: 0.7537/0.8392, hexane: 0.0012/0.0013, methanol: 0.2438/0.1005

The peak retention times were recorded for every injection in the calibration experiment. Table A.1 contains the mean value, standard deviation and standard error as well as the minimum and maximum retention times observed for each component. The mean values of the retention times are clearly different. Hence, it can be concluded that the GPC analytical method was effective for analyzing the components in the mixture reliably.

Table A.1 Mean retention time, standard error, standard deviation, minimum and maximum retention times observed in calibration experiments of each individual component

Component	Number of data points	Mean retention time (min)	Standard error	Standard deviation	Minimum retention time detected (min)	Maximum retention time detected (min)
FAME	106	29.02	0.015	0.15	28.68	29.73
glycerol	76	31.05	0.022	0.19	30.80	31.95
hexane	61	33.90	0.033	0.26	33.58	34.65
methanol	82	35.12	0.013	0.12	34.82	35.53
methyl oleate	31	29.00	0.040	0.21	28.68	29.75

A.3 Sample preparation

Standard solutions of each component were prepared separately by weighing required amounts (used a Mettler Toledo, model AG204 digital weighting device) of each in a volumetric flask and adding THF up to a volume of 100 mL or 200 mL. The mass of each component in the standard solution, final volume of the standard solutions and the concentration of the prepared solutions are presented in Table A.2. The standard solutions were then used to make several solutions with different but known concentrations of each component. This was carried out by pouring known volumes of the standard solutions (Table A.2) into a 10 or 25 mL volumetric flask by a graduated pipette and then adding THF to reach the specified volume (Table A.3).

Eventually out of the samples prepared with different concentrations for each component, two samples were made up in separate vials and two injections of each vial

were carried out into the GPC. Therefore, four replicated analyses for each concentration were obtained. Peak area, peak height and retention time of each sample injected into the GPC were recorded. Table A.3 summarizes the samples prepared from the standard solutions.

Table A.2 Standard solutions of the components used to prepare the calibration solutions

Component	Standard solution	Mass (gr)	Final volume with THF (mL)	Concentration (gr/mL)
FAME	1	2.0011	100	0.020011
	2	4.0016	200	0.020008
	3	0.1080	100	0.001080
glycerol	1	1.0036	100	0.010036
	2	1.0011	100	0.010011
	3	1.1012	100	0.011012
	4	1.5081	100	0.015081
hexane	1	2.5039	100	0.025039
	2	2.5053	100	0.025053
	3	0.8035	200	0.004018
methanol	1	2.0090	100	0.020090
	2	2.0016	100	0.020016
	3	0.0718	100	0.000718
methyl oleate	1	1.9990	100	0.019990
	2	2.0080	100	0.020080

Table A.3 Solutions prepared for each component using standard solutions

Component	Standard solution	Solution number	Amount (volume) taken from the standard solution (mL)	Final volume with THF (mL)
FAME	1	1	standard solution 1	
		2	18.75	25
		3	12.5	25
		4	6.25	25
	2	5	1.25	25
		6	2.5	25
		7	3.75	25
		8	5	25
		9	3	10
		10	3.5	10
		11	10	25
		12	11.25	25
		13	5.5	10
		14	15	25

Table A.3 Solutions prepared for each component using standard solutions (cont'd)

Component	Standard solution	Solution number	Amount (volume) taken from the standard solution (mL)	Final volume with THF (mL)
FAME	2	15	16.25	25
		16	17.5	25
		17	7.5	10
		18	20	25
		19	8.5	10
		20	9	10
		21	9.5	10
	3	22	18.75	25
		23	12.5	25
		24	4	10
		25	2.5	10
glycerol	1	1	standard solution 1	
		2	20	25
		3	15	25
		4	10	25
		5	2	10
	2	6	9	10
		7	8	10
		8	standard solution 2	
		9	17.5	25
		10	2.5	25
		11	22.5	25
	3	12	18.75	25
		13	12.5	25
		14	4	10
		15	2.5	10
		16	standard solution 3	
	4	17	11.6	25
		18	13.3	25
		19	15	25
		20	standard solution 4	
		21	6.8	10
		22	8	10
		23	8.6	10
		24	9.3	10
		25	16	25
hexane	1	1	standard solution 1	
		2	5	25
		3	10	25
		4	15	25
		5	8	10
	2	6	8	10
		7	5	10
		8	17.5	25
		9	22.5	25
		10	7.5	25

Table A.3 Solutions prepared for each component using standard solutions (cont'd)

Component	Standard solution	Solution number	Amount (volume) taken from the standard solution (mL)	Final volume with THF (mL)
hexane	3	11	1.56	25
		12	1.25	10
		13	2.5	10
		14	12.5	25
		15	standard solution 3	
		16	18.75	25
methanol	1	1	standard solution 1	
		2	18.75	25
		3	5	10
		4	2.5	10
	2	5	9.5	10
		6	9	10
		7	8.5	10
		8	8	10
		9	7.5	10
		10	7	10
		11	6.5	10
		12	6	10
		13	5.5	10
		14	4.5	10
		15	4	10
		16	3.5	10
		17	3	10
		18	2	10
		19	1.5	10
		20	1	10
		21	0.5	10
	3	22	3.3	10
		23	6.6	10
		24	standard solution 3	
		25	5	25
methyl oleate	1	1	18.75	25
		2	12.5	25
		3	9.375	25
		4	2.5	10
		5	2	10
		6	3.125	25
		7	1.25	25
		8	0.25	10
		9	0.125	10
		10	standard solution 2	
		11	0.3	25
		12	standard solution 2	
		13	6.2	10
		14	8.7	10

A.4 Model building

When carrying out the calibration, the independent and dependent variables are the injected mass and the peak areas, respectively. Thus, in contrast to what typically has been done, the form of the model to be fitted to the experimental calibration data should be as following:

$$\text{peak area} = f(\text{injected mass}) \tag{A.1}$$

where f represents a function. To indicate the form of the model, the first step is plotting all the observed data points. Figure A.2 shows the peak areas obtained for each component as a function of the mass injected into the GPC. At the first look, a linear model seemed to be an appropriate choice for all the components; although a slight quadratic curvature could also be detected. Thus, linear model was studied as the primary step of developing a calibration equation.

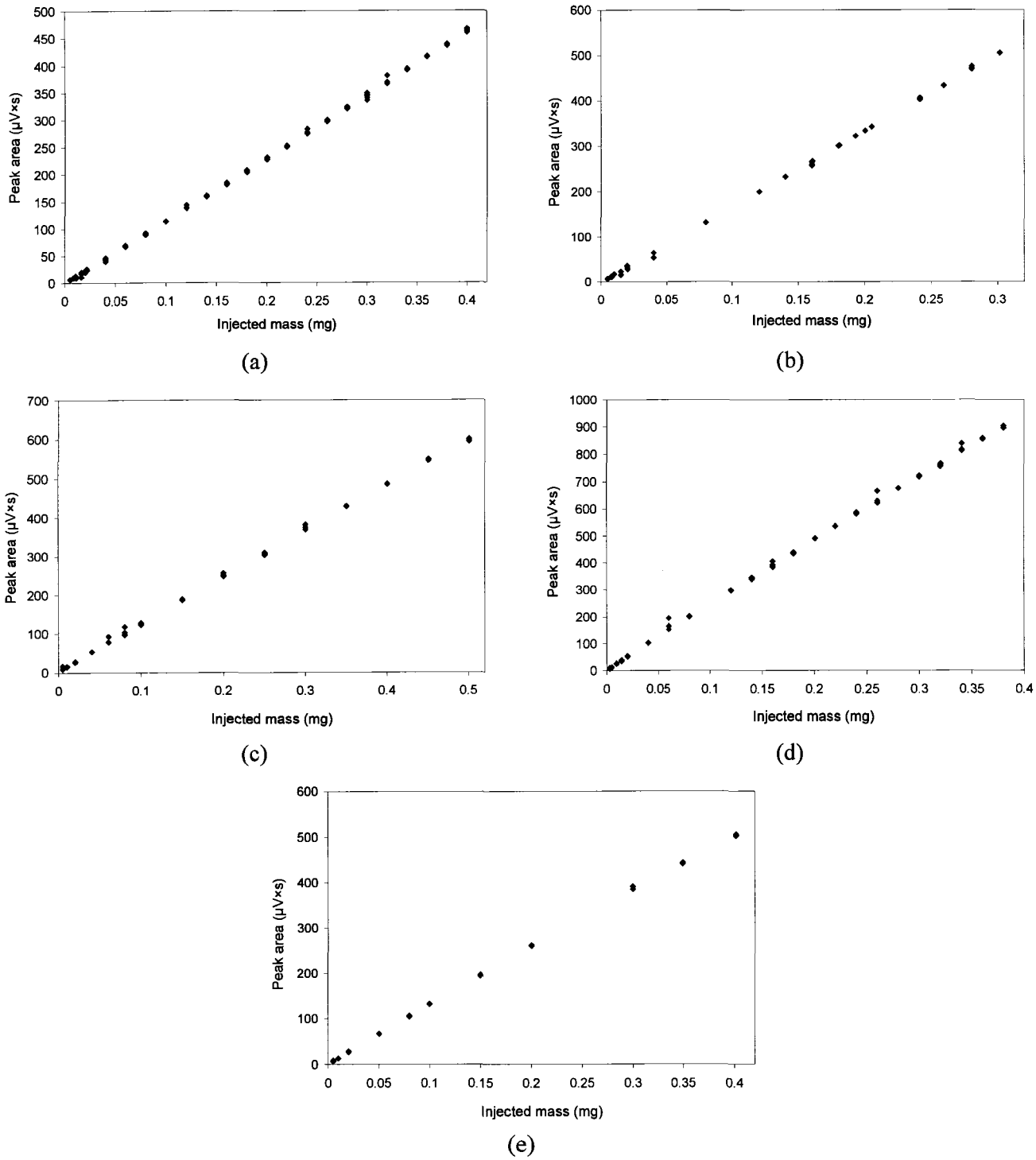

Figure A.2 Experimental calibration data for (a) FAME (b) glycerol (c) hexane (d) methanol (e) methyl oleate

A.4.1 Fitting a linear model

The linear model to be fitted to the calibration experimental data has the following form:

$$\text{peak area} = \beta_1^A \times \text{injected mass} + \beta_0^A \quad (\text{model } A) \tag{A.2}$$

Tables A.4 and 5 contain the regression statistics and ANOVA data (i.e., Analysis of Variance) data for each component. These data were obtained using the 'Data Analysis' and 'Regression' toolbox in Microsoft Office Excel (2003). As a part of the same toolbox, Table A.6 contains the fitted parameters, the precision of the parameters and other statistical variables found through regression of the calibration data.

Table A.4 Linear regression statistical data obtained using the regression toolbox in Excel

	FAME	glycerol	hexane	methanol	methyl oleate
Multiple R	0.9998	0.9998	0.9997	0.9995	0.9997
R Square	0.9997	0.9997	0.9993	0.9990	0.9994
Adjusted R Square	0.9997	0.9997	0.9993	0.9990	0.9994
R^2/R^2_{adj}	1.0000	1.0000	1.0000	1.0000	1.0000
Standard Error	2.625	2.952	5.0859	9.384	4.299
Observations	106	76	61	82	31

Table A.5 ANOVA table for the linear regression of calibration data using regression toolbox in Excel

		df	SS	MS	F	Significance F
FAME	Regression	1	2366285	2366285	343538	7.96E-185
	Residual	104	716	6.89		
	Total	105	2367001			
glycerol	Regression	1	2076914	2076914	238316	1.47E-131
	Residual	74	645	8.71		
	Total	75	2077559			
hexane	Regression	1	2332411	2332411	90170	1.18E-95
	Residual	59	1526	25.87		
	Total	60	2333937			
methanol	Regression	1	7182877	7182877	81570	3.93E-122
	Residual	80	7045	88.05		
	Total	81	7189922			
methyl oleate	Regression	1	959188	959188	51904	9.95E-49
	Residual	29	536	18.48		
	Total	30	959724			

Table A.6 Regression parameters of linear model to the calibration data points using regression toolbox in Excel

		Coefficients	Standard error	t-Stat	P-value	Lower 95%	Upper 95%
FAME	β_0^A	-1.5166	0.43	-3.54	0.001	-2.37	-0.67
	β_1^A	1156.1930	1.97	586.12	7.956E-185	1152.28	1160.10
glycerol	β_0^A	-3.3178	0.57	-5.83	1.379E-07	-4.45	-2.18
	β_1^A	1684.3809	3.45	488.18	1.472E-131	1677.51	1691.26
hexane	β_0^A	7.201	1.02	7.09	1.894E-09	5.17	9.23
	β_1^A	1195.7707	3.98	300.28	1.181E-95	1187.80	1203.74
methanol	β_0^A	9.4157	1.73	5.45	5.533E-07	5.97	12.86
	β_1^A	2375.8428	8.32	285.60	3.932E-122	2359.29	2392.40
methyl oleate	β_0^A	4.1289	1.18	3.51	0.002	1.72	6.54
	β_1^A	1260.7575	5.53	227.82	9.953E-49	1249.44	1272.08

A.4.2 Qualitative evaluation of goodness of fit (linear model)

To determine how well the linear model represents the experimental calibration data, qualitative and quantitative methods were used. Evaluating the residual plots, which are the difference between the observed and predicted peak areas versus the predicted peak areas, one is able to qualitatively check if the model represents the data points properly. Random distribution of the residual points around zero implies a reasonable fit. The residual plots of the linear model are presented in Figure A.3. The plots of FAME, glycerol and methanol show a random distribution of the data points around zero axes; however, a quadratic trend is detectable with respect to hexane and methyl oleate.

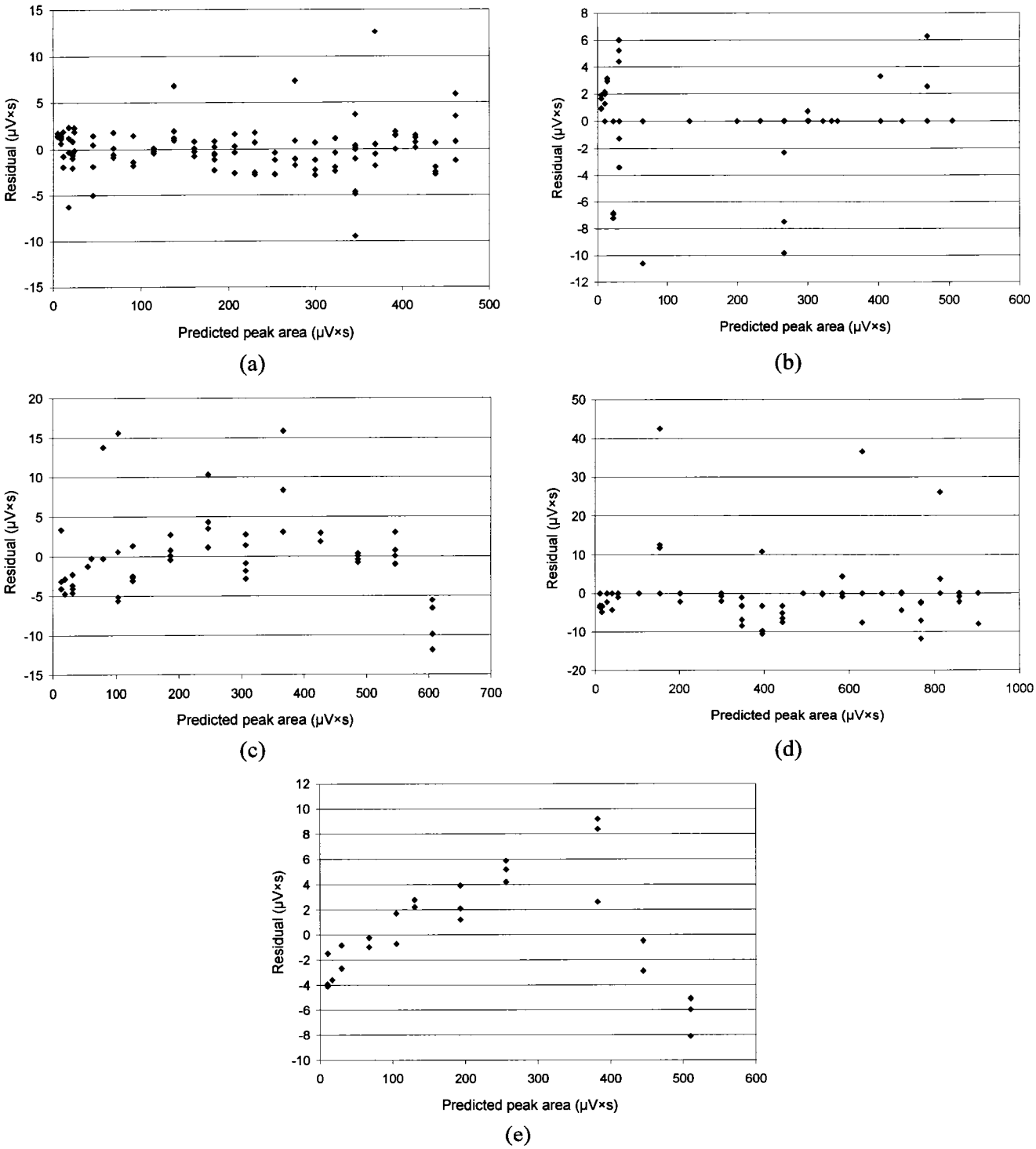

Figure A.3 Residual plots of the linear model for (a) FAME (b) glycerol (c) hexane (d) methanol (e) methyl oleate

A.4.3 Quantitative lack of fit test (linear model)

In order to carry out the quantitative lack of fit test, the test ratio (Equation 3) should be compared to the corresponding value of F-distribution. When R is greater than $F_{\nu_1,\nu_2,\alpha}$, the lack of fit is not significant. In that equation, ν_1, ν_2 and α are degree of freedom associated with the lack of fit $\left(\text{or } n-P-\sum_{i=1}^{l}(m_i-1)\right)$, degree of freedom associated with the pure error variance $\left(\text{or } \sum_{i=1}^{l}(m_i-1)\right)$ and the level of significance, respectively. Comparing the value of the test ratio with $F_{\nu_1,\nu_2,\alpha}$, one can find if the lack of fit is significant.

$$R=\frac{\sum_{u=1}^{n}\left(\bar{y}_u-\hat{y}_u\right)^2 \Big/ \left\{n-P-\sum_{i=1}^{l}(m_i-1)\right\}}{\hat{\sigma}_P^2} \tag{A.3}$$

In the Equation A.3, $\hat{y}_u$ and $\bar{y}_u$ are the predicted variables and the mean value of the replicated experimental points. $\hat{\sigma}_P^2$ is the pooled pure error variance and can be calculated by combining the variance of each set of replicated experimental data (Equations A.4 and 5). This combination can only be performed if the assumption of homoscedasticity or constant variability over the entire range of observed data points is valid. Homoscedasticity of the observed data can be simply checked by means of the residual plots. If the residual points are not increasing or decreasing systematically along the x-axis, homoscedasticity of the experimental data can be concluded.

Assessing the residual plots (Figures 7 through 11), one can observe no indication of heteroscedasticity in the experimental calibration data. Thus, the pooled pure error variance was calculated by Equation A.5 and is presented for each component in Table A.7.

$$\hat{\sigma}^2=\frac{\sum_{k}\left(PA_k-\overline{PA}\right)}{m-1} \tag{A.4}$$

$$\text{pooled pure error variance} = \hat{\sigma}_P^{\,2} = \frac{\sum_i (m_i - 1)\hat{\sigma}_i^{\,2}}{\sum_i (m_i - 1)} \qquad \text{(A.5)}$$

Table A.7 Pooled pure error variance associated with the GPC analyses of each component

Component	$\hat{\sigma}_P^{\,2}$ ($\mu V^2 \times s^2$)
FAME	1.90
glycerol	4.30
hexane	15.55
methanol	52.56
methyl oleate	2.69

The values of the test ratio (Equation 2) and the corresponding values of the *F*-distribution for each component are presented in Table A.8. The lack of fit was found not significant for glycerol, hexane, methanol and FAME. Although with respect to methyl oleate, the lack of fit was found significant. After assessing the linear model, the need for an additional term in the linear model (quadratic term) will be studied subsequently.

Table A.8 Results of quantitative test of lack of fit for the linear model

Component	R	v_1	v_2	$F_{v1,v2,\alpha}$
FAME	1.42	24	80	1.6
glycerol	1.14	22	52	1.8
hexane	1.00	13	46	1.97
methanol	0.98	20	60	1.75
methyl oleate	6.82	11	18	2.39

A.4.4 Testing the need for a quadratic term in the linear model

To evaluate if an additional term (a quadratic term) to the linear model results in a better fit, the *Q*-ratio (Equation A.6) should be compared to the corresponding *F*-distribution.

$$Q = \frac{1}{\hat{\sigma}_P^{\,2}} \frac{SSR_L^2 - SSR_Q^2}{n_Q - n_L} \tag{A.6}$$

SSR_L^2 and SSR_Q^2 are the sum of squares of residuals of the linear and quadratic models, respectively. n_Q, n_L and $\hat{\sigma}_P^2$ are the number of parameters in the quadratic model, number of parameters in the linear model and pooled experimental pure error variance, respectively.

If the value of Q is larger than the critical value of $F_{v1,v2,\alpha}$, it can be concluded that addition of a quadratic term to the linear model results in an improved fit. v_1 is the difference between the number of estimated parameters in the linear and quadratic models, v_2 is the degree of freedom associated with the pure error variance, $\sum_i (m_i - 1)$ (m_i is the number of data points in i^{th} set of replicates and the sum is over all the experiments) and α is the selected level of significance, 95% herein. This test is based on the significance test of the null hypothesis that the true value of the quadratic term in the model is zero. After fitting a second degree polynomial model (Equation 7) to the experimental calibration data, the sum of squares of residuals, the corresponding F-distribution and also the ratio Q (Equation 6) were determined and presented in Table A.9.

$$peak\ area = \beta_2^B \times (injected\ mass)^2 + \beta_1^B \times (injected\ mass) + \beta_0^B \quad (\text{model } B) \tag{A.7}$$

Table A.9 Values of SSR, Q and their corresponding F-distribution

Component	Q	SSR_{linear}	$SSR_{quadratic}$	$F_{v1,v2,\alpha}$
FAME	6.68	716.35	703.64	3.97
glycerol	7.61	644.91	612.19	4.04
hexane	29.08	1526.14	1074.05	4.07
methanol	34.52	7044.63	5230.26	3.99
methyl	151.41	535.92	128.94	4.41

Clearly, for all the components the ratio Q is significantly greater than $F_{v1,v2,\alpha}$ indicating that addition of a quadratic term to the linear model results in a better fit.

A.4.5 Fitting a quadratic model

Using the Data Analysis toolbox in Excel, the quadratic regression statistical data and ANOVA table have been presented in Tables A.10, 11 and 12.

Table A.10 Quadratic regression statistical data obtained using the regression toolbox in Excel

	FAME	glycerol	hexane	methanol	methyl oleate
Multiple R	0.9999	0.9999	0.9998	0.9996	0.9999
R Square	0.9997	0.9997	0.9995	0.9993	0.9999
Adjusted R square	0.9997	0.9997	0.9995	0.9993	0.9999
R^2/R^2_{adj}	1.0000	1.0000	1.0000	1.0000	1.0000
Standard Error	2.614	2.896	4.303	8.137	2.146
Observations	106	76	61	82	31

Table A.11 ANOVA table for the quadratic regression of calibration data using the regression toolbox in Excel

		df	SS	MS	F	significance F
FAME	Regression	2	2366298	1183149	173190	2.33E-182
	Residual	103	704	6.83		
	Total	105	2367001			
glycerol	Regression	2	2076946	103847	123832	1.35E-129
	Residual	73	612	8.39		
	Total	75	2077559			
hexane	Regression	2	2332863	1166432	62989	1.68E-97
	Residual	58	1074	18.52		
	Total	60	2333937			
methanol	Regression	2	7184692	3592346	54260	1.09E-124
	Residual	79	5230	66.21		
	Total	81	7189922			
methyl oleate	Regression	2	959595	479798	104190	6.24E-55
	Residual	28	129	4.61		
	Total	30	959724			

Table A.12 Regression parameters of the quadratic model to the calibration data points using regression toolbox in Excel

		Coefficients	Standard Error	*t*-Stat	*P*-value	Lower 95%	Upper 95%
FAME	β_0^B	-1.0635	0.54	-1.9660	0.0520	-2.14	0.0094
	β_1^B	1146.5514	7.34	156.2677	0.0000	1132.00	1161.10
	β_2^B	26.0755	19.12	1.3639	0.1756	-11.84	63.99
glycerol	β_0^B	-2.6395	0.66	-4.0250	0.0001	-3.95	-1.33
	β_1^B	1661.9926	11.83	140.4935	0.0000	1638.42	1685.57
	β_2^B	84.1593	42.61	1.9751	0.0520	-0.76	169.08
hexane	β_0^B	3.7599	1.11	3.3998	0.0012	1.55	5.97
	β_1^B	1256.4126	12.73	98.7182	0.0000	1230.94	1281.89
	β_2^B	-129.5565	26.21	-4.9410	0.0000	-182.04	-77.07
methanol	β_0^B	3.7010	1.85	1.9955	0.0494	0.0094	7.39
	β_1^B	2508.1186	26.28	95.4491	0.0000	2455.82	2560.42
	β_2^B	-377.1573	72.05	-5.2350	0.0000	-520.56	-233.75
methyl oleate	β_0^B	-0.4311	0.76	-0.5659	0.5760	-1.99	1.13
	β_1^B	1359.0024	10.81	125.7231	0.0000	1336.86	1381.14
	β_2^B	-247.8110	26.36	-9.4009	0.0000	-301.81	-193.81

A.4.6 Qualitative evaluation of goodness of fit (quadratic model)

As mentioned before, residual plots are helpful to qualitatively check the adequacy of the fitted model. Figures A.12 through 16 are the residual plots of the quadratic model for the components under study.

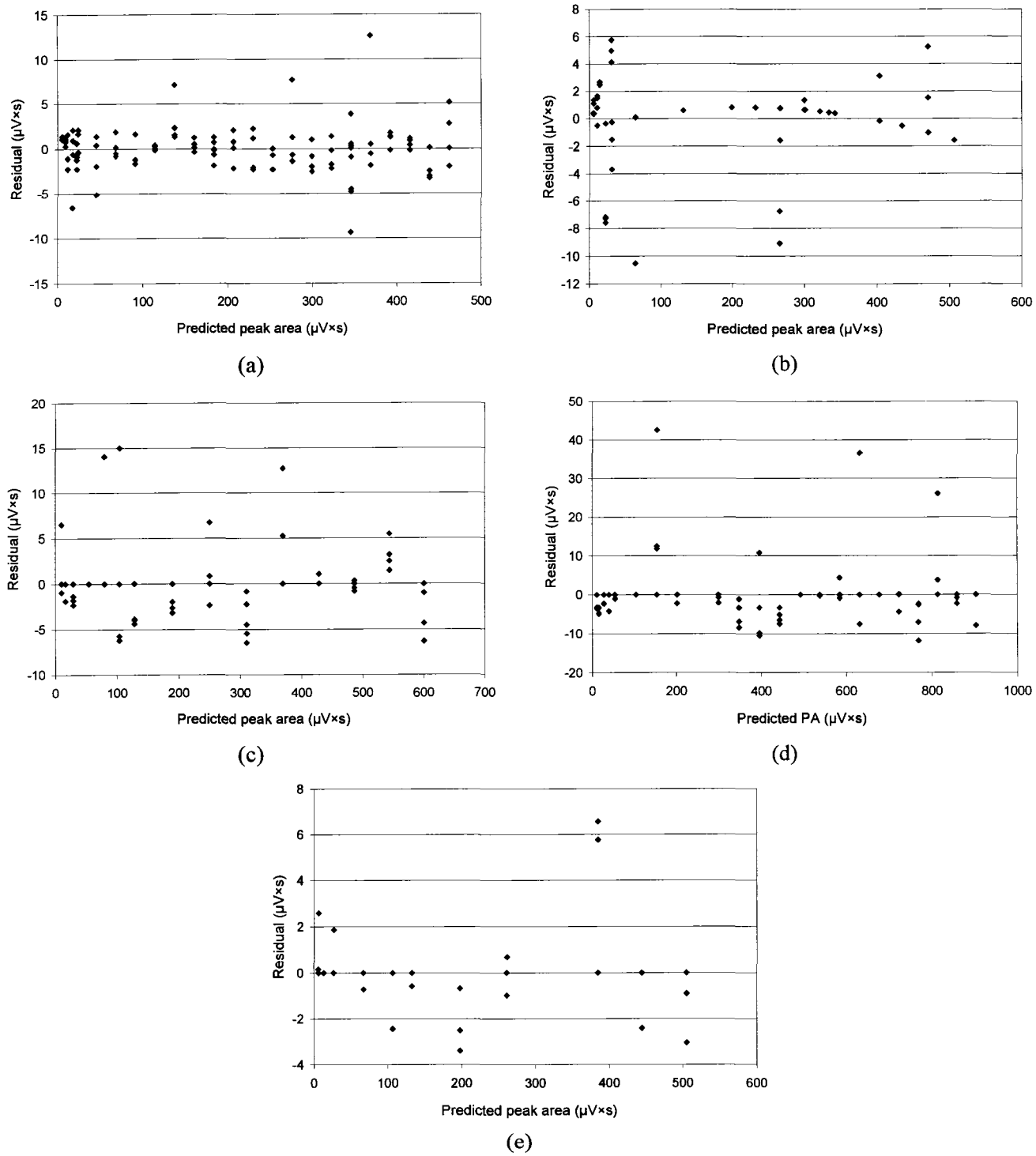

Figure A.4 Residual plots of the quadratic model for (a) FAME (b) glycerol (c) hexane (d) methanol (e) methyl oleate

A.4.7 Quantitative lack of fit test (quadratic model)

Table A.13 contains the results of the *R*-test for quantitative analysis of the lack of fit for the quadratic model. Although the quadratic model showed a better fir than the linear model and the linear model was an acceptable fit, the quantitative lack of fit test was carried out for the quadratic model. Based on the values in Table A.13, due to the lower values of *R* compared to the corresponding *F*-distribution, for all the components the quadratic model displays an acceptable fit.

Table A.13 Results of quantitative test of lack of fit for the quadratic model

Component	R	v_1	v_2	$F_{v1,v2,\alpha}$
FAME	1.41	23	80	1.72
glycerol	1.11	21	52	1.80
hexane	0.46	12	46	1.97
methanol	0.52	19	60	1.77
methyl oleate	1.08	10	18	2.41

A.5 Calibration curves

Figure A.5 shows the calibration curves of hexane, methanol and glycerol with peak area (μV×s) as a function of injected mass (mg). Figure A.6 is that of FAME and methyl oleate. When carrying out the liquid-liquid equilibria experiments, the injected masses of each species are to be determined by using the relevant calibration equations and measured peak areas. As discussed above, for all the components, a second degree polynomial model was tested to be the ultimate calibration model. Hence, the injected mass was found by solving a second order equation. One of the roots of the calibration equations was either a negative value or is unacceptably large and located out of the calibration range. As the mass of each species injected into the GPC, just one of the roots was acceptable. That reasonable root which was the injected mass into the GPC was then employed for further equilibrium calculations.

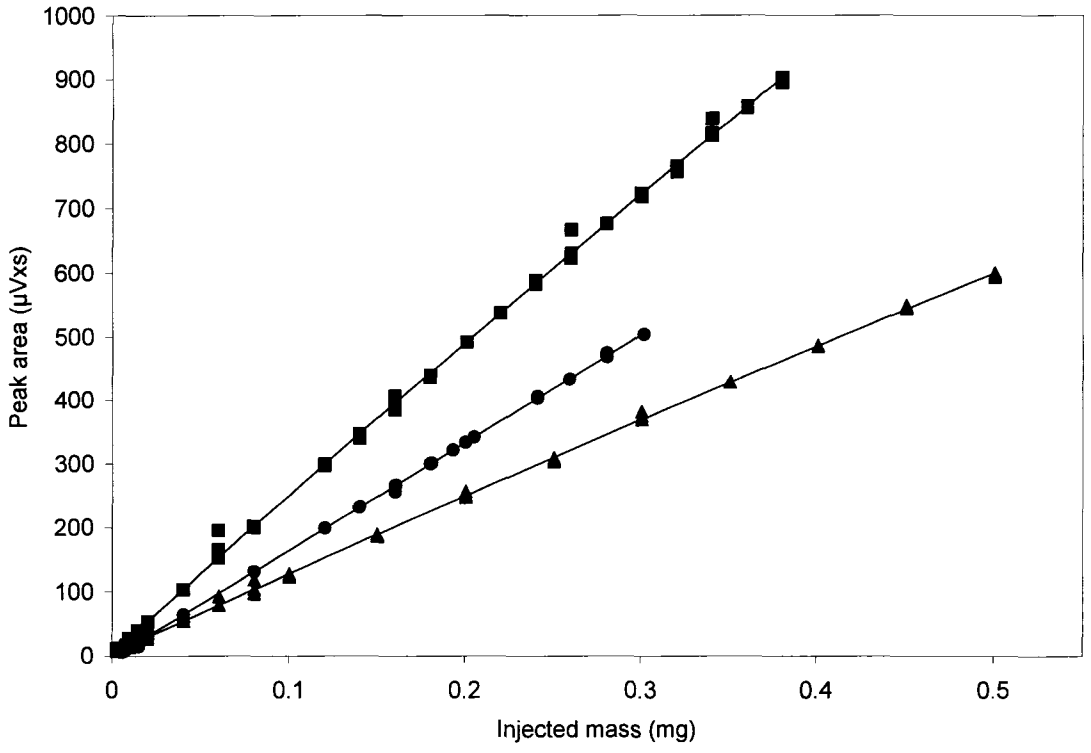

Figure A.5 Calibration curves of glycerol (●), hexane (▲) and methanol (■)

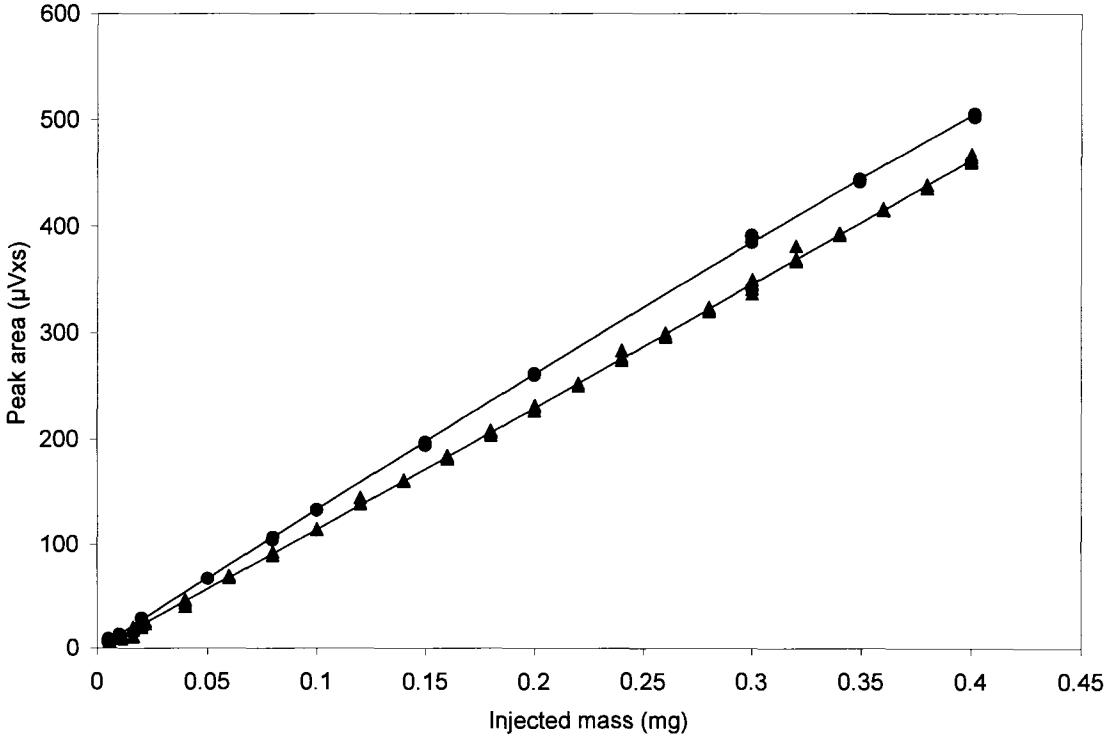

Figure A.6 Calibration curves of FAME (▲) and methyl oleate (●)

Reference

McLean, D. D. and Burn N. J., "Data Collection and Interpretation," course notes, CHG3337, University of Ottawa (2004).

Appendix B

Experimental Liquid-liquid Equilibria of the System Biodiesel, Glycerol, Hexane and Methanol at Room Temperature and Atmospheric Pressure

B.1 Preparation of biodiesel

Experimental liquid-liquid equilibria were conducted for the system biodiesel (i.e., fatty acid alkyl ester or FAME), glycerol, hexane and methanol. Biodiesel was produced in our laboratory by alkali-catalyzed transesterification of virgin vegetable oil with methanol at 65°C and 4 bar. The reaction time was 2 hours and in order to force the reaction to completion in a shorter time, methanol was initially fed into the batch reactor in excess (6:1 methanol to oil molar ratio). The reaction mixture containing biodiesel, glycerol by-product, alkali catalyst, unconverted oil and methanol was washed with water several times. Two phases were formed; biodiesel-rich phase and the aqueous phase which contained water, methanol, glycerol and the alkali catalyst. The biodiesel-rich phase was separated by decantation and the remaining moisture in biodiesel was evaporated. The final biodiesel product contained traces of unconverted oil and traces of moisture. In order to reduce the water content of the biodiesel, it was passed over anhydrous calcium sulphate.

B.2 Liquid-liquid equilibria

To carry out the liquid-liquid equilibrium experiments, several samples containing various quantities of biodiesel, glycerol, hexane and methanol were prepared by following the procedure, described in Chapter 3 of this thesis. GPC analysis of the upper and lower phases yielded chromatograms showing well separated peaks of the respective components and their peak areas. By using the GPC calibration equation for each component (see Appendix A for more details), the peak areas were converted to mass and mole fractions. The experimental tielines represent the average of one to four replicates

carried out for each overall composition. The variance associated with the composition of phase *I* (biodiesel-rich phase) and phase *II* (glycerol-rich phase) are presented in Table B.1. The experimental overall compositions and the tielines are given in mole and mass fractions in Tables B.2 and B.3, respectively.

Table B.1 Pooled pure error variance associated with the experimental mole and mass fractions of each component in each phase

	FAME	Glycerol	Hexane	Methanol
Mole fraction:				
Phase *I*	0.000074	0.000442	0.000298	0.000861
Phase *II*	0.000001	0.000054	0.000075	0.000210
Mass fraction:				
Phase *I*	0.000186	0.000226	0.000115	0.000083
Phase *II*	0.000041	0.000094	0.000215	0.000453

For each set of replicates, approximate 95% confidence intervals for the true mean compositions are given in the form of $\bar{x} \pm 2s/\sqrt{N}$, where $\bar{x}$ is the sample mean mole or mass fraction, s is the sample standard deviation associated with each set of replicated data and N is the number of replicates for each overall composition.

Table B.2 Overall compositions and average liquid-liquid equilibria mole fractions for the quaternary system: methyl oleate, glycerol, hexane and methanol at 20°C and 1 bar

Tieline	Overall composition				FAME-rich phase (upper phase)				Glycerol-rich phase (lower phase)			
	biodiesel	glycerol	hexane	methanol	FAME	glycerol	hexane	methanol	FAME	glycerol	hexane	methanol
1	0.1187	0.0394	0.1084	0.7335	$0.281^{\pm 0.014*}$	$0.059^{\pm 0.078}$	$0.259^{\pm 0.067}$	$0.401^{\pm 0.131}$	$0.011^{\pm 0.001}$	$0.089^{\pm 0.024}$	$0.056^{\pm 0.035}$	$0.844^{\pm 0.058}$
2	0.1200	0.0395	0.1986	0.6419	$0.261^{\pm 0.005}$	$0.020^{\pm 0.001}$	$0.368^{\pm 0.001}$	$0.351^{\pm 0.005}$	$0.008^{\pm 0.001}$	$0.085^{\pm 0.002}$	$0.025^{\pm 0.001}$	$0.882^{\pm 0.003}$
3	0.0597	0.0201	0.1993	0.7209	$0.119^{\pm 0.002}$	$0.017^{\pm 0.000}$	$0.350^{\pm 0.003}$	$0.514^{\pm 0.001}$	$0.022^{\pm 0.001}$	$0.035^{\pm 0.001}$	$0.082^{\pm 0.004}$	$0.861^{\pm 0.005}$
4	0.0917	0.0310	0.1867	0.6906	$0.194^{\pm 0.005}$	$0.017^{\pm 0.000}$	$0.350^{\pm 0.002}$	$0.439^{\pm 0.003}$	$0.012^{\pm 0.000}$	$0.059^{\pm 0.000}$	$0.037^{\pm 0.000}$	$0.892^{\pm 0.000}$
5	0.1205	0.0396	0.0901	0.7499	$0.328^{\pm 0.004}$	$0.024^{\pm 0.002}$	$0.203^{\pm 0.003}$	$0.445^{\pm 0.005}$	$0.013^{\pm 0.002}$	$0.070^{\pm 0.002}$	$0.020^{\pm 0.003}$	$0.897^{\pm 0.004}$
6	0.2504	0.0833	0.2229	0.4434	$0.427^{\pm 0.004}$	$0.019^{\pm 0.000}$	$0.348^{\pm 0.001}$	$0.206^{\pm 0.004}$	$0.004^{\pm 0.002}$	$0.241^{\pm 0.002}$	$0.008^{\pm 0.003}$	$0.747^{\pm 0.004}$
7	0.0600	0.0200	0.3998	0.5201	$0.092^{\pm 0.007}$	$0.014^{\pm 0.002}$	$0.581^{\pm 0.088}$	$0.313^{\pm 0.097}$	$0.007^{\pm 0.000}$	$0.056^{\pm 0.000}$	$0.057^{\pm 0.000}$	$0.880^{\pm 0.000}$
8	0.0603	0.0203	0.4991	0.4203	$0.088^{\pm 0.000}$	$0.014^{\pm 0.001}$	$0.699^{\pm 0.000}$	$0.199^{\pm 0.000}$	$0.003^{\pm 0.001}$	$0.073^{\pm 0.001}$	$0.046^{\pm 0.001}$	$0.878^{\pm 0.001}$
9	0.0596	0.0201	0.2983	0.6220	$0.107^{\pm 0.003}$	$0.015^{\pm 0.000}$	$0.510^{\pm 0.003}$	$0.368^{\pm 0.000}$	$0.011^{\pm 0.000}$	$0.043^{\pm 0.000}$	$0.072^{\pm 0.002}$	$0.874^{\pm 0.001}$
10	0.1174	0.0390	0.0237	0.8199	$0.374^{\pm 0.008}$	$0.023^{\pm 0.000}$	$0.077^{\pm 0.002}$	$0.526^{\pm 0.010}$	$0.016^{\pm 0.000}$	$0.060^{\pm 0.004}$	$0.011^{\pm 0.001}$	$0.913^{\pm 0.004}$
11	0.1184	0.0395	0.0537	0.7884	0.026	0.044	0.386	0.544	0.015	0.035	0.076	0.874
12	0.2508	0.0837	0.3309	0.3346	0.463	0.026	0.354	0.157	n.d.	$0.313^{\pm 0.003}$	$0.002^{\pm 0.002}$	$0.685^{\pm 0.001}$
13	0.1498	0.0505	0.3996	0.4002	$0.231^{\pm 0.004}$	$0.020^{\pm 0.041}$	$0.581^{\pm 0.022}$	$0.168^{\pm 0.015}$	$0.001^{\pm 0.000}$	$0.174^{\pm 0.001}$	$0.013^{\pm 0.001}$	$0.812^{\pm 0.001}$
14	0.1981	0.0656	0.3201	0.4162	$0.330^{\pm 0.006}$	n.d.	$0.484^{\pm 0.001}$	$0.186^{\pm 0.007}$	$0.001^{\pm 0.000}$	$0.211^{\pm 0.000}$	$0.008^{\pm 0.002}$	$0.780^{\pm 0.002}$
15	0.1252	0.0417	0.1665	0.6665	$0.273^{\pm 0.005}$	$0.017^{\pm 0.007}$	$0.325^{\pm 0.004}$	$0.385^{\pm 0.010}$	$0.007^{\pm 0.000}$	$0.082^{\pm 0.003}$	$0.024^{\pm 0.004}$	$0.887^{\pm 0.000}$
16	0.0415	0.1241	0.1659	0.6685	$0.180^{\pm 0.003}$	n.d.	$0.663^{\pm 0.013}$	$0.157^{\pm 0.014}$	$0.001^{\pm 0.000}$	$0.170^{\pm 0.005}$	$0.030^{\pm 0.002}$	$0.799^{\pm 0.003}$
17	0.0419	0.1250	0.1683	0.6648	$0.189^{\pm 0.016}$	$0.009^{\pm 0.010}$	$0.675^{\pm 0.007}$	$0.127^{\pm 0.018}$	$0.001^{\pm 0.000}$	$0.177^{\pm 0.002}$	$0.025^{\pm 0.002}$	$0.797^{\pm 0.001}$
18	0.0828	0.2496	0.3313	0.3363	$0.198^{\pm 0.002}$	n.d.	$0.769^{\pm 0.002}$	$0.033^{\pm 0.002}$	n.d.	$0.472^{\pm 0.001}$	$0.004^{\pm 0.002}$	$0.524^{\pm 0.002}$
19	0.1667	0.4949	0.1681	0.1703	$0.497^{\pm 0.008}$	n.d.	$0.483^{\pm 0.008}$	$0.020^{\pm 0.016}$	n.d.	$0.782^{\pm 0.002}$	$0.011^{\pm 0.003}$	$0.207^{\pm 0.001}$
20	0.0427	0.1243	0.6628	0.1702	$0.059^{\pm 0.004}$	n.d.	$0.915^{\pm 0.021}$	$0.026^{\pm 0.025}$	n.d.	$0.480^{\pm 0.010}$	$0.012^{\pm 0.003}$	$0.508^{\pm 0.013}$
21	0.1251	0.6242	0.1241	0.1266	$0.516^{\pm 0.012}$	n.d.	$0.468^{\pm 0.004}$	$0.016^{\pm 0.012}$	n.d.	$0.861^{\pm 0.002}$	$0.006^{\pm 0.003}$	$0.133^{\pm 0.002}$
22	0.1252	0.1229	0.1254	0.6266	$0.383^{\pm 0.007}$	n.d.	$0.358^{\pm 0.003}$	$0.259^{\pm 0.007}$	$0.002^{\pm 0.001}$	$0.199^{\pm 0.002}$	$0.008^{\pm 0.000}$	$0.791^{\pm 0.002}$
23	0.1237	0.1262	0.6215	0.1286	$0.163^{\pm 0.014}$	n.d.	$0.821^{\pm 0.008}$	$0.016^{\pm 0.015}$	$0.001^{\pm 0.001}$	$0.592^{\pm 0.003}$	$0.016^{\pm 0.007}$	$0.391^{\pm 0.004}$
24	0.2396	0.2396	0.2365	0.2843	$0.469^{\pm 0.015}$	n.d.	$0.456^{\pm 0.010}$	$0.075^{\pm 0.025}$	n.d.	$0.533^{\pm 0.016}$	$0.007^{\pm 0.002}$	$0.456^{\pm 0.015}$
25	0.1256	0.3748	0.4996	0.0000	$0.204^{\pm 0.004}$	n.d.	$0.796^{\pm 0.004}$	0.000	$0.004^{\pm 0.005}$	$0.959^{\pm 0.021}$	$0.037^{\pm 0.017}$	0.000

n.d. : not detectable

* : $\pm 2s/\sqrt{N}$; no value indicates a single observation.

Table B.3 Overall compositions and average liquid-liquid equilibria mass fractions for the quaternary system: methyl oleate, glycerol, hexane and methanol at 20°C and 1 bar

Tieline	Overall composition				Biodiesel-rich phase (upper phase)				Glycerol-rich phase (lower phase)			
	biodiesel	glycerol	hexane	methanol	biodiesel	glycerol	hexane	methanol	biodiesel	glycerol	hexane	methanol
1	0.4910	0.0506	0.1304	0.3280	$0.672^{\pm 0.059*}$	$0.044^{\pm 0.057}$	$0.180^{\pm 0.039}$	$0.104^{\pm 0.037}$	$0.075^{\pm 0.012}$	$0.189^{\pm 0.037}$	$0.111^{\pm 0.062}$	$0.624^{\pm 0.089}$
2	0.4628	0.0473	0.2225	0.2674	$0.633^{\pm 0.005}$	$0.015^{\pm 0.000}$	$0.260^{\pm 0.004}$	$0.092^{\pm 0.002}$	$0.058^{\pm 0.004}$	$0.193^{\pm 0.002}$	$0.053^{\pm 0.003}$	$0.696^{\pm 0.006}$
3	0.2960	0.0309	0.2870	0.3860	$0.423^{\pm 0.005}$	$0.019^{\pm 0.000}$	$0.361^{\pm 0.005}$	$0.197^{\pm 0.001}$	$0.147^{\pm 0.006}$	$0.073^{\pm 0.002}$	$0.159^{\pm 0.007}$	$0.621^{\pm 0.011}$
4	0.3983	0.0418	0.2358	0.3242	$0.557^{\pm 0.008}$	$0.015^{\pm 0.000}$	$0.292^{\pm 0.005}$	$0.136^{\pm 0.003}$	$0.087^{\pm 0.000}$	$0.133^{\pm 0.000}$	$0.078^{\pm 0.001}$	$0.701^{\pm 0.001}$
5	0.5020	0.0512	0.1091	0.3377	$0.741^{\pm 0.003}$	$0.017^{\pm 0.001}$	$0.133^{\pm 0.002}$	$0.109^{\pm 0.002}$	$0.095^{\pm 0.010}$	$0.158^{\pm 0.002}$	$0.042^{\pm 0.006}$	$0.705^{\pm 0.012}$
6	0.6437	0.0665	0.1666	0.1232	$0.768^{\pm 0.002}$	$0.011^{\pm 0.000}$	$0.182^{\pm 0.001}$	$0.040^{\pm 0.001}$	$0.025^{\pm 0.004}$	$0.462^{\pm 0.005}$	$0.014^{\pm 0.001}$	$0.499^{\pm 0.002}$
7	0.2516	0.0260	0.4869	0.2355	$0.308^{\pm 0.001}$	$0.015^{\pm 0.001}$	$0.565^{\pm 0.042}$	$0.113^{\pm 0.044}$	$0.051^{\pm 0.001}$	$0.128^{\pm 0.000}$	$0.122^{\pm 0.001}$	$0.699^{\pm 0.002}$
8	0.2346	0.0246	0.5642	0.1767	$0.278^{\pm 0.001}$	$0.014^{\pm 0.001}$	$0.641^{\pm 0.000}$	$0.068^{\pm 0.000}$	$0.022^{\pm 0.005}$	$0.169^{\pm 0.003}$	$0.100^{\pm 0.002}$	$0.708^{\pm 0.000}$
9	0.2711	0.0285	0.3945	0.3059	$0.357^{\pm 0.009}$	$0.016^{\pm 0.000}$	$0.495^{\pm 0.007}$	$0.133^{\pm 0.001}$	$0.079^{\pm 0.003}$	$0.096^{\pm 0.001}$	$0.150^{\pm 0.004}$	$0.676^{\pm 0.001}$
10	0.5218	0.0538	0.0306	0.3938	$0.812^{\pm 0.004}$	$0.016^{\pm 0.000}$	$0.049^{\pm 0.001}$	$0.123^{\pm 0.004}$	$0.117^{\pm 0.003}$	$0.137^{\pm 0.008}$	$0.023^{\pm 0.003}$	$0.723^{\pm 0.007}$
11	0.5115	0.0530	0.0674	0.3680	0.123	0.065	0.533	0.279	0.105	0.076	0.155	0.663
12	0.6130	0.0635	0.2351	0.0884	0.784	0.014	0.174	0.029	n.d.	$0.566^{\pm 0.005}$	$0.003^{\pm 0.003}$	$0.431^{\pm 0.001}$
13	0.4611	0.0483	0.3575	0.1331	$0.545^{\pm 0.010}$	$0.015^{\pm 0.030}$	$0.398^{\pm 0.016}$	$0.043^{\pm 0.004}$	$0.007^{\pm 0.001}$	$0.369^{\pm 0.001}$	$0.026^{\pm 0.002}$	$0.599^{\pm 0.001}$
14	0.5557	0.0571	0.2610	0.1262	$0.672^{\pm 0.004}$	n.d.	$0.287^{\pm 0.003}$	$0.041^{\pm 0.002}$	$0.007^{\pm 0.001}$	$0.428^{\pm 0.001}$	$0.015^{\pm 0.003}$	$0.550^{\pm 0.003}$
15	0.4842	0.0501	0.1871	0.2785	$0.659^{\pm 0.004}$	$0.013^{\pm 0.005}$	$0.228^{\pm 0.002}$	$0.100^{\pm 0.004}$	$0.052^{\pm 0.001}$	$0.188^{\pm 0.007}$	$0.052^{\pm 0.009}$	$0.708^{\pm 0.004}$
16	0.2069	0.1923	0.2405	0.3603	$0.462^{\pm 0.005}$	n.d.	$0.495^{\pm 0.007}$	$0.044^{\pm 0.004}$	$0.007^{\pm 0.000}$	$0.355^{\pm 0.009}$	$0.059^{\pm 0.005}$	$0.580^{\pm 0.004}$
17	0.2080	0.1928	0.2427	0.3566	$0.471^{\pm 0.024}$	$0.007^{\pm 0.008}$	$0.488^{\pm 0.018}$	$0.034^{\pm 0.006}$	$0.007^{\pm 0.003}$	$0.368^{\pm 0.000}$	$0.049^{\pm 0.003}$	$0.577^{\pm 0.002}$
18	0.2827	0.2647	0.3286	0.1240	$0.466^{\pm 0.006}$	n.d.	$0.526^{\pm 0.006}$	$0.008^{\pm 0.000}$	n.d.	$0.717^{\pm 0.002}$	$0.006^{\pm 0.003}$	$0.277^{\pm 0.002}$
19	0.4300	0.3965	0.1260	0.0475	$0.777^{\pm 0.002}$	n.d.	$0.219^{\pm 0.001}$	$0.003^{\pm 0.003}$	n.d.	$0.905^{\pm 0.002}$	$0.012^{\pm 0.003}$	$0.083^{\pm 0.000}$
20	0.1460	0.1321	0.6590	0.0629	$0.180^{\pm 0.008}$	n.d.	$0.811^{\pm 0.003}$	$0.009^{\pm 0.009}$	n.d.	$0.719^{\pm 0.006}$	$0.017^{\pm 0.005}$	$0.265^{\pm 0.000}$
21	0.3394	0.5258	0.0978	0.0371	$0.789^{\pm 0.005}$	n.d.	$0.208^{\pm 0.004}$	$0.003^{\pm 0.002}$	n.d.	$0.943^{\pm 0.002}$	$0.006^{\pm 0.003}$	$0.051^{\pm 0.000}$
22	0.4680	0.1427	0.1362	0.2531	$0.744^{\pm 0.005}$	n.d.	$0.202^{\pm 0.003}$	$0.054^{\pm 0.002}$	$0.013^{\pm 0.008}$	$0.408^{\pm 0.005}$	$0.015^{\pm 0.001}$	$0.564^{\pm 0.004}$
23	0.3461	0.1096	0.5054	0.0389	$0.404^{\pm 0.023}$	n.d.	$0.592^{\pm 0.019}$	$0.004^{\pm 0.004}$	$0.004^{\pm 0.006}$	$0.793^{\pm 0.007}$	$0.020^{\pm 0.008}$	$0.182^{\pm 0.003}$
24	0.5795	0.1800	0.1662	0.0743	$0.769^{\pm 0.005}$	n.d.	$0.217^{\pm 0.001}$	$0.013^{\pm 0.005}$	n.d.	$0.763^{\pm 0.013}$	$0.009^{\pm 0.003}$	$0.227^{\pm 0.011}$
25	0.3244	0.3006	0.3750	0.0000	$0.469^{\pm 0.006}$	n.d.	$0.531^{\pm 0.006}$	0.000	$0.013^{\pm 0.016}$	$0.953^{\pm 0.030}$	$0.034^{\pm 0.015}$	0.000

n.d. : not detectable

* : $\pm 2s/\sqrt{N}$; no value indicates a single observation.

The root mean squared deviation and average absolute deviation of the predicted tielines, using UNIFAC or Modified UNIFAC activity coefficient models, from the experimental tielines are given in Table B.4.

Table B.4 Deviation of the experimental and calculated mole fractions using UNIFAC and Modified UNIFAC activity coefficient models, as defined in Equations 3.2 and 3.3, Chapter 3 (Paper 1)

	UNIFAC	Modified UNIFAC
RMSD	0.0589	0.0404
AAD	0.0311	0.0217

Appendix C

Vapor-Liquid-Liquid Multicomponent Phase Equilibria Calculations

C.1 Isothermal-isobaric flash equations

In the current thesis, the phase equilibria determination (i.e., flash calculations) for the system methyl oleate, glycerol, hexane, methanol and water has been carried out by using the fugacity-matching method of Nelson (1987), and Bunz et al., (1991). This method is capable of predicting up to three coexisting phases at equilibrium (one vapor and two liquid phases). The following sets of equations (a), (b) and (c) are employed in this algorithm.

(a) Equations 1a and 2a are the defined conditions of phase equilibria based on the $\gamma - \Phi$ approach (Smith et al., 1996).

$$K_i^I = \frac{y_i}{x_i^I} = \frac{\widehat{\Phi}_i^I}{\widehat{\Phi}_i^V} = \frac{\gamma_i^I P_i^{sat} \Phi_i^{sat}}{P\widehat{\Phi}_i^V} \left[\exp \int_{P_i^{sat}}^{P} \frac{V_i^I}{RT} dP \right] \qquad (1a)$$

$$K_i^{II} = \frac{y_i}{x_i^{II}} = \frac{\widehat{\Phi}_i^{II}}{\widehat{\Phi}_i^V} = \frac{\gamma_i^{II} P_i^{sat} \Phi_i^{sat}}{P\widehat{\Phi}_i^V} \left[\exp \int_{P_i^{sat}}^{P} \frac{V_i^{II}}{RT} dP \right] \qquad (2a)$$

where the two correction terms, $\exp \int_{P_i^{sat}}^{P} \frac{V_i^I}{RT} dP$ and $\exp \int_{P_i^{sat}}^{P} \frac{V_i^{II}}{RT} dP$, are called Poynting factors. For liquid systems at low to moderate pressures, which is the case of this study, these factors were omitted because of the negligible dependency of liquid molar volume on pressure.

(b) Material balance equations for the individual components and also the overall material balance of the system are:

$$Fz_i = Vy_i + L^I x_i^I + L^{II} x_i^{II} \qquad (1b)$$

$$F = V + L^I + L^{II} \qquad (2b)$$

where F, V, L^I and L^{II} are the total number of moles in the mixture, the number of moles in the vapor phase, number of moles in liquid phases I and that of liquid phase II, respectively.

(c) The last set of equations is the Stoichiometric equation corresponding to the vapor phase and two liquid phases at physical equilibrium.

$$\sum_{i=1}^{C} y_i = \sum_{i=1}^{C} x_i^I = \sum_{i=1}^{C} x_i^{II} = 1 \qquad (1c)$$

In the above equation, C denotes the number of components in the mixture. By solving the above equations (Equations 1b, 2b and 1c) for compositions of the vapor and two liquid phases, the following equations will be obtained.

$$y_i = \frac{z_i F K_i^I K_i^{II}}{V K_i^I K_i^{II} + L^I K_i^{II} + L^{II} K_i^I} \qquad (1)$$

$$x_i^I = \frac{z_i F K_i^{II}}{V K_i^I K_i^{II} + L^I K_i^{II} + L^{II} K_i^I} \qquad (2)$$

$$x_i^{II} = \frac{z_i F K_i^I}{V K_i^I K_i^{II} + L^I K_i^I + L^{II} K_i^I} \qquad (3)$$

By substituting the phase fractions (Equations 4 and 5), equations 1, 2 and 3 are converted to equations 6, 7 and 8.

$$\Psi_I = \frac{L^I}{F} \qquad (4)$$

$$\Psi_{II} = \frac{L^{II}}{F} \qquad (5)$$

$$y_i = \frac{z_i K_i^I K_i^{II}}{(1-\Psi_I - \Psi_{II}) K_i^I K_i^{II} + \Psi_I K_i^{II} + \Psi_{II} K_i^I} \qquad (6)$$

$$x_i^I = \frac{z_i K_i^{II}}{(1-\Psi_I - \Psi_{II}) K_i^I K_i^{II} + \Psi_I K_i^{II} + \Psi_{II} K_i^I} \qquad (7)$$

$$x_i^{II} = \frac{z_i K_i^I}{(1-\Psi_I - \Psi_{II}) K_i^I K_i^{II} + \Psi_I K_i^{II} + \Psi_{II} K_i^I} \qquad (8)$$

Summing the above equations over all the species and applying equation 1c results in the following equations (Equations 9 and 10) which are more helpful and are the ones to be solved in the flash calculations.

$$Q_1(\Psi_I, \Psi_{II}) = \sum_{i=1}^{C} x_i^I - \sum_{i=1}^{C} y_i = \sum_{i=1}^{C} \frac{z_i K_i^{II}(1-K_i^I)}{K_i^I K_i^{II} + \Psi_1 K_i^{II}(1-K_i^I) + \Psi_1 K_i^I (1-K_i^{II})} = 0 \qquad (9)$$

$$Q_2(\Psi_I, \Psi_{II}) = \sum_{i=1}^{C} x_i^{II} - \sum_{i=1}^{C} y_i = \sum_{i=1}^{C} \frac{z_i K_i^I (1-K_i^{II})}{K_i^I K_i^{II} + \Psi_1 K_i^{II}(1-K_i^I) + \Psi_1 K_i^I (1-K_i^{II})} = 0 \qquad (10)$$

C.2 Stability test

As a part of the phase calculation of the phase equilibria determination method, the number and nature of phases at equilibrium can be determined by the "stability test". at the desired temperature and pressure. This type of test can handle up to three phases, one vapor and two liquid phases at equilibrium; therefore, seven different circumstances might happen, as follows (Nelson, 1987; Bunz, 1991).

(1) Single vapor phase:

$$\sum_{i=1}^{C} \frac{z_i}{K_i^I} < 1 \qquad \text{and} \qquad \sum_{i=1}^{C} \frac{z_i}{K_i^{II}} < 1$$

(2) Single liquid phase *I*:

$$\sum_{i=1}^{C} z_i K_i^I < 1 \quad \text{and} \quad \sum_{i=1}^{C} z_i \frac{K_i^I}{K_i^{II}} < 1$$

(3) Single liquid phase *II*:

$$\sum_{i=1}^{C} z_i K_i^{II} < 1 \quad \text{and} \quad \sum_{i=1}^{C} z_i \frac{K_i^{II}}{K_i^I} < 1$$

For the two phase systems, one of the following three situations might happen.

(4) Vapor phase and liquid phase *I*:

$$\sum_{i=1}^{C} \frac{z_i}{K_i^I} > 1 \quad \text{and} \quad \sum_{i=1}^{C} z_i K_i^I > 1$$

where $Q_2(\Psi_I, 0) < 0$ at the point $Q_1(\Psi_I, 0) = 0$

(5) Vapor phase and liquid phase *II*:

$$\sum_{i=1}^{C} \frac{z_i}{K_i^{II}} > 1 \quad \text{and} \quad \sum_{i=1}^{C} z_i K_i^{II} > 1$$

where $Q_1(0, \Psi_{II}) < 0$ at the point $Q_2(\Psi_{II}, 0) = 0$

(6) Liquid phase *I* and liquid phase *II*:

$$\sum_{i=1}^{C} z_i \frac{K_i^I}{K_i^{II}} > 1 \quad \text{and} \quad \sum_{i=1}^{C} z_i \frac{K_i^{II}}{K_i^I} > 1$$

where $Q_1(\Psi_I, 1-\Psi_I) > 0$ for $Q_2(\Psi_I, 1-\Psi_I) > 0$ at the point $Q_1(\Psi_I, 1-\Psi_I) - Q_2(\Psi_I, 1-\Psi_I) = 0$.

(7) Only if none of the one-phase or two phase tests, as shown above, resulted in an acceptable answer, it can be concluded that at the specified temperature and pressure, the three phases, one vapor and two liquid phases co-exist. For the case of three co-existing phases, the following criteria are required.

$Q_1(\Psi_I, \Psi_{II}) = 0$ and $Q_2(\Psi_I, \Psi_{II}) = 0$.

C.3 UNIFAC activity coefficient model

The activity coefficient of each component in each phase can be calculated using different activity coefficient models, such as NRTL (Non Random Two Liquid), UNIQUAC (Universal Quasi Chemical) and UNIFAC (Universal Quasi-Chemical Functional Group) are some of them. In Chapters 4 and 5 of this thesis, activity coefficients are calculated using the UNIFAC model (Magnussen et al., 1981). This model is based on the group contribution method and calculates the activity coefficient using the interaction parameters between bonds in each molecule. For instance, the methanol molecule, CH_3OH consists of one CH_3 and one OH group or glycerol, $C_3H_8O_3$, consists of two CH_2, one CH and three OH groups. In this way, the properties of the components in the mixture can be related to the binary interactions between the groups in each molecule.

$$\ln \gamma_i = \ln \gamma_i^C + \ln \gamma_i^R$$

$$\ln \gamma_i^C = \ln \frac{\phi_i}{x_i} + 1 - \frac{\phi_i}{x_i} - \frac{1}{2} z q_i \left(\ln \frac{\phi_i}{\theta_i} + 1 - \frac{\phi_i}{\theta_i} \right)$$

$$\phi_i = \frac{x_i r_i}{\sum_j x_j r_j}$$

$$\theta_i = \frac{x_i q_i}{\sum_j x_j q_j}$$

$$r_i = \sum_k \nu_{ki} R_k$$

$$q_i = \sum_k \nu_{ki} Q_k$$

where $\sum_j$ and $\sum_k$ are summations over all the components and all the groups respectively.

$$\ln \gamma_i^R = \sum_k \nu_{ki} \left(\ln \Gamma_k - \ln \Gamma_k^{(i)} \right)$$

$$\ln \Gamma_k = Q_k \left[1 - \ln\left(\sum_m \theta_m \psi_{mk} \right) - \sum_m \left(\frac{\theta_m \psi_{km}}{\sum_n \theta_n \psi_{nm}} \right) \right]$$

$$\psi_{nm} = \exp\left(\frac{-a_{nm}}{T} \right)$$

$$\theta_m = \frac{Q_m X_m}{\sum_n Q_n X_n}$$

$$X_m = \frac{\sum_j \nu_{mj} x_j}{\sum_j \sum_n \nu_{nj} x_j}$$

$\sum_m$ and $\sum_n$ are both summation over all the groups.

C.4 *SRK* equation of state

To find the properties of the vapor phase, the *SRK* (Soave-Redlich-Kwong) equation of state was employed (Walas, 1985; Holderbaum and Gmehling, 1991). The correlations are given below.

$$P = \frac{RT}{V-b} - \frac{a}{V(V+b)}$$

where $a = \frac{0.4278 R^2 T_C^2}{P_C} \alpha$

and $$\begin{cases} \alpha = \left[1 + C_1 \left(1 - T_r^{0.5} \right) + C_2 \left(1 - T_r^{0.5} \right) + C_3 \left(1 - T_r^{0.5} \right) \right]^2 & (T_r < 1) \\ \alpha = \left[1 + C_1 \left(1 - T_r^{0.5} \right) \right]^2 & (T_r > 1) \end{cases}$$

The value of C_1 for methyloleate and glycerol is equal to $\left[0.48 + 1.57\omega - 0.176\omega^2 \right]$, while the other two parameters, C_2 and C_3 are zero. For hexane, methanol and water, all the three parameters have been found in the literature (Holderbaum and Gmehling, 1991).

$$b = \frac{0.08664 R T_C}{P_C}$$

Up to this point, the given parameters of the *SRK* equation of state were properties of pure components. Appropriate mixing rules should be employed to make the equation of state applicable to the mixture of components. In *SRK* equation of state the parameters a and b of the pure species should be adjusted for the mixture of several components, as following (Walas, 1985),

$$a = \sum_{i=1}^{C} \sum_{j=1}^{C} x_i x_j \left(1 - K_{ij}\right) \sqrt{a_i a_j}$$

$$b = \sum_{i=1}^{C} x_i b_i$$

The summations are over all the components involved. x_i and x_j are the molar compositions and K_{ij} is the *SRK* binary interaction parameter between the components i and j.

C.5 Flash calculations algorithm

In this section, the algorithm followed to carry out the flash calculations will be summarized.

1. The three compositions x_i^I, x_i^{II} and y_i are estimated. Usually, reliable experimental data can be the first estimate for the mole fractions of the vapor and two liquid phases.

2. From an Antoine-type correlation, at the given temperature, the corresponding saturation pressure can be found for the pure components,

$$\log P^{sat} = A + \frac{B}{T} + C\log T + DT + ET^2$$

The parameters A, B, C and D are constants given for the pure species in tables (Yaws, 1999). P^{sat} is the saturation pressure in mmHg and T is temperature in K.

3. From the *SRK* equation of state, the values of the fugacity coefficients of each component as vapor in the mixture, $\widehat{\Phi}_i^V$, and also the fugacity coefficient at saturation pressure and known temperature for the pure species, Φ_i^{sat}, can be calculated (Smith, 1996).

4. By means of a suitable activity coefficient model, such as UNIFAC, at any temperature and composition, the activity coefficient of the liquid phases can be determined.

5. From equations 1a and 2a, in the $\gamma - \Phi$ approach, the values of the vapor-liquid distribution coefficients for each component, K_i^I and K_i^{II}, can be obtained.

6. Stability test, cases (a) to (g) as studied in C.2, can be performed and the number of stable equilibrium phases at a given temperature, pressure and overall composition can be found.

7. By solving equations 9 and 10 with Newton-Raphson method, the phase fractions, Ψ_I and Ψ_{II}, can be calculated.

8. Equations 6 through 8 can be used to calculate new values of the composition of the vapor and two liquid phases.

9. Repeating steps 3, 4 and 5, one can calculate the new values of the distribution coefficient.

10. Going back to step 6, the stability test can be carried out again employing the new values of the distribution coefficients.

11. Iteration continues until the values of the phase fractions, Ψ_I and Ψ_{II}, do not change significantly in a pre-determined number of consecutive iterations.

Nomenclature

K_i^I	Distribution coefficient with respect to liquid phase *I*
K_i^{II}	Distribution coefficient with respect to liquid phase *II*
y_i	Molar composition of the vapor phase
x_i^I	Molar composition of liquid phase *I*
x_i^{II}	Molar composition of liquid phase *II*
P^{sat}	Saturation pressure
P	Pressure
R	Universal gas constant (J/mol.K)
T	temperature (K)
V_I^I	Molar volume of liquid phase *I*
V_I^{II}	Molar volume of liquid phase *II*
F	Total number of moles in the mixture
L^I	Number of moles (liquid phase *I*)
L^{II}	Number of moles (liquid phase *II*)
z	Overall molar composition of the mixture
R_k	Volume parameter in UNIFAC model
Q_k	Surface parameter in UNIFAC model
a_{nm}	UNIFAC interaction parameter
C_1,C_2,C_3	SRK correction parameters
T_r	Reduced temperature
T_c	Critical temperature
P_c	Critical pressure
K_{ij}	SRK interaction parameter
A, B, C, D, E	Antoine constants

Greek letters:

$\widehat{\Phi}_i^I$	Fugacity coefficient in liquid phase *I*
$\widehat{\Phi}_i^{II}$	Fugacity coefficient in liquid phase *II*
$\widehat{\Phi}_i^V$	Fugacity coefficient in vapor phase
γ_i^I	Activity coefficient in liquid phase *I*
γ_i^{II}	Activity coefficient in liquid phase *II*
Φ_i^{sat}	Activity coefficient in saturation pressure (pure)
Ψ_I	Phase fraction of liquid phase *I*
Ψ_{II}	Phase fraction of liquid phase *II*
γ_i^C	Combinatorial activity coefficient
γ_i^R	Residual activity coefficient
υ_{ki}	Number of groups

Superscripts and subscripts:

i, j	Component
k, m, n	Groups

References

Bunz, A. P., Dohrnt, R. and Prausnitz, J. M., "Three Phase Flash Calculations for Multicomponent Systems," Computers Chem. Eng. 15, 47-51(1991).

Holderbaum, T. and Gmehling, J., "A Group Contribution Equation of State Based on UNIFAC," Fluid Phase Equilibria 70, 251-265 (1991).

Magnussen, T., Rasmussen, P. and Fedenslund, A., "UNIFAC Parameter Table for Prediction of Liquid-liquid Equilibria," Ind. Eng. Chem. Process Des. Dev. 20 331-339 (1981).

Nelson, P. A., "Rapid Phase Determination in Multi-Phase Flash Calculations," Computers Chem. Eng. 11(6), 581-591(1987).

Smith, J. M., Van Ness, H. C. and Abbott, M. M., "Introduction to Chemical Engineering Thermodynamics," 5th edition, McGraw Hill Companies, Inc., New York (1996), p. 434.

Walas, S. M., "Phase Equilibria in Chemical Engineering," Butterworth Publishers, Boston, MA (1985), pp. 202-203.

Yaws, C. L., "Chemical Properties Handbook: Physical, Thermodynamic, Environmental, Transport, Safety, and Health Related Properties for Organic and Inorganic Chemicals," McGraw Hill, New York (1999).

Appendix D

Sizing and Equipment Cost of Mixer, Settler, Heat Exchangers and Flash Separators

D.1 Mixer

D.1.1 Sizing

To calculate the cost of mixer, the residence time required for the proper mixing of the feed and solvents (T_M, min) and the ratio of length to diameter (i.e., L/D) of the mixer must be known. Typically, in a mixer, the residence time is estimated to be 5 minutes or even less and the ratio of L/D is 1 (Seider et al., 2004). The volume of the mixer (V, m^3) is then calculated by multiplying the residence time and volumetric flow rate of the entire stream entering the mixer (Q_V, $m^3/\min$), which consists of the feed and solvents. Specifying the ratio of L/D and volume of the mixer as a cylindrical vessel, both length (L, m) and diameter of the mixer (D, m) can be determined.

$$V = Q_V \times T_M$$

$$D = L = \sqrt[3]{\frac{4V}{\pi}}$$

D.1.2 Thickness

Thickness of the mixer is calculated using the design pressure (P_d), which is higher than the average operating pressure of the unit (Seider et al., 2004).

For an operating pressure of $0 < P_0 < 5\,\text{psig}$, the design pressure of 10 psig is used and for $10 < P_0 < 1000\,\text{psig}$, the following correlation can be employed.

$$P_d = \exp\left\{0.60608 + 0.91615\left[\ln\left(P_0\right)\right] + 0.0015655\left[\ln\left(P_0\right)\right]^2\right\}$$

By neglecting the corrosion, wind load and earthquake, the cylindrical shell wall thickness can be computed through the following correlation (Seider et al., 2004).

$$t_P = \frac{P_d D_i}{2SE - 1.2P_d}$$

t_p : wall thickness (in)

P_d : design gauge pressure (psig)

D_i : inside shell diameter (in)

S : maximum allowable stress of shell material (13750 psi for carbon steel, SA-285 C)

E : fractional weld efficiency (10% for t_P<1.25 in)

The minimum values for the vessel wall thickness is given by Seider at al. (2004). To consider the effect of wind load and earthquake, the following correlation can be applied to vessel thickness when the effect of wind is significant or when $1.34 < (L/D_i)^2 / P_d < 10$ (earthquake impact).

$$t_V = t_P \left[0.75 + 0.22E \frac{(L/D_i)^2}{P_d} \right]$$

where L and D_i are the length and inside diameter of the vessel respectively. To find the final value of the thickness, corrosion should be added to the value calculated above. In this study, the value of 1/16 in. was assumed for the corrosion of carbon steel.

D.1.3 Weight

The weight of the mixer can be calculated using the following formula, which is applicable to a 2:1 elliptical head vessel with equal shell and head thicknesses (Seider et al., 2004). D_i is the inside diameter of the vessel in inches. L and t_S are tangent to tangent length of the mixer and thickness of its shell respectively. ρ is the density of carbon steel and equal to 7.8 g/cm^3 (Forsberg et al., 2001).

$$W = \pi (D_i + t_S)(L + 0.8D_i) t_S \rho$$

D.1.4 Equipment cost

The purchase cost for carbon steel construction of platforms, ladder, nozzles and manhole, can be determined using the following correlation (Seider et al., 2004).

$$C_P = F_M C_V + C_{PL}$$

where F_M is the material factor and for carbon steel is assumed to be 1. C_V is the purchased cost of the vessel plus nozzles, manholes and supports and can be calculated employing W, the net weight of the vessel.

For a vertical vessel when $4,200 < W < 1,000,000$ lb

$$C_V = \exp\left\{6.775 + 0.18255\left[\ln(W)\right] + 0.02297\left[\ln(W)\right]^2\right\}$$

C_{PL} is the cost of platforms and ladder and is a function of vessel inside diameter (Seider et al., 2004).

In a vertical vessel for $3 < D_i < 21$ ft and $12 < L < 40$ ft :

$$C_{PL} = 258.1(D_i)^{0.73960}(L)^{0.70684}$$

D.2 Settler

D.2.1 Sizing

For the settler, the only parameter to be pre-determined is the ratio of length to diameter which is usually around 4 (Seider et al., 2004). Hence, in contrast to the mixer which was a vertical vessel, the settler can be assumed as a horizontal vessel. The residence time in the settler is a function of density of both liquid phases and the viscosity of the continuous phase, as shown as below (Branan, 2002). In this work, based on the observations, the continuous phase is the biodiesel/hexane rich phase.

$$T_S = 0.1\left[\frac{\mu}{\rho_h - \rho_l}\right]$$

T_S: residence time (h)

μ : viscosity of the continuous phase (cp)

ρ_b : specific gravity of the bottom phase (glycerol-rich phase)

ρ_t : specific gravity of the top phase (biodiesel-rich phase)

Same procedure as the mixer should be followed in order to calculate the volume, length and diameter of the settler.

D.2.2 Thickness and weight

The same procedure and formulas described for the mixer can also be applied for computation of the thickness and weight of the settler (Sections D.1.2 and D.1.3).

D.2.3 Equipment cost

The main difference between the cost calculations of a mixer (i.e., vertical vessel) with a settler (i.e, horizontal vessel) is in the formulation of the C_V and C_{PL}. The following equations were used to calculate the cost of the settler (Seider et al., 2004).

$$C_P = F_M C_V + C_{PL}$$

Horizontal vessel $1,000 < W < 920,000$ lb :

$$C_V = \exp\left\{8.717 - 0.2330\left[\ln(W)\right] + 0.04333\left[\ln(W)\right]^2\right\}$$

Horizontal vessel $3 < D_i < 12$ ft :

$$C_{PL} = 1,580\left(D_i\right)^{0.20294}$$

D.3 Flash separators (vertical drums)

D.3.1 Sizing (Branan, 2002)

Knowing the mass flow rate and density of the liquid ($mass_L$ and ρ_L) and vapor phases ($mass_V$ and ρ_V) entering the flash separator, one is able to calculate the separation factor (X), the term K_v and the maximum velocity of the vapor phase $\left(U_{vapor-\max}\right)$ as following:

$$X = \frac{mass_L}{mass_V}\sqrt{\frac{\rho_V}{\rho_L}}$$

$$x = \log(X)$$

$$K_v = \exp\left(-1.942936 - 0.814894x - 0.179390x^2 - 0.0123790x^3 + 0.000386235x^4 + 0.000259550x^5\right)$$

$$U_{vapor-\max} = K_v\left[\frac{\rho_L - \rho_V}{\rho_V}\right]^{0.5}$$

The minimum vessel cross section (A_{min}), minimum vessel diameter (D_{min}) and real vessel diameter (D) can be calculated as following:

$$A_{\min} = \frac{mass_V / \rho_V}{U_{vapor-\max}} \text{ and } D_{\min} = \sqrt{\frac{4A_{\min}}{\pi}}$$

Determining $D_{\min}$, one is able to find D, the actual diameter of the vessel by rounding $D_{\min}$ to the next largest 6 inches.

Assuming a fill time of T, which is usually around 10 minutes, the volume required by the liquid phase and then the heights required for the liquid and vapor phases (H_L and H_V respectively) can be determined by the following equations:

$$V_L = T\frac{mass_L}{\rho_L}$$

$$H_L = V_L\frac{4\pi}{D^2}$$

$$H_V = \begin{cases} D & if\ D \geq 1 \\ 1 & if\ D < 1 \end{cases}$$

The total height of the vertical flash drum can be calculated by summing the heights required for the liquid and vapor phases.

$$H_{total} = H_L + H_V$$

D.3.2 Thickness and weight

The same procedure and formulas described for the mixer can also be applied for computation of the thickness and weight of the settler (see Section D.1.2).

D.3.3 Equipment cost (Seider et al., 2004)

$$C_V = \exp\left\{7.0374 + 0.18255 \times \log(\mathrm{W}) + 0.02297 \times \left(\log(\mathrm{W})\right)^2\right\}$$

$$\mathrm{C_{PL}} = 237.1 \times \mathrm{D_{ft}}^{0.63316} \times \mathrm{H_{ft}}^{0.80161}$$

$$C_P = F_M C_V + C_{PL}$$

D.4 Heat exchangers

D.4.1 Heat transfer area

In this study, superheated steam at 185°C and water at 15°C were assumed as the heating and cooling media respectively. A fixed, average heat transfer coefficient of 50 $BTU/hr(sq.ft.)(^{\circ}F)$ in a fixed heat shell and tube heat exchangers was assumed (Branan, 2002).

The logarithmic mean value of the temperature difference in the heat exchanger is determined by the following equation.

$$T_{LM} = \frac{\left(T_{in}^{U} - T_{out}\right) - \left(T_{out}^{U} - T_{in}\right)}{\log\left(\frac{\left(T_{in}^{U} - T_{out}\right)}{\left(T_{out}^{U} - T_{in}\right)}\right)}$$

For the temperatures of the inlet and outlet streams, entering and exiting the heat exchanger (T_{in} and T_{out} respectively), the flash calculations can be carried out to determine the enthalpy of each stream. The total heat required to make the enthalpy change (q) and the corresponding area of the heat exchanger (A) is calculated by means of the following equations:

$$q = \left(H_{out} - H_{in}\right) \times flow$$

$$A = \frac{q}{U \times T_{LM}}$$

D.4.2 Equipment cost

For a fixed heat shell and tube heat exchanger, the following equation is applied to determine the basis cost of the heat exchanger (Seider et al., 2004):

$$C_B = \exp\left\{11.0545 - 0.9228\left[\ln\left(A\right)\right] + 0.0986\left[\ln\left(A\right)\right]^2\right\}$$

The final equipment cost can be determined by the following equation and correction factors.

$$C_P = F_P F_M F_L C_B$$

where F_M is the material factor and is 1.00 for a heat exchanger made from carbon steel completely (shell and tube both). F_L is the length factor and for a tube length of 8, 12, 16 and 20 is 1.25, 1.12, 1.05 and 1.00 respectively. F_P is the pressure factor and depends on the shell side pressure. For the pressure range from 100 to 2000 psig it can be determined by the following correlation (Seider et al., 2004):

$$F_P = 0.9803 + 0.018\left(\frac{P}{100}\right) + 0.0017\left(\frac{P}{100}\right)^2$$

References

Branan, C., "Rules of Thumb for Chmeical Engineers," 3rd edition, Gulf Professional Publishing, Houston (2002).

Forsberg et al., http://www.ornl.gov/~webworks/cppr/y2001/pres/111817.pdf, 2001.

Seider, W. D., Seader, J. D. and Lewin D. R., "Product and Process Design Principles: Synthesis, Analysis and Evaluation," 2nd edition, John Wiley and Sons, Inc.New York (2004).

Ulrich, G. D., "A Guide to Chemical Engineering Process Design and Economics," 1st edition, John Wiley and Sons, Inc., New York (1984).

Appendix E

MATLAB Codes

E.1 Biodiesel plant configuration

```
function ObjFun =
One_Mixer_Settler_6X_COMPLETE_HM(Ratio,Extractor,Ratio_Min,Ratio_Max)

for i=1:max(size(Ratio))
    if(Ratio(i)<Ratio_Min(i))
        Ratio(i)=Ratio_Min(i);
    elseif(Ratio(i)>Ratio_Max(i))
        Ratio(i)=Ratio_Max(i);
    end
end
%-------------------------------------------------------------------------
Ratio(4) = 0;
Ratio(3) = Ratio(2);
Ratio(2) = Ratio(1);
Ratio(1) = Extractor.XF(2)./Extractor.XF(1);
%-------------------------------------------------------------------------
XQQ(1) = Extractor.F .* Extractor.XF(1);
for i=2:5
    XQQ(i) = XQQ(1) .* Ratio(i-1);
end
Q = sum(XQQ);
XQ = XQQ./Q;
Extractor.solvent = Q - Extractor.F;

Extractor.XS(1) = 0;
for i = 2:5
    Extractor.XS(i) = (XQQ(1)*Ratio(i-1)-
    Extractor.F.*Extractor.XF(i))/Extractor.solvent;
end
%-------------------------------------------------------------------------
Error = 1;
while(Error>1e-4)

    Extractor.P0 = 1;                   % operating pressure (Bar)
    Extractor.T = 20+273.15;            % extraction unit temperature (K)
%-------------------------------------------------------------------------
    % mixer-settler cost
    % length to diameter ratio of the mixer (usually=1)
    Extractor.mixer_LD = 1;
    Extractor.mixer_rt = 5;             % mixing time (min)
    Extractor = cost_mixer(Extractor);

    % length to diameter ratio of the settler (usually = 3-5)
    Extractor.settler_LD = 3;
    Extractor = cost_settler(Extractor);
    if (Extractor.flag == -1)
```

```
        ObjFun = 1e120;
        return
    end
% ------------------------------------------------------------------------
    % drum 1: top phase of the settler
    drum1.XF = Extractor.TL.xI; % feed composition
    % the following T and P are to be adjusted
    drum1.T = 100+273.15;
    drum1.P = 1;

    drum1 = VLE(drum1.T,drum1.P,drum1.XF);
    drum1.XF = Extractor.TL.xI;
    drum1.Q = Extractor.TL.LI.*Q;
    drum1 = cost_drum_vertical_drum1(drum1);
    %drum1 = cost_drum_vertical(drum1);
    %drum1 = cost_drum_horizontal(drum1)
%------------------------------------------------------------------------
    % drum 2: bottom phase of the settler
    drum2.XF = Extractor.TL.xII; % feed composition
    % the following T and P are to be adjusted
    drum2.T = 70+273.15;
    drum2.P = 1;

    drum2 = VLE(drum2.T,drum2.P,drum2.XF);
    drum2.XF = Extractor.TL.xII;
    drum2.Q = Extractor.TL.LII.*Q;
    drum2 = cost_drum_vertical(drum2);
    %drum2 = cost_drum_horizontal(drum1)
%------------------------------------------------------------------------
    % drum 3:  After drum 1
    drum3.XF = drum1.xI; % feed composition
    % the following T and P are to be adjusted
    drum3.T = 140+273.15;
    drum3.P = 0.55;

    drum3 = VLE(drum3.T,drum3.P,drum3.XF);
    drum3.XF = drum1.xI;
    drum3.Q = drum1.Q*drum1.LI;
    drum3 = cost_drum_vertical_drum3(drum3);
    %drum3 = cost_drum_vertical(drum3)
    %drum3 = cost_drum_horizontal(drum1)
%------------------------------------------------------------------------
    % drum 4:  After drum 2
    drum4.XF = drum2.xI; % feed composition
    % the following T and P are to be adjusted
    % for hexane-methanol with mole ratio of [3.50   12.49]:
    %drum4.T = 129+273.15;
    %drum4.P = 1;

    % for hexane-methanol with mole ratio of [3.9672   15.0056]:
    drum4.T = 131+273.15;
    drum4.P = 1;

    % for hexane-methanol with mole ratio of [4.25 15.86]:
    %drum4.T = 131.5+273.15;
    %drum4.P = 1;
```

```
    drum4 = VLE(drum4.T,drum4.P,drum4.XF);
    drum4.XF = drum2.xI;
    drum4.Q = drum2.Q*drum2.LI;
    drum4 = cost_drum_vertical(drum4);
    %drum3 = cost_drum_horizontal(drum1)
% ------------------------------------------------------------------------
     % recycle streams:

     % hexane + methanol solvents
      [Q_out XQQ RR FreshSolvent Recycle] =
      RecycleStreams_Methanol(Extractor.F,Extractor.XF,Q,XQ,...
        drum1.V*drum1.Q,drum1.y,drum3.V*drum3.Q,drum3.y,...
        drum2.V*drum2.Q,drum2.y,drum4.V*drum4.Q,drum4.y);

      % hexane + water solvents
      %      [Q_out XQQ RR FreshSolvent Recycle] =
      RecycleStreams_Water(Extractor.F,Extractor.XF,Q,XQ,...
      %         drum1.V*drum1.Q,drum1.y,drum3.V*drum3.Q,drum3.y);

           % hexane + methanol + water solvents
      %    [Q_out XQQ RR FreshSolvent Recycle] =
      RecycleStreams_HMWater(Extractor.F,Extractor.XF,Q,XQ,...
      %        drum1.V*drum1.Q,drum1.y,drum3.V*drum3.Q,drum3.y,...
      %        drum2.V*drum2.Q,drum2.y,drum4.V*drum4.Q,drum4.y);

    Error = abs(Q_out - Q) + sum(abs(XQ-XQQ));
    Q = Q_out;
    XQ = XQQ;
    Extractor.Q = Q;
    Extractor.xQ = XQ;
    Extractor.XQ = XQ;

    Solvent = Q.*XQ - Extractor.F.*Extractor.XF;
    Extractor.solvent = Q - Extractor.F;
end
%------------------------------------------------------------------------
% heat exchangers:
heat1 = HEATEX(Extractor.T,drum2.T,Extractor.TL.xII,Extractor.P,
Extractor.TL.LII*Q,'steam');
heat2 = HEATEX(Extractor.T,drum1.T,Extractor.TL.xI,Extractor.P,
Extractor.TL.LI*Q,'steam');
heat3 = HEATEX(drum1.T,25+273.15,drum1.y,drum1.P,drum1.V*drum1.Q,
'coolingwater');
heat4 = HEATEX(drum1.T,drum3.T,drum1.xI,drum1.P,drum1.Q*drum1.LI,
'steam');
heat5 = HEATEX(drum2.T,25+273.15,drum2.y,drum2.P,drum2.V*drum2.Q,
'coolingwater');
heat6 = HEATEX(drum2.T,drum4.T,drum2.xI,drum2.P,drum2.LI*drum2.Q,
'steam');
heat7 = HEATEX(drum4.T,25+273.15,drum4.xI,drum4.P,drum4.LI*drum4.Q,
'coolingwater');
heat8 = HEATEX(drum3.T,25+273.15,drum3.xI,drum3.P,drum3.LI*drum3.Q,
'coolingwater');
heat9 = HEATEX(drum3.T,25+273.15,drum3.y,drum3.P,drum3.V*drum3.Q,
'coolingwater');
heat10 = HEATEX(drum4.T,25+273.15,drum4.y,drum4.P,drum4.V*drum4.Q,
'coolingwater');
```

```
%-------------------------------------------------------------------------
% profitability analysis:
Price.biodiesel = 280;                  % $/kmole
Price.glycerol = 120;                   % $/kmole
Price.Hex = 62;                         % $/kmole
Price.MeOH = 19;                        % $/kmole
Price.water = 0.004;                    % $/kmole
%Price.feed = 113;                      % $/kmole (virgin vegetable oil)
Price.feed = 60.*1306.3./1093.9;        % $/kmole (waste cooking oil)
Price.i = 0.06;                         % interest rate %
Price.pot = 10;                         % pay out time (year)
% working hours per year = (days per year)*(hours per day)
Price.wh = 334*24;
Price.tax = 0.5;                        % income tax rate
%-------------------------------------------------------------------------
% material costs (inlet and outlet)
[Prop Mat Prc] = data();
cost_solvent1 = sum(FreshSolvent.*([0 0 Price.Hex Price.MeOH
Price.water]));   % $/h
cost_solvent = cost_solvent1.*Price.wh;                          % $/year
%cost_phaseII = (Extractor.TL.LII.*Q.*Price.phaseII).*Price.wh  % $/year
%cost_phaseI = (Extractor.TL.LI.*Q.*Price.phaseI).*Price.wh;    % $/year
% biodiesel + glycerol as the main products:
cost_product = (drum3.Q*drum3.LI.*Price.biodiesel +
drum4.LI*drum4.Q.*Price.glycerol).*Price.wh;                     % $/year
cost_feed = Price.feed.*Extractor.F.*Price.wh;                   % $/year

Extractor.Cost.utility = heat1.utilityPrice + heat2.utilityPrice +
heat3.utilityPrice + heat4.utilityPrice +...
    heat5.utilityPrice + heat6.utilityPrice + heat7.utilityPrice +
heat8.utilityPrice + heat9.utilityPrice + heat10.utilityPrice;

% page 266 Timmerhaus (2003)
% transesterification + methanol distillation + neutralization + ...
% heat exchangers + pumps + miscelleneous + ...
% cost index 201 = 1093.9
% cost index 2005 = 1294.4
Extractor.Cost.PEC = (673000 + 358000 + 29000 + 6000 + 50000 +
20000).*1306.3./1093.9 + Extractor.cost_settler + Extractor.cost_mixer +
...
    drum1.Cp + drum2.Cp + drum3.Cp + drum4.Cp +...
    heat1.Cp + heat2.Cp + heat3.Cp + heat4.Cp + heat5.Cp + heat6.Cp +
    heat7.Cp + heat8.Cp + heat9.Cp + heat10.Cp;

% fixed capital investment ($)
% (PEC+land+installation+piping+services+electrical+matrial+buildings+
% yard improvement+engineering and supervision+contractor's
% fees+construction+contingency)

Extractor.Cost.FCI =
Extractor.Cost.PEC.*(1+0.06+0.25+0.80+0.16+0.20+0.45+0.15+0.75);
% total capital investment ($)
Extractor.Cost.TCI = Extractor.Cost.FCI./0.85;
% working capital investment ($)
Extractor.Cost.WCI = 0.15.*Extractor.Cost.TCI;
% raw material cost ($/year)
```

```
Extractor.Cost.Raw_Material = cost_solvent + cost_feed; TPC1 =
0.20*Extractor.Cost.FCI;
Extractor.Cost.TPC = (Extractor.Cost.Raw_Material + TPC1)/0.37;

%Extractor.Cost.TPC = Extractor.Cost.Raw_Material./0.35;
% total production cost ($/year)(waste cooking oil)

Extractor.Cost.plant_capacity = cost_product;                    % $/year
Extractor.Cost.ANP = Extractor.Cost.plant_capacity - Extractor.Cost.TPC;
Extractor.Cost.ANNP = (1-Price.tax).*Extractor.Cost.ANP;
Extractor.Cost.ABD = 0.1.*Extractor.Cost.FCI;
Extractor.Cost.ROI = (1-Price.tax).*(Extractor.Cost.plant_capacity-
Extractor.Cost.TPC)./Extractor.Cost.TCI;
OBJFUN = - Extractor.Cost.ROI;

% residence time in the settler
RT = 0.1.*Extractor.TL.viscI./((Extractor.TL.dens_Liquid_II)./1000-
(Extractor.TL.dens_Liquid_I)./1000);

% NEW OBJECTIVE FUNCTIONS:
      %purity_bio = drum3.xI.*[296.5 92.10 86.17 32.04
      18.02]./sum(drum3.xI.*[296.5 92.10 86.17 32.04 18.02]);
      %purity_gly = drum4.xI.*[296.5 92.10 86.17 32.04
      18.02]./sum(drum4.xI.*[296.5 92.10 86.17 32.04 18.02]);

ObjFun(1) = OBJFUN;
```

E.2 Mixer

```
function mixer = cost_mixer(mixer)

% mixer is a vertical pressure vessel with agitation and L/D=1

% Inputs:   mixer.F = feed flow rate  (kmol/hr)
%           mixer.solvent = solvent flow rate (kmol/hr)
%           mixer.XF = feed composition
%           mixer.XS = solvent composition
%           mixer.T = temperature of mixer (K)
%           mixer.P0 = pressure of mixer (Bar)

mixer.mixer_LD = 1; % length to diameter ratio of the mixer (usually=1)
mixer.mixer_rt = 5; % mixing time (min)

mixer.XQ =
(mixer.XF.*mixer.F+mixer.XS.*mixer.solvent)/(mixer.solvent+mixer.F);
% volume of the mixer-----------------------------------------------------
[Prp Mt Prc] = data();
dens_liquid = density(mixer.T,mixer.XQ);                         % (kg/m3)
mol_weight = 0;
for i=1:max(size(mixer.XQ))
    mol_weight = mol_weight + mixer.XQ(i).*Prp.MW(i);
end
% feed volumetric flowrate (m3/h)
```

```
QV = (mixer.solvent+mixer.F).*mol_weight./dens_liquid;
V = QV.*mixer.mixer_rt./60;              % total volume of the mixer (m3)

% diameter and height of the mixer-------------------------------------
D = (4.*V./(pi().*mixer.mixer_LD)).^(1/3);                          % (m)
L = D.*mixer.mixer_LD;                                              % (m)

% thickness-----------------------------------------------------------
% process and product synthesis, page 530
Di = D.*100./2.54;                          % conversion to in.
Li = L.*100./2.54;                          % conversion to in.

P0_psig = abs(mixer.P0.*14.7-14.7);         % conversion to psig
if(P0_psig<5)
    Pd = 10;
elseif (P0_psig<1000)                       % operating pressure (psig)
    Pd = exp(0.60608+0.91615.*(log(P0_psig))+0.0015655.*
         (log(P0_psig)).^2);                % design pressure (psig)
    Pd = Pd*(Pd>10)+(Pd<=10)*10;
else
    Pd = 1.1*P0_psig;
end

tp = Pd.*Di./(2*Mt.E*Mt.S-1.2.*Pd);         % thk of pressure load (in)

A = (L./D).^2./Pd;
if (A>1.34)
    tvp = tp.*(0.75+0.22*Mt.E.*(Li./Di).^2./Pd); % wind load
elseif (A<=1.34)
    tvp = tp;                                % no wind load detected
end

t_total = tvp+Mt.COR;

thk_min = THK_min(Di);
if (t_total<thk_min)
    thk = thk_min;
else
    thk = t_total;                                                  % [in]
end

% vertical vessel weight and cost--------------------------------------
% process and product synthesis
weight = pi().*(Di+thk).*(Li+0.8.*Di).*thk.*Mt.roi;                 % [lb]
if (weight>4200 & weight<=1E6)
   weight = weight;
elseif (weight<=4200)
   weight = 4200;
else
   weight = 1e6;
end
cv = exp(6.775+0.18255.*log(weight)+0.02297.*(log(weight)).^2);

Dft = Di./12;               % conversion to ft
Lft = Li./12;               % conversion to ft
```

```
if (Dft>3 & Dft<21)
    Dft = Dft;                                          % conversion to ft
elseif (Dft<=3)
    Dft = 3;
else
    Dft = 21;
end
if (Lft>12 & Lft<40)
    Lft = Lft;                                          % conversion to ft
elseif (Lft<=12)
    Lft = 12;
else
    Lft = 40;
end
cpl = 285.1.*(Dft.^0.73960).*(Lft.^0.70684);
cost_vessel = Mt.FM.*cv+cpl;

% agitation cost-------------------------------------------------------
cost_agitator = 2600.*(Mt.AG.*V./3.785).^0.17;                    % [$]

% total cost-----------------------------------------------------------
cost = cost_agitator + cost_vessel;

% power of the motor---------------------------------------------------
[visc_liquid visc_vapor MWm_liquid MWm_vapor] =
viscosity(mixer.T,mixer.XQ,mixer.XQ);
power = (mixer.mixer_rt.*60./(12000.*sqrt(V.*visc_liquid.*1E-
3).*V.^0.2)).^2;           % (Watts)

% outputs--------------------------------------------------------------
mixer.cost_mixer = cost;    % ($)
mixer.thk_mixer = thk;      % (in)
mixer.D_mixer = D;          % (m)
mixer.L_mixer = L;          % (m)
mixer.QV = QV;              % (m3/h)
mixer.power = power;        % (Watts)
%mixer.XF = mixer.XQ;
```

E.3 Settler

```
function settler = cost_settler(settler)

% Inputs: "output of mixer + Extractor.settler_LD = ratio of Length to
diameter"
% length to diameter ratio of the settler (usually=3-5)
settler.settler_LD = 3;

% settler can be a horizontal vessel
% usually the ratio of height to diameter is 3 to 5
[Prp Mt Prc] = data();

% volume of the settler------------------------------------------------
settler.TL = VLLE(settler.T,settler.P0,settler.XQ);
```

```
if(settler.TL.LI.*settler.TL.LII == 0)
    settler.flag = -1;
    return;
end
if (settler.TL.xII(1)>settler.TL.xI(1))
    settler.xI = settler.TL.xII;
    settler.xII = settler.TL.xI;
else
    settler.xI = settler.TL.xI;
    settler.xII = settler.TL.xII;
end

dens_liquid_II = density(settler.TL.T,settler.xII);% hexane-rich phase
dens_liquid_I = density(settler.TL.T,settler.xI);  % methanol-rich phase

[visc_liquid_I visc_vapor MWm_liquid MWm_vapor] =
   viscosity(settler.TL.T,settler.xI,settler.TL.y);

RT = 0.1.*visc_liquid_I./((dens_liquid_II./1000)-(dens_liquid_I./1000));
if (RT>=0)
    settler.settler_rt = RT;
else
    settler.settler_rt = RT.*(-1);
    display('phase flipping')
end
% residence time (hr)
% settler.settler_rt = 0.1.*visc_liquid_I./((max(dens_liquid_II,
% dens_liquid_I)./1000)-(min(dens_liquid_II,dens_liquid_I)./1000));
V = settler.QV.*settler.settler_rt;   % volume of the settler (m3)

% diameter and height of the settler-----------------------------------
D = (4.*V./(pi().*settler.settler_LD)).^(1/3);                    % (m)
L = D.*settler.settler_LD;                                        % (m)

% thickness calculation------------------------------------------------
% process and product synthesis, page 530
Di = D.*100./2.54;                                % conversion to in.
Li = L.*100./2.54;                                % conversion to in.

P0_psig = abs(settler.P0.*14.7-14.7);             % conversion to psig
if(P0_psig<5)
    Pd = 10;
elseif (P0_psig<1000)                        % operating pressure (psig)
    % design pressure (psig)
    Pd = exp(0.60608+0.91615.*(log(P0_psig))+
         0.0015655.*(log(P0_psig)).^2);
    Pd = Pd*(Pd>10)+(Pd<=10)*10;
else
    Pd = 1.1*P0_psig;
end

tp = Pd.*Di./(2*Mt.E*Mt.S-1.2.*Pd);          % thk of pressure load (in)
A = (L./D).^2./Pd;

if (A>1.34)
```

```
    tvp = tp.*(0.75+0.22*Mt.E.*(Li./Di).^2./Pd); % wind load
elseif (A<=1.34)
    tvp = tp;                                    % no wind load detected
end

t_total = tvp+Mt.COR;

thk_min = THK_min(Di);
if (t_total<thk_min)
    thk = thk_min;
else
    thk = t_total;                                                  % [in]
end

% weight and cost of the settler-----------------------------------------
% process and product synthesis
weight = pi().*(Di+thk).*(Li+0.8.*Di).*thk.*Mt.roi;                 % [lb]
if (weight<1000)
    weight = 1000;
elseif (weight>9.2E5)
    weight = 9.2E5;
else
    weight = weight;
end
cv = exp(8.717-0.2330.*log(weight)+0.04333.*(log(weight)).^2);

Dft = Di./12;                                       % conversion to ft
if (Dft>3 & Dft<12)
    Dft = Dft;                                      % conversion to ft
elseif (Dft<=3)
    Dft = 3;
else
    Dft = 12;
end
cpl = 1.580.*Dft.^0.20294;

% total cost-------------------------------------------------------------
cost = Mt.FM.*cv+cpl;

% outputs----------------------------------------------------------------
settler.cost_settler = cost;    % $
settler.thk_settler = thk;      % (in)
settler.D_settler = D;          % (m)
settler.L_settler = L;          % (m)
settler.flag = 1;
```

E.4 Vertical flash drum

```
function drum = cost_drum_vertical(drum)

% vessel diameter--------------------------------------------------------
dens_liquid = density(drum.T,drum.xI);                          % (kg/m3)
```

```
[visc_liquid visc_vapor MWm_liquid MWm_vapor] =
viscosity(drum.T,drum.xI,drum.y);
[Z Volume phi DH] = SRK(drum.T,drum.P,drum.y);

% average density of the vapor phase in the column (kg/m3)
dens_gas = MWm_vapor./Volume(2);
WWL = drum.LI.*drum.Q.*MWm_liquid./3600;                    % kg/s
WWV = drum.V.*drum.Q.*MWm_vapor./3600;                      % kg/s
% separation factor
sep_factor = (WWL./WWV).*sqrt(dens_gas./dens_liquid);
XX = log(sep_factor);
Kv = exp(-1.942936-0.814894*XX-0.179390*XX.^2-
0.0123790*XX.^3+0.000386235*XX.^4+0.000259550*XX.^5);
uv = (Kv.*sqrt((dens_liquid-dens_gas)./dens_gas)).*0.3048;          % m/s

Amin = (WWV./dens_gas)./uv;                                         % m2
Dmin = sqrt(4*Amin./pi());                                          % m
D = ceil((Dmin./0.3048).*2)./2.*0.3048;                             % m
% design time to fill (a guide to, page 203)
fill_time = 10.*60;                                                 % s
% required vessel liquid volume
VL = (WWL./dens_liquid).*fill_time;                                 % m3
HL = VL.*(4/(pi().*D.^2));  % m (liquid height)
HV = D.*(D>1)+1.*(D<=1);    % vapor height (a guide to, page 203) (m)
height = HV+HL;             % total height of drum (m)
LD = height./D;

% thickness-----------------------------------------------------------
[Prp Mt Prc] = data();
Di = D./0.0254;
Hi = height./0.0254;

P_psig = abs(drum.P.*14.7-14.7);                    % conversion to psig
if(P_psig<5)
    Pd = 10;
elseif (P_psig<1000)                          % operating pressure [psig]
    % design pressure (psig)
    Pd = exp(0.60608+0.91615.*(log(P_psig))+0.0015655.*
         (log(P_psig)).^2);
    Pd = Pd*(Pd>10)+(Pd<=10)*10;
else
    Pd = 1.1*P_psig;
end

tp = Pd.*Di./(2*Mt.E*Mt.S-1.2.*Pd);                 % pressure load [in]

% for vacuum vessel, tv:
tE = 1.3.*Di.*(Pd.*Hi./(Mt.Em.*Di)).^0.4;
tEC = Hi.*(0.18.*Di-2.2)*1e-5-0.19;
tvp = tp.*(0.75+0.22*Mt.E.*(Hi/Di).^2./Pd);
t_total = tvp+tEC+tE+Mt.COR;

thk_min = THK_min(Di);
if (t_total<thk_min)
    thk = thk_min;
```

```
else
    thk = t_total;                                                    % [in]
end

% vessel weight-------------------------------------------------------
weight = pi().*(Di+thk).*(Hi.*100./2.54+0.8.*Di).*thk.*Mt.roi;    % [lb]

% vertical vessel capital cost----------------------------------------
dft = Di./12;
hft = height.*100./(2.54*12);          % conversion of height in m to ft
Cpl = 237.1.*dft.^0.63316.*(hft).^0.80161;
Cv = exp(7.0374+0.18255*log(weight)+0.02297*(log(weight)).^2);
Cp = Mt.FM.*Cv+Cpl;                        % purchase cost (capital cost)

% outputs-------------------------------------------------------------
drum.Cp = Cp;
drum.weight = weight;
drum.thk = thk;
drum.LD = LD;
drum.height = height;
drum.HL = HL;
drum.HV = HV;
drum.D = D;
```

E.5 Heat exchanger

```
function heat = HEATEX(Tin,Tout,z,P,flow,HE)

FM = 1;          % (carbon steel) material factor (P. 523)
FL = 1.12;       % average tube length correction (P. 523)
% pressure factor
FP = 0.9803+0.018.*(P.*14.7-14.7)./100+0.0017.*((P.*14.7-14.7)./100).^2;
switch lower(HE)
    case 'steam'
        % utility Steam at 150 psig & 185 °C
        Tuin = 185+273.15;                                            % K
        Tuout = 184+273.15;                                           % K
        U = 50;
        TLM = ((Tuin-Tout)-(Tuout-Tin))./
              (log((Tuin-Tout)./(Tuout-Tin)));
        TLin = VLLE(Tin,P,z);
        TLout = VLLE(Tout,P,z);
        q = (TLout.Hstream - TLin.Hstream).*flow;                      % kJ/h
        A = q./(U.*TLM);

        % fixed head shell and tube heat exchanger:
        %p = 114.7./14.7;   % conversion to Bar
        if ((P.*14.7-14.7)>100) & ((P.*14.7-14.7)<2000)
            FP = FP;
        elseif ((P.*14.7-14.7)<=100) & ((P.*14.7-14.7)>0)
            FP = 1;
        elseif ((P.*14.7-14.7)<=0) | ((P.*14.7-14.7)>2000)
            FP = 2.03;
```

```
        end
        CB = exp(11.0545-0.9228.*log(A)+0.09861.*(log(A)).^2);        % $
        Cp = FP.*FM.*FL.*CB;  % $
        heat.Cp = Cp;
        heat.A = A;
        heat.q = q;
        % kJ/h /(kJ/1000Kg steam) * $/1000Kg steam  = $/h
        heat.utilityPrice = q / 1.994e6 * 4.4;
        heat.Utility = 'Steam 185°C';
        return

    case 'coolingwater'
        % utility cooling water
        Tuin = 15+273.15;                                              % K
        Tuout = 20+273.15;                                             % K
        U = 50;

        TLM = ((Tout-Tuin)-(Tin-Tuout))./(log((Tout-Tuin)/(Tin-Tuout)));

        TLin = VLLE(Tin,P,z);
        TLout = VLLE(Tout,P,z);
        q = -(TLout.Hstream - TLin.Hstream).*flow;
        A = q./(U.*TLM);

        % fixed head shell and tube heat exchanger:
        %p = 114.7./14.7;   % conversion to Bar
        if ((P.*14.7-14.7)>100) & ((P.*14.7-14.7)<2000)
            FP = FP;
        elseif ((P.*14.7-14.7)<=100) & ((P.*14.7-14.7)>0)
            FP = 1;
        elseif ((P.*14.7-14.7)<=0) | ((P.*14.7-14.7)>2000)
            FP = 2.03;
        end
        CB = exp(11.0545-0.9228.*log(A)+0.09861.*(log(A)).^2);        % $
        Cp = FP.*FM.*FL.*CB;                                           % $
        heat.Cp = Cp;
        heat.A = A;
        heat.q = q;
        % kJ/h /(kJ/1000Kg steam) * $/1000Kg steam  = $/h
        heat.utilityPrice = q / 2.092e4 * 0.08;
        heat.Utility = 'Cooling Water';
        return

    otherwise
        disp('error in selecting heat exchanger')
end
```

E.6 UNIFAC activity coefficient model

```
function [lngama Hp] = UNIFAC_LnGAMA(TT,xA,Groups,NU)

nnn = size(NU);
```

```
No_Comp = nnn(2);
max_subGroup = nnn(1);

RQ = [0.9011 0.848;0.6744 0.54;0.4469 0.228;0.2195 0;1.3454 1.176;1.1167
0.867;0.8886 0.676;1.1173 0.988;0.5313 0.4;0.3652 0.12;1.2663
0.968;1.0396 0.66;0.8121 0.348;1 1.2;3.2499 3.128;3.2491 3.124;0.92
1.4;0.8952 0.68;1.6724 1.488;1.4457 1.18;0.998 0.948;3.168 2.484;1.3013
1.224;1.528 1.532;1.9031 1.728;1.6764 1.42;1.145 1.088;0.9183
0.78;0.6908 0.468;0.9183 1.1];
a = [0 74.54 -114.8 -115.7 644.6 329.6 310.7 1300 2255 472.6 158.1 383
139.4 972.4 662.1;292.3 0 340.7 4102 724.4 1731 1731 896 0 343.7 -214.7
0 1647 -577.5 289.3;156.5 -94.78 0 167 703.9 511.5 577.3 859 1649 593.7
362.3 31.14 461.8 6 32.14;104.4 -269.7 -146.8 0 4000 136.6 906.8 5695
292.6 916.7 1218 715.6 339.1 5688 213.1;328.2 470.7 -9.21 1.27 0 937.3
991.3 28.73 -195.5 67.07 1409 -140.3 -104 195.6 262.5;-136.7 -135.7 -223
-162.6 -281.1 0 0 -61.29 -153.2 -47.41 -344.1 299.3 244.4 19.57 1970;-
131.9 -135.7 -252 -273.6 -268.8 0 0 5.89 -153.2 853.8 -338.6 -241.8 -
57.98 487.1 1970;342.4 220.6 372.8 203.7 -122.4 247 104.9 0 344.5 -171.8
-349.9 66.95 -465.7 -6.32 64.42;-159.8 0 -473.2 -470.4 -63.15 -547.2 -
547.2 -595.9 0 -825.7 0 0 0 -898.3 0;66.56 306.1 -78.31 -73.87 216 401.7
-127.6 634.8 -568 0 -37.36 120.3 1247 258.7 5.202;146.1 517 -75.3 223.2
-431.3 643.4 231.4 623.7 0 128 0 1724 0.75 -245.8 0;14.78   0 -10.44 -
184.9 444.7 -94.64 732.3 211.6 0 48.93 -311.6 0 1919 57.7 0;1744 -48.52
75.49 147.3 118.4 728.7 349.1 652.3 0 -101.3 1051 -115.7 0 -117.6 -
96.62;-320.1 485.6 114.8 -170 180.6 -76.64 -152.8 385.9 -337.3 58.84
1090 -46.13 1417 0 -235.7;1571 76.44 52.13 65.69 137.1 -218.1 -218.1
212.8 0 52.38 0 0 1402 461.3 0];
main_group = [1 1 1 1 2 2 2 2 3 3 4 4 4 5 6 7 8 9 10 10 11 12 13 13 14
14 15 15 15 15 16 16 16 17 17 17 18 18 19 20 21 21 22 23 23 23 24 25 26
27 27 27 28 29 30 31 32];
%-------------------------------------------------------------------------
for i=1:No_Comp
    rA(i)=0;
    qA(i)=0;
    for j = 1:max_subGroup
        rA(i) = rA(i) + NU(j,i).* RQ(Groups(j),1);
        qA(i) = qA(i) + NU(j,i).* RQ(Groups(j),2);
    end
end

hhrA = 0;
qqrA = 0;
for i=1:No_Comp
    hrA(i)=xA(i).*rA(i);
    hqA(i)=xA(i).*qA(i);
    hhrA = hhrA + hrA(i);
    qqrA = qqrA + hqA(i);
end

for i=1:No_Comp
    pAi(i)=hrA(i)/hhrA;
    tAi(i)=hqA(i)/qqrA;
end
z = 10;
for i=1:No_Comp
```

```
    gAC(i)=(log(pAi(i)/xA(i))+1-pAi(i)/xA(i))-
(z/2).*qA(i).*(log(pAi(i)/tAi(i))+1-pAi(i)/tAi(i));
end
%-------------------------------------------------------------------------
% for the mixture
N2 = 0;
for j=1:max_subGroup
    N1(j) = 0;
    for i = 1:No_Comp
        N1(j) = N1(j) + NU(j,i) * xA(i);
    end
    N2 = N2 + N1(j);
end
Xm = N1/N2;

M2 = 0;
for j=1:max_subGroup
    M1(j)= RQ(Groups(j),2)* Xm(j);
    M2 = M2 + M1(j);
end
tetm =M1/M2;

for m = 1:max_subGroup
    for k= 1:max_subGroup
        phimk(m,k)=exp(-
a(main_group(Groups(m)),main_group(Groups(k)))./TT);
        phikm(k,m)=exp(-
a(main_group(Groups(k)),main_group(Groups(m)))./TT);
    end
end

Kmmk = tetm * phimk;

for k = 1:max_subGroup
    KMS(k) = 0;
    for m= 1:max_subGroup
        Kmkm(k,m) = tetm(m).*phikm(k,m);
        Kmkm(k,m) = Kmkm(k,m)./Kmmk(m);
        KMS(k) = KMS(k) + Kmkm(k,m);
    end
end

for j = 1:max_subGroup
    g1A(j) = RQ(Groups(j),2)*(1- log(Kmmk(j))- KMS(j));
end
%-------------------------------------------------------------------------
% pure components
for i = 1:No_Comp
    PN2 = 0;
    for j=1:max_subGroup
       PN1(j) = NU(j,i);
       PN2 = PN2 + NU(j,i);
    end
    PXm = PN1/PN2;

    PM2 = 0;
```

```
    for j=1:max_subGroup
        PM1(j)= RQ(Groups(j),2)* PXm(j);
        PM2 = PM2 + PM1(j);
    end
    Ptetm =PM1/PM2;

    for m = 1:max_subGroup
        for k= 1:max_subGroup
            Pphimk(m,k)=exp(-
a(main_group(Groups(m)),main_group(Groups(k)))/TT);
            Pphikm(k,m)=exp(-
a(main_group(Groups(k)),main_group(Groups(m)))/TT);
        end
    end

    PKmmk = Ptetm * Pphimk;

    for k = 1:max_subGroup
        PKMS(k) = 0;
        for m = 1:max_subGroup
            PKmkm(k,m) = Ptetm(m) * Pphikm(k,m);
            PKmkm(k,m) = PKmkm(k,m) / PKmmk(m);
            PKMS(k) = PKMS(k) + PKmkm(k,m);
        end
    end

    for k = 1:max_subGroup
        Pg1A(k) = RQ(Groups(k),2)*(1- log(PKmmk(k))- PKMS(k));
    end
    lngamaR(i) = 0;
    for j = 1:max_subGroup
        lngamaR(i) = lngamaR(i) +  NU(j,i)*(g1A(j)-Pg1A(j));
    end
    lngama(i) = lngamaR(i) + gAC(i);
end
% enthalpy calculations ---------------------------------------------
R = 0.08314;                                              (m3.Bar/Kmol.K)

% mixture
for k = 1:max_subGroup
    Kmmkp(k) = 0;
    Kmmk(k) = 0;
    Kmkmp(k) = 0;
    Kmkm(k) = 0;
    for m = 1:max_subGroup
        Kmmkp(k) = Kmmkp(k) +
tetm(m).*phimk(m,k).*a(main_group(Groups(m)),main_group(Groups(k)));
        Kmmk(k) = Kmmk(k) + tetm(m).*phimk(m,k);
        Kmkmp(k) = Kmkmp(k) +
tetm(m).*phikm(k,m).*a(main_group(Groups(k)),main_group(Groups(m)));
        Kmkm(k) = Kmkm(k) + tetm(m).*phikm(k,m);
    end
end

for k = 1:max_subGroup
    KMS(k) = 0;
```

```
    for m= 1:max_subGroup
        KMS(k) = KMS(k) - tetm(m).*phikm(k,m).*Kmkmp(m)./(Kmkm(m).^2);
    end
    KMS(k) = KMS(k) + Kmkmp(k)./Kmkm(k) + Kmkmp(k);
end

for k = 1:max_subGroup
    Hk_RT2(k) = RQ(Groups(k),2).*KMS(k)./(TT.^2);
end
%-------------------------------------------------------------------------
% for pure components
for i = 1:No_Comp
    PN2 = 0;
    for j=1:max_subGroup
       PN1(j) = NU(j,i);
       PN2 = PN2 + NU(j,i);
    end
    PXm = PN1./PN2;

    PM2 = 0;
    for j=1:max_subGroup
        PM1(j)= RQ(Groups(j),2)* PXm(j);
        PM2 = PM2 + PM1(j);
    end
    Ptetm =PM1./PM2;

    for m = 1:max_subGroup
        for k= 1:max_subGroup
            Pphimk(m,k)=exp(-
a(main_group(Groups(m)),main_group(Groups(k)))/TT);
            Pphikm(k,m)=exp(-
a(main_group(Groups(k)),main_group(Groups(m)))/TT);
        end
    end

    for k = 1:max_subGroup
        PKmmkp(k) = 0;
        PKmmk(k) = 0;
        PKmkmp(k) = 0;
        PKmkm(k) = 0;
        for m = 1:max_subGroup
            PKmmkp(k) = PKmmkp(k) +
Ptetm(m).*Pphimk(m,k).*a(main_group(Groups(m)),main_group(Groups(k)));
            PKmmk(k) = PKmmk(k) + Ptetm(m).*Pphimk(m,k);
            PKmkmp(k) = PKmkmp(k) +
Ptetm(m).*Pphikm(k,m).*a(main_group(Groups(k)),main_group(Groups(m)));
            PKmkm(k) = PKmkm(k) + Ptetm(m).*Pphikm(k,m);
        end
    end

    for k = 1:max_subGroup
        PKMS(k) = 0;
        for m= 1:max_subGroup
            PKMS(k) = PKMS(k) -
Ptetm(m).*Pphikm(k,m).*PKmkmp(m)./(PKmkm(m).^2);
        end
```

```
            PKMS(k) = PKMS(k) + PKmkmp(k)./PKmkm(k) + PKmkmp(k);
        end

        for k = 1:max_subGroup
            PHk_RT2(k) = RQ(Groups(k),2).*PKMS(k)./(TT.^2);
        end

        DH(i) = 0;
        for k = 1:max_subGroup
            DH(i) = DH(i) + NU(k,i) * (Hk_RT2(k) - PHk_RT2(k));
        end
    end

    Hp = sum(DH.*xA);                                          % DHmixing/RT²
```